

APPLICATION OF GRIBOV CALCULUS
TO TWO-BODY PROCESSES

by

PETER KOEHLER

A Thesis presented for the Degree of Doctor of Philosophy
of the Royal Holloway College, University of London.

Department of Mathematics,
Royal Holloway College
Englefield Green
Surrey

June 1978

ProQuest Number: 10097448

All rights reserved

INFORMATION TO ALL USERS

The quality of this reproduction is dependent upon the quality of the copy submitted.

In the unlikely event that the author did not send a complete manuscript and there are missing pages, these will be noted. Also, if material had to be removed, a note will indicate the deletion.



ProQuest 10097448

Published by ProQuest LLC(2016). Copyright of the Dissertation is held by the Author.

All rights reserved.

This work is protected against unauthorized copying under Title 17, United States Code.
Microform Edition © ProQuest LLC.

ProQuest LLC
789 East Eisenhower Parkway
P.O. Box 1346
Ann Arbor, MI 48106-1346

ABSTRACT

A new model for two-body high energy scattering is presented as part of an investigation into the phenomenology of the non planar structure of Reggeon-particle scattering. The model is a modification of the weak cut reggeized for Pion-Nucleon scattering and is developed in form of a correlation modified quasi eikonal where the Reggeon number of Pomerons are allowed to change the projection of the nucleon spin. A correlation parameter - the β - has its origin in Gribov's theory, provides an indication about the failure of the traditional weak cut reggeized and restores its most profound shortcoming - the prediction of an incorrect phase behaviour of the helicity isovector amplitude in the reaction $\pi^- p \rightarrow \pi^0 n$ - while retaining the model's attractive simplicity. The vertex Reggeon-calculus depend in general on the angle between the momenta of the exchanged reggepoles. By parameter dependence we take into account the effective contribution of inelastic intermediate states in the unitarity expansion of Regge-particle scattering amplitude. We obtain a reasonable phase energy description of the isovector amplitude and demonstrate in detail the mechanism by which the correct phase behaviour is restored. The spin-structure of the amplitude is investigated and observables of πN scattering between 6 and 200 GeV/c within a range of momentum transfer are being produced.

PREFACE

The work described in this Thesis was carried out under the supervision of Dr. K. J. M. Moriarty in the Mathematics, Royal Holloway College, between October 1973 and September 1976.

The material presented in the text is original except in so far as explicit reference is made to the work which has been submitted for a Degree in this, or any other, University.

The author expresses his gratitude to Dr. K. J. M. Moriarty and Dr. R. W. B. Ardill with whom he collaborated in this and similar work, for their enthusiasm, guidance, support and friendship. He wishes to thank Professor Moriarty for encouragement in this work.

Thanks are also extended to P. Choudhury, Dr. A. Ungkitchanukit and Dr. N. Staton for many lively discussions during the various stages of this work.

I am indebted to H. Høgaasen, A. Krzywicki and A. P. Kaidalov for their detailed and useful correspondence.

The financial support of Royal Holloway College in the form of a Tutorial Research Fellowship from October 1973 to September 1976 is gratefully acknowledged.

I would like to thank my wife, Mary, who has typed and arranged the layout of this Thesis - without whom I could not have enjoyed the work as much as I did.

Finally, I would like to thank Dr. F. Gutierrez and Dr. J. O. Falcon-Vega for having introduced me into the world of particle physics.

C O N T E N T S

	Pa
ABSTRACT	(i)
PREFACE	(ii)
I <u>INTRODUCTION</u>	1
<u>PART ONE - THEORETICAL DISCUSSION</u>	10
II <u>THE REGGEON AND POMERON CONTRIBUTION TO THE S-CHANNEL HELICITY AMPLITUDE OF THE PROCESS $A + C \rightarrow B + D$</u>	11
III <u>GRIBOV'S REGGEON DIAGRAM TECHNIQUE</u>	22
III. I Gribov's Evaluation of the Mandelstam Diagram - the Basis of the Reggeon Diagram Technique	22
III. II The Regge Particle Scattering Amplitude	32
III. III Gribov Rules for the "Raleigh-Schrödinger" Perturbation Theory	38
IV <u>A CORRELATION MODIFIED EIKONAL MODEL</u>	45
V <u>THE "DERIVATIVE RULE" APPLIED TO THE CORRELATION MODIFIED WEAK ABSORPTION MODEL WITH (A) TRADITIONAL POMERON INPUT, AND (B) HARTLEY-KANE POMERON INPUT</u>	73

	<u>Pa</u>
<u>PART TWO - PHENOMENOLOGICAL INVESTIGATION</u>	7
VI <u>A DISCUSSION OF THE MECHANISM BY WHICH THE CORRELATION MODIFIED ABSORPTION MODEL RECTIFIES THE INCORRECT PHASE BEHAVIOUR PREDICTED BY TRADITIONAL REGGEIZED ABSORPTION</u>	7
VI.1 The Crossing Symmetric Weak Cut Reggeized Absorption Model as a Special Case of the Gribov Cut	8
VI.11 The Gribov Cut Represented as Vector in the Argand Diagram	10
VI.111 Several Model Variants Towards the Solution of the Phase Problem of the Helicity Nonflip Isovector Amplitude	12
VI.111.1 Model Variant Ia - Purely Real Correlation Model	12
VI.111.2 Model Variant Ib - Complex Correlation Model as a Crossing Symmetry Violating Solution to the Phase Problem of the Helicity Nonflip Isovector Amplitude	12
VI.111.3 Purely Real and Negative Correlation Modified Models as a Crossing Symmetry-Preserving Solution to the Phase Problem	14
VI.111.4 A Phase Energy Description of $\pi^-p \rightarrow \pi^0n$ at 6 GeV/c and FNAL Energies with a Good Prediction of both Inelastic and Elastic Polarization of $\bar{\pi} N$ Scattering (Model V and Model VI)	16
VII <u>SOME PURELY REAL AND POSITIVE CORRELATION MODIFIED MODELS</u>	18
VII.1 The Large Pomeron Phase Model	18
VII.1.1 The Zero Residue Version (Model VII)	18
VII.1.2 The Non-Zero Residue Version (Model VIII)	18

VIII	<u>THE CORRELATION MODIFIED "DERIVATIVE RULE" MODEL (MODEL IX)</u>	19
IX	<u>AN INTERPRETATION OF THE NEGATIVE SIGN OF THE CORRELATION PARAMETER</u>	20
X	<u>AN OUTLOOK TOWARDS A UNIFIED DESCRIPTION OF HADRONIC TWO-BODY INTERACTIONS</u>	20
XI	<u>APPENDIX</u>	20
XII	<u>REFERENCES</u>	22

I - INTRODUCTION

There is overwhelming evidence (1) that the simple power law energy behaviour predicted by the Regge formula at high energies is a good approximation to the real world of two body scattering. A particularly striking example has been provided by the recent data from Fermilab (2) on the Pion Nucleon charge exchange reaction $\pi^- p \rightarrow \pi^0 n$ at 20 and 200 GeV/c. The effective J-plane singularity moves on an only slightly curved trajectory which approximates the Regge pole excellently. The data, however, show a small bump at the nonsense wrong signature zero (NWSZ) around $t \approx -0.5$ and the slight deviation from a straight line further out in $|t|$ are the mild reflections of correction terms to the Regge pole exchange. These corrections arise as cuts in the complex angular momentum plane (3). They are traded for the pole by means of a version of the absorption model (4). Within such an approach one understands that, in the case of the $\pi^- p \rightarrow \pi^0 n$ reaction, the relative size of the helicity nonflip[#] compared to the pole needs to be particularly large to account for the real part of the helicity nonflip isovector amplitude. In addition, this zero has to occur before the zero of the real part of the amplitude with sufficient separation so as to account for the correct phase structure which is manifest in the data of the recoil nucleon in $\pi^- p \rightarrow \pi^0 n$ (5). None of the traditional absorption models can account for the observed features of the data.

Cuts have, due to their smaller slope ($\alpha'_{\text{cut}} < \alpha'_{\text{pole}}$) the tendency to "take over" further out in $|t|$ and a corresponding lack of shrinkage. The mild deviation of the effective trajectory from a straight line constitutes, therefore, a significant feature. On the other hand, $\pi^- p \rightarrow \pi^0 n$ is dominated by the helicity flip amplitude and cuts in this amplitude are relatively weak. The helicity flip amplitude has all the features of a NWSZ pole (5) up to $|t| \sim 6$. Beyond this the rise and fall of the symmetric part of the elastic polarization (6) in πN scattering seems to imply a rather important key role in the determination of elastic as well as inelastic polarization of πN scattering is played by the pole amplitude, i. e. the full elastic amplitude. Unfortunately this phase is unknown away from forward direction and the uncertainty of the phase is the major source of uncertainty in an otherwise model-independent amplitude analysis. Thus the first step for is to obtain a self consistent description of the πN system by constructing simultaneously the isoscalar and isovector amplitudes.

cut

The elastic amplitude enters the absorption model in form of strong dominantly elastic rescattering in the initial state. This is supposed to effectively take account of the many competing inelastic channels which open up in "head on collisions". The elastic amplitude replaces, in the high energy approximation of the absorption model, the initial and final state wave functions of a complex optical potential whose imaginary part is meant to simulate the effects of the competing channels. This high energy version of the distorted-wave Born approximation of low energy nuclear scattering introduced by Sopkovich (7) and has been applied successfully to correct the too exaggerated peak close to threshold and the too slow fall-off with momentum transfer predicted by the peripheral or one-particle exchange model for the production of quasi-two-body reactions. (8). Note that in the OPE model the couplings are constant and the factors for the couplings in the Born approximation exactly simulates, at fixed energies, the effects of absorption.

Traditionally the elastic amplitude has been taken from experiment, equal in initial and final states, diagonal in angular momentum, imaginary with no t -dependent phase and has been parameterized by a Gaussian. This produces the desired effect: it appears as a grey absorbing disc reducing the lower partial waves and leaving the higher ones unaffected, which sharpens the forward peak of the t -distribution.

Absorption and reggeization of the OPE model has led the Imperial College group to construct, in connection with the strong exchange degeneracy and couplings which are determined by a higher symmetry scheme: a very compact parameter-free reggeized weak cut absorption model for Meson-Baryon scattering with considerable predictive power (4). Although this model has failed to predict the correct phase behaviour of the isovector helicity amplitudes, the NWSZ input of the basic exchange seems to be strongly supported by the FNAL data.

The weak cut absorption originally proposed by Cohen-Tannoudji et al. and Arnold et al. (4) has qualitatively correct polarization in $\pi^- \rho \rightarrow \pi^0 n$. Its quantitative prediction, however, is drastically wrong. The reason is the strength and wrong phase of the cut amplitude. Absorption is essentially a convolution in momentum transfer. If the NWSZ input pole changes sign in the region of integration there will be a cancellation in the integral and the amplitude will tend to be small. It is in fact too small to obtain the zero of the imaginary part of the isovector amplitude which is much further inwards in t than predicted by the pure NWSZ pole. If one were to introduce a strength factor to pull the zero further in, this would completely destroy the already displaced dip position.

a zero in the imaginary part implies, due to the wrong cut phase, a nearby zero of the real part. But to polarization of $\pi^- p \rightarrow \pi^0 n$ the zero of the imaginary part has to occur before the real one and both sufficiently enough apart.

The lack of strength of the weak cut model in other reactions such as $\gamma p \rightarrow \pi^+ n$ and $n p \rightarrow p n$ is also on the theoretical side, the intuitive basis of the Sopkovich formula has led to serious doubts. This concerns, truncation of rescattering in the initial and final states to on-mass shell states. The weak absorption model neglects the contribution of inelastic diffractive intermediate states. These intermediate states are, however, a consequence of s-channel unitarity. Furthermore, the very existence of cuts is due to the presence of the third order double spectral function. These functions cause fixed pole singularities at wrong signature points for the partial wave amplitudes which cannot be made to vanish by a superconvergence relation. These fixed poles would, due to unitarity, be essential singularities violating the Froissart bound were it not for cuts specially invoked for these reasons to prevent this happening. In the presence of the third order double spectral function it is not unlikely that the occurring fixed poles are strong and enter the Regge residues multiplicatively. They then would cancel the unstructured pole amplitude.

In combining both points of view, namely the necessity to incorporate the inelastic diffractive intermediate states and the factor λ and the absence of NWSZ in the input pole, the Michigan group Henyey et al (4) have constructed an absorption model and also successfully fitted a great amount of data. In particular the dip structure of the polarization is now being produced by pole-cut interference. The polarization, however, has been equally as wrongly produced by the cut model. The relatively large strength of the Michigan cut actually once produced the crossover position which was paid for with over absorption, which could be restored by eikonolization (9), while losing the crossover position.

The failure of traditional absorption-irrespective whether weak or strong - to account for positive polarization (both versions result in an approximately 90% negative peak) has stimulated a great number of successful models with and without NWSZ input poles (10). Despite their different appearance they all have one factor in common, they are completely ad hoc and consists essentially in a broadening of the J-plane discontinuity due to the addition of a J-plane singularity, $(11a,b)$ a circumstance which led these models into strong conflict with duality. $(11c)$ Duality, a property of two body amplitudes, is definitely a property of \mathcal{P} exchange. The zero of the imaginary part

amplitude already occurs in the lower energy resonances. All phase modified model amplitudes when FE compare wrongly in their $/t/$ dependence with the phase shift FESR integral. Ironically the only alternative scheme - Barger and Phillips' $\rho + \rho'$ pole model (12) - has predicted positive πN inelastic polarization symmetry of elastic πN polarization, though not the double zero. It is in excellent agreement (13) with the and in addition is compatible with FESR and local-average duality. (11 a)

Polarization generated by two different trajectories, however, changes rapidly with a fixed power of the e in the case of a cut this power is proportional to the momentum transfer consequently resulting in a mild e within the range of the diffraction cone. The $\rho + \rho'$ model, in fact, changes the shape of the polarization that already at 18 GeV/c it shows the tendency to approach the unwanted shape of the absorption model. (9) resonances have yet been identified along the ρ' trajectory causes further doubt about the validity of such although it seems to serve as a surprisingly good parameterization.

The circumstance that at an early stage of the development of the absorption model the introduction of strong factors into the Born term of the OPE model could simulate exactly the effect of absorption shows how sensible empirical factors in order to suit a first intuitive guess. On the theoretical side there is the necessity to absorption model contributions from inelastic diffractive intermediate states; on the phenomenological side the reggeized absorption model is too weak and has a wrong phase and energy behaviour. A source of strength available by the Michigan approach through a vague enhancement coefficient in connection with an unfavourable celling the NWSZ in the Regge pole amplitude. All phase modified models have taught us that the imaginary helicity nonflip isovector exchange should be more absorbed than the real part. This, as we saw, however with duality. The FNAL data on the other hand suggest that the energy dependence of cuts should be rather

The result of a closer examination into the origin of the phase problem may be summarized in the two major traditional absorption cut:

- (1) the relative cut pole phase is too close to 180° at $/t/ \neq 0$
- (2) although the absorptive cut rotates with increasing $/t/$ away from the pole, it does so too slowly by comparison with the fast following pole. Thus, the pole catches up with the cut at the critical

phase difference of 180° already at very small $|t|$ and there it causes the polarization to change its sign from positive to negative.

As the phenomenological investigation performed in this thesis has shown, it is possible to obtain a re description of $\pi^-p \rightarrow \pi^0n$ including the elastic polarization of π^+p scattering by simulation of the inelastic intermediate states in the following way:

- (1) The size of the effective interaction region of the Reggeon involved in the cut has to shrink considerably smaller value in comparison with the size of the Reggeon in the Born term. The same holds for the elastic amplitude.
- (2) In addition, the elastic amplitude has to have a $|t|$ dependent phase.
- (3) At last there is an overall damping form factor which renormalizes the shape of the cut.

The combined effect of this prescription on the phase - while keeping the attractive NWSZ - is that:

- (1) The cut is strengthened in forward direction
- (2) The initial phase angle at $|t| = 0$ has been rotated in anti-clockwise direction resulting in a purely imaginary cut term.
- (3) The cut's traditional slow rotation becomes accelerated.

The new cut is now able to reverse the sense of rotation of the helicity nonflip pole so strongly that the part of the amplitude moves into the vicinity of the actual cross over position.

When extrapolating the amplitudes to FNAL energies one can stabilize the helicity nonflip phase angle with considerably stable polarization over a wide range in energy. By doing this the logarithmic energy denominator vanishes. This promises agreement with duality. In fact, the phase modification has not been achieved by broadening the J -plane singularity structure but by enhancing the ratio between the slope of the "Pomeron" and the effective interaction size which results in a larger phase and greater strength of the cut. The t

problems further out in t and for large energies remain, however, causing a slower fall off of the differential cross section and a spread between both effective trajectories at 6 and 200 GeV/c. Thanks to the NWSZ pole, however, the discrepancy is not so severe as it otherwise would be.

This procedure of modifying the cut sounds as ad hoc as many modification attempts of the past. But a great deal of it disappears if we see it in connection with Gribov's theory, from which it emerges quite naturally. Gribov's theory is as the most general frame for the whole strong interaction physics. Its basic assumption is the absence of singular forces. This convergence property in conjunction with analyticity led to Gribov's Reggeon diagram technique (14).

The fundamental postulate in connection with multiperipheral kinematics which governs the multiparticle production bound up in the two-body amplitude through unitarity, generated a two dimensional field theory of high energy and small momentum transfer reactions.

The following picture of two body scattering emerged: During the scattering process the two colliding hadrons act as sinks to produce and absorb respectively the energy momentum of Reggeons in form of quasi particles. The Reggeons interact with each other while they diffuse over one time and two space dimensions. The sum over all such interaction diagrams is the result of the non-relativistic theory for asymptotic energies. Each diagram corresponds to a term in a Rayleigh-Schrödinger expansion of the amplitude in powers of $(\ln s)^{-1}$. The rules for evaluating the diagrams are reminiscent of Feynman diagrams.

Compositeness enters the theory - emphasising its multiperipheral origin - via unitarity when the colliding hadrons are broken up into constituents in a cascade of decays. The interaction of the corresponding constituents from both hadrons causes the production of multiperipheral showers which correspond in turn to the exchanged reggeons. For clarification of Gribov's theory and of the simultaneous contribution of multiperipheral and diffractive intermediate states to the two body amplitude we refer to the exhaustive exposition by Baker and Ter-Martirosyan (15), a rich encyclopaedia of reggeon diagrams which await their phenomenological implications.

Gribov's Reggeon diagram technique (14) can indeed serve as a powerful tool in practical calculations for vacuum and number exchange at attainable energies. The vertices of the theory are, however, unknown and are expected not to be known because of their non-planar nature. These vertices describe transitions between external particles and reggeons, and reggeons. The diagrams of the expansion of the scattering amplitude have been systematically computed by Ter-Martirosyan selecting the importance of their contributions which have been determined according to powers of $(\ln s)^{-1}$.

The phenomenology of two-body reactions investigated by means of unenhanced diagrams has been performed by Ter-Martirosyan and collaborators. (18) A Gaussian model of the two particle \rightarrow several reggeon transition is allowed for a closed eikonal expression of the scattering amplitude. A more general exponential parameterization, however, though considered by Ter-Martirosyan has not yet been carried out.

The success with which Gribov's reggeon-diagram technique has been applied in the eikonal approximation to the two-body system is very impressive. The region of applicability in t of the model, however, is limited to the diffraction region. This is manifest in its failure to compare with the experimental data in the following three cases -

(1) Inelastic polarization of $\pi^- p \rightarrow \pi^0 n$

The eikonal or optical approximation which has no extra parameter than the one as already introduced by the Regge pole (without NWSZ) generates at 11 GeV/c a negative 65% spike around $t = .6$, whereas the data are compatible with vanishing polarization. This large negative spike is also characteristic for all absorption models, irrespective of whether they are weak or strong. Glebov et al. (13) include in their calculations however the $g \otimes P'$ cut and give the Pomeron pole a slope of $\alpha'_P = .6$. As a result the pomeron obtained in this way helps to improve the polarization (see also (19)) such that it does not change sign before $t \approx .4$ and agrees with the data for $t \lesssim .4$. The contribution of the $g \otimes P'$ cut however decreases rapidly with increasing energy and the model predicts for 200 GeV/c a very small polarization up to $t \approx .2$. The polarization changes sign and drops rapidly to its 90% spike at $t \approx .6$ which is in contrast to what the data at low energy lead us to expect.

(2) Elastic polarization of $\pi^+ p \rightarrow \pi^+ p$

The model fails to produce the double zero. The polarization changes sign instead and grows in magnitude with energy.

(3) Elastic and inelastic differential cross section

Both cross sections are too small in magnitude for $t \gtrsim .6$ in particular the elastic one, which has a minimum at $t \approx 1.2$ in contrast to the data, and the inelastic underestimates the dip at $t \approx 1.2$.

In addition, the growth of total cross section at Serphukov energies was not predicted by the optical model.

A correct description of total cross section for various two-body processes at Serphukov energies was achieved by Ter-Martirosyan et al. (20) with modified eikonal approximation by taking account of the formation of particle beams in the interaction region.

such shower corrections to the eikonal approximation, the so-called quasi-eikonal model* (21), could account in energy, while the "old problems" in t of πN scattering still remain.

A close analysis by Eremyan (22) of the structure of the πN scattering amplitudes demonstrated the impossibility of a correct description of both helicity amplitudes of the isovector exchange within the frame of the quasi-eikonal model. A modification of the quasi-eikonal model,** Eremyan (23) has given a successful description of the πN system in the energy range up to $|t| = 2.00 (\text{GeV}/c)^2$. The modified quasi-eikonal model introduces in particular a slow $|t|$ dependence of the shower enhancement coefficients in connection with a more complex parameterization of the P, P' and ρ

The present thesis describes a further modification of the quasi-eikonal model by giving the Gribov vertices an exponential parameterization, as has been suggested by Ter-Matirosoyan (16,18). This then corresponds to a prescription for the modified absorption cut and takes into account the effective contribution of inelastic interactions. The optical approximation treats multiple scattering as the independent re-scattering of the colliding hadrons on the target structure. We, however, show that this independence is responsible for the poor description of the phase structure of the isovector amplitude. Gribov's analysis of the Mandelstam cut implies that the diffractively dissociated hadrons are mutually correlated exchange of the reggeons. The vertices are non planar. They allow for the temporary exchange of hadrons and depend on the angle between the momenta of the reggeons exchanged by the constituents.

A Gribov vertex in the second order unenhanced diagram corresponds to the t -channel partial wave amplitude of the particle-particle-reggeon-reggeon and is the residue of the fixed pole at the first nonsense wrong signature zero. Putting the reggeons on their mass shell. There exists a super-convergent sum rule through which the vertex can be expressed as a contour-integral over the corresponding absorptive part of the off-mass-shell particle-reggeon scattering amplitude in an appropriate sub energy plane.

The first approximation of the reggeon-particle scattering amplitude by its Born term establishes the link between the quasi-eikonalized absorption model. Indeed, the fits to the pion-nucleon system produced by the first generation of the reggeon-diagram technique to two-body phenomenology are very similar to those of the eikonal model.

* QEM
** MQEM

As we see Eikonal/Absorption follows as a special case from Gribov's Reggeon diagram technique where Gribov's hypothesis is realized, when one replaces the coupling constants by two body form factors which allow for the structure of the colliding particle. This produces a cut off preventing large momenta from travelling across the diagram. In the limit eikonal and Reggeon calculus correspond to the same physical picture of colliding hadrons which scatter off each other's internal structure. This amounts formally to Glauber scattering of nuclei (24). This formalism of scattering suggests an extension of the eikonal model: here the nth order terms of a Glauber expansion of the scattering amplitude are taken between nuclei (composite hadrons) in powers of the nucleon-nucleon (quark-quark) scattering amplitude. The nucleon-nucleon (quark-quark) scattering amplitude corresponds to the Reggeon propagators. Formally in physics one could regard such an extended eikonal as the multiple scattering expansion of an optical potential of a nuclear correlation function. (25) Whereas in first order the target remains in its ground state directly adjacent to the nuclear density next to the elementary nucleon-nucleon scattering amplitude, in higher order it experiences nuclear excitations. When in higher order the target has been lifted out of its ground state after the first encounter, it establishes the connection with the final scattering in that particular higher order and allows for the nucleus to return to its ground state. The closure as the sum over all excited nuclear states is related to the many body correlation function form factor.

The correspondence between Gribov and q-number Glauber scattering has been stressed by Lovelace (26) and applied to future phenomenology. We have listed the ingredients of Gribov's multiple scattering expansion and related it to different approaches and corresponding terms from nuclei scattering.

	<u>Particles</u>		<u>Nuclei</u>
(1)	Hadron	~	Nucleus
(2)	Constituent e. g. quark, parton	~	Nucleon
(3)	Gribov vertex i. e. impact factor (27), fixed pole residue, Veneziano fixed pole residue (26), Dispersion (superconvergent) sum rule of absorptive part of Regge-particle scattering (28), in connection with Gribov-Migdal reggeon unitarity condition (29) Feynman integral over Mandelstam cross (14) Evaluated harmonic oscillator matrix elements: partition functions of two dimensional Coulomb gases (26)	~	Generalized form factor Fourier transform of integral Hadron viewed as non-resonant bound state and due to closure sum over the infinite number of states (30)
(4)	Reggeon propagator	~	Nucleon-nucleon scattering

Our phenomenological purposes are to take into account the effective contribution of the inelastic intermediate states to the wrong phase of the cut predicted by the absorption model. We therefore include the mutual orientations of the momenta of the reggeons by relating the Gribov vertex to the hadronic quark-antiquark oscillator model of Pagnamenta (30). We do this by expressing the Gribov vertex product as a correlation kernel parameter representation. The correlation parameter - the "Gribov c" - corresponds, if interpreted in the $q\bar{q}$ model, to the oscillator or fluctuation length, which gives the average separation of the quarks. We have, however, found that the phase of the cut is not suitably reproduced and produce the polarization of $\pi^-p \rightarrow \pi^0n$ the Gribov c becomes persistently a negative value which obscures the relation to the oscillator length. This implies that when Reggeon and Pomeron poles are both present the range of the cut is shrinking by comparison to the single exchanged poles. The shrinking of range is then reflected in the phase of the helicity nonflip isovector amplitude: it reverses the sense of rotation around the origin in the t - u diagram. There are, on the other hand, two essentially different models which actually produce an excellent fit to the data. One of these models assumes a pole residue zero at the crossover position. The other chooses a large residue. For both models the c has, to a greater or lesser extent, only a cosmetic effect in the sense that it forces the fit to agree but it is not responsible for the change of the phase. For those models c is positive, however, it is not determined by the oscillator length. For this reason we do not interpret c. We merely state that it is the parameter which measures the effective contribution from inelastic intermediate states. Any analogy to nuclear physics can only help in the interpretation of the Gribov vertices. It will, therefore, come as no surprise that the totally different world of nuclear physics leads to parameter values which are in contradiction to their non-relativistic counterparts.

but see IX p202

- 10 a -

PART ONE

THEORETICAL DISCUSSION

II - THE REGGEON AND POMERON CONTRIBUTION TO THE S-CHANNEL HELICITY AMPLITUDE OF THE PROCESS A + C --> B + D

When studying hadronic interactions at high energies with hadrons made up of constituents one chooses appropriate momentum frame IMF (31). In such a frame of reference the hadron moves with nearly the speed of light : effect freezes the internal motion of the constituents. We therefore decompose (28) the four momenta of the process A + C --> B + D into longitudinal and transverse components

$$p_i = p_{i\parallel} + p_{i\perp} \quad \text{where} \quad p_{i\parallel} = (E_i, 0, 0, p_{iz})$$

$$\text{and} \quad p_{i\perp} = (0, p_{ix}, p_{iy}, 0)$$

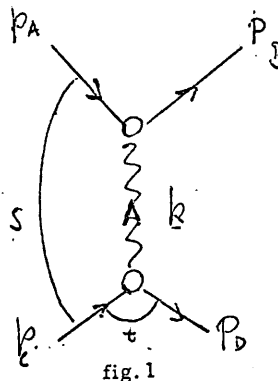
The longitudinal components are large $p_{i\parallel} \approx \frac{1}{2} \sqrt{s} \rightarrow \infty$ and the transverse components are of the order of the mass m . The total c. m. energy squared $s = (p_c + p_A)^2 \gg m^2$ with p_A and p_B the four momenta of the particles A and B. The four momentum transfer is

$$t = (p_c - p_D)^2 = q^2$$

In the IMF one has $q^2 = t = -\underline{k}^2$

with the Reggeon momenta \underline{k}

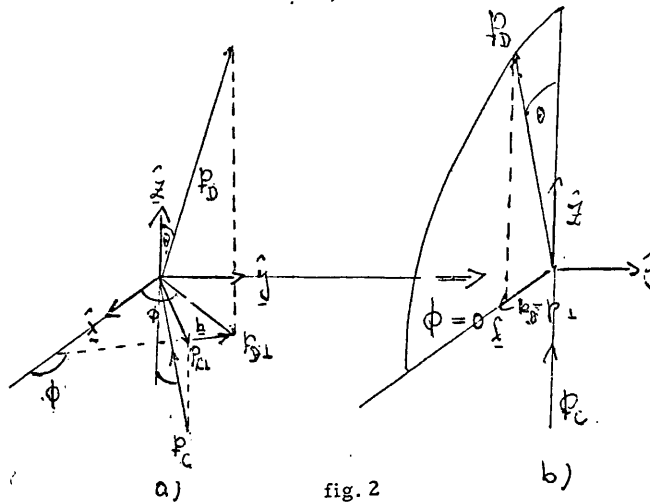
in the exchange diagram of fig. 1



is two dimensional and is given by the sum of the transverse components of the initial and final three momenta

with $\vec{p}_i = (p_{i1}, p_{i2})$ $i = A, B, C, D$

This situation is demonstrated in fig. 2



- a) Scattering of $A + C \rightarrow B + D$ in the infinite momentum frame
- b) One can always put the azimuthal angle ϕ equal to zero such that the scattering takes place in the

The relation between the relativistic invariant scattering amplitude and the centre of mass scattering amplitude

$$M(s, t) = \frac{\sqrt{u}}{p_{i2}} M_{CM}(\theta)$$

with \vec{p}_{in} and \vec{p}_{fin} the three dimensional initial and final momentum, E the total energy and Θ the angle. The differential cross section in the c. m. system reads then

$$\frac{d\sigma}{d\Omega} = \frac{1}{(2s_1+1)(2s_2+1)} \frac{p_{fin}}{p_{in}} |M(E, \Theta)|^2$$

with Ω the solid angle in the c. m. system, s_1 and s_2 are the spins of the colliding particles.

Replacing the c. m. scattering amplitude by the invariant amplitude we obtain the invariant differential cross section

$$\frac{d\sigma}{dt} = \frac{1}{p_{in} p_{fin}} \frac{d\sigma}{d\Omega} = \frac{1}{(2s_1+1)(2s_2+1)} |M(s, t)|^2$$

Our normalization factor N is consequently $N = 1$ whereupon the optical theorem

$$\sigma_{tot} = (16\pi N)^{1/2} \text{Im} M(s, t=0)$$

reads

$$\sigma_{tot} = 4\sqrt{s} \text{Im} M(s, t=0) \frac{\sqrt{mb}}{\text{GeV}/c}$$

We have used the isospin decomposition for πN scattering

$$M(\pi^\pm \rightarrow \pi^\pm) = {}^0M + {}^1M$$

$$M(\pi^+p \rightarrow \pi^+p) = \sqrt{2} {}^1M$$

with the index 0 denoting isoscalar and 1 isovector exchange.

The formalism will enable us to construct for the πN system in principal the isoscalar amplitude by

$${}^0M = P + P' + P \otimes P + P' \otimes P + P' \otimes P' \\ + P \otimes P \otimes P + P' \otimes P \otimes P \dots \text{etc}$$

and the isovector amplitude by

$${}^1M = P + P \otimes P + P \otimes P + P \otimes P \otimes P + P \otimes P \otimes P \dots \text{etc}$$

where P, P', P denote Pomeron, P' and P Regge poles respectively. \otimes symbolises the cut theory Regge-Reggecuts should in case of $\pi^+p \rightarrow \pi^+p$ be cancelled due to Finkelstein's selection rules

We denote a general isospin s-channel helicity amplitude by

$${}_{0,1} M_{\lambda_A \lambda_C \rightarrow \lambda_B \lambda_D}^{m(p)}(s, \underline{\Delta})$$

with the helicities λ_i of the external particles $i = A, B, C, D$. $\underline{\Delta}$ is the total momentum transfer $\underline{\Delta} =$

where \underline{k}_j is the jth Reggeon momentum such that for the Born term we have $\underline{\Delta} = \underline{k}$

Further we have $\underline{\Delta}^2 = \left(\sum_{j=1}^n \underline{k}_j \right)^2 = -t = |t|$

and $k_j^2 = -t_j = |t_j|$

$m(p)$ indicates the overall net helicity. It is a function of the net helicities from the contribution of the individual exchanges μ_j with $\mu = |\lambda_i - \tilde{\lambda}_i|$ with $\lambda = \lambda_A - \lambda_B$ and $\tilde{\lambda} = \lambda_C - \lambda_D$

$\mu_j = 0$ indicates that the jth Reggeon has net helicity nonflip

$\mu_j = 1$ net helicity flip

The sum overall net helicities $p = \sum_{j=1}^n \mu_j$ defines the overall net helicity in $m(p)$ such that to the net helicity nonflip total amplitude is obtained when an even number of poles change the projection of the an odd number produces a contribution to the net helicity nonflip total amplitude.

Thus $m(p = \text{even}) = 0$ and $m(p = \text{odd}) = 1$

We obtain the meson-nucleon helicity amplitude for the single scattering of the ρ pole and an arbitrary number by the Pomeron. There is growing confirmation (5) that the isoscalar amplitude is not diagonal in helicity and does not conserve helicity. It is for this reason that we allow the vacuum pole to change the projection of the nucleon.

We decompose any amplitude in a helicity nonflip and helicity flip contribution indicated by 0 and 1 respectively

$$M = M^0 + i \sigma \hat{p}_{in} \times \hat{k} \cdot M^1 = M^0 + i \sigma_y M^1$$

where

$$\sigma_y = \begin{pmatrix} 0 & -i \\ i & 0 \end{pmatrix}$$

and the polarization vector is perpendicular to the scattering plane fig. 2b and points along the \hat{y} axis.

$$\frac{\hat{p}_{in}}{|\hat{p}_{in}|} \times \frac{\hat{k}}{|\hat{k}|} = \hat{y}$$

We write down the propagator of the ρ regge pole and the Pomeron P (P'). They differ in so far as we assume a fixed pole in its residue sufficiently strong to cancel the present nonsense wrong signature zero (NWSZ) when such a fixed pole. We accomplish the reggeization of the Feynman propagator for the elementary particle exchange by the replacement:

$$\frac{1}{t - m^2} \rightarrow \frac{d\alpha}{d\alpha} \frac{\tau}{\sin \pi(\alpha - J)} \frac{1 + \tau e^{-i\pi\alpha}}{2} \left(\frac{s + \frac{1}{2}t - \frac{1}{2} \sum_{i=1}^4 m_i^2}{s_0} \right)$$

where $\alpha = J$ at the pole $t = m^2$ and τ is the signature m_i are the masses of the external particles and n exchanged particles, s is the total c.m. energy squared and s_0 the energy scale factor traditionally chosen since any other choice is equivalent to the introduction of an exponential factor into the residue. α is the

falling with t and exchange degenerate $\alpha = \alpha_0 + \alpha' t$ or otherwise $\int_4 C_3$ mass formula constraint via intercept of the trajectory such that $\alpha(0) = J - \alpha' m^2$.

The Reggeization is due to the expansion of $\sin \pi (\alpha - J)$ in a Taylor series about $t = m^2$ plus ins

signature factor $\frac{1 + \tau e^{-i\pi\alpha}}{2}$ and the energy factor $\left(\frac{s + \frac{1}{2}t - \frac{1}{2} \frac{t}{s_0} m^2}{s_0} \right)^{\alpha - J}$

Thus $\sin \pi (\alpha - J) \approx \sin \pi (\alpha - J) \Big|_{t=m^2} + \frac{d}{dt} \sin \pi (\alpha - J) \Big|_{t=m^2} (t - m^2)$

$$\approx \pi \frac{d\alpha}{dt} \Big|_{t=m^2} (t - m^2)$$

noting that the signature and $\int \alpha - J$ factor are unit at $t = m^2$ (for high energy the masses of the four p irrelevant) we see that this relation is exact at the pole $t = m^2$. The Gell Mann ghost eliminating mechanism by making the replacement

$$\frac{1}{\sin \pi \alpha} = \Gamma(\alpha) \Gamma(1 - \alpha)$$

and dividing by $\Gamma(\alpha)$ for natural parity exchange $(-1)^J = \eta$ where η is the intrinsic p

For natural parity exchange $(-1)^J = \eta$ we make the replacement $\frac{\pi}{\sin \pi \alpha} = -\Gamma(-\alpha) \Gamma(1 + \alpha)$ and divide through $\Gamma(1 + \alpha)$

In the case of ρ exchange we obtain

$$\frac{1}{t - m_\rho^2} \rightarrow -\alpha' \Gamma(1 - \alpha) \frac{1 - e^{-i\pi\alpha}}{2} \left(\frac{s}{s_0} \right)^{\alpha - 1}$$

This agrees with the Regge limit of the Veneziano formula if the couplings are constant.

The poles of the Gamma function are at 0 and negative integer values, hence there are only poles in the resonance region $\alpha = 1, 2, 3, \dots$. This resembles the propagator of the one particle exchange model. The first pole at $\alpha = 1$. In the scattering region the Gamma function can be approximated by, let us say $\Gamma(1-\alpha) \approx 1/\alpha$. For simplicity, however, we use only one.

The signature factor gives a zero at integer values of α which correspond to wrong signature points (val that $(-1)^\alpha = -1$). This means that in the resonance region poles occur on a trajectory in steps ΔJ where $(-1)^\alpha = 1$ that is to say for the ρ pole with $\tau = -1$ at 1, 3 etc. The wrong signature zero since then $(-1)^\alpha = -1$ i.e. the wrong signature $\tau = -(-1)$. These zeros are, since they occur in responsible for the dip structure of the differential cross section - a triumph for the NWSZ Regge pole.

We separate the t-dependence in the regge energy factor

$$(s/s_0)^{\alpha_p(t)-1} = (s/s_0)^{\alpha_p(\omega)-1} e^{-\alpha'_p \ln(s/s_0) |t|}$$

since we are in the scattering region we have $t = -|t|$ always.

The Gamma function we parameterize for convenience just by one exponential (there are no poles nor zeros i

$$\Gamma(1-\alpha C(t)) = A_p e^{-B_p |t|}$$

We split, for calculational reasons (performing the cut) the negative signature factor $\sum_{\tau=-1}^{\omega} C(t) = 1 - e^{-\dots}$
 Thus we write the propagator as

$$G_p^{\tau=-1}(s, |t|) = (s/s_0)^{\alpha_p(\omega)-1} \sum_{i=1}^2 \chi_i(\omega) e^{-B_i |t|}$$

where $\chi_2(\omega) = \alpha'_p A_p / 2$ $\chi_1(\omega) = -\frac{\chi_2(\omega)}{2} e^{-i\pi \alpha_p(\omega)}$

with the Regge interaction region of the nonrotating part -

$$B_1 = B_P + \alpha'_P \ln(s/s_0)$$

and the Regge interaction region of the rotating part

$$B_2 = B_P + \alpha'_P (\ln(s/s_0) - i\pi)$$

When we just consider the pole alone then it is more convenient to use the half angle form of the signature and write then for the propagator -

$$G_P^{\tau-1}(s, H) = i \alpha'_P (s/s_0)^{\alpha'_P(\omega)-1} A_P \sin \frac{\pi}{2} (\alpha'_P(\omega) - \alpha'(H)) e^{-i\pi \alpha'_P(\omega)} e^{-B_P + \alpha'_P (\ln(s/s_0) - i\pi)}$$

We replace the coupling constant (Veneziano limit) with form factors and write for the exponentially parameterized Regge residue i. e. for Particle-Regge-Particle vertex where α indicates the Regge term

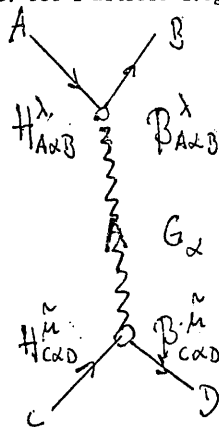


fig. 3

$$\longrightarrow H_{AxB}^{\lambda} B_{AxB}^{\lambda} G_{\alpha} H_{CxD}^{\mu} B_{CxD}^{\mu}$$

$$B^{\mu}(t) = B_{CxD}^{\mu}(\omega) B_{AxB}^{\lambda}(\omega) e^{-\frac{1}{2} (R_{CxD}^2 + R_{AxB}^2) |t|}$$

The once fitted values of the residues are expected to be not too far away from the values of the coupling constant extrapolated to the resonance region $t = m^2$

Conservation of angular momentum and parity requires the introduction of the factors $H^{\tilde{\lambda}} H^{\lambda}$

$$H^{\tilde{\lambda}} H^{\lambda} = \left(\frac{|k|}{2m_p} \right)^{(|\lambda|+|\tilde{\lambda}|)} e^{i\phi(|\lambda|-\tilde{\lambda})}$$

with m_p the nucleon mass introduced for dimensional reasons. ϕ is measured against the \hat{x} axis the phase angle of the Reggeon momentum \underline{k} . It is measured in addition to the conventional Regge phase which is \hat{z} axis. The phase had to be introduced since the scattering plane $\underline{p}_0, \underline{k}$ is not fixed due to the integration convolution.

We express the full ρ -Regge pole amplitude by

$$M_{\rho}^{\mu}(s, k) = \left(\frac{|k|}{2m_p} \right)^{\mu} e^{i\mu\phi} \sum_{\lambda=1,2} \beta_{\rho}^{\mu}(s) e^{-\gamma_{\rho}^{\mu} k^2}$$

with $\beta_{\rho_1}^{\mu}(s) = \beta_{\rho_1}^{\mu}(s/s_0)^{\alpha_{\rho}^{\mu}(s)-1}$ since $\beta_{\rho_1}^{\mu}(s) = \beta_{\rho_1 \rho_2}^{\mu}(s) \beta_{\rho_2}^{\mu}(s) \sum_1^{\rho}(s) = \beta_{\rho_2}^{\mu}(s)$

$$\beta_{\rho_2}^{\mu}(s) = \beta_{\rho_1}^{\mu}(s) \sum_2^{\rho}(s) = -\beta_{\rho_1}^{\mu} e^{-i\pi\alpha_{\rho}^{\mu}(s)}$$

$$\gamma_{\rho_1}^{\mu}(s) = R_{\rho}^{\mu} + B_{\rho} + \alpha' \ln(s/s_0) \quad \text{since} \quad R_{\rho}^{\mu} = \frac{1}{2} (R_{\rho_1 \rho_2}^{\mu} + R_{\rho_2 \rho_1}^{\mu})$$

$$\gamma_{\rho_2}^{\mu}(s) = \gamma_{\rho_1}^{\mu}(s) - i\pi\alpha'_{\rho}$$

For the Pomeron propagator on the other hand we write -

$$G_P(s, k) = \frac{1 + \rho^{-i\pi\alpha_P(k)}}{\sin\pi\alpha_P(k)} (s/s_0)^{\alpha_P(k)-1}$$

and since

$$\frac{1 + \rho^{-i\pi\alpha(k)}}{\sin\pi\alpha(k)} = i\tau \frac{\rho^{\frac{i\pi}{2}(\frac{\tau+1}{2} - \alpha(k))}}{\cos\frac{\pi}{2}(\frac{\tau+1}{2} - \alpha(k))}$$

we obtain for the propagator $\tau=1$

$$G_P(s, k) = i \rho^{\frac{i\pi}{2}(1 - \alpha_P(s)) - \alpha'_P(\ln(s/s_0) - i\pi/2)k^2} \frac{1}{\cos\left\{\frac{\pi}{2}(1 - \alpha_P(s)) + \frac{\pi\alpha'_P}{2}k^2\right\}}$$

and the full expression for the Pomeron pole amplitude reads now (with the slow varying $\cos\left(\frac{(1 - \alpha_P(s))\pi}{2} + \frac{\pi\alpha'_P}{2}k^2\right)$ into the residue)

$$M_P^u(s, k) = i(-1)^M \left(\frac{|k|}{2m_p}\right)^M \rho^{iM\phi} \beta_P^M(s) \rho^{\frac{i\pi}{2}(1 - \alpha_P(s)) - \gamma_P^M(s)}$$

with $\beta_P^M(s) = \beta_P^M(s_0) (s/s_0)^{\alpha_P(s)-1}$

and $\gamma_P^M(s) = R_P^{2M} + \alpha'_P(\ln(s/s_0) - i\pi/2)$ where $R_P^{2M} = \frac{1}{2} C$

III - GRIBOV'S REGGEON DIAGRAM TECHNIQUE

III.1 - Gribov's evaluation of the Mandelstam diagram - the basis of the Reggeon diagram technique (14)

In Gribov's determination of the asymptotic form of Mandelstam's diagram the use of Sudakov variables has proven in order to separate between negligible and important invariants, e. g. in separating the effect for large energy and from the transverse momentum space. This is mainly achieved by decomposing the internal momentum into a vector plane of large vectors and into a vector perpendicular to this plane. Equally one can achieve the same by working in the momentum frame, this is because the hadrons are decaying while they are moving with high velocity and the Gribov the probability amplitudes for decay and recombination which are in the Glauber picture analogous to the wave function in the momentum frame.

In order to succeed in picking out the essential regions of integration, Gribov applied the Sudakov variables to the left and right cross of the Mandelstam diagram. For large s , the two body amplitudes comparable with the Glauber scattering amplitude will be large but will fall off considerably fast when t is beyond the exchanged square mass. The Regge feature; therefore Gribov factorised the two body amplitude. These restrictions put heavy constraints on integration. Further avoiding that the asymptotic contribution of the Mandelstam cut disappears, one has to restrict 0 and l so the Sudakov contours cannot be distorted to infinity because they are pinched between the singularities on either side of the contour. One can work this out by representing the propagator of the left or right hand cross by

In applying the Mellin transforms to the Green's function of the Regge poles, one obtains a partial wave decomposition function à la Sommerfeld-Watson, whereas the partial wave amplitude is expressed as the Mellin pole. Now one obtains for the asymptotic behaviour of the Mandelstam cut built up from two Gribov vertices and two Mellin poles. The G incorporate our ignorance of decay and recombination of hadrons.

Let us now look closely at how the dominant region of integration is picked out. The main result will be that the final Mandelstam cut will be a two dimensional integral of the Regge poles over a plane perpendicular to the incident momentum supported by our intuition, namely by imagining two interacting hadrons at high energy as two flat absorbing discs, a two-dimensional transverse world. We consider the two Gribov vertices which represent the left and the right hand themselves are complicated Feynman diagrams. We already mentioned the condition for the internal propagators to be infinitely away from their mass shell. So one obtains an integral over α^* and over the four dimensional momentum

* see next page

1 stands for the left and 2 for the right hand cross $i = 1$ (left)
 $i = 2$ (right)

This 4-dimensional momentum is decomposed into α_1 and α_2 and into the two -dimensional transverse momenta $k_{1\perp}$ and $k_{2\perp}$. α_1 and α_2 are the Sudakov variables when the momenta are expressed by

$$k_i = \alpha_i P_1 + \beta_i P_2 + k_{i\perp}$$

The propagator expressed in these variables gives the mass conditions namely the 4 masses depend only on

$$\alpha_1, \beta_1, k_{1\perp}, q_{1\perp}, k_{1\perp}, \alpha_2$$

These are the same variables on which the integrand over α_1, β_1 and $k_{1\perp}$ depends, thus making a further integration over α_2, β_2 and $k_{2\perp}$ is left with a function which depends only on q and k . Since the left and the right hand cross are symmetrical in the exchange of the incoming momenta P_1 and P_2 , these conclusions also apply to the right hand cross, so that one is actually left with a two-dimensional integral over $\alpha^2 k_{1\perp}$ as already mentioned above. How can we now understand that the exchange is analogous to the production and decay of a non-relativistic quasi particle moving in a two dimensional world of imaginary time dimension, namely rapidity, from a source provided by the annihilation of 2 incoming hadrons to the sink again by the annihilation of 2 outgoing hadrons?

One can find the single partial wave explicitly by applying the Mellin transformation to the absorptive part of the Green's function. This absorptive part is just the imaginary part of this amplitude which is finally found by evaluating the amplitude over the cut which gives the discontinuity. By applying the Mellin transform to the absorptive part of the diagram in the energy plane to the complex angular momentum plane, therefore the power behaviour of the absorptive part in the energy plane is the behaviour of the complex angular momentum. Since the Regge poles are Mellin poles one can now express the pole part of the amplitude by the two Regge trajectories. Thus the partial wave amplitude is obtained as an integral over the two dimensional momentum and the ℓ_1 contour which is pinched between the two Mellin poles, hence the integral does not disappear as one cannot distort the contour towards infinity. The form found for the partial wave amplitude can now be expressed in terms of functions conserving angular momentum and "energy" namely the angular momentum and energy of the produced and decaying relativistic particles. So Gribov showed that the discontinuity across the Mandelstam cut looks very similar to the discontinuity of two quasi particles with conserved momentum and "energy" in its intermediate states and on its mass shell. In the Reggeon picture with a non-relativistic quasi particle one can talk about its "mass" which is inverse twice its slope and also about its velocity and further on the Green's function for it either in energy or transfer momentum or in its conjugate variables rapidity and parameter and rapidity ("time"). This gives us almost a picture for Reggeons which diffuse along in space and time.

We have to notice that only pairs of hadrons serve as a source and as a sink of produced and absorbed quasi particles. In other words, say the two Gribov vertices give the production and absorption probability. The Reggeon propagators represent the exchange of particles, the integration is over the first angular momentum and the transverse momentum and energy and momentum are conserved. We can further say that the Gribov vertices do not depend on energy if we are in the high energy limit. The essential singularities appear in Sudakov variables which are of the order of inverse s so that the integral works. The vertex function is inversely proportional to s . Further the vertices are real because of the space like Reggeon exchange. Alternatively to the Gribov perturbation approach to the Mandelstam diagram, White⁽³³⁾ derived the genuine rigorous footing: He started from t-channel unitarity and projected out the partial wave of the 4 particle integral to the complex j plane by a helicity contour integral. The contour got pinched in the helicity plane between the Regge poles and "nonsense wrong signature inverse square root branch points" of the product of the scattering amplitudes which led to the t-channel integral which in turn generates a cut at the moment it hits the end point of the integral. However, this analysis was complicated because one has to treat the signature involved very carefully. The main conclusion of White's analysis was that this cut has a negative sign, which was always intuitively felt from the phenomenological point of view.

A brief outline of Gribov's method (14)

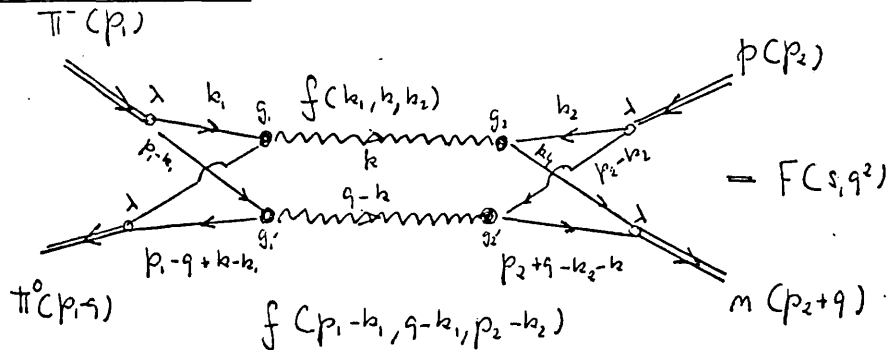


fig. 4 The Mandelstam diagram

equal mass, spinless, $d = q^2 = (p_1 - p_2)^2$ small and fixed

Gribov found asymptotic value for $s \rightarrow \infty$ by applying Sudakov variables to loop momenta:

decompose inner momenta in plane of light like fourvector and space like two vector perpendicular to this plane:

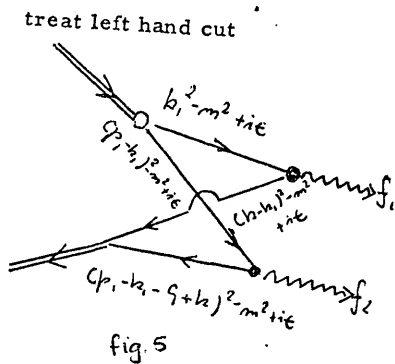
$$k_i = \alpha_i p_2' + \beta_i p_1' + k_{i\perp}$$

$$p_1' = p_1 - \frac{m^2}{s} p_2$$

$$p_2' = p_2 - \frac{m^2}{s} p_1$$

volume of integration:

$$d^4k = \frac{1}{2} |s| d\alpha d\beta d^2k_{\perp}$$



put close to mass shell

$$d_1 = \alpha_1 \beta_1 s + k_{1\perp}^2 - m^2 + i\epsilon$$

$$d_2 = (\beta_1 - 1) (\alpha_1 - \frac{m^2}{s}) s + k_{1\perp}^2 - m^2 + i\epsilon$$

$$d_3 = (\alpha_1 - \alpha) (\beta_1 - \beta) s + (k_{1\perp} - k_{\perp})^2 - m^2 + i\epsilon$$

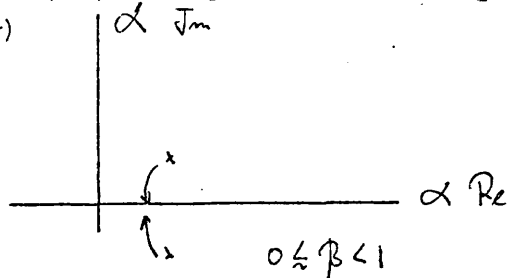
$$d_4 = -(\alpha_1 - \alpha) s - (\beta_1 - \beta) m^2$$

$$+ (\alpha_1 - \alpha) (\beta_1 - \beta) s +$$

$$+ (k_{1\perp} - k_{\perp} + q_{\perp})^2 - q_{\perp}^2 (1 - \beta_1 + \beta)$$

with similar expression for the right hand cut.

After integration over α_1 the integrand still has singularities in α on both sides of $\text{Re } \alpha$ due to the intersection from the third order $(s-u)$ double spectral function i. e. $(\alpha - 1)$ and $(\alpha_1 - \alpha)$ consequently the integration contour (Pinch singularity)



The assumptions made are -

(1) f_i large when energy large: $\rightarrow f_i \sim O(s)$

$$S_1 = (k_1 + k_2)^2 \sim 2k_1 k_2$$

$$S_2 = (p_1 + p_2 - k_1 - k_2)^2 \sim 2(p_1 - k_1)(p_2 - k_2)$$

(2) Momentum transfer $k^2, (q - k)^2$
 and masses $k_1^2, k_2^2, (k_1 - k)^2, (k_2 + k)^2, \dots \} O(1)$

If these variables become of order $s \rightarrow$ amplitude decreases sharply and region is unimportant.

Regions of interest:

$$k_{\perp}^2 \sim k_{i\perp}^2 \sim m^2$$

$$\alpha_1 \sim \beta_2 \sim m^2/s$$

$$\beta \ll \beta_1 \sim 1$$

$$\alpha \ll \alpha_1 \sim \alpha_2 \sim 1$$



From there it follows

$$S_1 \sim \beta_1 \alpha_2 s$$

$$S_2 \sim (1 - \beta_1)(1 - \alpha_2) s$$

$$k^2 = \alpha \beta s + k_{\perp}^2 \sim k_{\perp}^2$$

Factorization of Regge amplitude $s \rightarrow \infty$

$$f_1 = g_1(k_1^2, (k-k_1)^2, k^2) g_2(k_1^2, (k+k_2)^2, k^2) G(k_1^2, 2k, k_2)$$

$$f_2 = g_1'(p_1, -k_1)^2, (k_1 - k_1 - q + k)^2, (q - k)^2) g_2'(p_2 - k_2)^2, (p_2 - k_2 + q - k)^2, (q - k)^2) G'(q)$$

Sommerfeld-Watson G's: (Green's function)

$$G = - \int \frac{dl_1}{k_i} \oint_{\mathcal{L}_1} G_{l_1}(k^2) (\alpha_2 \beta_1 s)^{l_1}$$

$$G' = - \int \frac{dl_2}{k_i} \oint_{\mathcal{L}_2} G_{l_2}'((q-k)^2) ((1-\alpha_2)(1-\beta_1)s)^{l_2}$$

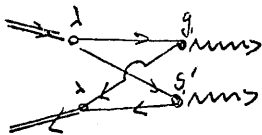
where $\oint_{\mathcal{L}_i}$ are the signature factors.

Insert the G's into the Feynman integral and use $k^2 = \alpha\beta s + k_{\perp}^2 \sim k_{\perp}^2$, $(q-k)^2 \sim (q_{\perp} - k_{\perp})^2$

The result of all integrations :

$$F(s, q^2) = \frac{i\pi}{2(4\pi)} \int_{c_1}^{\infty} \frac{dl_1}{2i\pi} \int_{c_2}^{\infty} \frac{dl_2}{2i\pi} \int \frac{d^2 k_{\perp}}{(2\pi)^2} N_{l_1, l_2}^2(q_1, k_{\perp}) G_{l_1}(k_{\perp}^2) G_{l_2}(q_1 - k_{\perp})^2$$

signature $\int_{l_i}^{\infty} = - \frac{1 + \pi l_i}{2i\pi l_i} e^{-i\pi l_i}$, $G_{l_i}(q^2) = \frac{1}{l_i - \alpha_i(q^2)}$ Mellin pole



$= N_{l_1, l_2}(q_1, k_{\perp}) =$ Reggeon production amplitude = Gribov vertex

$$= \frac{1}{4(4\pi)^2} \int \frac{d^2 k_{\perp} d\beta_1 d\alpha_1 d\alpha_2}{(2\pi)^4} s^{\alpha} \chi^2 g_1 g_2 \beta_1^{l_1} (1-\beta_1)^{l_2} \{ (k_{\perp}^2 - m^2) (q_1 - k_{\perp})^2 - m^2 \} (k_{\perp} - k)^2 - m^2 (q_1 - k)^2 - m^2$$

$$\text{Im} F(s, q^2) = \frac{\sqrt{s}}{2} \int \frac{dl_1}{2i\pi} \int \frac{dl_2}{2i\pi} \gamma_{l_1} \gamma_{l_2} \int \frac{d^2 k}{(2\pi)^2} N_{l_1 l_2}^2 (k, q) G_{l_1}(k, q^2) G_{l_2}(q-k, q^2) s^{l_1}$$

with $\text{Re} \frac{d}{dz} \gamma_{l_2} = \gamma_{l_2}$

t-channel partial wave amplitude
$$f_j(q^2) = \frac{2}{\pi} \int_{s_0}^{\infty} ds' (s')^{-j-1} \text{Im} F(s', q^2)$$

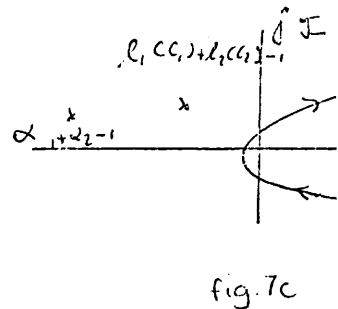
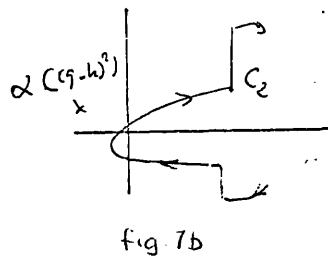
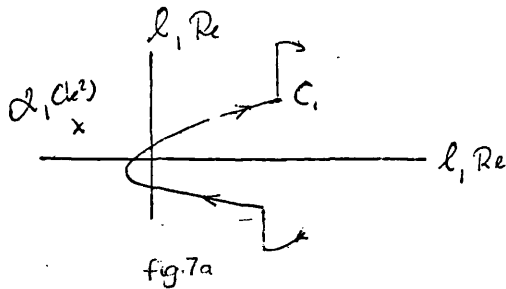
partial wave amplitude = Mellin projection x Absorptive part of the scattering amplitude

↷

$$f_j(q^2) = \int_{C_1} \frac{dl_1}{2i\pi} \int_{C_2} \frac{dl_2}{2i\pi} \int \frac{d^2 k}{(2\pi)^2} \frac{G_{l_1}(k, q^2) G_{l_2}(q-k, q^2)}{j+1-l_1-l_2} N_{l_1 l_2}^2$$

The partial wave amplitude is well defined and analytic in the region to the right of its singularities

\Rightarrow l_1, l_2 integrations run to the right of the singularities of G_{l_1}, G_{l_2} and f_j is anal
the right of $l_1 (C_1) + l_2 (C_2) - 1$

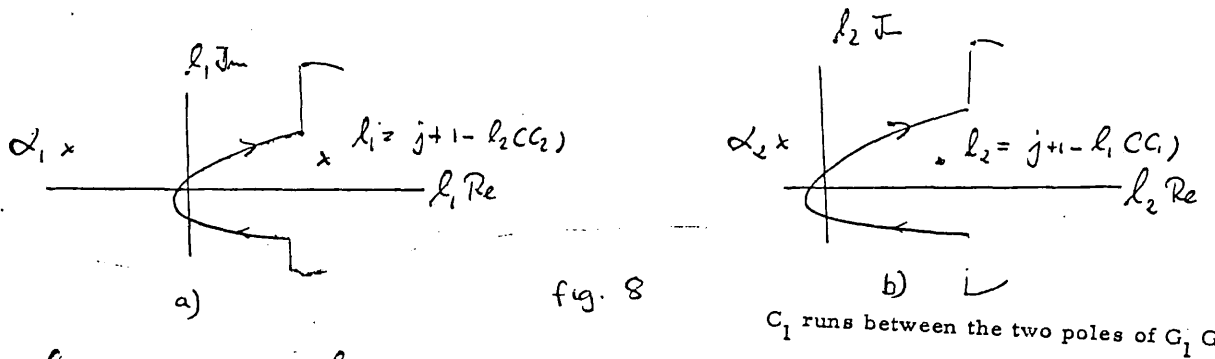


integration over l_2 and evaluated pole at $l_2 = j+1 - l_1$

$\text{Re } j > \text{Re } (l_1 C_1) + l_2 C_2 - 1 \Rightarrow$ domain of validity $j+1 - l_1 C_1 > l_2 C_2$

fixed j ;

\Rightarrow pole in l_2 i. $l_2 = j+1 - l_1 C_1$ lies to the right of C_2
similarly for l_1

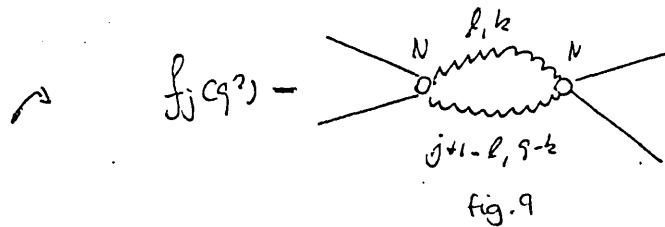


now deform C₂ around the pole in l₂

$$\rightarrow f_j(q^2) = \int_{C_1} \frac{\alpha l_1}{2i\pi} \int \frac{\alpha^2 k_1}{(\alpha\tau)^2} G_{l_1}(k_1^2) G_{j+l-l_1}((q-k_1)^2) N_{l_1, j+1-l}^2 dl_1$$

the singularity from G is at $l_1 = \alpha_1 (k_1^2) < l_1(C_1)$

the singularity from G' is at $j+1-l_1 = \alpha_2 (C(q-k_1)^2)$



Momentum conservation: $q = k_1 + k_2$ in the vertices

Energy: $j+1$

Energy conservation: $j-1 = l_1-1 + l_2-1$

On the other hand evaluating the pole contribution of G, G' $\rightarrow f_j(q^2) = \int \frac{\alpha^2 k}{(\alpha\tau)^2} \frac{\int \alpha_1 N_{\alpha_1}^2}{j+1-\alpha_1 C}$

III. 11-THE REGGE PARTICLE SCATTERING AMPLITUDE

Gribov's theory indeed concentrates the unknown into one function - its Gribov vertex N . The Regge-particle amplitude \tilde{N} factorizes due to the factorization property of the Regge residues.

Thus, let us consider the nucleon vertex $\alpha_p \alpha_p \rightarrow \bar{p} n$ of

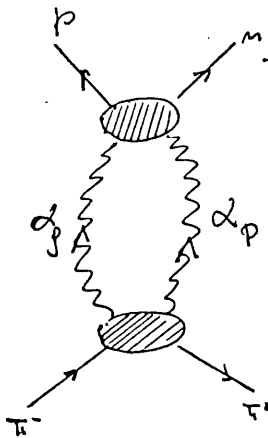


fig.10
Gribov two-Reggeon cut

The three momenta \vec{p} , \vec{p} and \vec{p}_n define the scattering in the \hat{x}, \hat{z} plane in fig.11

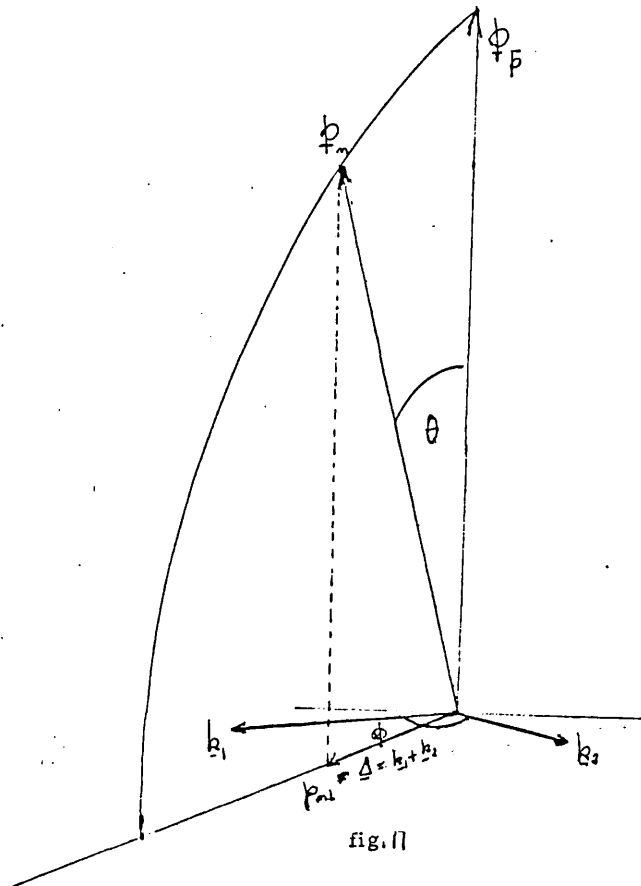


Fig. 11 demonstrates that the Regge particle amplitude in fig. 12

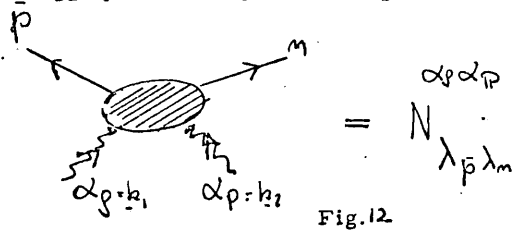


Fig. 12

is a function of the angle ϕ between the two dimensional Reggeon momenta.

The Regge-particle scattering amplitude has the same analytic properties in the subenergy plane as the ordinary amplitude. (29) That is to say it has poles and cuts due to the presence of physical intermediate states. the third order double spectral function is symbolized by the Mandelstam cross -

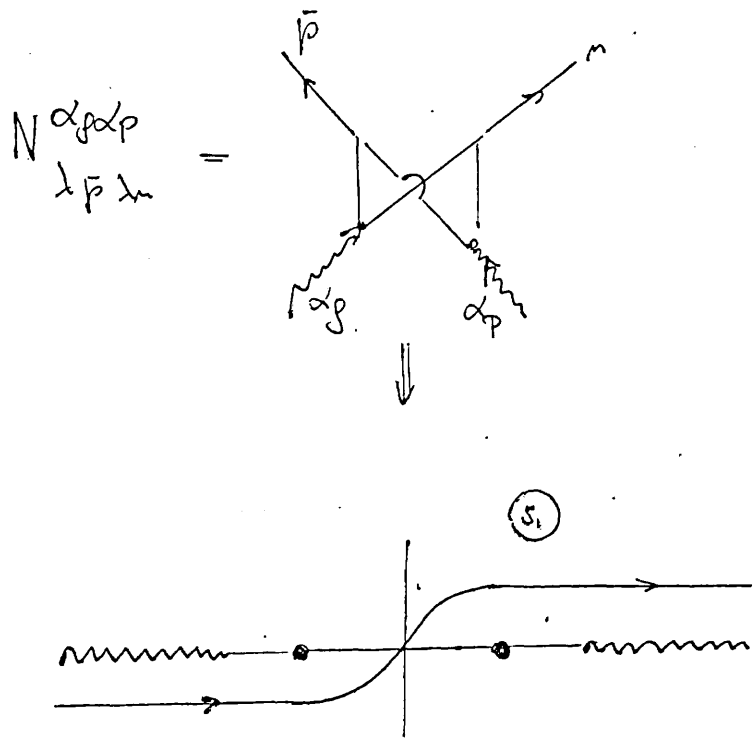


fig.13

singularities in the sub-energy plane due to third order double spectral function $s - u$

$$N_{\bar{p}\mu}^{(2)} \alpha p d p_i \sim \int_{-b}^b \text{disc}_{s_1} \tilde{N}_{\bar{p}\mu}^{(2)} \alpha p d p_i \alpha s_1$$

The convergence for large internal masses $s_1 = k_1^2$ is rapid enough that one can rotate the contour and one can neglect the contributions from integrands over large semi-circles, hence -

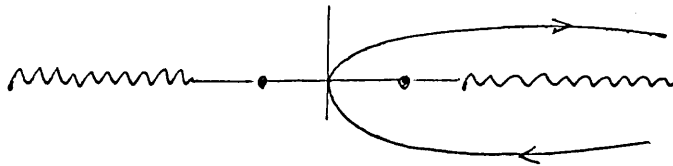


fig. 14

$$N_{\bar{p}\mu}^{(2)} \alpha p d p_i \sim \int_{km^2}^b \text{disc}_{s_1} \tilde{N}_{\bar{p}\mu}^{(2)} \alpha p d p_i \alpha s_1$$

Now let us consider the AFS cut

$$N_{AFS} = \int_{-b}^b \text{disc}_{s_1} \tilde{N}_{AFS} \alpha s_1$$

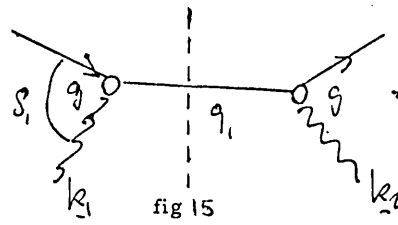
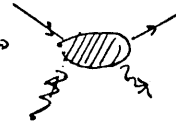


fig 15

The dashed line denotes that the discontinuity is taken through the pole (elastic intermediate state) of the propagator. AFS unitarity integral then leads to a spurious cut with positive sign -

$q_1^2 = s_1 > m_1^2$ is the total sub energy squared flowing through the blob 

\tilde{N} falls off more rapidly than $1/s_1$ when $s_1 \rightarrow \infty$

$$\tilde{N}(s_1) = \beta(s_1, k_1^2) \frac{1}{q_1^2 - m^2 + i\epsilon} \beta(s_1, k_2^2)$$

The Regge residues possess poles and branch points in the sub energy plane s_1 . The vertices depend on their s_1 when s_1 increases. The vertices are cut analytic, i. e. they only have a right hand cut. Thus, drawing the sub-energy plane $S_1 = q_1^2$ we see that at fixed t

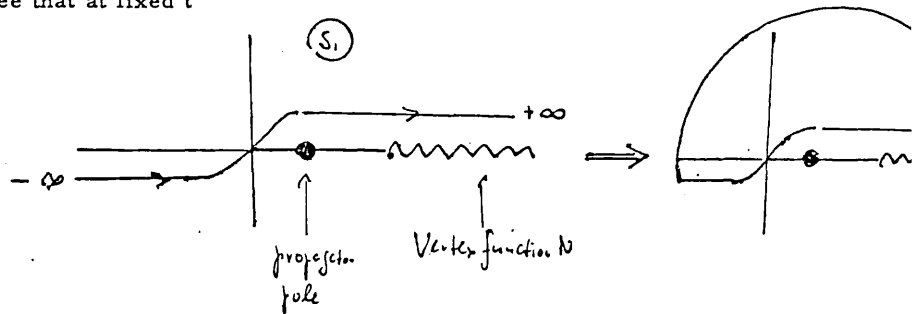
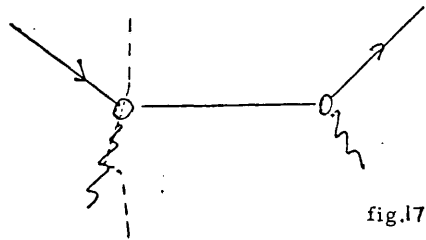


fig. 16.

$$\rightarrow N = \int_{-\infty}^{+\infty} \frac{\text{disc}_{s_1} \tilde{N}}{q_1^2 - m^2 + i\epsilon} dq_1 = 0 = \text{pole} + \int_{4m^2}^{\infty} \text{cut}$$

Which demonstrates that the cut singularity (if integrated up to $+\infty$) exactly cancels the pole from the propagator. see this even more clearly by wrapping the contour individually around pole and cut. This example emphasizes the nature of Gribov's theory in comparison to ϕ^3 : The AFS model is sufficiently convergent so as to rotate in the sub energy plane. However, the integrand does not fall off rapidly enough, i. e. it is still sizeable for q_1^2 or even $s_1 = s$. Thus values $q_1^2 \sim \mu^2$ do not give the dominant contribution. This in turn demonstrates why

produce a genuine cut. AFS performs all unitarity integrals represented by fig.16 by taking the discontinuity through the pole of the propagator. The discontinuity across the cut exactly cancels is in fact the discontinuity which cuts through the vertex function due to which this cancellation occurs.



Since a reggeon can be represented by a multiperipheral ladder, it needs a large number of rungs to cut through cancel the positive contribution obtained by AFS. Then, however, the threshold of the discontinuity is large, where n' is the number of ladders. Such a large mass is possible for AFS but not for Gribov. In Gribov's the assumption is the sufficiently rapid fall off in the virtual masses such as s_1 . This rapid fall off dampens the of the cuts with a high number of rungs cut through.

An underlying field theory with convergence properties such as the ones assumed by Gribov - the damping of v and momentum transfers when they exceed a particle mass m^2 - has not yet been found. But it is assumed the gauge theories could provide such a theory. (15)

III. 111 - GRIBOV RULES FOR THE "RALEIGH-SCHRÖDINGER" PERTURBATION THEORY

Gribov's analysis of the asymptotic behaviour of Feynman diagrams produced a two dimensional field theory. The fluctuations described by this field take place in impact parameter space and a variable (rapidity) which formally corresponds to time and which is conjugate to a quantity which formally corresponds to the energy.

The Laplace-Mellin transform plays in this a central role (15).

$$\phi(j, k^2) = \int_0^\infty d\alpha \log s \, e^{-\log s (j-1)} \text{Im } M(s, k^2)$$

$$J-M(s, k^2) = \int_{C \uparrow} \frac{d\alpha}{2i\pi} e^{(j-1) \log s} \phi(j, k^2)$$

Gribov's interpretation of fig. 18

the one Reggeon exchange graphs -

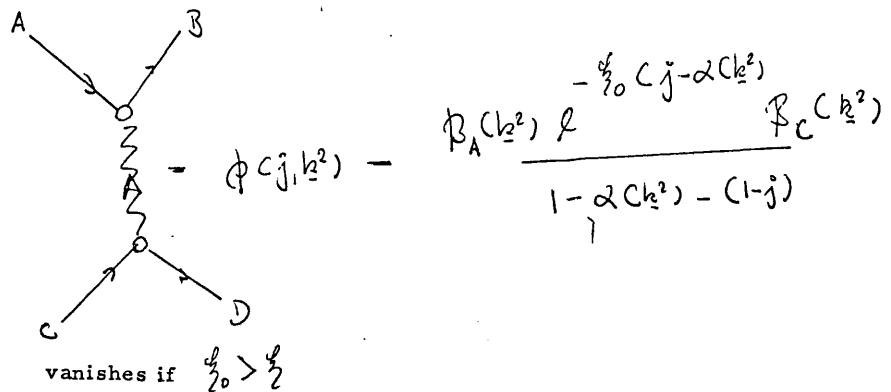


fig. 18

A source C of energy $1 - j$ and nonrelativistic momentum \underline{k} creates a quasi particle, a Reggeon of momentum \underline{k} energy $1 - \alpha(\underline{k}^2)$. It will be annihilated at the sink A where it transfers its momentum.

Note

$$1 - \alpha(\underline{k}^2) - (1 - j) = j - \alpha(\underline{k}^2)$$

$$\frac{\mathcal{E}}{\mathcal{E}_0} < \frac{\mathcal{E}}{\mathcal{E}_0} \quad \frac{\mathcal{E}}{\mathcal{E}_0} = \ln s$$

minimum

Gribov rules for the one-reggeon exchange graph -

- (1) The creation vertex (CD in our diagram) is given by $\beta_{CD}(\underline{k}^2) e^{-\frac{\mathcal{E}}{\mathcal{E}_0} (j - \alpha(\underline{k}^2))}$
- (2) Annihilation vertex (AB) - $\beta_{AB}(\underline{k}^2)$
- (3) Into the propagator enters the difference between the energy of the source C and the energy of the Reggeon

$$\frac{1}{1 - \alpha(\underline{k}^2) - (1 - j)}$$

↑ Energy of Reggeon ↑ Energy of source

$$= \frac{1}{j - 1 - \alpha'(\underline{k}^2) + (1 - \alpha(0))} \quad \text{for linear trajectory}$$

$$= \frac{1}{E - \frac{\underline{k}^2}{2m} + (1 - \alpha(0))} \quad \begin{array}{l} \text{Non-relativistic} \\ \text{quasi particle} \\ \text{Energy gap: } 1 - \alpha(0) \end{array}$$

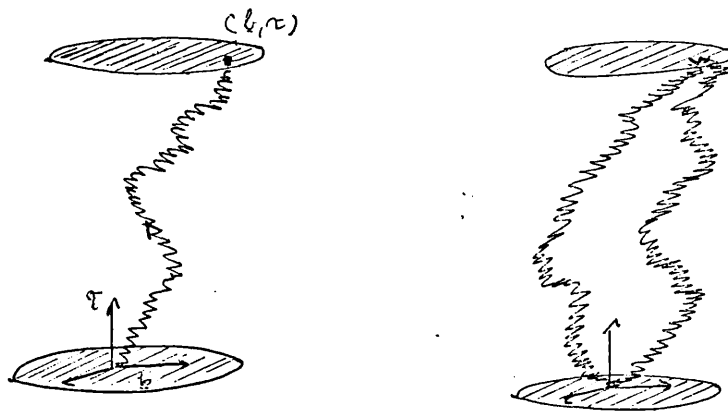
E is the conjugate variable to $\tau = i \log s$ i. e. rapidity in "time". The mass is $\frac{1}{2}\alpha' = m$ and the velocity in $(\underline{b}, \underline{x})$ space

$$\mu = \frac{q \ell \underline{b}}{c \ell \tau} = (4\alpha' C E - 1 + \alpha(\omega))^{1/2}$$

The Green's function for the diffusion of a Reggeon, see Abarbanel (34)

$$G(\underline{b}, \tau) = \frac{\Theta(\tau) \ell^{-\tau(1-\alpha(\omega))}}{4\pi\alpha'\tau} \ell^{-\underline{b}^2/4\alpha'\tau}$$

and is shown in fig. 19



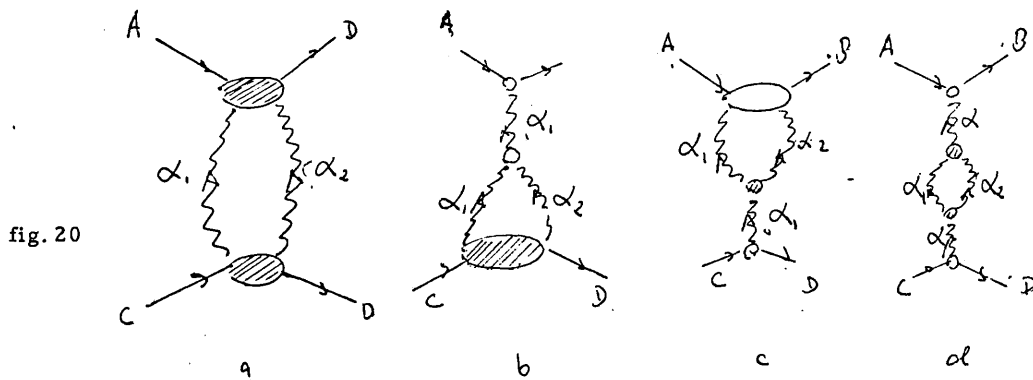
a) Space-time picture of a Reggeon (34)

b) for Mandelstam cut

The damping factor $e^{-\tau(1-\alpha(s))}$ in the Green's function implies that for $\tau \rightarrow \infty$ only Reggeons with $(1-\alpha(s)) \rightarrow 0$ Pomeron survive in the case of diffractive scattering. At attainable energies, however simple picture does not hold as there are many complicated interactions involved.

Gribov rules for the two-Reggeon exchange graphs

(e.g. The leading cut contribution to $\bar{u}p \rightarrow \bar{u}p$)




1) The vertex for the production of a pair of Reggeons with momenta k_1, k_2 during the scattering of a pion is given

$$\text{Vertex} = f_{\alpha_1, \alpha_2} e^{-\frac{q}{2} (j+1 - \alpha_1 - \alpha_2)} N C(k_{21}, k_{22})$$


with the product of the signature - $\text{Im sign } \alpha_1 \text{ sign } \alpha_2$.

2) The annihilation vertex




$$= N C(k_1, k_2)$$

3) A Reggeon decay amplitude



$$= \gamma_{\alpha_1, \alpha_2} l^{-\frac{1}{2} (j+1 - \alpha_1 - \alpha_2)} r_{\alpha}^{\alpha_1, \alpha_2} C(k_1, k_2)$$

4) Annihilation amplitude of two Reggeons into one



$$= r_{\alpha}^{\alpha_1, \alpha_2} C(k_1, k_2) l^{-\frac{1}{2} (j - \alpha)}$$

5) One Reggeon propagator

$$\frac{1}{j - \alpha(k^2)}$$

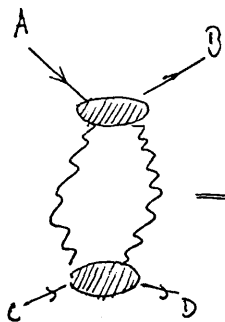
6) Two Reggeon propagator

$$\frac{1}{\underbrace{1 - \alpha_1}_{\text{Energy of 1st reggeon}} + \underbrace{1 - \alpha_2}_{\text{Energy of 2nd reggeon}} - \underbrace{(1-j)}_{\text{Initial energy}}}$$

7) Momentum transfer integration

$$= \frac{1}{j + 1 - \alpha_1 - \alpha_2}$$

Partial wave of the unenhanced Reggeon cut and absorptive part



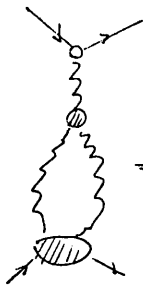
$$\Rightarrow \int \frac{d^2 k_1}{\pi} \frac{\Gamma_{\alpha_1, \alpha_2} N_{C_j}(k_1, k_2) N_{A_j}(k_1, k_2) e^{-\frac{c_j}{2} (j+1-\alpha_1-\alpha_2)}}{j+1-\alpha_1-\alpha_2} = \phi C_j$$

Laplace-Mellin transform:

$$\begin{aligned} \text{Im} M(\frac{c_j}{2}, \Delta) &= \int_{C_j} \frac{d^j}{d^2 s_i} e^{(j-1)\frac{c_j}{2}} \phi C_j(\Delta) \\ &= \int \frac{d^2 k_1}{\pi} \Gamma_{\alpha_1, \alpha_2} N_{C_j}(k_1, k_2) N_{D_j}(k_1, k_2) e^{\frac{c_j}{2} (\alpha_1 + \alpha_2 - 2)} \end{aligned}$$

where the N's are taken at $j = \alpha_1 + \alpha_2 - 1$

Semi enhanced cut



$$\Rightarrow \int \frac{d^4 k_1}{\alpha} \frac{\beta_A(k_2) \ell^{-\frac{d}{2}(j-\alpha)} \gamma_{\alpha}^{\alpha_1, \alpha_2}(k_1, k_2) \ell^{\alpha_2} \ell^{-\frac{d}{2}(j+1-\alpha_1-\alpha_2)} N(k_{11}, k_{21})}{(j-\alpha)(j+1-\alpha_1-\alpha_2)}$$

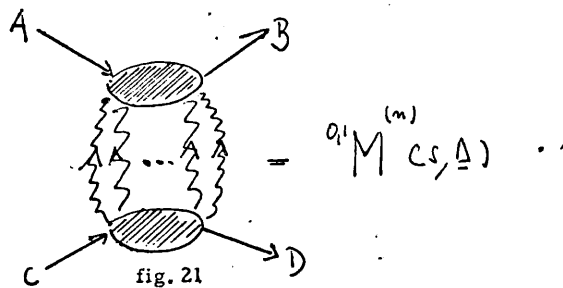
Gribov rules indicate that -

- 1) the unenhanced graph vanishes unless $\frac{d}{2} > \frac{d}{2}_0$
- 2) the semi-enhanced graph vanishes unless $\frac{d}{2} > 2\frac{d}{2}_0$
- 3) the full enhanced graph vanishes unless $\frac{d}{2} > 3\frac{d}{2}_0$

IV - A CORRELATION MODIFIED EIKONAL MODEL

With our basic ingredients explicitly defined[#] we enter the main part of the thesis. The derivation and justification of the modified eikonal model where one Reggeon and n-1 Pomerons can be exchanged and where non vacuum asymptotic states are allowed to change the projection of the nucleon spin.

We symbolize such a model by the typical Gribov diagram



We understand the scattering amplitude $M(s, \Delta)$ as expanded into a series consisting of nth order cut term helicity contribution. Thus we put

$${}^{0,1}M(s, \Delta) = \sum_{n=1, u_1, u_2, \dots, u_m} {}^{0,1}M^{(n)}(p; k_1, k_2, \dots, k_m)$$

and write down the s-channel helicity contribution to the nth order term in Gribov's 'multiple expansion' of the $A + C \rightarrow B + D$

$${}^{0,1}M^{(n)}(s, \Delta) = \sum_{u_1, u_2, \dots, u_m} p^{(n)} \int_{-\infty}^{\infty} m(p) N^{u_1, u_2, \dots, u_m}(\Delta, k_1, \dots, k_m) \prod_{k=1}^m \Gamma(C_{k_i}, s) d\Omega^{(n)}$$

pp 11-21

The reggeon 4-momenta are $q = (0, \underline{k}_i, 0)$ since, for high energy small angle scattering the reggeon momentum is approximated by the transverse component of the final three momentum of the colliding particle projected onto a plane perpendicular to the scattering plane. The longitudinal momentum transfer of the projectile has been neglected. In scattering (24) the two dimensional integration approximates the integration over the sphere by an integration over a plane which is tangent to the sphere at forward direction.

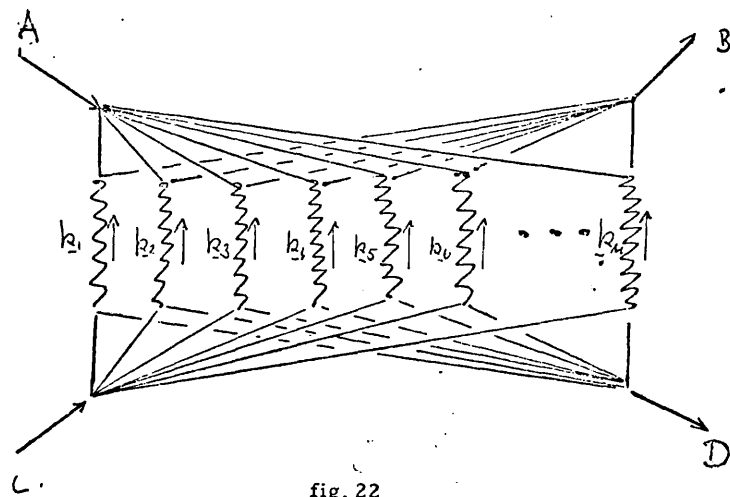
Thus we use $\underline{k}_i^2 = -t_i$ and $\Delta^2 = -t$ for the total momentum transfer $\Delta = \sum_{i=1}^n \underline{k}_i$

The helicity sum splits into net helicity nonflip and net helicity flip indicated by $m(p)$ which is a function of the helicities u_i carried by the exchanged reggeons, counted by the index i from 1 up to n the order of exchange. The $u_i = 0$ denote reggeon helicity nonflip and the $u_i = 1$ reggeon helicity flip. $p = \sum u_i$ defines the net helicity such that even p is net helicity nonflip and odd p is net helicity flip. Gribov's two body amplitude has been written as corresponding to a multiple scattering expansion in powers of the basic nucleon-nucleon (quark-quark) scattering amplitude - resembles nuclei scattering - and in increasing orders of a many-body transition form factor taking into account the contribution of inelastically excited intermediate states between the internal structure of the colliding hadrons. In addition, the amplitude includes factors for shower formation which are reminiscent of the Michigan λ .

The momentum conserving delta function enters the reggeon phase space as

$$d\Omega^{(m)} = \int^2 \left(\Delta - \sum_{i=1}^n \underline{k}_i \right) \prod_{i=1}^n d^2 k_i$$

We consider the nth order term of the correlation modified eikonal and symbolize the dependence of the Gribov vertices on the angle of the exchanged Reggeon and Pomerons by the nth order extension of the Mandelstam diagram



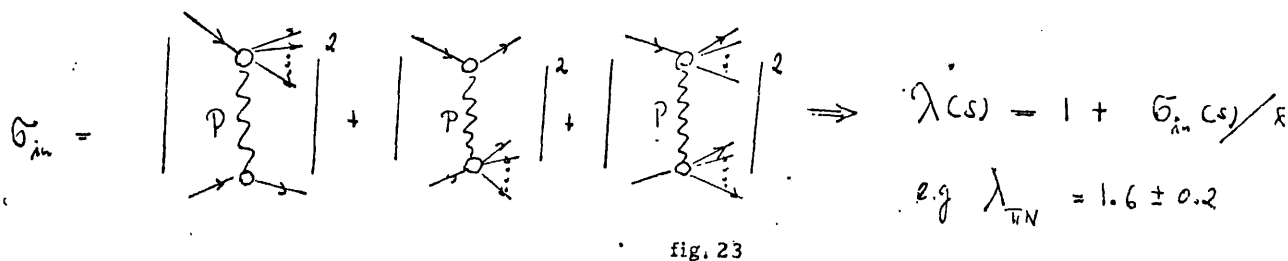
The Gribov vertex factorizes in the case of πN scattering into a nucleon (AB) and pion vertex (CD). Only nucleon vertex can helicity change take place. We give N the following functional expression -

$$N^{m(p)} \left(\mu_1, \mu_2, \dots, \mu_n \right) \left(k_1, \dots, k_n, \Delta \right) = \hat{N}^{m(p)} \left(n \right) \tilde{N}_N^{m(p)} \left(\mu_1, \mu_2, \dots, \mu_n \right) \left(k_1, \dots, k_n, \Delta \right) \tilde{N}_\pi \left(k_1, \dots, k_n, \Delta \right) \prod_{i=1}^n H^{\mu_i} \left(i k_{i-1} \right)$$

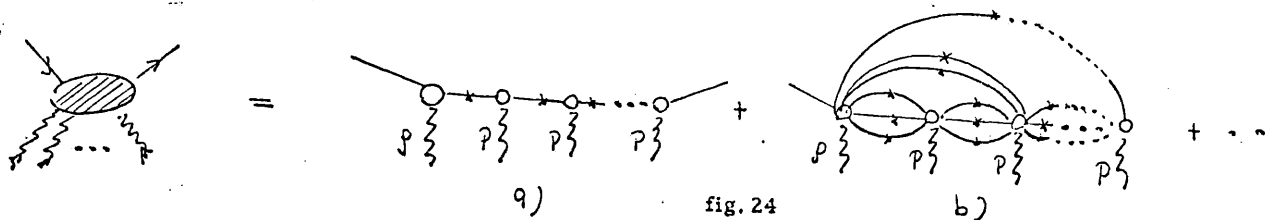
The H's and β 's are angular momentum factors and Regge residues respectively as defined in II (page 19). T

runs from 1 to n where $i = 1$ indicates the Reggeon and $i = 2 \dots n$ the Pomeron-exchange. The interesting to any deviation from 1 reflects the effective contribution of inelastic intermediate states besides the elastic p. The shower factor λ measures the normalization of the contribution of such inelastic intermediate states, their dependence on momentum transfer.

In a modification of the eikonal model, Ter-Martirosyan (21) has proposed the quasi-eikonal model by introducing a factor reminiscent of the Michigan λ . Kaidalov (35) has determined its value from pomeron induced production represented by the following three diagrams -



The λ then takes account of the formation of particle beams in the intermediate states and is experimentally a deviation from the eikonal model due to the ratio of the cross sections for diffractive dissociation to the cross section for elastic scattering. They can be s -dependent, see Kaidalov (36) and for applications see Boreskov et al (20). The way to take into account shower formations in intermediate states in the frame of the quasi-eikonal model is the factorized Gribov vertices as expanded in a series in the complete system of physical intermediate states in the language of nuclear physics to the expansion in an increasing order of the nuclear correlation function



The crosses on the intermediate lines indicate that the approximation of the Gribov diagram (second order)

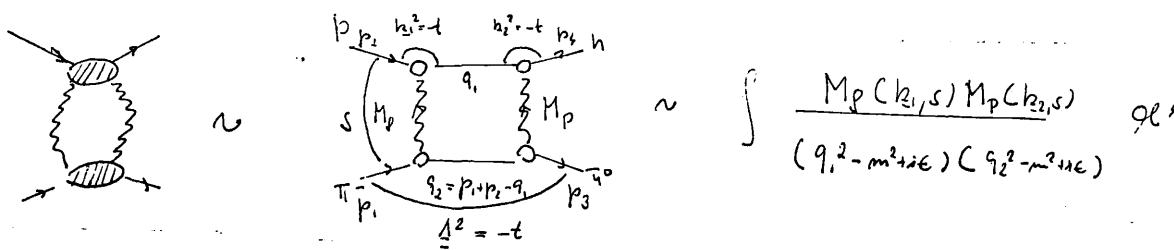
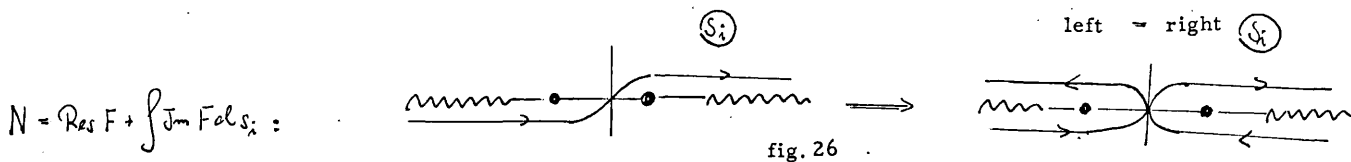


fig. 25

is not a Feynman diagram nor an AFS diagram since the intermediate particles are taken on mass shell

$$\frac{1}{q_j^2 - m_j^2 + i\epsilon} \longrightarrow -i\pi \delta(q_j^2 - m_j^2) \quad j=1,2 \quad \text{see Ter-Martirosyan (16)}$$

the M do not depend on the masses $s_1 = q_1^2$ and $s_2 = q_2^2 = (p_1 + p_2 - q_1)^2$. This procedure leads to the "optical" contribution which leads to the eikonal model. The optical contribution agrees with the Absorption model. The singularities are on the left and right hand side of the s plane. In the absence of enhanced branch points, i. e. small masses s_i the absorptive part of the Regge-scattering amplitude falls off more rapidly than $1/s_i$. One can then rotate both contours such that -



and obtain a superconvergent relation for the Regge-particle scattering amplitude which leads in the case of dominance to the equality of initial and final state rescattering, i. e. the absorption model see Kaidalov (28).

The contribution of each link in fig. 24 b) increases due to the shower formation in comparison with the elastic states in fig. 24 a). The Reggeon-induced production of a cascade of particles will be different from the one by the Pomeron. Also helicity flip might contribute differently from non-flip. In practice we only fit one number per helicity.

$$\lambda_{PN}^{m(p)} \lambda_{PN}^{m(p)} \lambda_{PN}^{m-2} = \lambda_{PN}^{m(p)} \lambda_{PN}^{m-2} = \lambda^{m(p)}(m)$$

Note that a determination by Ravenhall and Wyld (38) led to the result that from four diffractively produced states

$$\pi + N^*(1500), \quad \bar{\pi} + N^*(1520), \quad \bar{u} + N^*(1690), \quad A_1 + N \text{ in } \bar{u} - p \rightarrow \bar{u}^0 n$$

only two, namely $A_1 + N$ and $\bar{u} + N^*(1690)$ made a significant contribution leading to $\lambda \sim 1.2$

to be generally assumed that only pomeron-induced production is significantly large. In contrast, those induced by helicity flips are small (21).

What remains, and promises to be of considerable effect by comparison with the absorption/eikonal, is the dependence on momentum transfer, not only on the overall one Δ but also on $k_1 \cdot k_2$ which leads to a similar dependence on Δ and k_1 and k_2 i. e. a renormalization of the shape of the cut and of the poles of higher order exchanges. Thus the resulting eikonal will be modified in its overall Δ dependence and in addition phase undergoes a modification. This $k_1 \dots k_n, \Delta$ and possible s -dependence is represented by \tilde{N} in the case of second order exchange one could parameterize \tilde{N} algebraically by

$$\tilde{N} = \frac{1}{(1 + (k_1 + k_2)^2 R^2)} \quad \text{or exponentially} \quad \tilde{N} = e^{-c_1 C (k_1 + k_2)^2 - c_2 k_1 \cdot k_2}$$

as sug

These form factors reflect the composite structure of the colliding particles as they do in the quark model calculation of Benofy, Shrauner and Cho (39) and Harrington and Pagnamenta (30). We choose the exponential representation as to obtain simple Gaussian integrals. In the case of the nth order contribution we parameterize such that \tilde{N} factorize. This is accomplished by the following parameterization:

$$m(p) \tilde{N}_N(k_1, \dots, k_n; \Delta) = \exp \left[-\frac{m(p)}{2} \left\{ (k_1 - k_2)^2 + (k_2 - k_3)^2 + \dots - C_1 \right. \right. \\ \left. \left. + (k_2 - k_3)^2 + (k_3 - k_4) + \dots - C_2 \right. \right. \\ \left. \left. \dots \right. \right. \\ \left. \left. + (k_{n-2} - k_{n-1})^2 + (k_{n-2} - k_n) \right. \right. \\ \left. \left. + (k_{n-1} - k_n)^2 \right] \right]$$

We write an analogous expression for

$$\hat{N}_N(k_1, \dots, k_n, \Delta) = \exp \left[-\frac{C_N}{2} \left\{ (k_1 - k_2)^2 + \dots - (k_{n-1} - k_n)^2 \right. \right. \\ \left. \left. + (k_2 - k_3)^2 + \dots - (k_{n-1} - k_n)^2 \right. \right. \\ \left. \left. \dots \right. \right. \\ \left. \left. + (k_{n-1} - k_n)^2 \right] \right]$$

In a further simplification we set $C_N = C_{\overline{N}}$:

in this case

$$m(p) \sim \int_{\overline{N}}^{k_1, k_2, \dots, k_n} (k_1 \dots k_n, \Delta) \sim \int_{\overline{N}}^{k_1, k_2, \dots, k_n} (k_1 \dots k_n, \Delta) = \int_{\overline{N}}^{k_1, k_2, \dots, k_n} K(k_1 \dots k_n, \Delta) = \int c \Delta^{2-n} c$$

due to conservation momentum transfer $\underline{\Delta} = \sum \underline{k}_i$ we call K the correlation kernel and the correlation p the "Gribov c". The n in the exponent is the order of exchange. The introduction of a correlation kernel in cut integral has been strongly suggested by Høgaasen and Krzywicki (40). There the forms

$$K = \int \mathcal{D}k_1 k_2 \quad \text{and} \quad K = \int e^{-c(k_1 - k_2)^2}$$

were put forward.

Another form is the one by Lovelace (26). $K = \int \mathcal{D}k_1 k_2$

We write the nth order contribution to the s-channel helicity scattering amplitude as

$${}^{0,1} M^{(m)}{}^{mcp_1}(s, \underline{\Delta}) = \mathcal{V}^{(m)} \int_{-\infty}^{\infty} M^{\mu_1}(s, k_1^2) \dots M^{\mu_n}(s, k_n^2) K^{mcp_1}(k_1, \dots, k_n, \underline{\Delta}) \delta^4(\underline{\Delta} - \sum_{i=1}^n k_i) d^2 k_1 \dots d^2 k_n$$

with
$$M_{\mathcal{P}}^{\mu_i}(s, k_i^2) = \left(\frac{|k_i|}{2m_N}\right)^{\mu_i} e^{i\mu_i \phi_i} \left[\beta_{\mathcal{P}}^{\mu_i}(s) e^{-\gamma_{\mathcal{P}}^{\mu_i}(s) k_i^2} \right]$$

and
$$M_{\mathcal{P}}^{\mu_j}(s, k_j^2) = \left(\frac{|k_j|}{2m_N}\right)^{\mu_j} i (-1)^{\mu_j} e^{i\mu_j \phi_j} \beta_{\mathcal{P}}^{\mu_j}(s) e^{-\gamma_{\mathcal{P}}^{\mu_j}(s) k_j^2}$$

as defined in II pages 20 and 21. Further, we put the correlation kernel as on page 52 of this chapter

$$K(k_1, \dots, k_n, \underline{\Delta}) = e^{mcp_1 \underline{\Delta}^2 - n \sum_{i=1}^n k_i^2}$$

Before we discuss the normalization $\mathcal{V}^{(m)}$ we remark on the crossing symmetry (up to $1/s$) of the Gribov cut. The sym of the cut under crossing $s \rightarrow -s$ is the product of the symmetries of the Reggeons, (Pomerons) $\eta^{\mu_1}, \eta^{\mu_2}, \eta^{\mu_3}, \dots, \eta^{\mu_n}$. The signature of the cut is the product of the signatures of the poles.

In this respect it is interesting to remark that the absorption model as mentioned in the introduction (page 2) traditionally calculated with the help of the Sopkovich prescription which lacks $s \leftrightarrow u$ crossing symmetry, i. e. it is not line reversal. We mentioned that the Gribov cut corresponds to the absorption model, see page 49, if initial and final rescatterings are equal. This is however, generally not necessarily the case. How one can actually restore crossing symmetry in the absorption model has been nicely demonstrated by Quigg (41). It consists of adding the crossed graphs to the conventional graphs of the absorption model, i. e. to add elastic scattering of an initial state particle with a final state particle, as shown in fig. 27

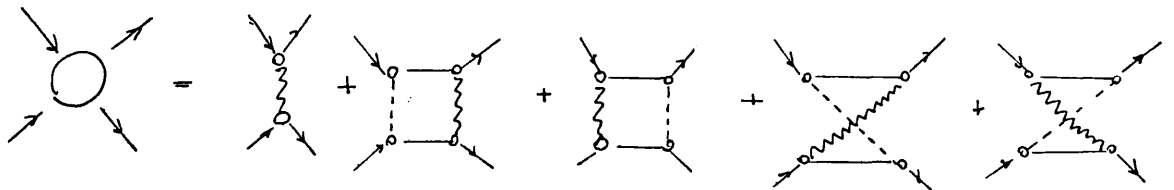
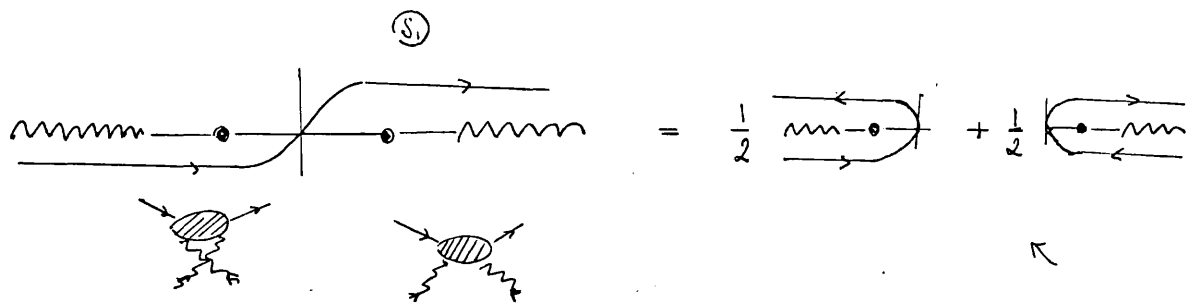


fig. 27

Quigg's crossing symmetric absorption model

Quigg demonstrated further how the crossed terms are already included in the Gribov cut. The Regge-particle scattering amplitude contains all possibilities - thus also the production of crossed reggeons.



Averaging over narrow resonances in two channels

fig. 28

Quigg's argument

The Gribov cut includes crossed and uncrossed graphs. The absorption model can be made crossing symmetric by averaging the crossed graphs with the uncrossed graphs. The crossed graphs can be understood since the Regge-particle scattering amplitude contains all possible orderings of the constituents namely a and b interchanged and c and d interchanged give crossed graph as in fig. 29

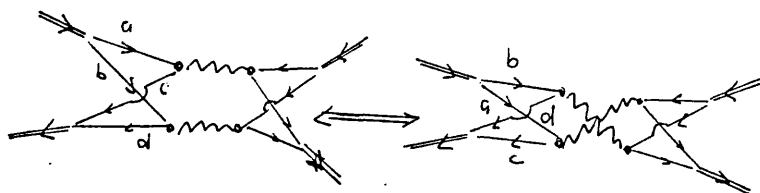


fig. 29 Gribov cut including crossed graphs

We can now state more precisely the limit cases of the Gribov cut in the case of second order exchange

We write

$$M^{(2)} = \int N^{(2)} G_1 G_2 d\Omega$$

which reduces in the case of $N = \text{const.}$ to the absorption model with coupling constants - see Adjei et al (4) initial and final rescatterings are equal. The contour integral in the sub energy plane includes only the residue of the intermediate elastic pole. The residue is a constant. The N 's can contain form factors instead of coupling constants. Any deviation, however, of N from the product of the pole residues involved in the exchange is a way to pick up contributions of other singularities in the sub energy plane. By writing $M^{(2)}$ as

$$M^{(2)} = \int M_1 M_2 K d\Omega$$

one can say that any deviation of K from 1 takes effectively account of the contribution of inelastic intermediate states and $K = \text{const.}$ corresponds to the crossing symmetric i. e. line reversal version of the absorption model such as the one developed by Quigg. However $K = \text{const} \neq 1$ only determines the normalization of the Gribov cut, i. e. the contribution of the inelastic intermediate states to the cut in forward direction. $K \neq \text{const.}$ on the other hand measures the effect these intermediate states have at $t \neq 0$. This has a considerable effect on the Gribov cut. Note, however that K has to be real so as not to destroy the crossing symmetry. In practice a small deviation might be feasible as long as it does not break the symmetry too drastically.

Now we are going to fix the normalization $\nu^{(n)}$ in $M^{(n)} = \nu^{(n)} \int M_1 M_2 \dots M_n k \delta^2 d^2 b_1 \dots d^2 b_n$

First let us consider spinless scattering. $M^{(n)}$ is the nth order term in an eikonal expansion of K factor. For this reason we have chosen it as on page 51.

Other forms, such as

$${}^{m(p)} N_N \sim e^{-\frac{1}{2} c_N \sum_{i=2}^m (k_i - \frac{1}{2} k_i)^2} \quad \text{and} \quad N_T \sim e^{-\frac{1}{2} c_T \sum_{i=2}^m k_i^2}$$

leading to ${}^{m(p)} K = e^{-m(p) c \Delta^2 + 4 c \sum_{i=2}^m k_i \frac{1}{2} k_i}$ when $c_N = c_T$

do not factorize at once. However, the quadratic forms with crossed terms can be diagonalized by carrying out similarity transformations.

We now write down the s-channel partial wave series for an elastic scattering amplitude. With our normalization see I, page 12, and Appendix page 207 we find

$$M(s, \Delta) = \frac{\sqrt{4\pi}}{q^2} \sum_j (2j+1) M_j^s(s) P_j(\cos \theta_s)$$

We are going over to the impact parameter representation, see Appendix page 211 and make the replacement

$$\sum_j (2j+1) \rightarrow 2q^2 \int_0^\infty b db \quad \text{and} \quad P_j(\cos \theta_s) \rightarrow J_0(q|b|)$$

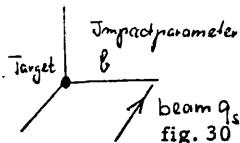
thus

$$M(s, \Delta) = \frac{\sqrt{4\pi}}{i} \int_0^\infty b M(b, s) J_0(q|b|) db$$

$M(b, s)$ is the sum over all nth order products of the phase shifts, i. e. the Regge pole amplitudes which are Fourier transformed from momentum transfer space into impact parameter space. If we call these phase shifts $\delta(b, s)$ then the s-channel partial wave reads

$$M(b, s) = \sum_{m=1}^{\infty} \frac{(2i\delta(b, s))^m}{m!} = e^{-2\delta(b, s)}$$

$M(b, s)$ is the partial wave amplitude for the angular momentum $J = q_s b - \frac{1}{2}$ where q_s is the magnitude of the s-channel centre of mass three momentum $|p_C| = |p_D|$ for the scattering $A + C \rightarrow B + D$ and b the impact parameter



$M(s, \Delta)$ Fourier transform back into impact parameter space $\times M(s, b)$

$$\sim \int_{-\infty}^{\infty} e^{i \Delta \cdot b} M(s, b) \frac{d^2 b}{2\pi}$$

The connection with $M(s, \Delta) = \frac{\sqrt{\pi}}{i} \int_0^{\infty} b M(s, b) J_0(\Delta |b|) db$ is found by making use of the

identity $J_m(x) = \frac{(-i)^m}{2\pi} \int_0^{2\pi} e^{ix \cos \phi} \cos m\phi d\phi$

thus $\int_{-\infty}^{\infty} e^{i \Delta \cdot b} d^2 b = \int_0^{\infty} b db \int_0^{2\pi} e^{i |\Delta| |b| \cos \phi} d\phi = 2\pi \int_0^{\infty} b db J_0(\Delta |b|)$

then $M(s, \Delta) = \frac{\sqrt{\pi}}{2i\pi} \int_{-\infty}^{\infty} e^{i \Delta \cdot b} M(s, b) d^2 b$

the partial wave amplitude $M(s, b)$ can be obtained by inverting $M(s, \Delta) = \frac{\sqrt{\pi}}{i} \int_0^{\infty} b M(s, b) J_0(\Delta |b|) db$

by using the Fourier-Bessel integral

$$f(x) = \int_0^b J_n(\alpha x) \alpha \left\{ \int_0^b f(x') J_n(\alpha x') x' dx' \right\} d\alpha$$

$$\Rightarrow M(s, b) = \frac{i}{\sqrt{\pi}} \int_0^b |\Delta| M(s, \Delta) J_0(|\Delta| b) d|\Delta|$$

Or $M(s, b) \sim$ Fourier transform from momentum transfer space into impact parameter space

$$= \frac{i}{\sqrt{\pi}} \int_{-\infty}^{\infty} e^{-i\Delta b} M(s, \Delta) \frac{d^2\Delta}{2\pi} = \sum_{n=1}^{\infty} f^{(n)}(s, b)$$

and since $M(s, b) = \sum_{n=1}^{\infty} \frac{(2i f(s, b))^{2n}}{n!} \Rightarrow f^{(1)}(s, b) = 2i f(s, b)$

and we define the eikonal phase in terms of the phase shift:

$$\chi(s, b) = 2 f(s, b)$$

then we have $f^{(1)}(s, b) = 2i f(s, b) = i \chi(s, b)$

and
$$i \chi(s, b) = \frac{i}{\sqrt{\pi}} \int_{-b}^{\infty} e^{-i k_1 b} M^{(1)}(s, k_1^2) \frac{d^2 k_1}{2\pi}$$
 where $M^{(1)}(s, \Delta)$ is the Reggepo

now
$$M^{(m)}(s, \Delta) = \sum_{n=1}^{\infty} M^{(m)}(s, \Delta) \quad \text{and} \quad M^{(m)}(s, \Delta) = \frac{\sqrt{\pi}}{i} \int_{-b}^{\infty} e^{i \Delta b} \int^{(m)}(s, b) \frac{d^2 b}{2\pi}$$

but
$$\int^{(m)}(s, b) = \frac{(i \chi(s, b))^m}{m!} \quad \text{thus}$$

$$M^{(m)}(s, \Delta) = \frac{\sqrt{\pi} i^{m-1}}{m! 2\pi} \int_{-b}^{\infty} e^{i \Delta b} \chi(s, b)_1 \chi(s, b)_2 \dots \chi(s, b)_m d^2 b$$

now we compare this with our nth order Gribov integral:

$$M^{(m)}(s, \Delta) = \int_{-b}^{\infty} M_1(s, k_1^2) M_2(s, k_2^2) \dots M_m(s, k_m^2) K(k_1, \dots, k_m, \Delta)$$

in order to be able to work in the impact parameter representation we choose the Fourier integral representation of the delta function:

$$\delta^2(\underline{A} - \sum \underline{k}_i) = \frac{1}{(2\pi)^2} \int_{-\infty}^{\infty} e^{i(\underline{A} - \sum \underline{k}_i) \cdot \underline{b}} d^2b$$

then the Gribov integral becomes

$$M^{(m)}(s, \underline{A}) = v^{(m)} \int_{-\infty}^{\infty} e^{i\underline{A} \cdot \underline{b}} \left\{ \int_{-\infty}^{\infty} e^{-i\underline{k}_1 \cdot \underline{b}} M_1(s, \underline{k}_1^2) d^2k_1 \int_{-\infty}^{\infty} e^{-i\underline{k}_2 \cdot \underline{b}} M_2(s, \underline{k}_2^2) d^2k_2 \dots \int_{-\infty}^{\infty} e^{i\underline{k}_m \cdot \underline{b}} \right.$$

$$\begin{aligned} & \Updownarrow \\ & = \frac{\sqrt{\pi} i^{m-1}}{m! 2\pi} \int_{-\infty}^{\infty} e^{i\underline{A} \cdot \underline{b}} \chi_1(s, \underline{b}) \chi_2(s, \underline{b}) \dots \chi_m(s, \underline{b}) d^2b \end{aligned}$$

by inspection \curvearrowright

$$v^{(m)} = \int_{\text{cut}}^{(m)} \frac{i^{m-1} 2\pi \sqrt{\pi}}{m! (\sqrt{\pi})^m (2\pi)^m} \int_{\text{cut}} P^m \text{ Pomeron and cut } \lambda \frac{i^{m-1} 2\pi \sqrt{\pi}}{(m-1)! (\sqrt{\pi})^m C}$$

Thus we write for the nth order contribution to the s-channel helicity scattering amplitude for the exchange of a Reggeon (the $\int i_n \bar{u} \rightarrow p \rightarrow \bar{u}_n$) and n-1 Pomerons which are allowed to change the projection of the nucleon spin is not helicity conserving.

$$M^{m(p)}(s, \Delta) = \frac{\lambda_{cut}^{(m)} i^{-m-1}}{(m-1)! (\sqrt{s})^{m-1} (\alpha\sqrt{s})^{m-1}} \int_{-b}^b M^{(1)}(s, k_1^2) \dots M^{(m)}(s, k_m^2) K^{m(p)}(k_1, \dots, k_m, \Delta) \delta^2(\Delta - \dots)$$

with Reggeon, Pomeron and the correlation kernel as defined on page 53 and in addition the Fourier integral representation of the delta function we obtain -

$$M^{m(p)}(s, \Delta) = \zeta(m) e^{C^{m(p)} \Delta^2} \int_{-b}^b e^{i(\Delta \cdot b + m(p)\phi)} \left\{ \int_{-b}^b |k_1|^{n_1} e^{i(\tau_1 \phi - k_1 \cdot b)} - \hat{M}_{P_+}^{n_1} k_1^2 \right. \\ \left. \int_{-b}^b \prod_{j=2}^m |k_j|^{n_j} e^{i(\tau_j \phi_j - k_j \cdot b)} - \hat{M}_P^{n_j} k_n^2 \right\} \frac{d^2 b}{(\alpha\sqrt{s})^2}$$

$$\text{with } \tilde{V}^{(m)} = \frac{\lambda_{Cut}^{(m)} \lambda^{2m-2} (-1)^{\sum_{j=2}^m M_j} \sum_{r=1,2} \beta_{Pr}^{M_1} \prod_{j=2}^m \beta_P^{M_j}}{(m-1)! (\sqrt{5})^{m-1} (2\sqrt{5})^{m-1} (2m_N)^{M_1 + \sum_{j=2}^m M_j}}$$

$$\text{and } \hat{M}_{Pr}^{M_1} = \gamma_{Pr}^{M_1} + n C^{m(p)} \quad \text{and} \quad \hat{M}_P^{M_j} = \gamma_P^{M_j} + m C^{m(p)}$$

The conventional Regge phase has been defined along the \hat{x} axis, see also part II, page 12, fig. 2. The plane of the Reggeon momenta $\underline{k}_1, \underline{k}_2$ and the total momentum transfer Δ is then as shown in fig. 31

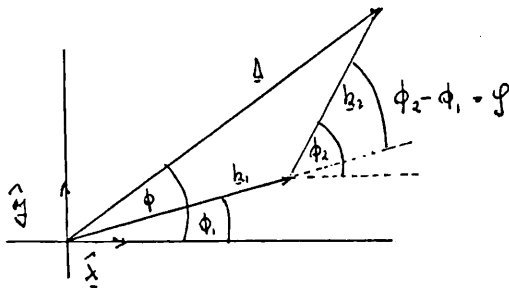


fig. 31

the mutually orientated transverse components of the Reggeon momenta.

We then write

$$\int_{-\infty}^{\infty} |k_1|^{\lambda_1} e^{i(\lambda_1 \phi_1 - k_1 \cdot b)} - \hat{\gamma}_{P_r}^{\lambda_1} k_1^2 e^{i k_1^2} = (-i)^{\lambda_1} \int_0^{\infty} |k_1|^{\lambda_1+1} e^{-\hat{\gamma}_{P_r}^{\lambda_1} k_1^2} J_{\lambda_1}(|k_1| |b|) dk_1$$

$$\int_{-\infty}^{\infty} |k_j|^{\lambda_j} e^{i(\lambda_j \phi_j - k_j \cdot b)} - \hat{\gamma}_P^{\lambda_j} k_j^2 e^{i k_j^2} = (-i)^{\lambda_j} \int_0^{\infty} |k_j|^{\lambda_j+1} e^{-\hat{\gamma}_P^{\lambda_j} k_j^2} J_{\lambda_j}(|k_j| |b|) dk_j$$

and consequently the Regge eikonal reads

$$\chi_{\text{Regge}}^{\lambda_1}(s, b) = \sum_{n=1,2} \beta_{P_r}^{\lambda_1}(s) \frac{(-i)^{\lambda_1}}{(\alpha_{P_r})^{\lambda_1}} \int_0^{\infty} |k_1|^{\lambda_1+1} e^{-\hat{\gamma}_{P_r}^{\lambda_1} k_1^2} J_{\lambda_1}(|k_1| |b|) dk_1$$

$$= \frac{\sum \beta_{P_r}^{\lambda_1}(s) (-i)^{\lambda_1}}{\sqrt{s} (\alpha_{P_r})^{\lambda_1}} \int_{-\infty}^{\infty} |k_1|^{\lambda_1} e^{-i(k_1 \cdot b + \mu_1 \phi) - \hat{\gamma}_{P_r}^{\lambda_1} k_1^2} \frac{d^2 k_1}{2\pi}$$

and the Pomeron eikonal

$$\chi_{\text{Pomeron}}^{\lambda_j}(s, b) = \frac{(-i)^{\lambda_j}}{\sqrt{s} (\alpha_{P_r})^{\lambda_j}} \beta_P^{\lambda_j}(s) \int_0^{\infty} |k_j|^{\lambda_j+1} e^{-\hat{\gamma}_P^{\lambda_j} k_j^2} J_{\lambda_j}(|k_j| |b|) dk_j$$

$$= \frac{(-i)^{\lambda_j} \beta_P^{\lambda_j}(s) (-i)^{\lambda_j}}{\sqrt{s} (\alpha_{P_r})^{\lambda_j}} \int_{-\infty}^{\infty} |k_j|^{\lambda_j} e^{-i(\lambda_j \phi_j + k_j \cdot b) - \hat{\gamma}_P^{\lambda_j} k_j^2} \frac{d^2 k_j}{2\pi}$$

We now carry out the integration over momentum-transfer \underline{k}_1 and \underline{k}_j , i. e. the Bessel integrals:
in order to evaluate the integrals we make use of the Fourier-Bessel transforms:

$$\int_0^{\infty} x^{2\mu+1} J_{\nu}(\beta x) e^{-\alpha x^2} dx = \frac{\beta^{\nu}}{(2\alpha)^{\mu+1}} e^{-\frac{\beta^2}{4\alpha}} \quad \begin{array}{l} x = |k| \\ \mu = \nu \\ \beta = |b| \\ \alpha = \hat{\eta}^{\mu} \end{array}$$

Thus we obtain

$$(-i)^{\mu} \int_0^{\infty} |k|^{\mu+1} e^{-\hat{\eta}^{\mu} k^2} J_{\mu}(|k||b|) dk = \frac{(-i)^{\mu} |b|^{\mu}}{(2\hat{\eta}^{\mu})^{\mu+1}} e^{-\frac{b^2}{4\hat{\eta}^{\mu}}}$$

$$\text{thus } \int_{-b}^b d^2k_1 \dots d^2k_n = \frac{(-i)^{\mu} |b|^{\mu}}{\prod_{j=1}^n (2\hat{\eta}^{\mu_j})^{\mu_j+1}} e^{-\mathcal{H}^{\mu_1, \mu_2, \dots, \mu_n}(c)} \quad \text{now } j \text{ runs from } 1 \text{ to } n$$

$$\mathcal{H}^{\mu_1, \mu_2, \dots, \mu_n}(c) = \frac{\mathcal{H}^{\mu_1, \mu_2, \dots, \mu_n}(c)}{4} \quad \text{and} \quad \mathcal{H}^{\mu_1, \mu_2, \dots, \mu_n}(c) = \frac{\sum_i \eta^{\mu_i} + (n)^{\mu} c^{m(c)}}{\prod_{j=1}^n (\eta^{\mu_j} + n c^{m(c)})}$$

Using the identity

$$J_m(x) = \frac{(-i)^m}{2\pi} \int_0^{2\pi} e^{i x \cos \phi} \cos m\phi \, d\phi$$

we obtain -

$$\begin{aligned} \int_{-\infty}^{\infty} e^{i(A-b + mcp_1)\phi} \phi^{2b} \, d\phi &= \int_0^{2\pi} b \, d\phi \int_0^{2\pi} e^{i(|A|b_1 \cos \phi + mcp_1)\phi} \, d\phi = \\ &= (i)^{mcp_1} 2\pi \int_0^1 b \, b \, J_{mcp_1}(|A|b_1) \end{aligned}$$

and

$$\int_{-\infty}^{\infty} e^{i(A-b + mcp_1)\phi} \left\{ \int_{-\infty}^{\infty} \prod_{j=1}^m |k_j|^{2j} e^{i(c_{1j}\phi_j - k_j \phi)} - \hat{\gamma}^{2i} k_r^2 \, d^2 k_r \right\}$$

$$\Rightarrow M^{mcp_1}(s, \underline{A}) = e^{c^{mcp_1} \underline{A}^2}$$

The nth order formula for the $\int_0^{\infty} p^{2n-1}$ helicity cut contribution to the s-channel helicity scattering amplitude

$$M_{(s, \underline{\Delta})}^{m(p)} = \hat{V}^{(n)} e^{c^{m(p)} \Delta^2} \int_0^{\infty} |t|^{p+1} e^{-\hat{\alpha}(t)} J_{m(p)}(|\Delta| |t|) dt$$

$$= \hat{V}^{(n)} e^{c^{m(p)} |t|} \times |t|^{m(p)/2} \left(-\frac{\partial}{\partial \hat{\alpha}(t)} \right)^{\frac{p-m(p)}{2}} \frac{e^{-\frac{|t|}{\hat{\alpha}(t)}}}{(2 \hat{\alpha}(t))^{m(p)}}$$

with

$$\hat{V}^{(n)} = \frac{\binom{n}{c} (i)^{2n-2} (-i)^p (i)^{m(p)} (-1)^{\sum_{j=2}^n u_j} \prod_{r=1}^n \beta_{p_r}^{u_r}(s) \prod_{j=2}^n \beta_p^{u_j}(s)}{(n-1)! (7\bar{v})^{n-1} (2\bar{v})^{n-1} (2\bar{v})^2 (2m_N)^{u_1 + \sum_{j=2}^n u_j} (2\hat{\gamma}_{p_r}^{u_1})^{u_1 + \sum_{j=2}^n u_j}}$$

$$\hat{\alpha}(t) = \frac{\gamma_{p_r}^{u_1} + \sum \gamma_p^{u_j} + (n)^n e^{m(p)}}{4 (\gamma_{p_r}^{u_1} + m c^{m(p)}) \prod_{j=2}^n (\gamma_p^{u_j} + n c^{m(p)})}$$

$p = \sum_{j=1}^n u_j$ $m(p)$ is net helicity

In II page 16, we have decomposed an amplitude by

$$M = M^0 \cdot \delta_0 + i \delta (\hat{p}_m \times \hat{k}) M^1 \quad \text{with } \delta_0 \text{ the unit matrix}$$

Thus we obtain for the second order helicity cut -

$${}^{(2)} M_{PP}^{m(p)=0} = M_P^0 \otimes M_P^0 - M_P^1 \otimes M_P^1 \quad \text{and} \quad {}^{(2)} M_{PP}^{m(p)=1} = M_P^1 \otimes M_P^0 +$$

and for the third order contribution

$${}^{(3)} M_{PP^2}^{m(p)=0} = M_P^0 \otimes M_P^0 \otimes M_P^0 - M_P^1 \otimes M_P^1 \otimes M_P^0 - M_P^0 \otimes M_P^1 \otimes M_P^1 - M_P^1 \otimes M_P^0 \otimes M_P^1$$

$${}^{(3)} M_{PP^2}^{m(p)=1} = M_P^1 \otimes M_P^0 \otimes M_P^1 - M_P^0 \otimes M_P^1 \otimes M_P^1 + M_P^0 \otimes M_P^1 \otimes M_P^0 + M_P^1 \otimes M_P^1 \otimes M_P^0$$

Our correlation modified eikonal model then reads -

Pomeron exchange only

$$M^0(s, \Delta, c) = \frac{c^{0/4}}{\sqrt{\pi} \lambda_{cut}} \int_{-b}^b e^{2i\lambda \delta_p^0} \text{ch} (2\lambda_{cut} \delta_p' - 1) e^{i\sqrt{H} \cdot b} d^2b$$

$$M^1(s, \Delta, c) = \frac{\sqrt{\pi} i e^{c/4}}{2\pi \lambda_{cut}} \int_{-b}^b e^{2i\lambda_{cut} \delta_p^0} \text{sh} (2\lambda_{cut} \delta_p') e^{i(\sqrt{H} \cdot b + \phi)} d^2b$$

Pomeron exchange + one Reggeon

$$M^0(s, \Delta, c) = \frac{c^{0/4}}{\sqrt{\pi} \lambda_{cut}} \int_{-b}^b \lambda \delta_p^0 \text{ch} (2\lambda \delta_p' - \lambda \delta_p^0 \text{sh} (2\lambda \delta_p')) e^{2i\lambda \delta_p^0}$$

$$M^1(s, \Delta, c) = \frac{\sqrt{\pi} e^{c/4}}{\pi \lambda_{cut}} \int_{-b}^b \lambda \delta_p^0 \text{ch} (2\lambda \delta_p' - \lambda \delta_p^0 \text{sh} (2\lambda \delta_p')) e^{2i\lambda \delta_p^0 + i}$$

The partial wave amplitude for the contribution of the Pomeron, which can change the projection of the nucleon spin

$$\begin{aligned}
 \int_P^{J_1}(s, b) &= \frac{i (-1)^{J_1} \beta_P^{J_1}(cs)}{\sqrt{4} (2m_N)^{J_1}} \int_{-b}^{\infty} |k_{\perp}|^{J_1} e^{i(J_1 \phi_1 - k_{\perp} b) - \gamma_P^{J_1} k_{\perp}^2} \frac{d^2 k_{\perp}}{2\pi} \\
 &= \beta_P^{J_1}(cs) \frac{i (-1)^{J_1} (-i)^{J_1} 2^{J_1}}{\sqrt{4} (2m_N)^{J_1}} \int_0^{\infty} |k_{\perp}|^{J_1+1} e^{-\gamma_P^{J_1} k_{\perp}^2} J_{J_1}(k_{\perp} b) \frac{dk_{\perp}}{2\pi} \\
 &= \frac{(-i)^{J_1}}{\sqrt{4} (2m_N)^{J_1}} \frac{(-1)^{J_1} |b|^{J_1}}{(2\hat{\gamma}_P^{J_1})^{J_1+1}} i \beta_P^{J_1}(cs) e^{-\frac{b^2}{4\hat{\gamma}_P^{J_1}}}
 \end{aligned}$$

and for the Reggeon:

$$\int_R^{J_1}(s, b) = \frac{(-i)^{J_1}}{\sqrt{4} (2m_N)^{J_1}} \sum_{n=1,2} \beta_{P_n}^{J_1}(cs) \frac{e^{-\frac{b^2}{4\hat{\gamma}_{P_n}^{J_1}}}}{(2\hat{\gamma}_{P_n}^{J_1})^{J_1+1}} \quad \hat{\gamma}_P^{J_1} = \gamma_P^{J_1}$$

Eikonal $\rightarrow \chi = 2\delta \leftarrow$ partial wave

And finally we state as the second order example, i. e. the correlation modified Gribov-Absorption cut:
 (it is this formula which we use in our phenomenological investigation)

Helicity nonflip

$$\begin{aligned}
 & - (2) \lambda_{cut}^0 \frac{\sqrt{\pi}}{2\pi} \frac{\sum_{\alpha, \beta} \beta_{pr}^0(c_s) \beta_p^0(c_s)}{(\gamma_{pr}^0 + \kappa c^0 + \gamma_p^0)} \rho - \frac{\gamma_{pr}^0 \gamma_p^0 + c^0 (\gamma_p^0 + \gamma_{pr}^0)}{\gamma_{pr}^0 + \kappa c^0 + \gamma_p^0} |t| \\
 & + (2) \lambda_{cut}^0 \frac{\sqrt{\pi}}{2\pi} \frac{\sum_{\alpha, \beta} \beta_{pr}^1(c_s) \beta_p^1(c_s)}{(\gamma_{pr}^1 + \kappa c^0 + \gamma_p^1)} \left(1 - \frac{(\gamma_{pr}^1 + 2c^0)(\gamma_p^1 + 2c^0)}{\gamma_{pr}^1 + \kappa c^0 + \gamma_p^1} |t| \right) \rho - \frac{\gamma_{pr}^1 \gamma_p^1}{\gamma_{pr}^1 + \kappa c^0 + \gamma_p^1} |t|
 \end{aligned}$$

Helicity flip

$$\begin{aligned}
 & - (2) \lambda_{cut}^1 \sqrt{|t|} \frac{\sqrt{\pi}}{2\pi} \frac{\sum_{\alpha, \beta} \beta_{pr}^1(c_s) \beta_p^0(c_s) (\gamma_p^0 + 2c^1)}{4m_N \pi (\gamma_{pr}^1 + \kappa c^1 + \gamma_p^0)^2} \rho - \frac{\gamma_{pr}^1 \gamma_p^0 + c^1 (\gamma_{pr}^1 + \gamma_p^0)}{\gamma_{pr}^1 + \kappa c^1 + \gamma_p^0} |t| \\
 & + (2) \lambda_{cut}^1 \sqrt{|t|} \frac{\sqrt{\pi}}{4m_N \pi} \frac{\sum_{\alpha, \beta} \beta_{pr}^0(c_s) \beta_p^1(c_s) (\gamma_{pr}^0 + 2c^1)}{(\gamma_{pr}^0 + \kappa c^1 + \gamma_p^1)^2} \rho - \frac{\gamma_{pr}^0 \gamma_p^1 + c^1 (\gamma_{pr}^0 + \gamma_p^1)}{\gamma_{pr}^0 + \kappa c^1 + \gamma_p^1} |t|
 \end{aligned}$$

V - THE "DERIVATIVE RULE" APPLIED TO THE CORRELATION MODIFIED WEAK ABSORPTION MODEL WITH (A) TRADITIONAL POMERON INPUT AND (B) HARTLEY-KANE POMERON INPUT

(A) At a preliminary stage of our investigation we applied the "derivative rule" in order to obtain the helicity flip amplitude. We change our notation such that -

$$\beta_p = \frac{1}{2} s^{\alpha_p(\omega)-1} A \quad \lambda_p = B \quad \beta_p = \frac{1}{2} \sqrt{s} C_p R^2 ; C_p = \frac{\sigma_{tot}}{2\pi R^2} \quad \lambda_p = R^{3/4}$$

and write for the Regge pole, $M_1(s, k_1^2) = \frac{1}{2} \sum_{i=1}^2 A_i s^{\alpha_i(\omega)} e^{-B_i k_1^2}$ and for the Pomeron, $M_2(s, k_2^2) = \frac{1}{2} i \gamma$

where $A_1 = A, A_2 = -A_1 e^{-i\pi\alpha(\omega)}$ $B_1 = B, B_2 = B_1 - i\pi\alpha'$

Inserting the pole, the pomeron and the correlation kernel into the Gribov expression we obtain -
Helicity nonflip cut amplitude

$$M(s, \Delta) = -\frac{1}{2} C_p (R^{3/4}) e^{-(R^{3/4} + c)|t|} s^{\alpha(\omega)} \sum_{i=1,2} \frac{A_i}{R^{3/4} + B_i + t c} e^{+ \frac{(R^{3/4} + c)|t|}{R^{3/4} + B_i + t c}}$$

We now apply the derivative rule $\phi_{\pm}(s, |t|) = c_0 \frac{\partial}{\partial \sqrt{|t|}} \phi_{\pm}(s, |t|)$ where c_0 is an arbitrary constant

Helicity flip cut amplitude of correlation modified weak absorption by means of the "derivative rule" with traditio

Pomeron input

we obtain -

$$M(s, k_1^2)_{+}^{\text{Pole}} = c_0 (-\alpha k_1) \left\{ \frac{1}{2} s^{\alpha(s)} [A_1 B_1 e^{-B_1 k_1^2} + A_2 B_2 e^{-B_2 k_1^2}] \right\}$$

$$M(s, \Delta)_{+}^{\text{Cut}} = c_0 (2\sqrt{|\Delta|}) \left\{ -\frac{1}{2} c_{op} \frac{R^2}{4} e^{-(R^2/4 + c)|\Delta|} s^{\alpha(s)} \right\}$$

$$\times \sum_{i=1,2} \frac{A_i}{R^2/4 + B_i + c} \left[\frac{(R^2/4 + 2c)^2}{(R^2/4 + B_i + c)} - (R^2/4 + c) \right] e^{-(R^2/4 + 2c)|\Delta|} + \frac{(R^2/4 + 2c)^2}{R^2/4 + B_i + c} |\Delta| \right\}$$

(B) We now state our correlation modified version of a HARTLEY-KANE POMERON INPUT (10) although the phenomenological investigation has not yet been carried out.

$$M_{HK}(s, k_1^2) = -i s \left[a e^{-b k_1^2} + a_0 e^{-b_0 k_1^2} \right] J_0 \left(R_0 \sqrt{\ln s - i\pi/2} k_1 \right)$$

Correlation modified weak absorption with Pomeron input à la Hartley-Kane

$$\begin{aligned}
 M(s, t)_{++} &= - \frac{\lambda s^{\alpha(s)+1}}{4\sqrt{5}} \left[a e^{-(b+c)|t|} \sum_{i=1,2} \frac{A_i}{(b + \beta_i + \epsilon_c)} e^{\frac{(b+2c)^2}{(b + \beta_i + \epsilon_c)} |t|} \right. \\
 &+ a_0 e^{-(b_0+c)|t|} \sum_{i=1,2} \frac{A_i}{b_0 + \beta_i + \epsilon_c} e^{\frac{(R_0^2/4)(\ln s - i\sqrt{5}/2)}{b_0 + \beta_i + \epsilon_c}} + \left. \frac{(b_0+2c)^2}{(b_0 + \beta_i + \epsilon_c)} \right] \\
 &= J_0 \left\{ - \frac{(\beta_i + 2c) R_0 \sqrt{\ln s - i\sqrt{5}/2}}{(b_0 + \beta_i + \epsilon_c) \sqrt{|t|}} \right\}
 \end{aligned}$$

We now use the "derivative rule"

$$\phi_{+-}(s, |t|) = C_0 \frac{\partial}{\partial \sqrt{|t|}} \phi_{++}(s, |t|)$$

And find the following result: Correlation modified weak absorption with Pomeron input a la Harte helicity flip cut amplitude by means of the "derivative rule" -

$$\begin{aligned}
 M(s, \Delta')_{+-} &= c_0 \left(- \frac{\lambda s^{\alpha(0)+1}}{4\sqrt{\pi}} \right) \left[2a \ell^{-(b+c)|t|} \sqrt{|t|} \sum_{i=1,2} \frac{A_i}{(b+\beta_i+\zeta c)} \right. \\
 &\left. \left\{ - (b+c) + \frac{(b+2c)^2}{(b+\beta_i+\zeta c)} \right\} \ell^{+\frac{(b+2c)^2}{(b+\beta_i+\zeta c)}|t|} + a_0 \ell^{-(b+c)|t|} \right. \\
 &\left. \sum_{i=1,2} \frac{A_i}{b_0+\beta_i+\zeta c} \ell^{\frac{(R_0^2/4)(\ln s - i\pi/2)}{b_0+\beta_i+\zeta c}} + \frac{(b_0+2c)^2}{b_0+\beta_i+\zeta c} |t| \right. \\
 &\left. \times \left[-2 \left\{ (b_0+c) - \frac{(b_0+2c)^2}{(b_0+\beta_i+\zeta c)} \right\} \sqrt{|t|} J_0 \left\{ - \frac{(\beta_i+2c) R_0 \sqrt{\ln s - i\pi/2}}{(b_0+\beta_i+\zeta c)} \right. \right. \right. \\
 &\left. \left. + \frac{(\beta_i+2c) R_0 \sqrt{\ln s - i\pi/2}}{b_0+\beta_i+\zeta c} J_1 \left\{ - \frac{(\beta_i+2c) R_0 \sqrt{\ln s - i\pi/2}}{b_0+\beta_i+\zeta c} \right. \right. \right.
 \end{aligned}$$

PART TWO

PHENOMENOLOGICAL INVESTIGATION*

* Figure numbers start again from 1.

VI A discussion of the mechanism by which the correlation modified absorption model rectifies the incorrect behaviour predicted by traditional reggeized absorption.

The pion-nucleon system is completely determined by 4 complex amplitudes, namely both isoscalar amplitudes in their helicity non-flip and helicity flip states. These amplitudes can, in turn, be extracted experimentally if there exists a complete set of measurements of the observables, i. e. the differential cross-section, the polarization and the spin-rotation parameters R and A. Such a complete set of data exists only at laboratory momentum of the incident pion at 6 GeV/c and small momentum transfer. Beyond $|t| = 0.3$ GeV² the lack of spin-rotation data prevents us from having a non-ambiguous view of the amplitudes' structure. In such a case such an amplitude analysis (5) is model-independent only up to an overall phase unless the method of analyticity[#] (5) is used. The overall phase is associated with the dominating amplitude, namely the isoscalar amplitude. The phase away from the forward direction of this amplitude, as found by Pietarinen (5) to considerably exceed the value as predicted by Barger and Phillips (12). This is consistent with the results of Ambats et al. (5). By assuming that the helicity flip isovector amplitude is strongly regge-dominated, we conclude from the constant phase difference which they have found to exist between the helicity flip and helicity non-flip isoscalar amplitude, that the effective trajectories of the two amplitudes have equal real parts. Pietarinen (5) found a ratio of real to imaginary part of the isoscalar helicity non-flip amplitude up to -50% at 6 GeV/c for $|t| = 0.3$ GeV². We have incorporated this piece of information into the model of our effective pomeron.

[#] Pietarinen

We now discuss how the gradual alteration of the effective Pomeron phase in connection with the introduction of correlation between the simultaneously exchanged pomeron and reggeon in an absorption model can produce the structure of the helicity amplitudes as found by the amplitude analysis at least at small momentum transfer and fixed laboratory momentum of 6 GeV/c.

We represent the amplitudes in the complex plane such that they are characterized by the following quantities:

1. Their strength \mathcal{Y} in forward direction
2. The slope Ψ of the assumed exponential fall-off with $|t|$ of this strength
3. Their initial phase ϕ
4. The rotation velocity $\dot{\Phi}$ of this phase in dependence on $|t|$

Thus we write any amplitude as

$$T_{1,2}^{\mu_1, \mu_2} P_{i,C,th,exp} = \mathcal{Y} \exp \left\{ -\Psi |t| + i(\phi + \dot{\Phi} |t|) \right\}$$

Its particular type is specified by its indices. These indices indicate -

1. The upper left indices μ_1, μ_2 correspond to the t-channel isospin state
2. The right indices denote individual s-channel helicity states. The net helicity state m is the sum of individual helicity states n_i where $n_i = 0$ is helicity nonflip and $n_i = 1$ helicity flip if $n_1 + n_2 = 0$ helicity nonflip if $n_1 + n_2 = 1$ helicity flip.
3. P, C, th, stand for the pole, the cut, their sum which makes up our theoretical total helicity amplitude. exp denotes the amplitude as extracted by amplitude analysis from experiment.
4. The lower left indices 1, 2 refer to the non-rotating and rotating parts respectively into which the theoretical amplitudes due to their regge signature.

VI.1 - The Crossing Symmetric Weak Cut Reggeized Absorption Model as a special case of the Gribov cut.

By setting in the Gribov cut integral the correlation kernel equal to 1 we recover the absorption model in its original form. We use the weak-cut version of this model as a starting point for the discussion about the possible modifications to traditional absorption. Gradually we then introduce the correlation in several model variants and observe in each case the deviation of these model variants with respect to the reference model. We mean, by weak-cut, that the fixed poles present at wrong signature points will not contribute multiplicatively to the regge residues. Thus they are not considered as nonsense wrong signature zeros (NWSZ). Since the pomeron stays positive throughout t and the pole changes sign, the deviation will occur in the convolution integral and the resulting cut turns out to be small. This is not the case in the strong-cut model which was the alternative version originally adopted by the Michigan group. In this view, the third order polynomial function is assumed to have strong influence on the regge-residue in the form of strong fixed poles which cancel the help of an enhancement factor $1 \gg \lambda \geq 3$ pole and cut become comparable and generate the dip by interference in the cross-section. The weak-cut version, in contrast, just fills in the zeros already predicted by the pole. (Unfortunately the dip to smaller values in t .) The weak-cut model does not add any parameter beyond those already present in the traditional model, i. e. $\lambda = 1$. There is still a considerable amount of flexibility within the frame of the traditional weak-cut regge model, e. g. the reggeization allows a choice of ghost-eliminating mechanisms, exponential factors in the residues and the trajectories. We adopt the exponential factors in the residue and choose an energy scale factor $s_0 = 1$ (GeV). This choice is equivalent to the introduction of an exponential factor in the residue. Thus we absorb any deviation from the traditional model. Our trajectory chooses nonsense. Thus both helicity poles vanish at $t = .647$ for our particular choice of initial rho-trajectory. We employ the Gell-Mann ghost-killing mechanism and the Gamma function left over by this mechanism in the exponential parameterization of the residue function.

The parameters in Table I provide a reasonable choice for treating pion-nucleon charge exchange at 6 GeV/c. We state explicitly the dependence of the cut characterizing quantities on all parameters: initial cut strength, shrinking velocity of this strength, initial phase angle and rotation velocity of it. This is done on the level of amplitudes, what is needed to improve absorption and trace the effect the correlation has on the absorption. We use six Regge-parameters which are -

1. the two helicity dependent residues $\hat{B}_s^{o,1}$ at $t = 0$
2. the two helicity-dependent residue slopes $\hat{\lambda}_s^{o,1}$ of their exponential fall-off with increasing t .
3. the two helicity-independent parameters which determine the linear regge-trajectory i. e. the intercept α'_ρ and the slope α_ρ . We relate intercept and slope via the following expression $\alpha_\rho^{(o)} = 1 - \alpha'_\rho m_\rho^2$ where m_ρ is the mass of the rho meson with $m_\rho = .773 \text{ GeV}/c^2$.

There are four parameters for the effective pomeron. The traditional absorption model is characterized by its use of a helicity conserving purely imaginary and stationary pomeron as the absorptive factor. In this way we have effectively only for the pomeron, the residue \hat{P}_P^0 at $/t/ = 0$ and the slope $\hat{\lambda}_P^0$ of the exponential fall-off with increasing $/t/$. Parameters by fitting the helicity nonflip isoscalar amplitude as taken from the amplitude analysis by Ambats et al. the opacity is fixed at $C_{Op} = .79$. Then the model will involve altogether five free parameters in order to describe the cross-section and predict the non-vanishing polarization of the recoil nucleon. The parameter values in Table I do a "best fit" to the differential cross-section. They rather provide a good set of initial values liable to systematic improvement. I clearly demonstrate success and failure of the traditional weak-cut reggeized absorption model. For this reason we present in I and IIb the characteristic complex vectors of the helicity nonflip and helicity flip amplitudes respectively. These are the cut, the theoretical total amplitude obtained as sum of pole and cut, and the total amplitude as found in the amplitude analysis by Ambats et al. One comment to the amplitude analysis is in order. Because of the arbitrary nature of the overall phase, we denote all the phases relative to the helicity nonflip isoscalar amplitude. They denote a parallel component pointing in the direction of the reference amplitude and a perpendicular one orthogonal to this direction. At $/t/ = 0$ their reference amplitude denoted is purely imaginary and corresponds to 101° . Moreover by assuming a regge-behaved helicity flip isovector amplitude and the phase difference observed between the isovector helicity flip and the isoscalar helicity nonflip amplitude of about 60° we draw that both amplitudes rotate counterclockwise with increasing $/t/$ and with the same velocity. This phase behavior is respected by transferring from "parallel-perpendicular" plane to the complex plane. However, beyond $/t/ = .4$, the phase difference diminishes increasingly fast. We present in Table IIa and IIb the numerical values of the amplitudes at $/t/$ values by Ambats et al in their analysis. These values are: $/t/ = .00, .05, .15, .25, .35, .45, .55$. For the values $/t/ = .45$ and $.55$ we can only compare with Ambats total amplitude at $/t/$ values up to $/t/ = .35$. For the values $/t/ = .45$ and $.55$ we compare only the magnitude but not with the phase, since this phase depends on a model for the isoscalar reference amplitude. (In Table IIc we arrange real and imaginary total theoretical amplitudes as calculated by the traditional absorption model and the polarization according to the formula -

$$\text{Polarization} = -2\text{Im}T^0 T^1 / \text{differential cross section}$$

The observables as given in Table IIc are given by Ambats for the additional $/t/$ values of $/t/ = .65$ and $.8$. These values exhibit clearly the structure of the observables. We see in fig. 1 the differential cross section measured in mb/GeV^2 contributions to the momentum transfer distributions from the pole, the cut, and the pole + cut. Compare Table IIc results, the theoretical differential cross section in column 3 and the experimental values in column 4. Immediate

theoretical curve deviates from an excellent description of the experimental differential cross section up to $t/ = . .$ this value. Although the dip up to $t/ = .025$ is at the correct position, it is vastly underestimated. Furthermore, at $t/ = .8$ cannot be reached at the heights it should be. Nevertheless, beyond $t/ = .4$ the theoretical curve still qualitative feature of the data.

In Fig. 2 we see that the predicted polarization is disastrously wrong. This is particular to the traditional absorptive strong or weak nature, and demonstrates its most serious failure. Since the rate of change of the differential cross to the scattering angle is proportional to the polarization, we observe that the 90% minimum of the polarization is r position as the dip in the differential cross section. This dip in turn originates in NWSZ of both helicity poles at $t/$ fills in the zero insufficiently, yet moves it to the desired position. A different choice of the parameters for the tr exert a strong influence on the position of the dip, and the minimum of the polarization. They could both be moved i for $\Delta p (t/) = .5 - 1.00 t/$ for example. We see in fig. 1 that the single rho pole fits the differential cross section the zero which has to be filled in. In particular the pole alone exhibits the forward turn over around $t/ = .05$, giving the dominating presence of the helicity flip amplitude which was only suppressed by the angular momentum factor at to Table IIa).

Of greater importance to our discussion, however, is the specific way in which the traditional absorption happens to polarization. The three parts of Table II contain all the information on amplitude level necessary to understand the. The helicity regge poles do not differ in their phase. They start (in our particular case) at 43.20° and rotate anticlockwise 72.36° per units in $t/$ around the origin of the Argand diagram. With a confidence up to $t/ = .35$ the amplitude anal behaviour only for the helicity flip amplitude. The helicity nonflip amplitude, on the contrary, rotates in a clockwise polarization is generated by the relative phase difference between the helicity flip and the helicity nonflip amplitude, should be positive. Traditional absorption treats the helicity nonflip pole as relatively strong by comparison with the strong absorption in the helicity nonflip case is accompanied by a phase of the cut relative to the one of the pole which let us say, typically 5° . Such a cut makes the pole lose about one degree at $t/ = 0$. By comparison, although the h out of phase with the pole, its strength is so weak that it affects the pole less in phase. For this reason traditional a with positive polarization, due to the small positive phase difference. We have chosen the slope of the helicity flip r helicity nonflip residue. (See Table I). This increases both the relative phase of flip cut to flip pole and the flip cut roughly in comparison to equal residue slopes. Due to this the positive start of the polarization is lost. This differen

with respect to the major alterations which traditional absorption has to undergo. The reason that traditional absorption is only in a very small $t/$ region $0 \leq t/ \leq .075$, is due to the different strengths by which the helicity pole and helicity flip pole loses slightly on strength after it has been absorbed, the effect on its phase, especially for small $t/$ behaviour is sharply in contrast to that of the helicity nonflip pole. See Tables IIb and IIa. Away from $t/ = 0$ the pole is shifted by the relative rotation velocity per $t/$ of helicity nonflip cut and pole. In the traditional absorption the rotation velocity with the pole is almost negligible about 4-5 degree per $t/$ compared with the 72° of the pole. Thus, although the cut and pole the pole is already at very small $t/$ out of phase with the cut by 180° . From then onward, the absorbed pole starts to rotate away from the weakly absorbed helicity flip pole whose phase remains virtually unaffected. Thus, in principle the phase difference between helicity nonflip cut and pole passes through 180° the phase difference between the two helicity amplitudes is going from positive to negative.

We have, in fig. 3-9 displayed the structure of the helicity amplitudes for the isovector exchange as obtained with the traditional reggeized absorption model. Fig 3 shows the moduli of the helicity nonflip amplitude. Its structure reflects the two pole absorption - the NWSZ has been shifted from $t/ = .65$ to a smaller value in $t/$. At the same time the zeros of the real part become separated. This separation converts the zero of the regge-pole in the differential cross section into a dip in the differential cross section. Thus the separation is actually needed, but what the differential cross section cannot do is that separation has unfortunately been arranged the wrong way round by traditional absorption. This could only be revealed by data now available for larger values in $t/$. The Argand diagram in fig. 8a clearly demonstrates the zero structure of the amplitude where we have given the pole and show that the cut places the zero of the real part at $t/ = .25$ and the zero of the imaginary part at $t/ = .325 (\text{GeV}/c)^2$. For comparison we have drawn, in the same figure, the amplitude as obtained in the amplitude by Ambats et al. which places the zero of the real part at about $t/ = .25 (\text{GeV}/c)^2$ and the zero of the imaginary part at $t/ = .325 (\text{GeV}/c)^2$. Note, however, that those values are found in the parallel perpendicular plane in reference to the isoscalar helicity nonflip amplitude has been taken as the parallel component. There these values are determined by Ambats et al. with a precision which is in doubt. The value of the crossover is known in this plane with an accuracy up to .025 and placed at $t/ = .15 (\text{GeV}/c)^2$. The crossover into the complex plane requires a model for the phase of the reference amplitude. One assumption about this phase is taken by Ambats et al have taken it, that the phase of the isoscalar nonflip amplitude behaves in a very similar fashion to the helicity flip amplitude. It rotates anticlockwise with the velocity of a regge pole starting by being out of phase of about 60° which amounts to

This initial value and its sense of rotation agrees with dispersion relations. This assumption is only reliable for a value of about $t = .35$ (GeV/c). For larger values in t however, a rotation in the opposite direction seems to occur such that the amplitude crosses the positive imaginary axis at about $.84/t \approx 1.00$ into the first quadrant again. This is not involving elastic scattering as an absorptive factor, which takes in form of an appropriate parameterization of the isoscalar amplitude into account can satisfy within the frame of strong absorption a positive polarization. Our final aim, however, is to construct both isospin amplitudes out of poles with the correct absorption properties. This absorption, if applied to a complicated effective Pomeron, seems to lead occasionally to correct results in some cases. This generally involves a great number of parameters whose origin remains unknown (10). On the other hand, the residues of the pomeron quasi eikonalise and complicate the regge residues of the rho-pole and quasi eikonalise. The introduction of t dependent shower factors and in this way obtain a satisfying description for the pion-nucleon range in t up to $t = 2.00$ (GeV/c)² and for different energies as accomplished within the frame of Gribov-Sh.H. Eremyan (23). This is the best description ever achieved. The number of parameters is still great and we are searching for an alternative, which hopefully would result in less parameters or, if not, then at least those parameters which are less obscure. We are going to gradually build up such a model. At this stage we have discussed the weak cut absorption by assuming a simple form of the elastic scattering amplitude - namely the Pomeron - purely imaginary and fixed pole and the effective amplitude namely the total isoscalar amplitude itself. The isovector amplitude through the process of absorption.

The incorrect relative phase between the two helicity amplitudes as seen in fig. 5 causes the polarization to be wrong. Note the proportionality between fig. 2 and fig. 5. Fig. 3 also shows the modulus of the helicity flip amplitude with a distinct minimum due to the NWSZ though it is shifted down to .55, the actual position of the dip. Note that the helicity nonflip amplitude which is the cause of the wrong polarization. The phase of the helicity flip amplitude is $t = .35$ or $.4$, in accordance with the amplitude analysis. Fig. 6 and fig. 7 visualise the amplitudes at $t = .35$ and demonstrate suggestively the rotation and shrinking properties of the pole before and after absorption. Fig. 8a shows the acceleration of the pole due to absorption in anticlockwise direction and observe the little effect absorption has on the flip pole at small t . We have in fig. 8b enlarged the Argand diagram of fig. 8a for larger values of t/n . This will be particularly relevant in the case of the helicity flip amplitude displayed in the Argand diagram. The amplitude is governed by the elastic polarization unambiguously known up to $t = 2.00$. Elastic polarization is the rise and fall of models in strong interactions.

Traditional reggeized Absorption model at fixed energy: (fixed energy is indicated through hats on the reggeons)

The Pomeron is s-channel helicity conserving, purely imaginary and stationary.

Helicity non-flip - (Non-rotating part of the cut)

(Rotating part of the cut)

$$\chi_1^{00} = \frac{\lambda_{\text{cut}}^0 \hat{\beta}_{\beta_1}^0 \hat{\beta}_P^0}{2\sqrt{\pi} (\text{Re} \hat{\lambda}_P^0 + \hat{\lambda}_{\beta_1}^0)}$$

$$\chi_2^{00} = \frac{\lambda_{\text{cut}}^0 \hat{\beta}_P^0 \hat{\beta}_{\beta_1}^0}{2\sqrt{\pi} \{ (\text{Re} \hat{\lambda}_P^0 + \hat{\lambda}_{\beta_1}^0)^2 + (\text{Im} \hat{\lambda}_P^0)^2 \}}$$

$$\phi_1^{00} = 0$$

$$\phi_2^{00} = -\pi \alpha_P(0) - \text{arctg} \frac{-\text{Im} \hat{\lambda}_P^0}{\text{Re} \hat{\lambda}_P^0}$$

$$\Psi_1^{00} = \frac{\text{Re} \hat{\lambda}_P^0 \hat{\lambda}_{\beta_1}^0}{\text{Re} \hat{\lambda}_P^0 + \hat{\lambda}_{\beta_1}^0}$$

$$\Psi_2^{00} = \frac{\text{Re} \hat{\lambda}_P^0 \{ \hat{\lambda}_{\beta_1}^0 (\text{Re} \hat{\lambda}_P^0 + \hat{\lambda}_{\beta_1}^0) \}}{(\text{Re} \hat{\lambda}_P^0 + \hat{\lambda}_{\beta_1}^0)^2 + (\text{Im} \hat{\lambda}_P^0)^2}$$

$$\Phi_1^{00} = 0$$

$$\Phi_2^{00} = \frac{-\pi \alpha_P' \text{Re} \hat{\lambda}_P^0}{(\text{Re} \hat{\lambda}_P^0 + \hat{\lambda}_{\beta_1}^0)^2 + (\text{Im} \hat{\lambda}_P^0)^2}$$

Traditional reggeized Absorption model at fixed energy

(fixed energy is indicated through hats on the relevant parameters, see Table I for parameter values).

The Pomeron is s-channel helicity conserving, purely imaginary and stationary

Helicity flip - (Non-rotating part of the cut)

(Rotating part of the cut)

$$\zeta_1^{01} = \frac{\lambda_{cut} \hat{\beta}_P^0 \hat{\beta}_P^1 \text{Re} \hat{\lambda}_P^0}{2\sqrt{\pi} (\text{Re} \hat{\lambda}_P^0 + \hat{\lambda}_P^1)^2}$$

$$\zeta_2^{01} = \frac{\lambda_{cut} \hat{\beta}_P^0 \hat{\beta}_P^1 \text{Re} \hat{\lambda}_P^0}{2\sqrt{\pi} \{ (\text{Re} \hat{\lambda}_P^0 + \hat{\lambda}_P^1)^2 \}}$$

$$\phi_1^{01} = 0$$

$$\phi_2^{01} = -\pi \alpha_P(0) - 2 \arctan \dots$$

$$\psi_1^{01} = \frac{\text{Re} \hat{\lambda}_P^0 \hat{\lambda}_P^1}{\text{Re} \hat{\lambda}_P^0 + \hat{\lambda}_P^1}$$

$$\psi_2^{01} = \frac{\text{Re} \hat{\lambda}_P^0 \{ \hat{\lambda}_P^1 (\text{Re} \hat{\lambda}_P^0 + \dots) \}}{(\text{Re} \hat{\lambda}_P^0 + \hat{\lambda}_P^1)^2}$$

$$\Phi_1^{01} = 0$$

$$\Phi_2^{01} = \frac{-\pi \alpha_P (\text{Re} \hat{\lambda}_P^0 + \dots)}{(\text{Re} \hat{\lambda}_P^0 + \hat{\lambda}_P^1)^2 + \dots}$$

TABLE I
Model 0a

The parameters of the traditional reggeized absorption model used as a set of parameters. We introduce in several model variants a correlation between the exchanged Regge Pomeron and measure this correlation with respect to this fixed set of parameters of the traditional absorption model. The given values of the parameters are not determined by a minimization procedure. They nevertheless provide a reasonable choice to start a discussion about the mechanism of the correlation as set against the independent parameters typical for the traditional absorption. (The indices β for Rho Regge pole and

Parameter type		Value	Unit	Parameter type	Value
Inc. lab momentum	P_{lab}	6.00	GeV/c	Residue slope	$\hat{\lambda}_\rho^0$
Tot. c. m. energy	S	12.163	(GeV/c) ²	Initial Pomeron phase	δ_ρ^0
Energy scale	S_0	1.00	(GeV/c) ²	Correlation real part	$Re c^0$
Intercept of trajectory	$\alpha_\rho^{(0)}$.52		Correlation imaginary part	$Im c^0$
Slope of trajectory	α_ρ'	.804	(GeV/c) ⁻²	Cut enhancement	λ_{cut}^0
Residue const.	$\hat{\beta}_\rho^0$.431	$\frac{\sqrt{s_{mb}}}{GeV/c}$	Helicity flip	$\hat{\beta}_\rho^1$
Residue slope	$\hat{\lambda}_\rho^0$	8.00	(GeV/c) ⁻²	Helicity flip	$\hat{\lambda}_\rho^1$
Intercept of trajectory	$\alpha_\rho^{(0)1}$	1.00		Helicity flip	$'Re c^1$
Slope of trajectory	$\alpha_\rho'^1$	0.00	(GeV/c) ⁻²	Helicity flip	$Im c^1$
Residue const.	$\hat{\beta}_\rho^0$	6.16	$\frac{\sqrt{s_{mb}}}{GeV/c}$	Helicity flip	λ_{cut}^1

Traditional Absorption model (parameters from Table I)

$$T_{\rho}^{\circ} = .958 \sin \frac{\pi}{2} (.52 - .804 |t|) e^{-8.00 |t|} e^{i(43.20^{\circ} + 72.36^{\circ} |t|)}$$

$$T_{c}^{\circ\circ} = -.071 e^{-2.53 |t|} e^{i(0.00^{\circ} + 0.00^{\circ} |t|)} \\ + .07 e^{-2.58 |t|} e^{i(-81.36^{\circ} + 13.8^{\circ} |t|)}$$

$$T_{\rho}^I = 4.75 (|t|)^{1/2} \sin \frac{\pi}{2} (.52 - .804 |t|) e^{-4.00 |t|} e^{i(43.20^{\circ} + 72.36^{\circ} |t|)}$$

$$T_{c}^{oI} = -.257 (|t|)^{1/2} e^{-1.92 |t|} e^{i(0.00^{\circ} + 0.00^{\circ} |t|)} \\ + .233 (|t|)^{1/2} e^{-2.09 |t|} e^{i(-57.36^{\circ} + 36.4^{\circ} |t|)}$$

TABLE IIa Traditional Absorption model (helicity nonflip amplitudes given in $(\text{mb})^{1/2}/\text{GeV}/c$)

$ t = 0$	$ t = .05$	$ t = .15$
$T_p^0 = .621 e^{i 43.20^\circ}$	$= .395 e^{i 46.89^\circ}$	$= .152 e^{i 54.1^\circ}$
$T_c = .083 e^{i 228.52^\circ}$	$= .073 e^{i 228.72^\circ}$	$= .056 e^{i 22^\circ}$
$T_{th} = .546 e^{i 42.39^\circ}$	$= .322 e^{i 46.47^\circ}$	$= .096 e^{i 56^\circ}$
$T_{\text{hyp}} = .607 e^{i 38.79^\circ}$	$= .302 e^{i 39.00^\circ}$	$= .100 e^{i 28^\circ}$
$ t = .25$	$ t = .35$	$ t = .45$
$T_p^0 = .056 e^{i 61.29^\circ}$	$= .026 e^{i 68.53^\circ}$	$= .0057 e^{i 7^\circ}$
$T_c = .042 e^{i 229.7^\circ}$	$= .032 e^{i 230.18^\circ}$	$= .0243 e^{i 2^\circ}$
$T_{th} = .017 e^{i 91.98^\circ}$	$= .01 e^{i 82.68^\circ}$	$= .02 e^{i 2^\circ}$
$T_{\text{hyp}} = .074 e^{-i 90.00^\circ}$	$= .084 e^{-i 96.00^\circ}$	$= .063 e^{i 1^\circ}$

TABLE IIa Traditional Absorption model (helicity nonflip amplitudes given in $(\text{mb})^{1/2}/\text{GeV}/c$)

	<u>$t = .55$</u>	<u>$t = .65$</u>	<u>$t = .8$</u>
T_P	$= .001 e^{i 83.00^\circ}$	$= .00$	$= .00$
T_C	$= .0186 e^{i 230.91^\circ}$	$= .014 e^{i 230.15^\circ}$	$= .0097 e^{i ?}$
T_{t_4}	$= .0179 e^{i 229.09^\circ}$	$= .014 e^{i 230.19^\circ}$	$= .0097 e^{i ?}$
T_{ep}	$= .055 e^{i ?}$	$= ?$	$= ?$

TABLE II b Traditional Absorption model (helicity flip amplitudes given in $(\text{mb})^{1/2}/\text{GeV}/c$)

	<u>$t = .05$</u>	<u>$t = .15$</u>	<u>$t = .25$</u>	<u>$t = .35$</u>
T_{ρ}^1	$.626 e^{i 44.82^\circ}$	$.623 e^{i 54.05^\circ}$	$.441 e^{i 61.29^\circ}$	$.267 e^{i 6^\circ}$
T_C^{01}	$.049 e^{i 236.31^\circ}$	$.066 e^{i 235.8^\circ}$	$.066 e^{i 235.8^\circ}$	$.061 e^{i 23^\circ}$
T_{th}^1	$.578 e^{i 46.03^\circ}$	$.557 e^{i 53.85^\circ}$	$.375 e^{i 62.16^\circ}$	$.208 e^{i 72^\circ}$
$T_{\rho p}^1$	$.578 e^{i 48.10^\circ}$	$.502 e^{i 56.62^\circ}$	$.319 e^{i 66.57^\circ}$	$.176 e^{i 74^\circ}$
	<u>$t = .45$</u>	<u>$t = .55$</u>	<u>$t = .65$</u>	
T_{ρ}^1	$.136 e^{i 75.76^\circ}$	$.050 e^{i 83.00^\circ}$	$.001 e^{i 90.21^\circ}$	
T_C^{01}	$.053 e^{i 235.44^\circ}$	$.046 e^{i 234.61^\circ}$	$.039 e^{i 234.253^\circ}$	
T_{th}	$.081 e^{i 88.09^\circ}$	$.023 e^{i 119.75^\circ}$	$.039 e^{i 235.13^\circ}$	
$T_{\rho p}$	$.094 e^{i ?^\circ}$	$.074 e^{i ?^\circ}$	$?$	

TABLE IIc Polarization Chart (traditional reggeized Absorption model with parameters from Table I). Real and imaginary part of the helicity amplitudes are arranged according to $Polarization = -2ImT^0 T^1 / \text{differential cross section}$

$ t $	$Re T^0 \times Im T^1$	$- Im T^0 \times Re T^1$	t_1	$\frac{d\sigma}{dt}$	ϵ_p
.00	.403 × .00	- .368 × .00	.298	.362 ± .07	.
.05	.222 × .387	- .231 × .373	.393	.423 ± .03	-
.15	.053 × .419	- .08 × .306	.278	.266 ± .02	-
.25	- .001 × .309	- .017 × .163	.122	.110 ± .012	--
.35	- .01 × .185	- (-.001) × .059	.038	.038 ± .004	-
.45	- .015 × .081	- (-.014) × .0027	.007	.013 ± .002	-
.55	- .012 × .021	- (-.014) × (-.012)	.00093	.0059 ± .0011	-
.65	- .009 × (-.032)	- (-.011) × (-.023)	.0017	.0059 ± .0011	+
.8	- .005 × (-.057)	- (-.008) × (-.011)	.0035	.0082 ± .0009	+

TABLE III Polarization chart analogous to Table IIc with one difference - λ cut = 2.00
The boost factor improves the differential cross section - but not the polarization

k_1	$Re T^0 - J^0 T^0$	$- Im T^0 Re T^0$	$\frac{d\sigma/d\Omega}{\mu\mu}$	P	
.00	.405 x .00	- .357 x .00	.291	.362 ± .07	.00
.05	.204 x .402	- .21 x .401	.408	.423 ± .03	-.010
.15	.02 x .425	- .048 x .313	.481	.266 ± .02	-.046
.25	-.032 x .484	- (-.0179) x .1372	.112	.110 ± .12	-.124
.35	-.04 x .158	- (-.036) x .0315	.029	.038 ± .004	-.358
.45	-.034 x .0475	- (-.036) (-.0294)	.0057	.013 ± .002	-.96
.55	-.027 (-.0263)	- (-.0315) (-.0503)	.005	.0055 ± .001	-.919
.65	-.0126 (-.0693)	- (-.0149) (-.0443)	.0077	.0055 ± .001	-.606
.8	-.0126 (-.0753)	- (-.0149) (-.0303)	.0077	.0082 ± .001	-.402

TABLE IIe In order to show that the failure of traditional absorption is mainly due to the amplitude as far as the polarization is concerned (this applies in particular for ρ_{pp} if we combine the theoretical helicity flip values with the helicity nonflip values of et al (Model for isoscalar had to be used however)

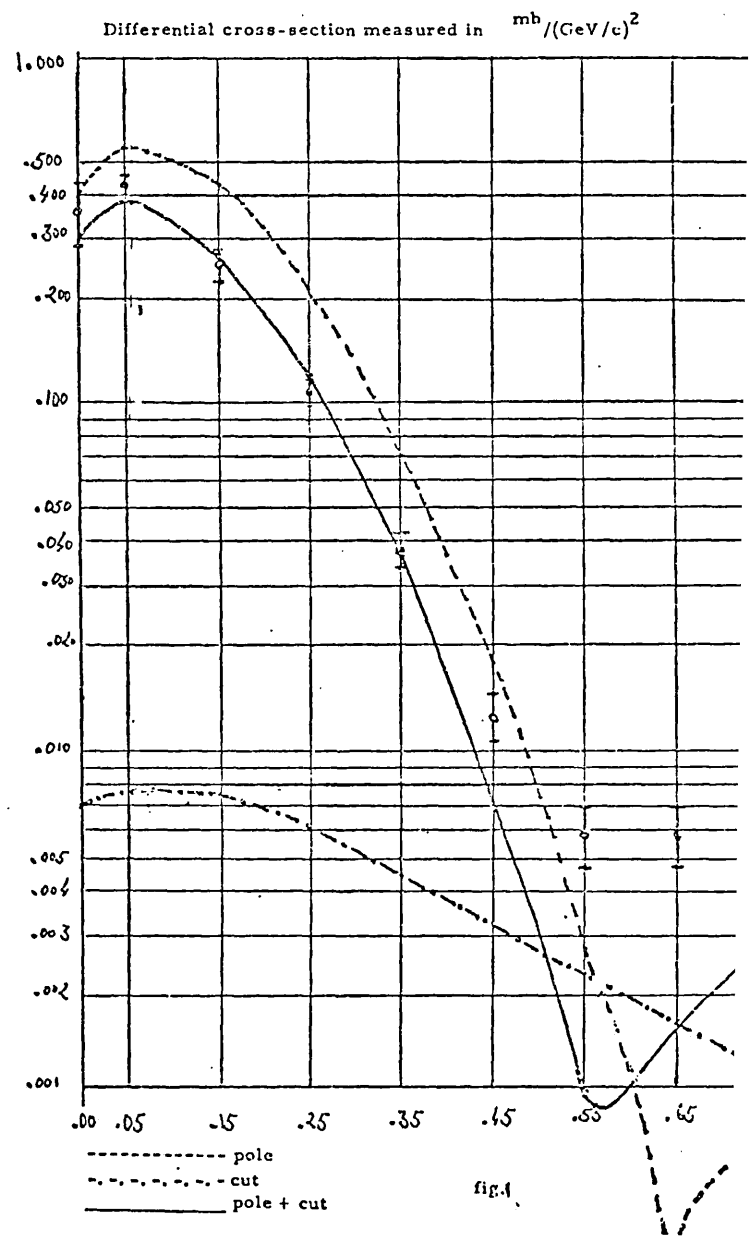
t	$Re T^0 J T^1 - J T^0 Re T^1$		d^0/dt	
	ρ_{pp}	ρ_{pp}	ρ_{pp}	ρ_{pp}
.00	.473 x .00	- .380 x .00	.367	-.362 ± .07
.05	.235 x .387	- .190 x .373	.380	.423 ± .07
.15	.088 x .419	- .048 x .306	.279	.266 ± .05
.25	.00 x .309	- (-.074) .163	.127	-.110 ± .02
.35	-.009 x .165	- (-.084) .255	.045	-.038 ± .008
.45	.0169 x .071	- (-.019) .0027	.011	-.013 ± .002
.55	.034 x .021	- (-.018) (-.012)	.0036	.0055

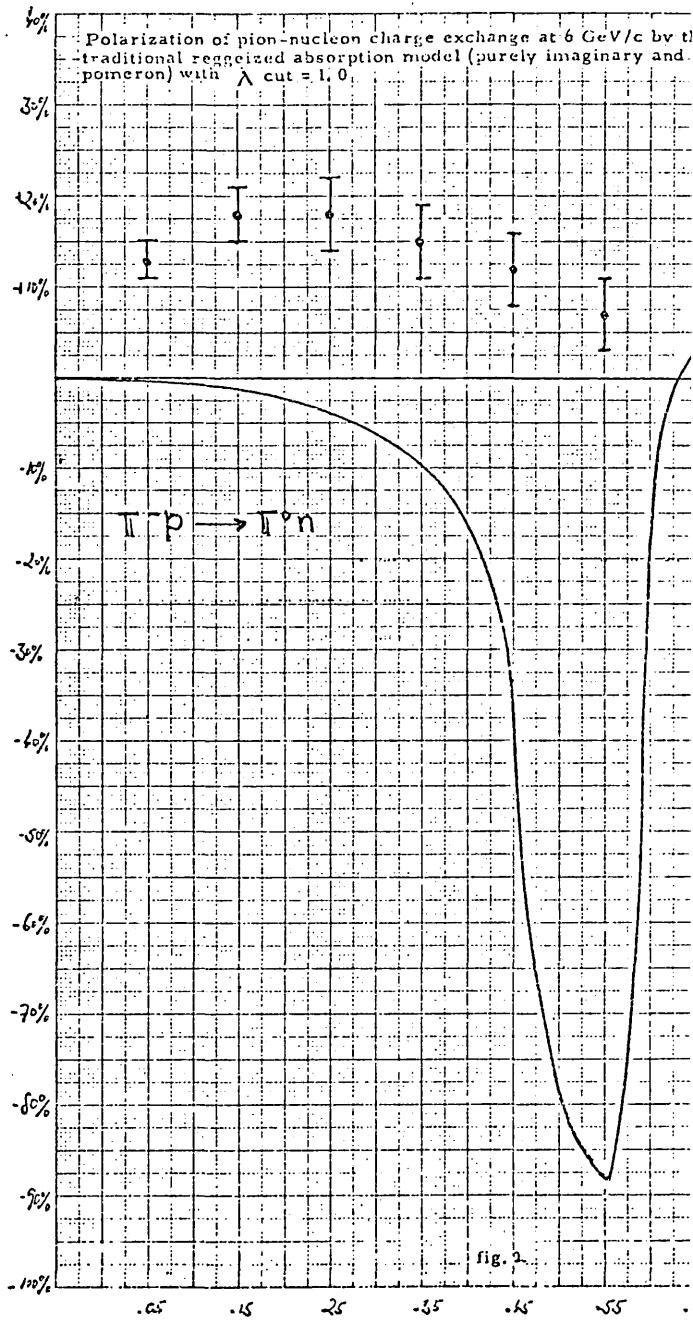
MODEL Ia Elastic chart

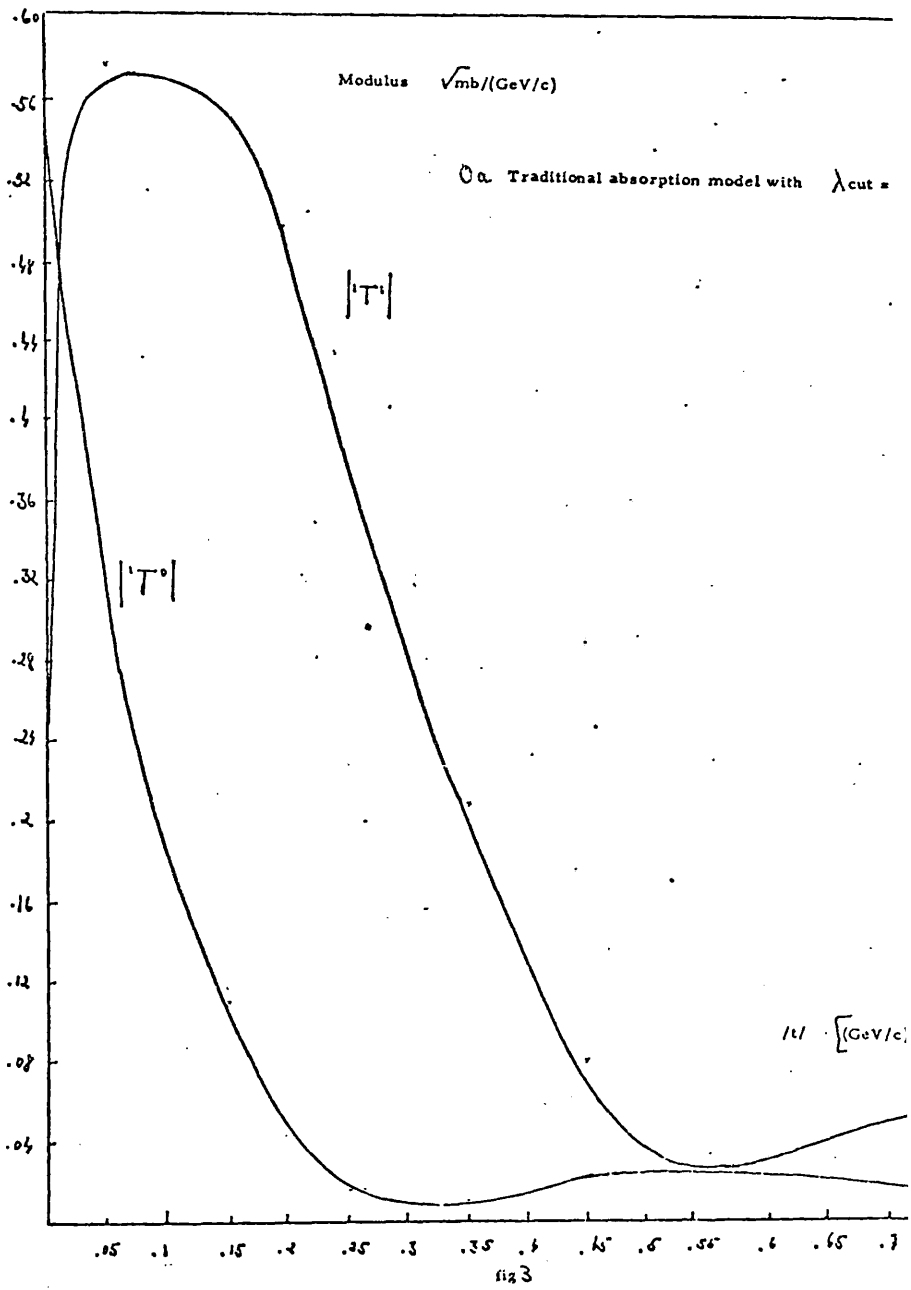
	$\bar{J}_m^0 T^0 \times Re^1 T^1$	$d\delta^+ / dt$	$d\delta^- / dt$	P^+
.00	6.16 x .00	33.71	42.78	.00
.05	5.12 x .373	24.21	29.00	.158
.15	3.54 x .306	12.24	13.38	.177
.25	2.443 x .163	6.01	6.01	.133
.35	1.65 x .055	2.89	2.85	.069
.45	1.17 x .027	1.38	1.37	.005
.55	.805 x (-.012)	.645	.645	-.03
.65	.556 x (-.023)	.311	.311	-.022
.8	.319 x (-.011)	.105	.105	-.062
1.00	.152 x .004	.026	.026	.047
1.2	-.073 x .010	.006	.006	.243
1.5	.024 x .006	.001	.001	.288
2.00	.004 x (-.001)	.00002	.00002	-.4

Data

0a. Traditional reggeized absorption model with λ cut = 1.00







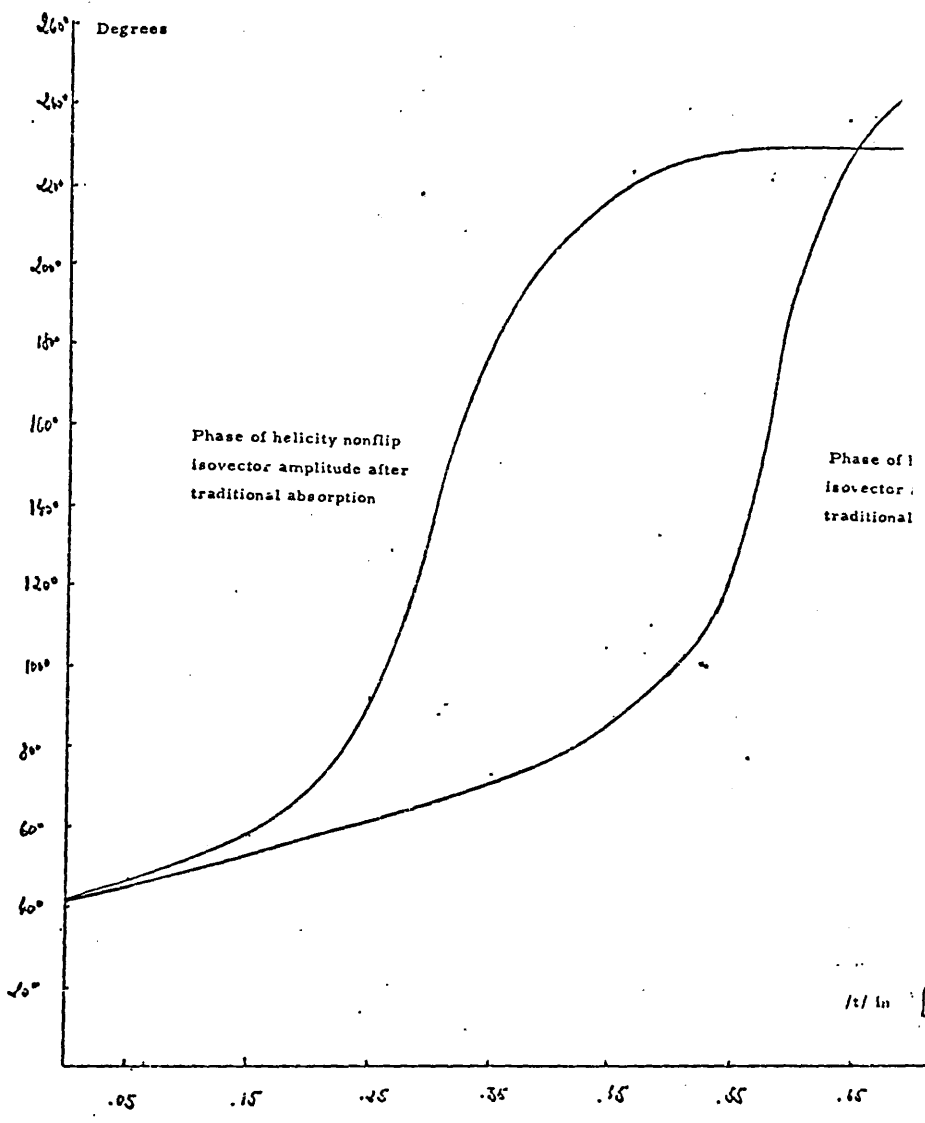
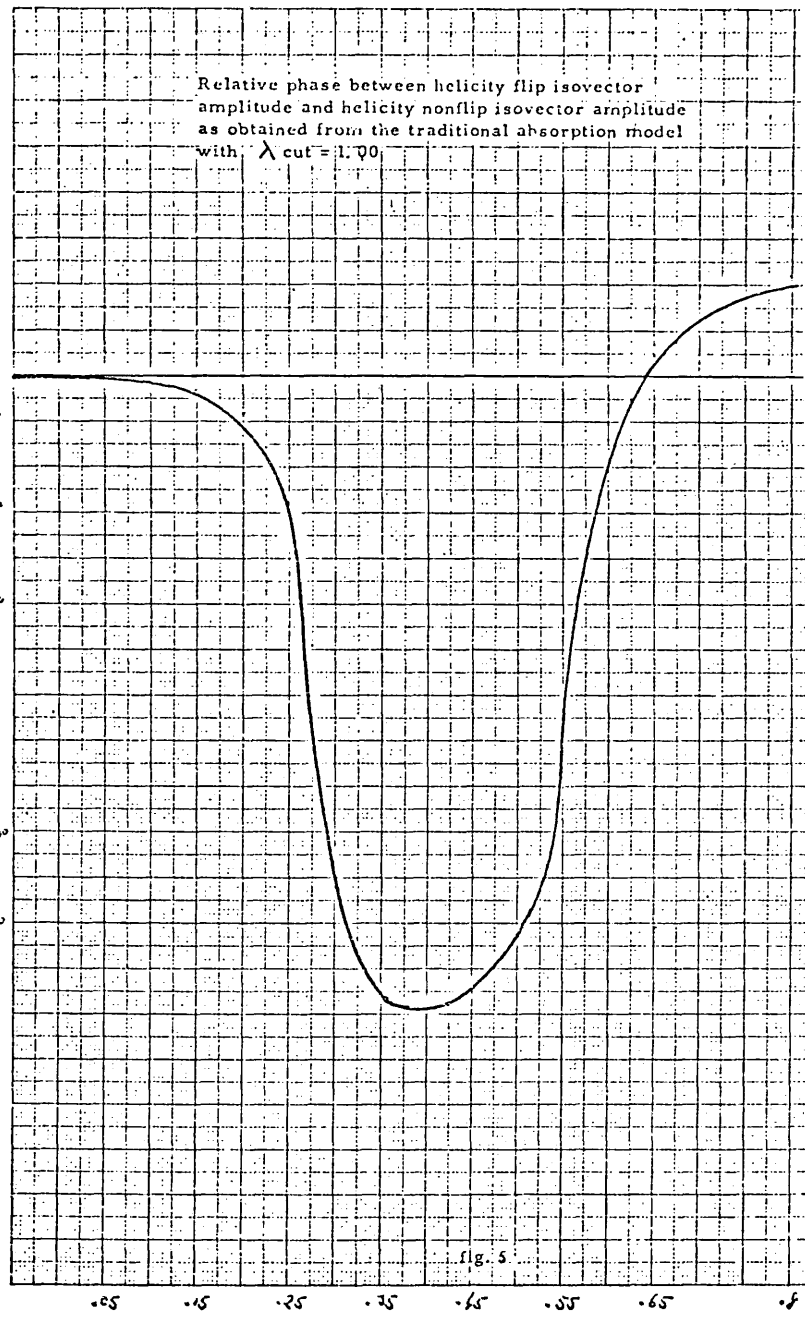


fig 4



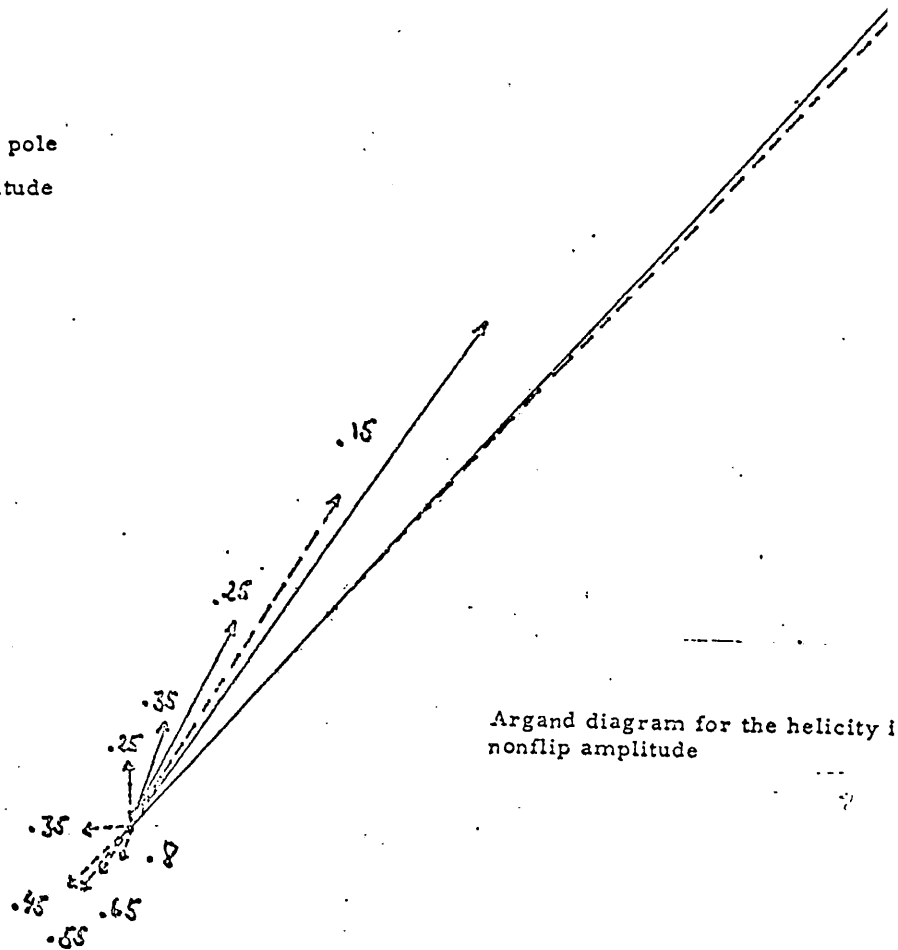
Traditional absorption model (purely imaginary and stationary Pomeron
and λ cut = 1.00)

See Table IIa for numerical values

—————→ Helicity nonflip pole
- - - - -→ Absorbed amplitude

Numbers indicate $|t|$ values

Scale -
1 cm = $.019(\text{mb})^{1/2}/\text{GeV}/c$



Argand diagram for the helicity nonflip amplitude

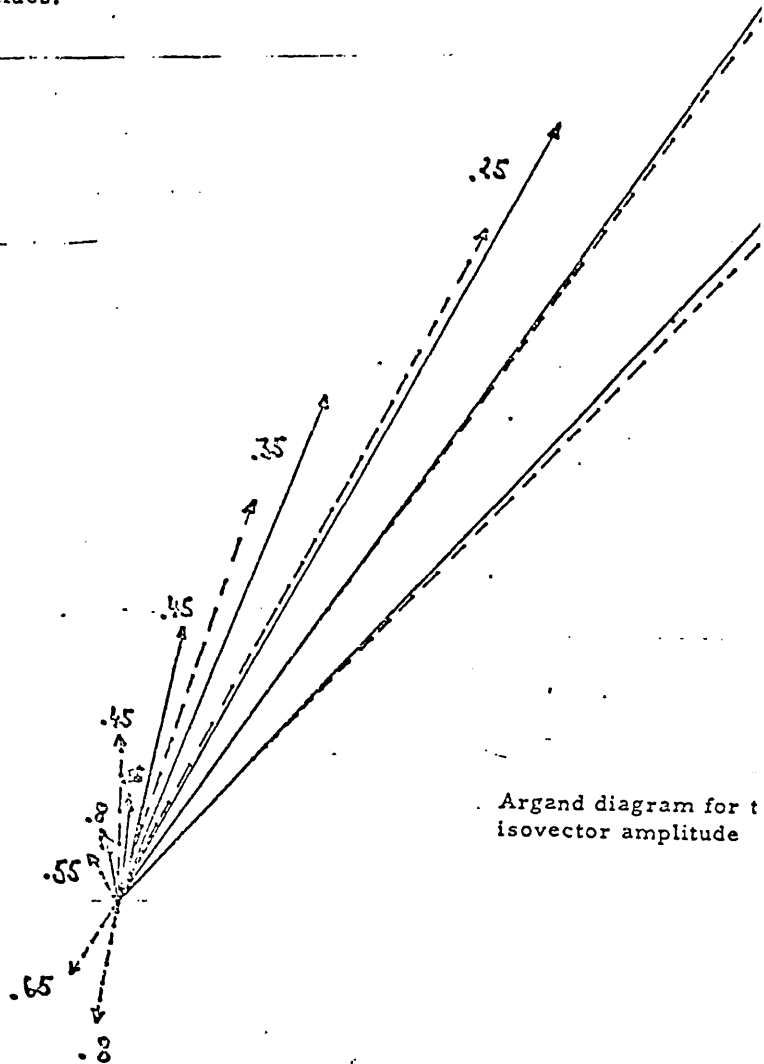
Traditional absorption model (purely imaginary and stationary Pomeron and λ cut = 1.00)

See Table IIb for numerical values.

—————→ Helicity flip pole
-----→ Absorbed amplitude

Numbers indicate $|t|$ values

Scale -
1 cm = $.038(\text{mb})^{1/2}/\text{GeV}/c$



Argand diagram for t isovector amplitude

fig 7

Argand diagram for the helicity nonflip isovector amplitude obtained with the help of traditional absorption model (purely imaginary and stationary Pomeron and λ cut =

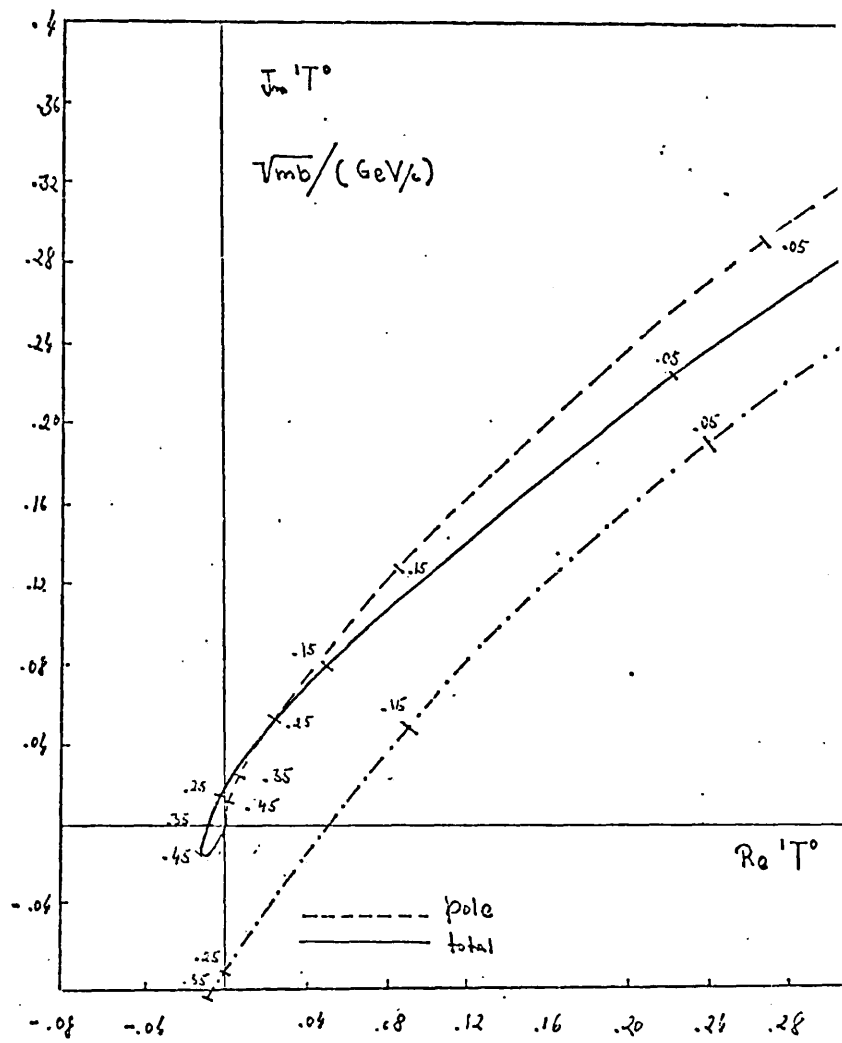


fig 8a

Previous diagram for the helicity nonflip isovector amplitude enlarged for large t region

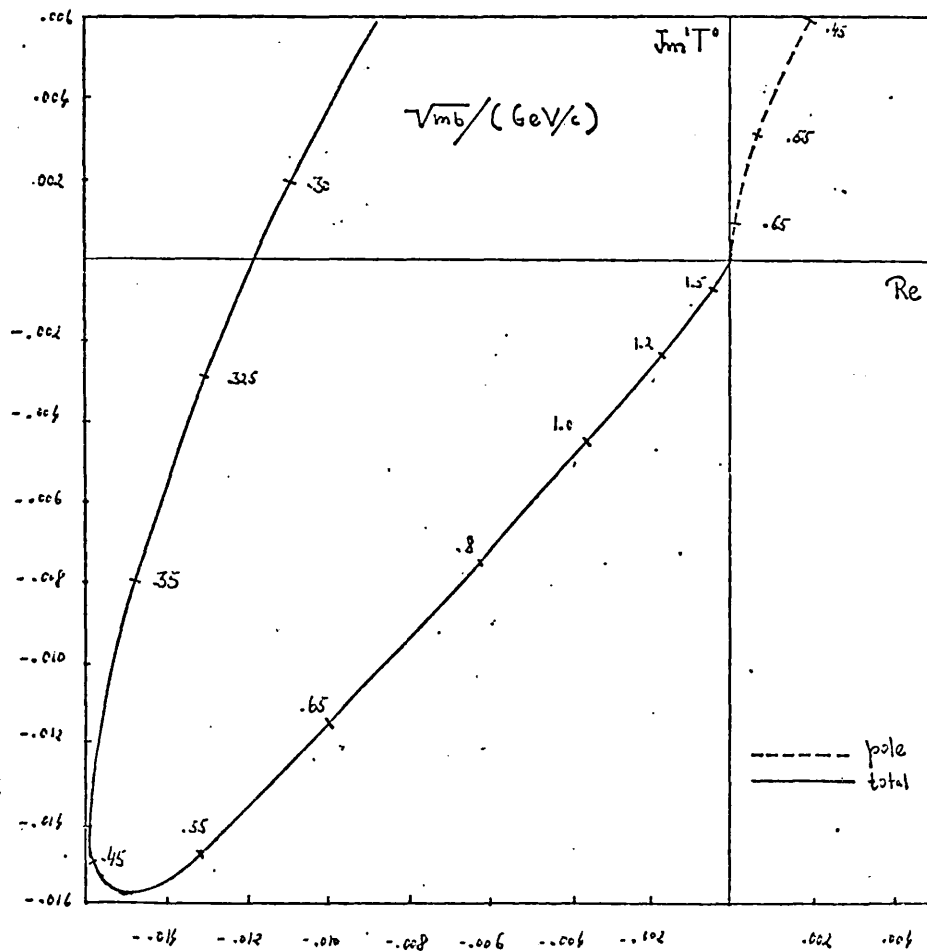


fig 8b

Argand diagram for the helicity flip isovector amplitude for small $t/$ of traditional absorption model (purely imaginary and stationary Pomeron). The numbers on the curve indicate values in $t/$.

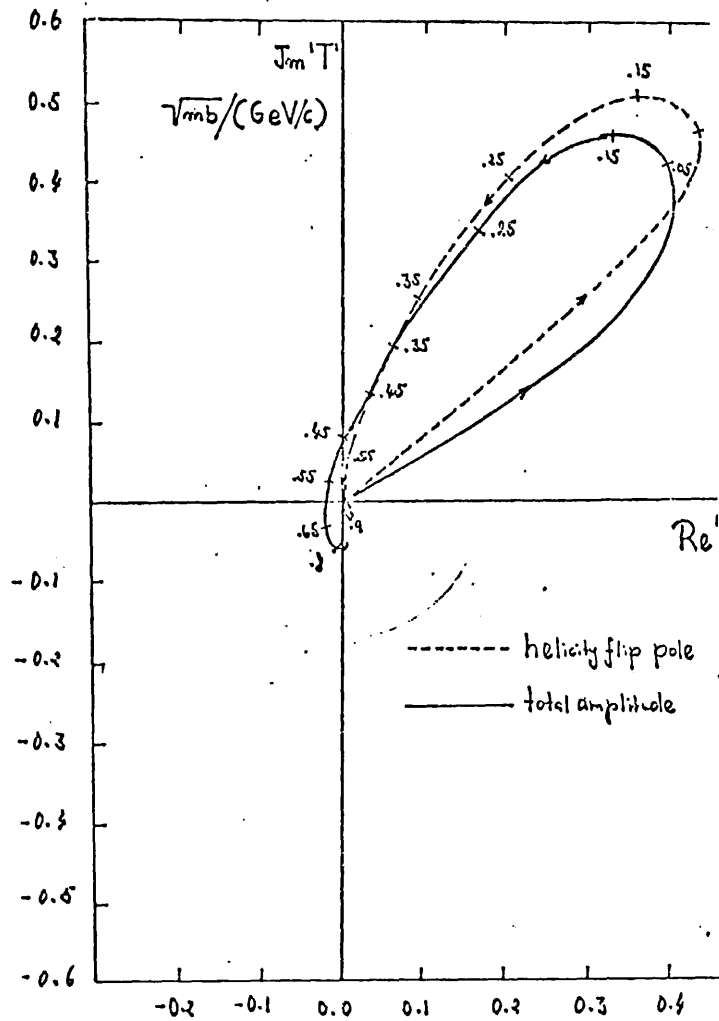
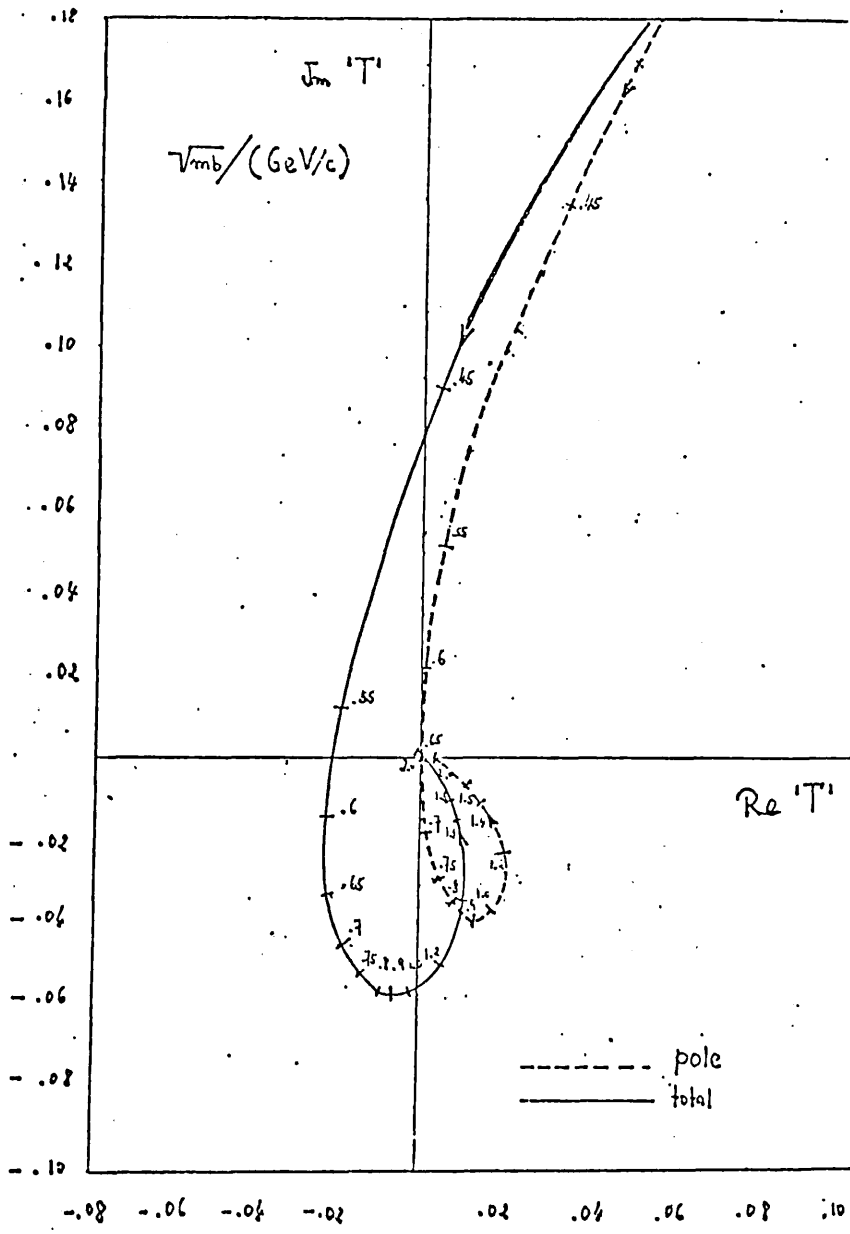


Fig. 9a

Previous diagram for helicity flip isovector amplitude enlarged for large t/t' region



VI. 11 - The Gribov Cut represented as vector in the Argand Diagram

The parameterization of the cut allows for a moving helicity conserving Pomeron with real part in forward direction. correlation parameter c can be helicity dependent and has a slow energy dependence in order to stabilize a possible dependence of the phase. The actual values of the parameters give rise to a set of models, out of which we choose the one that satisfies the optimum between theoretical constraints and phenomenological necessity.

Helicity non-flip cut $T_{cut}^{00}(s, s_0, \lambda_{cut}^0, \beta_p^0, \lambda_p^0, \alpha_p^0, \alpha_p^{(0)}, \beta_p^0, \lambda_p^0, \alpha_p^0, \delta_p^0, Re c_1^0, Re c_2^0, Im c_1^0, Im c_2^0)$

$$= - \sum_1^{\psi^{00}} e^{-\Psi_1^0 |t|} e^{i(\phi_1^0 - \Phi_1^0 |t|)} + \sum_2^{\psi^{00}} e^{-\Psi_2^0 |t|} e^{i(\phi_2^0 - \Phi_2^0 |t|)}$$

Helicity flip cut $T_{cut}^{01}(s, s_0, \lambda_{cut}^1, \beta_p^1, \lambda_p^1, \alpha_p^1, \alpha_p^{(0)}, \beta_p^0, \lambda_p^0, \alpha_p^0, \delta_p^0, Re c_1^1, Re c_2^1, Im c_1^1, Im c_2^1)$

$$= - \sum_1^{\psi^{01}} (|t|)^{1/2} e^{-\Psi_1^1 |t|} e^{i(\phi_1^1 - \Phi_1^1 |t|)} + \sum_2^{\psi^{01}} (|t|)^{1/2} e^{-\Psi_2^1 |t|} e^{i(\phi_2^1 - \Phi_2^1 |t|)}$$

We have split the cut into "non rotating" and "rotating" vectors in the complex plane indicated by 1 and 2 respectively.

Their explicit dependence on all parameters involved is as follows -

Strength of the "non rotating part" of the helicity non flip cut in forward direction

$$\sum_1^{\infty} = \frac{(2\sqrt{\pi})^{-1} \lambda_{cut}^0 \beta_p^0 \beta_p^0 (s/s_0)^{\alpha_p(0)-1}}{\left\{ (\lambda_p^0 + \alpha_p' \ln(s/s_0) + \lambda_p^0 + \alpha_p' \ln(s/s_0) + 4 \operatorname{Re}(c_1^0 + c_2^0 \ln(s/s_0)))^2 + (4 \operatorname{Im}(c_1^0 + c_2^0 \ln(s/s_0)))^2 \right\}}$$

Strength of the "rotating part" of the helicity non flip cut in forward direction

$$\sum_2^{\infty} = \frac{(2\sqrt{\pi})^{-1} \lambda_{cut}^0 \beta_p^0 \beta_p^0 (s/s_0)^{\alpha_p(0)-1}}{\left\{ (\lambda_p^0 + \alpha_p' \ln(s/s_0) + \lambda_p^0 + \alpha_p' \ln(s/s_0) + 4 \operatorname{Re}(c_1^0 + c_2^0 \ln(s/s_0)))^2 + (4 \operatorname{Im}(c_1^0 + c_2^0 \ln(s/s_0)))^2 - (\pi \alpha_p) \right\}}$$

Slope of the exponential fall off with /t/ of the strength of the non rotating part of the helicity non flip cut

$$\begin{aligned}
 \Psi_1^{\infty} = & \left[\left\{ (\lambda_p^0 + \alpha_p' \ln(s/s_0)) (\lambda_p^0 + \alpha_p' \ln(s/s_0)) + \operatorname{Re} (c_1 + c_2 \ln(s/s_0)) (\lambda_p^0 + \alpha_p' \ln(s/s_0)) + \lambda_p^0 + \alpha_p' \ln(s/s_0) \right. \right. \\
 & \left. \left. + \operatorname{Im} (c_1 + c_2 \ln(s/s_0)) \frac{\pi \alpha_p'}{2} \right\} \left\{ \lambda_p^0 + \alpha_p' \ln(s/s_0) + \lambda_p^0 + \alpha_p' \ln(s/s_0) + 4 \operatorname{Re} (c_1 + c_2 \ln(s/s_0)) \right. \right. \\
 & \left. \left. + \left\{ \operatorname{Im} (c_1 + c_2 \ln(s/s_0)) (\lambda_p^0 + \alpha_p' \ln(s/s_0)) + \lambda_p^0 + \alpha_p' \ln(s/s_0) - \frac{\pi \alpha_p'}{2} (\lambda_p^0 + \alpha_p' \ln(s/s_0)) \right. \right. \right. \\
 & \left. \left. + \operatorname{Re} (c_1 + c_2 \ln(s/s_0)) \right\} \left\{ 4 \operatorname{Im} (c_1 + c_2 \ln(s/s_0)) - \frac{\pi \alpha_p'}{2} \right\} \right] \left[\left\{ \lambda_p^0 + \alpha_p' \ln(s/s_0) \right. \right. \\
 & \left. \left. + \lambda_p^0 + \alpha_p' \ln(s/s_0) + 4 \operatorname{Re} (c_1 + c_2 \ln(s/s_0)) \right\}^2 + \left\{ 4 \operatorname{Im} (c_1 + c_2 \ln(s/s_0)) - \frac{\pi \alpha_p'}{2} \right\}^2 \right]
 \end{aligned}$$

Slope of the exponential fall-off with /t/ of the strength of the rotating part of the helicity non flip cut

$$\begin{aligned}
 \Psi_2^{\circ\circ} = & \left[\left\{ (\lambda_p^{\circ} + \alpha_p^{\circ} \ln(s/s_0)) (\lambda_p^{\circ} + \alpha_p^{\circ} \ln(s/s_0)) + \operatorname{Re} (c_1 + c_2 \ln(s/s_0)) (\lambda_p^{\circ} + \alpha_p^{\circ} \ln(s/s_0)) \right. \right. \\
 & \left. \left. + \lambda_p^{\circ} + \alpha_p^{\circ} \ln(s/s_0) \right\} + \operatorname{Im} (c_1 + c_2 \ln(s/s_0)) \left(\frac{\pi \alpha_p^{\circ}}{2} + \pi \alpha_p^{\circ} \right) - \pi \alpha_p^{\circ} \frac{\pi \alpha_p^{\circ}}{2} \right] \\
 & \cdot \left\{ \lambda_p^{\circ} + \alpha_p^{\circ} \ln(s/s_0) + \lambda_p^{\circ} + \alpha_p^{\circ} \ln(s/s_0) + \frac{1}{2} \operatorname{Re} (c_1 + c_2 \ln(s/s_0)) \right\} + \left\{ -\pi \alpha_p^{\circ} (\lambda_p^{\circ} + \right. \\
 & \left. + \operatorname{Re} (c_1 + c_2 \ln(s/s_0)) + \operatorname{Im} (c_1 + c_2 \ln(s/s_0)) (\lambda_p^{\circ} + \alpha_p^{\circ} \ln(s/s_0)) + \lambda_p^{\circ} + \alpha_p^{\circ} \ln(s/s_0) \right. \\
 & \left. - \frac{\pi \alpha_p^{\circ}}{2} (\lambda_p^{\circ} + \alpha_p^{\circ} \ln(s/s_0)) + \operatorname{Re} (c_1 + c_2 \ln(s/s_0)) \right\} \left\{ 4 \operatorname{Im} (c_1 + c_2 \ln(s/s_0)) \right. \\
 & \left. - (\pi \alpha_p^{\circ} + \frac{\pi \alpha_p^{\circ}}{2}) \right\} \left[\left\{ \lambda_p^{\circ} + \alpha_p^{\circ} \ln(s/s_0) + \lambda_p^{\circ} + \alpha_p^{\circ} \ln(s/s_0) + 4 \operatorname{Re} (c_1 + c_2 \ln(s/s_0)) \right. \right. \\
 & \left. \left. + \left\{ 4 \operatorname{Im} (c_1 + c_2 \ln(s/s_0)) - (\pi \alpha_p^{\circ} + \frac{\pi \alpha_p^{\circ}}{2}) \right\}^2 \right]^{-1}
 \end{aligned}$$

Initial angle of the "non rotating part" of the helicity non flip cut

$$\phi_1^{00} = \delta_P^0 - \pi/2 - \arctg \frac{4 \operatorname{Im} (c_1^0 + c_2^0 \ln(s/s_0)) - \frac{\pi \alpha'_P}{2}}{\lambda_P^0 + \alpha'_P \ln(s/s_0) + \lambda_J^0 + \alpha'_J \ln(s/s_0) + 4 \operatorname{Re} (c_1^0 + c_2^0 \ln(s/s_0))}$$

Initial angle of the "rotating part" of the helicity non flip cut

$$\phi_2^{00} = -\pi \alpha'_g(0) + \delta_P^0 - \pi/2 - \arctg \frac{4 \operatorname{Im} (c_1^0 + c_2^0 \ln(s/s_0)) - (\pi \alpha'_g + \frac{\pi \alpha'_P}{2})}{\lambda_P^0 + \alpha'_P \ln(s/s_0) + \lambda_J^0 + \alpha'_J \ln(s/s_0) + 4 \operatorname{Re} (c_1^0 + c_2^0 \ln(s/s_0))}$$

Rotation velocity per /t/ of the "non rotating part" of the helicity non flip cut

$$\begin{aligned}
 \Phi_1^{00} = & \left[\left\{ \text{Im} (c_1^0 + c_2^0 \ln(s/s_0)) (\lambda_p^0 + \alpha_p' \ln(s/s_0) + \lambda_p^0 + \alpha_p' \ln(s/s_0)) - \frac{\pi \alpha_p'}{2} (\lambda_p^0 + \right. \right. \\
 & \left. \left. + \alpha_p' \ln(s/s_0) + \text{Re} (c_1^0 + c_2^0 \ln(s/s_0)) \right\} \left\{ \lambda_p^0 + \alpha_p' \ln(s/s_0) + \lambda_p^0 + \right. \right. \\
 & \left. \left. + \alpha_p' \ln(s/s_0) + 4 \text{Re} (c_1^0 + c_2^0 \ln(s/s_0)) \right\} - \left\{ (\lambda_p^0 + \alpha_p' \ln(s/s_0)) + \right. \right. \\
 & \left. \left. + (\lambda_p^0 + \alpha_p' \ln(s/s_0)) + \text{Re} (c_1^0 + c_2^0 \ln(s/s_0)) (\lambda_p^0 + \alpha_p' \ln(s/s_0) + \lambda_p^0 + \right. \right. \\
 & \left. \left. + \alpha_p' \ln(s/s_0)) + \text{Im} (c_1^0 + c_2^0 \ln(s/s_0)) \frac{\pi \alpha_p'}{2} \right\} \left\{ 4 \text{Im} (c_1^0 + c_2^0 \ln(s/s_0)) - \frac{\pi \alpha_p'}{2} \right\} \\
 & \times \left[\left\{ \lambda_p^0 + \alpha_p' \ln(s/s_0) + \lambda_p^0 + \alpha_p' \ln(s/s_0) + 4 \text{Re} (c_1^0 + c_2^0 \ln(s/s_0)) \right\}^2 + \left\{ 4 \text{Im} (c_1^0 + c_2^0 \ln(s/s_0)) \right. \right. \\
 & \left. \left. - \frac{\pi \alpha_p'}{2} \right\}^2 \right]^{-1}
 \end{aligned}$$

Rotation velocity per /t/ of the "rotating part" of the helicity non flip cut

$$\begin{aligned}
 \Phi_{\alpha}^{\circ\circ} = & \left[\left\{ -\pi \alpha'_{\rho} (\lambda_{\rho}^{\circ} + \alpha'_{\rho} \ln(s/s_0) + \text{Re}(c_1 + c_2 \ln(s/s_0))) + \text{Im}(c_1 + c_2 \ln(s/s_0)) \right. \right. \\
 & \times (\lambda_{\rho}^{\circ} + \alpha'_{\rho} \ln(s/s_0) + \lambda_{\rho}^{\circ} + \alpha'_{\rho} \ln(s/s_0)) - \frac{\pi \alpha'_{\rho}}{2} (\lambda_{\rho}^{\circ} + \alpha'_{\rho} \ln(s/s_0) \\
 & + \text{Re}(c_1 + c_2 \ln(s/s_0))) \left. \right\} \left\{ \lambda_{\rho}^{\circ} + \alpha'_{\rho} \ln(s/s_0) + \lambda_{\rho}^{\circ} + \alpha'_{\rho} \ln(s/s_0) \right. \\
 & + 4 \text{Re}(c_1 + c_2 \ln(s/s_0)) \left. \right\} - \left\{ (\lambda_{\rho}^{\circ} + \alpha'_{\rho} \ln(s/s_0)) (\lambda_{\rho}^{\circ} + \alpha'_{\rho} \ln(s/s_0)) \right. \\
 & + \text{Re}(c_1 + c_2 \ln(s/s_0)) (\lambda_{\rho}^{\circ} + \alpha'_{\rho} \ln(s/s_0) + \lambda_{\rho}^{\circ} + \alpha'_{\rho} \ln(s/s_0)) \\
 & + \text{Im}(c_1 + c_2 \ln(s/s_0)) (\pi \alpha'_{\rho} + \frac{\pi \alpha'_{\rho}}{2}) - \pi \alpha'_{\rho} \frac{\pi \alpha'_{\rho}}{2} \left. \right\} \left\{ 4 \text{Im}(c_1 + c_2 \ln(s/s_0)) \right. \\
 & - (\pi \alpha'_{\rho} + \frac{\pi \alpha'_{\rho}}{2}) \left. \right\} \left[\left\{ \lambda_{\rho}^{\circ} + \alpha'_{\rho} \ln(s/s_0) + \lambda_{\rho}^{\circ} + \alpha'_{\rho} \ln(s/s_0) + 4 \right. \right. \\
 & \left. \left. (c_1 + c_2 \ln(s/s_0)) \right\}^2 + \left\{ 4 \text{Im}(c_1 + c_2 \ln(s/s_0)) - (\pi \alpha'_{\rho} + \frac{\pi \alpha'_{\rho}}{2}) \right\} \right]
 \end{aligned}$$

Strength of the "non rotating part" of the helicity flip cut in forward direction

$$\left. \begin{matrix} c_1^{c_1} \\ \left. \right\} \\ 1 \end{matrix} \right\} = \frac{(\alpha \sqrt{s})^{-1} \lambda_{int}^1 \beta_P^0 \beta_P^1 \left\{ (\lambda_P^0 + \alpha_P^1 \ln(s/s_0) + 2 \operatorname{Re}(c_1 + c_2 \ln(s/s_0)))^2 + (2 \operatorname{Im}(c_1 + c_2 \ln(s/s_0)) - \frac{\pi}{2}) \right\}}{\left\{ \lambda_P^0 + \alpha_P^1 \ln(s/s_0) + \lambda_P^1 + \alpha_P^2 \ln(s/s_0) + 4 \operatorname{Re}(c_1 + c_2 \ln(s/s_0)) \right\}^2 + \left\{ 4 \operatorname{Im}(c_1 + c_2 \ln(s/s_0)) - \frac{\pi}{2} \right\}^2}$$

Strength of the "rotating part" of the helicity flip cut in forward direction

$$\left. \begin{matrix} c_2^{c_1} \\ \left. \right\} \\ 2 \end{matrix} \right\} = \frac{(\alpha \sqrt{s})^{-1} \lambda_{int}^1 \beta_P^0 \beta_P^1 \left\{ (\lambda_P^0 + \alpha_P^1 \ln(s/s_0) + 2 \operatorname{Re}(c_1 + c_2 \ln(s/s_0)))^2 + (2 \operatorname{Im}(c_1 + c_2 \ln(s/s_0)) - \frac{\pi}{2}) \right\}}{\left\{ \lambda_P^0 + \alpha_P^1 \ln(s/s_0) + \lambda_P^1 + \alpha_P^2 \ln(s/s_0) + 4 \operatorname{Re}(c_1 + c_2 \ln(s/s_0)) \right\}^2 + \left\{ 4 \operatorname{Im}(c_1 + c_2 \ln(s/s_0)) - \frac{\pi}{2} \right\}^2}$$

Slope of the exponential fall-off with /t/ of the strength of the non rotating part of the helicity flip cut

$$\begin{aligned}
 \underline{\Psi}_1^{01} = & \left[\left\{ (\lambda_p^0 + \alpha_p' \ln(s/s_0)) (\lambda_p^1 + \alpha_p' \ln(s/s_0)) + \operatorname{Re} (c_1' + c_2' \ln(s)) (\lambda_p^0 + \alpha_p' \ln(s) \right. \right. \\
 & + \lambda_p^1 + \alpha_p' \ln(s/s_0)) + \operatorname{Im} (c_1' + c_2' \ln(s/s_0)) \frac{\sqrt{s} \alpha_p'}{2} \left. \left. \right\} \left\{ \lambda_p^0 + \alpha_p' \ln(s/s_0) \right. \right. \\
 & + \lambda_p^1 + \alpha_p' \ln(s/s_0) + \operatorname{Re} (c_1' + c_2' \ln(s/s_0)) \left. \left. \right\} + \left\{ \operatorname{Im} (c_1' + c_2' \ln(s/s_0)) \right. \right. \\
 & \cdot (\lambda_p^0 + \alpha_p' \ln(s/s_0) + \lambda_p^1 + \alpha_p' \ln(s/s_0)) - \frac{\sqrt{s} \alpha_p'}{2} (\lambda_p^1 + \alpha_p' \ln(s/s_0)) \\
 & + \operatorname{Re} (c_1' + c_2' \ln(s/s_0)) \left. \left. \right\} \left\{ 4 \operatorname{Im} (c_1' + c_2' \ln(s/s_0)) - \frac{\sqrt{s} \alpha_p'}{2} \right\} \right] \cdot \\
 & \cdot \left[\left\{ \lambda_p^0 + \alpha_p' \ln(s/s_0) + \lambda_p^1 + \alpha_p' \ln(s/s_0) + 4 \operatorname{Re} (c_1' + c_2' \ln(s/s_0)) \right\}^2 + \right. \\
 & \left. \left\{ 4 \operatorname{Im} (c_1' + c_2' \ln(s/s_0)) - \frac{\sqrt{s} \alpha_p'}{2} \right\}^2 \right]^{-1}
 \end{aligned}$$

Slope of the exponential fall-off with t of the strength of the "rotating part" of the helicity flip cut

$$\begin{aligned}
 \underline{\Psi}_2^{01} = & \left[\left\{ (\lambda_p^0 + \alpha_p' \ln(s/s_0)) (\lambda_p^1 + \alpha_p' \ln(s/s_0)) + \text{Re} (c_1 + c_2 \ln(s/s_0)) (\lambda_p^0 + \alpha_p' \ln(s/s_0) \right. \right. \\
 & \left. \left. + \lambda_p^1 + \alpha_p' \ln(s/s_0)) + \text{Im} (c_1 + c_2 \ln(s/s_0)) (\pi \alpha_p' + \frac{\pi \alpha_p'}{2}) - \pi \alpha_p' \pi \right. \right. \\
 & \left. \left. * \left\{ \lambda_p^0 + \alpha_p' \ln(s/s_0) + \lambda_p^1 + \alpha_p' \ln(s/s_0) + 4 \text{Re} (c_1 + c_2 \ln(s/s_0)) \right\} + \left\{ - \right. \right. \\
 & \left. \left. \cdot (\lambda_p^0 + \alpha_p' \ln(s/s_0) + \text{Re} (c_1 + c_2 \ln(s/s_0)) + \text{Im} (c_1 + c_2 \ln(s/s_0)) (\lambda_p^0 \right. \right. \\
 & \left. \left. + \alpha_p' \ln(s/s_0) + \lambda_p^1 + \alpha_p' \ln(s/s_0)) - \frac{\pi \alpha_p'}{2} (\lambda_p^1 + \alpha_p' \ln(s/s_0) + \text{Re} (c_1 \right. \right. \\
 & \left. \left. * \left\{ 4 \text{Im} (c_1 + c_2 \ln(s/s_0)) - (\pi \alpha_p' + \frac{\pi \alpha_p'}{2}) \right\} \right] \right] \left\{ \lambda_p^0 + \alpha_p' \ln(s/s_0) + \lambda_p^1 \right. \\
 & \left. \left. + 4 \text{Re} (c_1 + c_2 \ln(s/s_0)) \right\}^2 + \left\{ 4 \text{Im} (c_1 + c_2 \ln(s/s_0)) - (\pi \alpha_p' + \frac{\pi \alpha_p'}{2}) \right\} \right]
 \end{aligned}$$

Initial angle of the "non rotating part" of the helicity flip cut

$$\phi_1^{01} = \delta_P^0 - \pi/2 - 2 \rho_1 \alpha_1 \eta \frac{4 \operatorname{Im} (c_1' + c_2' \ln(s/s_0)) - \frac{\pi \alpha_P'}{2}}{\lambda_P^0 + \alpha_P' \ln(s/s_0) + \lambda_P^1 + \alpha_P' \ln(s/s_0) + 4 \operatorname{Re} (c_1' + c_2' \ln(s/s_0))} + \rho_1 \alpha_1 \eta \frac{2 \operatorname{Im} (c_1' + c_2' \ln(s/s_0)) - \frac{\pi \alpha_P'}{2}}{\lambda_P^0 + \alpha_P' \ln(s/s_0) + 2 \operatorname{Re} (c_1' + c_2' \ln(s/s_0))}$$

Initial angle of the "rotating part" of the helicity flip cut

$$\phi_2^{01} = -\pi \alpha_P(0) + \delta_P^0 - \pi/2 - 2 \rho_2 \alpha_2 \eta \frac{4 \operatorname{Im} (c_1' + c_2' \ln(s/s_0)) - (\pi \alpha_P' + \frac{\pi \alpha_P'}{2})}{\lambda_P^0 + \alpha_P' \ln(s/s_0) + \lambda_P^1 + \alpha_P' \ln(s/s_0) + 4 \operatorname{Re} (c_1' + c_2' \ln(s/s_0))} + \rho_2 \alpha_2 \eta \frac{2 \operatorname{Im} (c_1' + c_2' \ln(s/s_0)) - \frac{\pi \alpha_P'}{2}}{\lambda_P^0 + \alpha_P' \ln(s/s_0) + 2 \operatorname{Re} (c_1' + c_2' \ln(s/s_0))}$$

Rotation velocity per /t/ of the "non rotating part" of the helicity flip cut

$$\begin{aligned}
 \Phi_1^{01} = & \left[\left\{ \text{Im} (c_1 + c_2 \ln(s/s_0)) \right\} \left(\lambda_p^0 + \alpha_p' \ln(s/s_0) + \lambda_p^1 + \alpha_p' \ln(s/s_0) - \frac{\pi \alpha_p'}{2} \right. \right. \\
 & + \alpha_p' \ln(s/s_0) + \text{Re} (c_1 + c_2 \ln(s/s_0)) \left. \left. \right\} \left\{ \lambda_p^0 + \alpha_p' \ln(s/s_0) \right. \right. \\
 & + \alpha_p' \ln(s/s_0) + \frac{1}{2} \text{Re} (c_1 + c_2 \ln(s/s_0)) \left. \left. \right\} - \left\{ \left(\lambda_p^0 + \alpha_p' \ln(s/s_0) \right. \right. \right. \\
 & \times \left. \left. \left(\lambda_p^1 + \alpha_p' \ln(s/s_0) \right) + \text{Re} (c_1 + c_2 \ln(s/s_0)) \left(\lambda_p^0 + \alpha_p' \ln(s/s_0) \right. \right. \right. \\
 & \left. \left. \left. \lambda_p^1 + \alpha_p' \ln(s/s_0) \right) + \text{Im} (c_1 + c_2 \ln(s/s_0)) \frac{\pi \alpha_p'}{2} \right\} \left\{ \frac{1}{2} \text{Im} (c_1 \right. \right. \\
 & - \left. \left. \frac{\pi \alpha_p'}{2} \right\} \right] \left[\left\{ \lambda_p^0 + \alpha_p' \ln(s/s_0) + \lambda_p^1 + \alpha_p' \ln(s/s_0) + \frac{1}{2} \text{Re} \right. \right. \\
 & \left. \left. + \left\{ \frac{1}{2} \text{Im} (c_1 + c_2 \ln(s/s_0)) - \frac{\pi \alpha_p'}{2} \right\} \right]^{-1}
 \end{aligned}$$

Rotation velocity per /t/ of the "rotating part" of the helicity flip cut

$$\begin{aligned}
 \bar{\Phi}_2^{01} = & \left[\left\{ -\pi\alpha'_p (\lambda_p^0 + \alpha'_p \ln(s/s_0)) + \text{Re} (c_1 + c_2 \ln(s/s_0)) \right\} + \text{Im} (c_1 + c_2 \ln(s/s_0)) \right. \\
 & + (\lambda_p^0 + \alpha'_p \ln(s/s_0) + \lambda_p^1 + \alpha'_p \ln(s/s_0)) - \frac{\pi\alpha'_p}{2} (\lambda_p^1 + \alpha'_p \ln(s/s_0)) \\
 & + \text{Re} (c_1 + c_2 \ln(s/s_0)) \left. \right\} \left\{ \lambda_p^0 + \alpha'_p \ln(s/s_0) + \lambda_p^1 + \alpha'_p \ln(s/s_0) \right. \\
 & + 4\text{Re} (c_1 + c_2 \ln(s/s_0)) \left. \right\} - \left\{ (\lambda_p^0 + \alpha'_p \ln(s/s_0)) (\lambda_p^1 + \alpha'_p \ln(s/s_0)) \right. \\
 & + \text{Re} (c_1 + c_2 \ln(s/s_0)) (\lambda_p^0 + \alpha'_p \ln(s/s_0) + \lambda_p^1 + \alpha'_p \ln(s/s_0)) \\
 & + \text{Im} (c_1 + c_2 \ln(s/s_0)) (\pi\alpha'_p + \frac{\pi\alpha'_p}{2}) - \pi\alpha'_p \frac{\pi\alpha'_p}{2} \left. \right\} \left\{ 4\text{Im} (c_1 + c_2 \ln(s/s_0)) \right. \\
 & - \left. \left[\pi\alpha'_p + \frac{\pi\alpha'_p}{2} \right] \right\} \left[\left\{ \lambda_p^0 + \alpha'_p \ln(s/s_0) + \lambda_p^1 + \alpha'_p \ln(s/s_0) + \right. \right. \\
 & \left. \left. (c_1 + c_2 \ln(s/s_0)) \right\}^2 + \left\{ 4\text{Im} (c_1 + c_2 \ln(s/s_0)) - (\pi\alpha'_p + \frac{\pi\alpha'_p}{2}) \right\} \right]
 \end{aligned}$$

Correlation modified Absorption model - Gribov cut

The explicit dependence of the helicity nonflip cut characterizing quantities at $t = 0$ and fixed energy
initial cut strength and initial phase angle of non-rotating and rotating part

$$\zeta_1^{\circ\circ} = \frac{\lambda_{a1}^{\circ} \hat{\beta}_{p1}^{\circ} \hat{\beta}_p^{\circ}}{2\sqrt{\pi} \left\{ (\text{Re } \hat{\lambda}_p^{\circ} + \hat{\lambda}_{p1}^{\circ} + 4\text{Re}c^{\circ})^2 + (4\text{Im}c^{\circ} - \frac{\pi\alpha_p^{\circ}}{2})^2 \right\}^{1/2}}$$

$$\zeta_2^{\circ\circ} = \frac{\lambda_{a2}^{\circ} \hat{\beta}_{p2}^{\circ} \hat{\beta}_p^{\circ}}{2\sqrt{\pi} \left\{ (\text{Re } \hat{\lambda}_p^{\circ} + \hat{\lambda}_{p2}^{\circ} + 4\text{Re}c^{\circ})^2 + (4\text{Im}c^{\circ} - \frac{\pi\alpha_p^{\circ}}{2} - \pi\alpha_p^{\circ})^2 \right\}^{1/2}}$$

$$\phi_1^{\circ\circ} = \delta_p^{\circ} - \frac{\pi}{2} - \arctg \frac{4\text{Im}c^{\circ} - \frac{\pi\alpha_p^{\circ}}{2}}{\text{Re } \hat{\lambda}_p^{\circ} + \hat{\lambda}_{p1}^{\circ} + 4\text{Re}c^{\circ}}$$

$$\phi_2^{\circ\circ} = \delta_p^{\circ} - \frac{\pi}{2} - \pi\alpha_p^{\circ} - \arctg \frac{4\text{Im}c^{\circ} - \frac{\pi\alpha_p^{\circ}}{2} - \pi\alpha_p^{\circ}}{\text{Re } \hat{\lambda}_p^{\circ} + \hat{\lambda}_{p2}^{\circ} + 4\text{Re}c^{\circ}}$$

Correlation modified Absorption model - Gribov cut

The explicit dependence of the helicity nonflip cut characterizing quantities at $t \neq 0$ and fixed energy
Shrinking velocity with t of cut strength of non-rotating and rotating part

$$\begin{aligned}
 \Psi_1^{\infty} &= \frac{\left\{ (\text{Re } \hat{\lambda}_P^{\circ}) \hat{\lambda}_P^{\circ} (\text{Re } \hat{\lambda}_P^{\circ} + \hat{\lambda}_P^{\circ}) + \left(\frac{\pi \alpha_P^{\circ}}{2}\right)^2 \hat{\lambda}_P^{\circ} \right\} + \text{Re } c^{\circ} \left\{ 4 (\text{Re } \hat{\lambda}_P^{\circ}) \hat{\lambda}_P^{\circ} + \right.}{(\text{Re } \hat{\lambda}_P^{\circ} + \hat{\lambda}_P^{\circ} + 4 \text{Re } c^{\circ})^2 + (4 \text{Im } c^{\circ} - \frac{\pi \alpha_P^{\circ}}{2})^2} \\
 &+ \frac{(\text{Re } c^{\circ})^2 \left\{ 4 (\text{Re } \hat{\lambda}_P^{\circ} + \hat{\lambda}_P^{\circ}) \right\} - \text{Im } c^{\circ} \left\{ 4 \hat{\lambda}_P^{\circ} \frac{\pi \alpha_P^{\circ}}{2} \right\} + (\text{Im } c^{\circ})^2 \left\{ 4 (\text{Re } \hat{\lambda}_P^{\circ} + \hat{\lambda}_P^{\circ}) \right\}}{(\text{Re } \hat{\lambda}_P^{\circ} + \hat{\lambda}_P^{\circ} + 4 \text{Re } c^{\circ})^2 + (4 \text{Im } c^{\circ} - \frac{\pi \alpha_P^{\circ}}{2})^2} \\
 \Psi_2^{\infty} &= \frac{\left\{ (\text{Re } \hat{\lambda}_P^{\circ}) \hat{\lambda}_P^{\circ} (\text{Re } \hat{\lambda}_P^{\circ} + \hat{\lambda}_P^{\circ}) + \left(\frac{\pi \alpha_P^{\circ}}{2}\right)^2 \hat{\lambda}_P^{\circ} + (\pi \alpha_P^{\circ})^2 \text{Re } \hat{\lambda}_P^{\circ} \right\}}{(\text{Re } \hat{\lambda}_P^{\circ} + \hat{\lambda}_P^{\circ} + 4 \text{Re } c^{\circ})^2 + (4 \text{Im } c^{\circ} - \frac{\pi \alpha_P^{\circ}}{2} - \pi \alpha_P^{\circ})^2} \\
 &+ \frac{\text{Re } c^{\circ} \left\{ 4 (\text{Re } \hat{\lambda}_P^{\circ}) \hat{\lambda}_P^{\circ} + (\text{Re } \hat{\lambda}_P^{\circ} + \hat{\lambda}_P^{\circ})^2 + \left[\left(\frac{\pi \alpha_P^{\circ}}{2}\right)^2 - (\pi \alpha_P^{\circ})^2 \right] \right\}}{(\text{Re } \hat{\lambda}_P^{\circ} + \hat{\lambda}_P^{\circ} + 4 \text{Re } c^{\circ})^2 + (4 \text{Im } c^{\circ} - \frac{\pi \alpha_P^{\circ}}{2} - \pi \alpha_P^{\circ})^2} \\
 &+ \frac{(\text{Re } c^{\circ})^2 \left\{ 4 (\text{Re } \hat{\lambda}_P^{\circ} + \hat{\lambda}_P^{\circ}) \right\} - \text{Im } c^{\circ} \left\{ 4 \hat{\lambda}_P^{\circ} \frac{\pi \alpha_P^{\circ}}{2} + 4 \text{Re } \hat{\lambda}_P^{\circ} \pi \alpha_P^{\circ} \right\} + (\text{Im } c^{\circ})^2 \left\{ 4 (\text{Re } \hat{\lambda}_P^{\circ} + \hat{\lambda}_P^{\circ}) \right\}}{(\text{Re } \hat{\lambda}_P^{\circ} + \hat{\lambda}_P^{\circ} + 4 \text{Re } c^{\circ})^2 + (4 \text{Im } c^{\circ} - \frac{\pi \alpha_P^{\circ}}{2} - \pi \alpha_P^{\circ})^2}
 \end{aligned}$$

Correlation modified Absorption model - Gribov cut

The explicit dependence of the helicity nonflip cut characterizing quantities at $t/ \neq 0$ and fixed energy on :

Phase angle rotation velocity with $t/$ of non-rotating and rotating part

$$\Phi_1^{00} = -\left(\frac{\pi\alpha'_p}{2}\right) \frac{(\hat{\lambda}_{p,1}^0)^2 + \text{Re}c^0 \{4\hat{\lambda}_{p,1}^0\} + 4(\text{Re}c^0)^2 + 4(\text{Im}c^0)^2}{(\text{Re} \hat{\lambda}_{p,1}^0 + \hat{\lambda}_{p,1}^0 + 4 \text{Re}c^0)^2 + (4 \text{Im}c^0 - \frac{\pi\alpha'_p}{2})^2}$$

$$+ \frac{\text{Im}c^0 \{ (\text{Re} \hat{\lambda}_{p,1}^0 - \hat{\lambda}_{p,1}^0)^2 + (-\frac{\pi\alpha'_p}{2})^2 \}}{(\text{Re} \hat{\lambda}_{p,1}^0 + \hat{\lambda}_{p,1}^0 + 4 \text{Re}c^0)^2 + (4 \text{Im}c^0 - \frac{\pi\alpha'_p}{2})^2}$$

$$\Phi_2^{00} = -\left(\frac{\pi\alpha'_p}{2}\right) \frac{(\hat{\lambda}_{p,2}^0)^2 + \text{Re}c^0 \{4\hat{\lambda}_{p,2}^0\} + 4(\text{Re}c^0)^2 + 4(\text{Im}c^0)^2 + (\pi\alpha'_p)^2}{(\text{Re} \hat{\lambda}_{p,2}^0 + \hat{\lambda}_{p,2}^0 + 4 \text{Re}c^0)^2 + (4 \text{Im}c^0 - \frac{\pi\alpha'_p}{2} - \pi\alpha'_p)^2}$$

$$+ \frac{\text{Im}c^0 \{ (\text{Re} \hat{\lambda}_{p,2}^0 - \hat{\lambda}_{p,2}^0)^2 + (\pi\alpha'_p - \frac{\pi\alpha'_p}{2})^2 \}}{(\text{Re} \hat{\lambda}_{p,2}^0 + \hat{\lambda}_{p,2}^0 + 4 \text{Re}c^0)^2 + (4 \text{Im}c^0 - \frac{\pi\alpha'_p}{2} - \pi\alpha'_p)^2}$$

$$- \pi\alpha'_p \frac{(\hat{\lambda}_{p,2}^0)^2 + (\frac{\pi\alpha'_p}{2})^2 + \text{Re}c^0 \{4\text{Re} \hat{\lambda}_{p,2}^0\} + 4(\text{Re}c^0)^2 + 4(\text{Im}c^0)^2}{(\text{Re} \hat{\lambda}_{p,2}^0 + \hat{\lambda}_{p,2}^0 + 4 \text{Re}c^0)^2 + (4 \text{Im}c^0 - \frac{\pi\alpha'_p}{2} - \pi\alpha'_p)^2}$$

Correlation modified absorption model - Gribov cut (isovector amplitude)

The explicit dependence of the helicity flip cut characterizing quantities at $t/t = 0$ and fixed energy on all parameters

Initial cut strength and initial phase angle of non-rotating and rotating part

$$\chi_1^{01} = \frac{\lambda_{cut}^1 \hat{\beta}_P^0 \hat{\beta}_{P_i}^1 \left\{ (Re \hat{\lambda}_P^0 + 2 Re c')^2 + (2 J c' - \frac{\sqrt{5} \alpha_P^0}{2})^2 \right\}^{1/2}}{2 \sqrt{5} \left\{ (Re \hat{\lambda}_P^0 + \hat{\lambda}_{P_i}^1 + 4 Re c')^2 + (4 J c' - \frac{\sqrt{5} \alpha_P^0}{2})^2 \right\}}$$

$$\chi_2^{01} = \frac{\lambda_{cut}^1 \hat{\beta}_P^0 \hat{\beta}_{P_i}^1 \left\{ (Re \hat{\lambda}_P^0 + 2 Re c')^2 + (2 J c' - \frac{\sqrt{5} \alpha_P^0}{2})^2 \right\}^{1/2}}{2 \sqrt{5} \left\{ (Re \hat{\lambda}_P^0 + \hat{\lambda}_{P_i}^1 + 4 Re c')^2 + (4 J c' - \frac{\sqrt{5} \alpha_P^0}{2} - \sqrt{5} \alpha_P^0)^2 \right\}}$$

$$\phi_1^{01} = \delta_P^0 - \frac{\pi}{2} - 29.0^\circ \arctan \frac{4 J c' - \frac{\sqrt{5} \alpha_P^0}{2}}{Re \hat{\lambda}_P^0 + \hat{\lambda}_{P_i}^1 + 4 Re c'} + 9.0^\circ \arctan \frac{2 J c' - \frac{\sqrt{5} \alpha_P^0}{2}}{Re \hat{\lambda}_P^0 + 2 Re c'}$$

$$\phi_2^{01} = \delta_P^0 - \frac{\pi}{2} - \sqrt{5} \alpha_P^0 \cos \theta - 29.0^\circ \arctan \frac{4 J c' - \frac{\sqrt{5} \alpha_P^0}{2} - \sqrt{5} \alpha_P^0}{Re \hat{\lambda}_P^0 + \hat{\lambda}_{P_i}^1 + 4 Re c'} + 9.0^\circ \arctan \frac{2 J c' - \frac{\sqrt{5} \alpha_P^0}{2}}{Re \hat{\lambda}_P^0 + 2 Re c'}$$

Correlation modified absorption model - Gribov cut (isovector amplitude)

The explicit dependence of the helicity flip cut characterizing quantities at $t/ \neq 0$ and fixed energy on all parameters in

Shrinking velocity with $t/$ of cut strength of non-rotating and rotating part

$$\Psi_{1,1}^{01} = \frac{\{ (\text{Re } \hat{\lambda}_P^0) \hat{\lambda}_{P,1}' (\text{Re } \hat{\lambda}_P^0 + \hat{\lambda}_{P,1}') + (\frac{\sqrt{\alpha_P^0}}{2})^2 \hat{\lambda}_{P,1}' \} + \text{Re } c' \{ 4 (\text{Re } \hat{\lambda}_P^0) \hat{\lambda}_{P,1}' + (\text{Re } \hat{\lambda}_P^0 + \hat{\lambda}_{P,1}')^2 \}}{(\text{Re } \hat{\lambda}_P^0 + \hat{\lambda}_{P,1}' + 4 \text{Re } c')^2 + (4 \text{Im } c' - \frac{\sqrt{\alpha_P^0}}{2})^2}$$

$$+ \frac{(\text{Re } c')^2 \{ 4 (\text{Re } \hat{\lambda}_P^0 + \hat{\lambda}_{P,1}') \} - \text{Im } c' \{ 4 \hat{\lambda}_{P,1}' \frac{\sqrt{\alpha_P^0}}{2} \} + (\text{Im } c')^2 \{ 4 (\text{Re } \hat{\lambda}_P^0 + \hat{\lambda}_{P,1}') \}}{(\text{Re } \hat{\lambda}_P^0 + \hat{\lambda}_{P,1}' + 4 \text{Re } c')^2 + (4 \text{Im } c' - \frac{\sqrt{\alpha_P^0}}{2})^2}$$

$$\Psi_{1,2}^{01} = \frac{\{ (\text{Re } \hat{\lambda}_P^0) \hat{\lambda}_{P,2}' (\text{Re } \hat{\lambda}_P^0 + \hat{\lambda}_{P,2}') + (\frac{\sqrt{\alpha_P^0}}{2})^2 \hat{\lambda}_{P,2}' + (\sqrt{\alpha_P^0})^2 \text{Re } \hat{\lambda}_P^0 \}}{(\text{Re } \hat{\lambda}_P^0 + \hat{\lambda}_{P,2}' + 4 \text{Re } c')^2 + (4 \text{Im } c' - \frac{\sqrt{\alpha_P^0}}{2} - \sqrt{\alpha_P^0})^2}$$

$$+ \frac{\text{Re } c' \{ 4 (\text{Re } \hat{\lambda}_P^0) \hat{\lambda}_{P,2}' + (\text{Re } \hat{\lambda}_P^0 + \hat{\lambda}_{P,2}')^2 + [(\frac{\sqrt{\alpha_P^0}}{2}) - (\sqrt{\alpha_P^0})]^2 \}}{(\text{Re } \hat{\lambda}_P^0 + \hat{\lambda}_{P,2}' + 4 \text{Re } c')^2 + (4 \text{Im } c' - \frac{\sqrt{\alpha_P^0}}{2} - \sqrt{\alpha_P^0})^2}$$

$$+ \frac{(\text{Re } c')^2 \{ 4 (\text{Re } \hat{\lambda}_P^0 + \hat{\lambda}_{P,2}') \} - \text{Im } c' \{ 4 \hat{\lambda}_{P,2}' \frac{\sqrt{\alpha_P^0}}{2} + 4 \text{Re } \hat{\lambda}_P^0 \sqrt{\alpha_P^0} \} + (\text{Im } c')^2 \{ 4 (\text{Re } \hat{\lambda}_P^0 + \hat{\lambda}_{P,2}') \}}{(\text{Re } \hat{\lambda}_P^0 + \hat{\lambda}_{P,2}' + 4 \text{Re } c')^2 + (4 \text{Im } c' - \frac{\sqrt{\alpha_P^0}}{2} - \sqrt{\alpha_P^0})^2}$$

Correlation modified absorption model - Gribov cut (isovector amplitude)

The explicit dependence of the helicity flip cut characterizing quantities at $t/ \neq 0$ and fixed energy on all

Phase angle rotation velocity with $t/$ of non-rotating and rotating part

$$\Phi_{1,1}^{01} = - \left(\frac{\sqrt{s} \alpha'_p}{2} \right) \frac{(\hat{\lambda}'_p)^2 + \text{Re} c' \{ \hat{\lambda}'_p \} + 4(\text{Re} c')^2 + \{ C \text{J-c}' \}^2}{(\text{Re} \hat{\lambda}'_p + \hat{\lambda}'_p + \{ \text{Re} c' \})^2 + (\{ \text{J-c}' - \frac{\sqrt{s} \alpha'_p}{2} \})^2} + \frac{\text{J-c}' \{ (\text{Re} \hat{\lambda}'_p - \hat{\lambda}'_p)^2 + (- \frac{\sqrt{s} \alpha'_p}{2})^2 \}}{(\text{Re} \hat{\lambda}'_p + \hat{\lambda}'_p + \{ \text{Re} c' \})^2 + (\{ \text{J-c}' - \frac{\sqrt{s} \alpha'_p}{2} \})^2}$$

$$\Phi_{2,2}^{01} = - \left(\frac{\sqrt{s} \alpha'_p}{2} \right) \frac{(\hat{\lambda}'_p)^2 + \text{Re} c' \{ \hat{\lambda}'_p \} + \{ \text{Re} c' \}^2 + \{ \text{J-c}' \}^2 + (\sqrt{s} \alpha'_p)^2}{(\text{Re} \hat{\lambda}'_p + \hat{\lambda}'_p + \{ \text{Re} c' \})^2 + (\{ \text{J-c}' - \frac{\sqrt{s} \alpha'_p}{2} - \sqrt{s} \alpha'_p \})^2} + \frac{\text{J-c}' \{ (\text{Re} \hat{\lambda}'_p - \hat{\lambda}'_p)^2 + (\sqrt{s} \alpha'_p - \frac{\sqrt{s} \alpha'_p}{2})^2 \}}{(\text{Re} \hat{\lambda}'_p + \hat{\lambda}'_p + \{ \text{Re} c' \})^2 + (\{ \text{J-c}' - \frac{\sqrt{s} \alpha'_p}{2} - \sqrt{s} \alpha'_p \})^2} - \sqrt{s} \alpha'_p \frac{(\hat{\lambda}'_p)^2 + (\frac{\sqrt{s} \alpha'_p}{2})^2 + \text{Re} c' \{ \text{Re} \hat{\lambda}'_p \} + \{ \text{Re} c' \}^2 + \{ \text{J-c}' \}^2}{(\text{Re} \hat{\lambda}'_p + \hat{\lambda}'_p + \{ \text{Re} c' \})^2 + (\{ \text{J-c}' - \frac{\sqrt{s} \alpha'_p}{2} - \sqrt{s} \alpha'_p \})^2}$$

VI. III - Several Model Variants towards the solution of the phase problem of the helicity nonflip isovector amplitude

VI. III. 1 - Model Variant Ia - Purely Real Correlation Model

- the s - channel helicity conserving effective pomeron is purely imaginary and stationary.

$t/ = 0$

Purely real correlation parameter c given in units of $(\text{GeV}/c)^{-2}$

It is known that by comparison to the helicity flip amplitude the helicity non-flip amplitude needs to be strengthened. Without having to invoke an enhancement factor of the Michigan type, one can, with the help of the correlation parameter, strengthen or weaken the cut in forward direction at will, depending on whether one chooses a negative or positive value for c . However, the ratio of non-rotating to rotating strength will quickly deviate from 1 towards larger values. Because, if the model has any chance to rectify the situation, one would expect a cut which is stronger in its real part. Traditionally, both parts are approximately equally strongly absorbed. The increase of the rotating part matters even worse. In fact, although the initial phase of the rotating cut is strongly rotated in anticlockwise direction, the cut strength, there is no way to rotate the non-rotating part of the cut, since we have used a stationary ratio prevents any substantial net gain in phase for the total cut from being more than a few degrees at a $t=0$ to a Michigan enhancement factor of about $\lambda = 2$. Any further attempt to increase the strength with the help of c results in a severe loss in phase. For example, using the parameters specified in table I, we obtain a total phase angle of 228.51° with a strength of about $1/10$ of the pole in the complex plane, which leaves a relative angle of 185.31 degrees. This is much too close to the critical value of 180° where the polarization changes its sign. The correlation parameter corresponding to $\lambda = 2$ has the value $c = -1.8$ keeping everything else fixed. A larger c has reached the optimal net gain in phase namely 3.18° . With $c = -2.2$ corresponding to a $\lambda = 2.52$, the total phase angle is more than the traditional absorption would give, namely 227.77° . The reason for this behaviour is that for a stationary cut the non-rotating part of the cut possesses a singularity due to the introduction of c . For the particular parameter values this singularity occurs at $c = -2.925$. The rotating part of the cut, by contrast, cannot possess such a singularity and thus has a slope of the Regge slope in the denominator.

Model Variant Ia

$$0 < /t/ \leq .35 \text{ (GeV/c)}^2$$

Purely real correlation parameter c

Although the introduction of a purely real c namely $\text{Re } c = -1.8 \text{ (GeV/c)}^{-2}$ resulted only in a negligible net g a few degrees, there is still hope that the situation might improve once $/t/$ starts to increase.

The nature of the failure of the traditional absorption model is the unfortunate effect of the combination of its features -

- (1) The relative cut pole phase is too close to 180° at $/t/ = 0 \text{ (GeV/c)}^2$
- (2) Although the cut rotates with increasing $/t/$ away from the pole, it does so too slowly by comparison with the fast following pole, thus the pole already catches up with the cut at the critical phase difference of 180° at very small $/t/$ values and there causes the polarization to change its sign from positive to negative.

By switching on the negative and purely real correlation one not only increases the cut strength at forward weakens the exponential fall-off of the cut strength with increasing $/t/$ e. g. for $\text{Re } c = -1.8 \text{ (GeV/c)}^{-2}$ the slope is reduced by a quarter of its former value. Also, nonrotating and rotating slope fall-off in the case of the traditional model are slightly different (the rotating part a bit faster than the non rotating part). At $\text{Re } c = -1.8 \text{ (GeV/c)}^{-2}$ the slopes are exactly equal. A further increase in $\text{Re } c$ lowers both slopes considerably quickly, but does so for the non-rotating part increasingly faster than for the rotating part. Again this is a consequence of the singularity at $\text{Re } c = -2.92$.

The hope that the disappointing situation met in forward direction might improve away from $/t/ = 0 \text{ (GeV/c)}^2$ model variant is unsubstantiated because we observe that $\text{Re } c$ not only cannot initiate a rotation of the non-rotating part but also slows down the already existing rotation velocity of the rotating part of the traditional absorption model and causes a complete standstill.

VI. III. 2 - Model Variant Ib - complex correlation model as a crossing symmetry violating solution to the phase problem of the helicity nonflip isovector amplitude

$$\underline{/t/ = 0 \text{ (GeV/c)}^2$$

Complex correlation parameter c

Due to the unwanted increase in strength of the non-rotating part of the cut relative to the rotating part, the real correlation parameter has so far been disappointing. By allowing for an imaginary part of the correlation parameter and keep the ratio at 1 if one accompanies the $\text{Re}c = -1.8 \text{ (GeV/c)}^{-2}$ with an $\text{Im}c = +.63 \text{ (GeV/c)}^{-2}$ the presence of the imaginary part of the correlation causes the non-rotating part, which is traditionally purely real, to acquire an imaginary part. Unfortunately the ratio stabilizing positive $\text{Im}c$ rotates both non-rotating part and rotating part clockwise such that the net effect for the total cut phase at $/t/ = 0 \text{ (GeV/c)}^2$ is much worse than it would be for a traditional absorption.

A negative imaginary part of c can, however, account in forward direction exactly for the strong absorptive part of the pole partially or even totally at the expense of the real part. Absorption modifying models (10) have such a behaviour of their cut in an ad hoc fashion and have produced several basic features of the observable correctly. By introducing a complex correlation we produce this behaviour naturally. If we choose for example $\text{Re}c = -1.35 \text{ (GeV/c)}^{-2}$ and $\text{Im}c = -0.63 \text{ (GeV/c)}^{-2}$ we obtain a purely imaginary cut at forward direction whose strength corresponds

Model variant Ib

$$0 < /t/ \leq .35 \text{ (GeV/c)}^2$$

Complex correlation parameter c

We have remarked that the reason for the persistent failure of the traditional absorption cut is due to its too early diagram at $/t/ = 0 \text{ (GeV/c)}^2$ together with its too slow rotation with increasing $/t/$. This causes the total amplitude to rotate clockwise which speeds up when the 180° relative cut-pole phase border has been crossed. This is in complete contrast to the actual behaviour of the amplitude, as has been revealed by model independent determinations of the amplitude. The feature of the amplitude in the $/t/$ region under consideration is its zero structure. Especially where the "crossover" to the zero of the parallel part is concerned (parallel with respect to the dominating helicity non flip isoscalar ρ meson) the analysis by Ambats et al has a definite advantage over others. The more precise determination of this zero at $/t/ = .2 \text{ (GeV/c)}^2$ due to their particle-anti-particle relative normalization uncertainty of $\pm 1.5\%$ which leads to an uncertainty of only $\pm .025 \text{ (GeV/c)}^2$ whereas a normalization uncertainty of $\pm 5\%$ as in previous determinations led to an uncertainty of $\pm .125 \text{ (GeV/c)}^2$. Although the zero in the imaginary part is close to the zero in the parallel part of the amplitude, its precise position is model independent unless it is determined by the method of fixed-t analyticity.

Whereas the zero of the parallel part seems to be a fairly reliable constraint for model building, the knowledge of the zero of the perpendicular part suffers from an uncertainty due to the inconsistency present in the polarization data measurements. The ARGONNE data are persistently 20% lower than the CERN data which affects mostly the perpendicular part of the amplitude. If the ARGONNE data are taken, the perpendicular part has a zero at $/t/ = .25 \text{ (GeV/c)}^2$ whereas in the case of the CERN data the perpendicular part of the amplitude remains positive throughout.

Our model variant Ib with $\text{Re}c = -1.8 \text{ (GeV/c)}^{-2}$ and $\text{Im}c = -1.35 \text{ (GeV/c)}^{-2}$ leads to the correct clockwise rotation of the total amplitude and in particular to a zero of the imaginary part at $/t/ = .2 \text{ (GeV/c)}^2$ not too far away from the actual "crossover". The real part on the other hand stays positive throughout the $/t/$ region under consideration as implied by the CERN data. As in the case of the RRRT-Phase angle, [#] (10) our model absorbs the imaginary part at the expense of the real part. RRRT provide the non-rotating part of the cut with a positive ad hoc phase angle of 90° which amounts essentially to multiplying the imaginary part of the cut by a $/t/$ independent enhancement factor $\lambda = 2$ and a nullif

Ringland et al.

of the real part of the cut, This model is the most extreme of its kind. Intermediate versions are for example the model by J. Anderson et al (10) which correct only the rotating part of the pole, and the model by Sadoulet (10) which corrects the non-rotating and rotating parts of the cut differently and employs a non flat pomeron. The newest determination of the crossover zero position by Ambats et al puts a severe constraint on model building. Although all three models mentioned above reproduce the observables and several features of the amplitude, the difficulties which these models encounter when they try to move the imaginary zero in the vicinity of the actual position of the crossover at $t/t = .15$ demonstrate the lack of cut strength in the imaginary part. (That this is so is clearly seen in the fact that RRRT can move its zero from $t/t = .2$ to the crossover position, and this is so only because its additional resource of strength comes from the rotating part. The non-rotating part is, due to the phase angle, fully transformed into the imaginary part. This effect doubles the cut strength.) No other model has such a resource in cut strength. The introduction of a complex parameter can somehow simulate the various versions of these phase-modifying models. A purely imaginary change can change the cut phase. However, both parts of the cut obtain an equal amount of change. A purely imaginary change also changes the approximate equality of the size of the two cut parts. Thus one can arrange for a 45° positive phase angle and obtain $Imc = -2.6 (GeV/c)^{-2}$ and obtain a purely imaginary cut at least at $t/t = 0$. However, although we obtain the correct rotation we lose in comparison with RRRT on strength. This happens firstly because of the 45° additional phase rotation which applies to both parts of the cut and reduces in principle the effective strength with respect to RRRT from $\lambda = 2$ to $\lambda = 1.4$. Secondly, a purely imaginary change weakens the cut and the net effect is such that for the optimal phase angle there will be no enhancement (nor loss) in strength of the imaginary part of the cut and there will be total cancellation of the real part. Our phase modification is not t/t independent. Both phases have a small rotation velocity. Such a purely imaginary change is effectively the model by J. Anderson apart from the weak t/t dependence. Both models fail at the crossover corner due to their lack in cut strength. For both models the simulating λ is $\lambda = 1$. Our zero, as well as that of Anderson, is at $t/t = .4$. By switching on the real part of the correlation we encounter a new source of strength and also a change in phase. In order to avoid the additional unwanted contribution in phase we have to turn down the size of Imc . This provides in turn a further boost in strength. The values for c which move the crossover to $t/t = .15$ are $Re c = -1.025 (GeV/c)^{-2}$ and $Imc = -1.025 (GeV/c)^{-2}$. The effective cut strength is then $\lambda = 2.14$ and we see that in the real part of c we have a resource of strength which a purely ad hoc phase modification cannot provide.

Helicity nonflip isovector amplitude (parameters used from Table I)

Model variant Ia - purely real correlation parameter, purely imaginary and stationary pomeron

Non-rotating part

Rotating part

$$\phi_1^{00}(c) = \frac{.749}{11.7 + 4c^0}$$

$$\phi_2^{00}(c) = \frac{.749}{\{(11.7 + 4c^0)^2 + 6.35\}^{1/2}}$$

$$\phi_1^{01}(c) = 0$$

$$\phi_2^{01}(c) = -93.6^\circ - \rho \cdot \text{ctg} \frac{-2.52}{11.7 + 4c^0}$$

$$\Delta \psi_1^{00}(c) = \frac{346.32 + 255.29c^0 + 46.8c^2}{11.7 + 4c^0}$$

$$\Delta \psi_2^{00}(c) = \frac{369.817 + 261.64c^0 + 46.8c^2}{(11.7 + 4c^0)^2 + 6.35}$$

$$\bar{\Phi}_1^{00}(c) = 0$$

$$\bar{\Phi}_2^{00}(c) = \frac{34.5 + 37.296c^0 + 10.08c^2}{(11.7 + 4c^0)^2 + 6.35}$$

Model variant Ib

(purely imaginary and stationary pomeron)

Helicity nonflip isovector amplitude (parameters used from Table I)

Dependence of the cut characterizing quantities on a complex correlation parameter

Non-rotating part

$$\phi_1^{00}(c^0) = \frac{.749}{\{(11.7 + 4 \operatorname{Re} c^0)^2 + (4 \operatorname{Im} c^0)^2\}^{1/2}}$$

$$\phi_1^{00}(c^0) = -g_1 c_1^0 \frac{4 \operatorname{Im} c^0}{11.7 + 4 \operatorname{Re} c^0}$$

$$\psi_1^{00}(c^0) = \frac{346.32 + 255.29 \operatorname{Re} c^0 + 46.8 \{ (\operatorname{Re} c^0)^2 + (\operatorname{Im} c^0)^2 \}}{(11.7 + 4 \operatorname{Re} c^0)^2 + (4 \operatorname{Im} c^0)^2}$$

$$\bar{\Phi}_1^{00}(c^0) = \frac{18.49 \operatorname{Im} c^0}{(11.7 + 4 \operatorname{Re} c^0)^2 + (4 \operatorname{Im} c^0)^2}$$

Model variant Ib

(purely imaginary and stationary pomeron)

Helicity nonflip isovector amplitude (parameters used from Table I)

Dependence of the cut characterizing quantities on a complex correlation parameter

Rotating part

$$\frac{d_{2,2}^{00}(c)}{d_{2,2}^{00}(c)} = \frac{.749}{\{ (11.7 + \frac{1}{2} \text{Re } c^0)^2 + C (\frac{1}{2} \text{Im } c^0 - 2.52)^2 \}^{1/2}}$$

$$\phi_{2,2}^{00}(c) = -93.6^\circ - \arctan \frac{\frac{1}{2} \text{Im } c^0 - 2.52}{11.7 + \frac{1}{2} \text{Re } c^0}$$

$$\Psi_{2,2}^{00}(c) = \frac{369.817 + 261.6 \frac{1}{2} \text{Re } c^0 - 37.296 \text{Im } c^0 + 46.8 \{ (\text{Re } c^0)^2 + (\text{Im } c^0)^2 \}}{C (11.7 + \frac{1}{2} \text{Re } c^0)^2 + C (\frac{1}{2} \text{Im } c^0 - 2.52)^2}$$

$$\Phi_{2,2}^{00}(c) = \frac{34.5 + 37.296 \text{Re } c^0 - 24.84 \text{Im } c^0 + 10.08 \{ (\text{Re } c^0)^2 + (\text{Im } c^0)^2 \}}{C (11.7 + \frac{1}{2} \text{Re } c^0)^2 + C (\frac{1}{2} \text{Im } c^0 - 2.52)^2}$$

Model variant Ib - parameters as in Table I. Complex correlation parameter and purely imaginary and s

in addition

$$\text{Re } c^0 = -2.2 \text{ (GeV/c)}^{-2} \quad \text{Im } c^0 = -1.025 \text{ (GeV/c)}^{-2}$$

$$T_P^0 = .862 \sin \frac{\Sigma}{2} (.52 - .80s|t|) e^{-.8.00|t|} e^{i(43.20^\circ + 72.36^\circ|t|)}$$

$$T_c^0 = -.149 e^{-2.39|t|} e^{i(54.728^\circ + 43.056^\circ|t|)} \\ + .107 e^{-2.06|t|} e^{i(-27.26^\circ + 40.9^\circ|t|)}$$

For Helicity flip (keep traditional absorption ; $\text{Re } c' = \text{Im } c' = 0$)

$$T_P^1 = 4.656 (|t|)^{1/2} \sin \frac{\Sigma}{2} (.52 - .80s|t|) e^{-4.00|t|} e^{i(43.20^\circ + 72.36^\circ|t|)}$$

$$T_c^1 = -.253 (|t|)^{1/2} e^{-1.92|t|} e^{i(0.00^\circ + 0.00^\circ|t|)} \\ + .228 (|t|)^{1/2} e^{-2.09|t|} e^{i(-57.36^\circ + 30.11^\circ|t|)}$$

TABLE III Model variant Ib (complex correlation, purely imaginary and stationary Pomeron)

$ t = 0$	$ t = .05$	$ t = .15$	$ t = .25$	$ t = .35$	$ t = .45$
$T_P = .621 e^{i 43.20}$	$.395 e^{i 46.89}$	$.152 e^{i 54.05}$	$.056 e^{i 61.29}$	$.021 e^{i 68.53}$	$.0057 e^{i 75.62}$
$T_C = .17 e^{i 271.90}$	$.152 e^{i 274.48}$	$.121 e^{i 279.613}$	$.096 e^{i 284.748}$	$.077 e^{i 289.88}$	$.061 e^{i 295.02}$
$T_{t_1} = .524 e^{i 29.11}$	$.313 e^{i 25.91}$	$.109 e^{i 1.94}$	$.067 e^{i -40.79}$	$.059 e^{i -53.36}$	$.057 e^{i -61.63}$
$T_{t_2} = .607 e^{i 38.79}$	$.302 e^{i 35.00}$	$.100 e^{i 28.61}$	$.074 e^{i -19.00}$	$.074 e^{i -19.00}$	$.063 e^{i ?}$

TABLE III Model variant Ib (complex correlation, purely imaginary and stationary Pomeron)

<u>$t = .55$</u>	<u>$t = .65$</u>	<u>$t = .8$</u>
$T_p = .001 e^{i 2.00^\circ}$	$= .00$	$= .00$
$T_c = .039 e^{i 300.153^\circ}$	$= .039 e^{i 305.29^\circ}$	$= .028 e^{i 312.99^\circ}$
$T_{th} = .038 e^{i -58.87^\circ}$	$= .039 e^{i 305.29^\circ}$	$= .028 e^{i 312.99^\circ}$
$T_{pp} = .055 e^{i ?}$	$=$	

<u>$t = 1.00$</u> in this region	$T_c \sim T_{th}$	<u>$t = 1.4$</u>	<u>$t = 1.8$</u>
$T_{th} \approx .0177 e^{i 323.26^\circ}$		$T_{th} = .0072 e^{i 343.8^\circ}$	$T_{th} =$

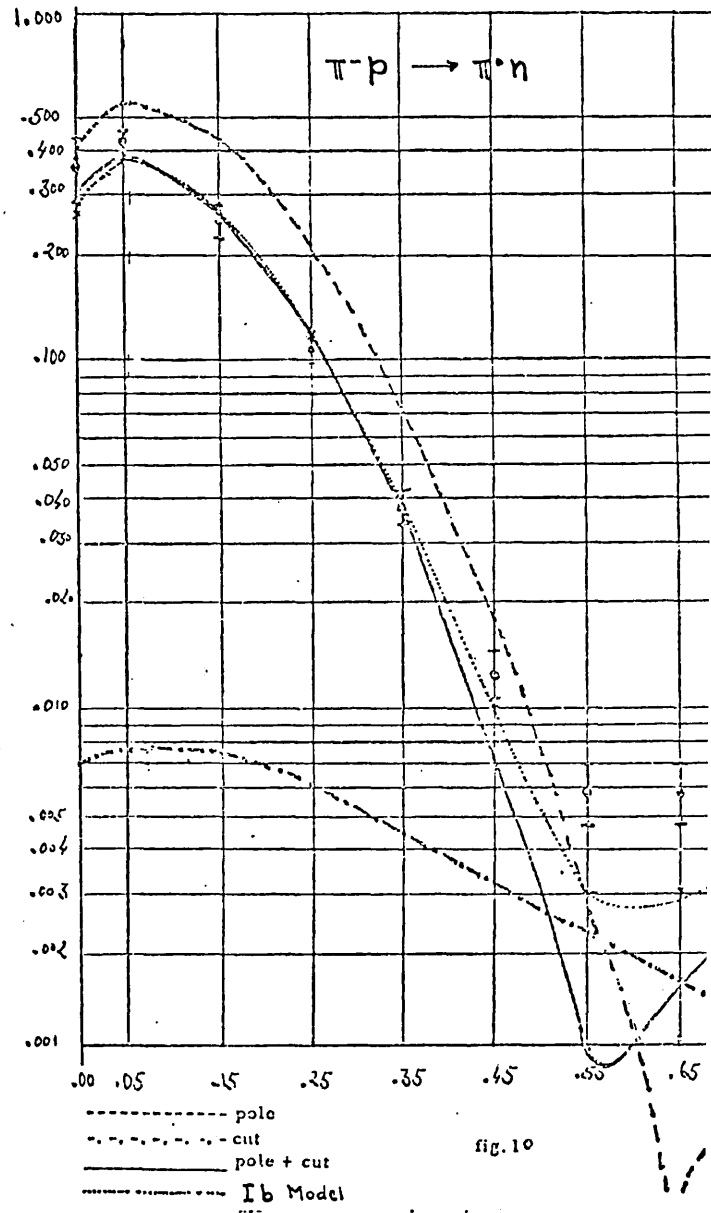
<u>$t = 1.200$</u>	<u>$t = 1.6$</u>	<u>$t = 2.0$</u>
$T_{th} = .0113 e^{i 333.53^\circ}$	$T_{th} = .0046 e^{i 354.07^\circ}$	$T_{th} =$

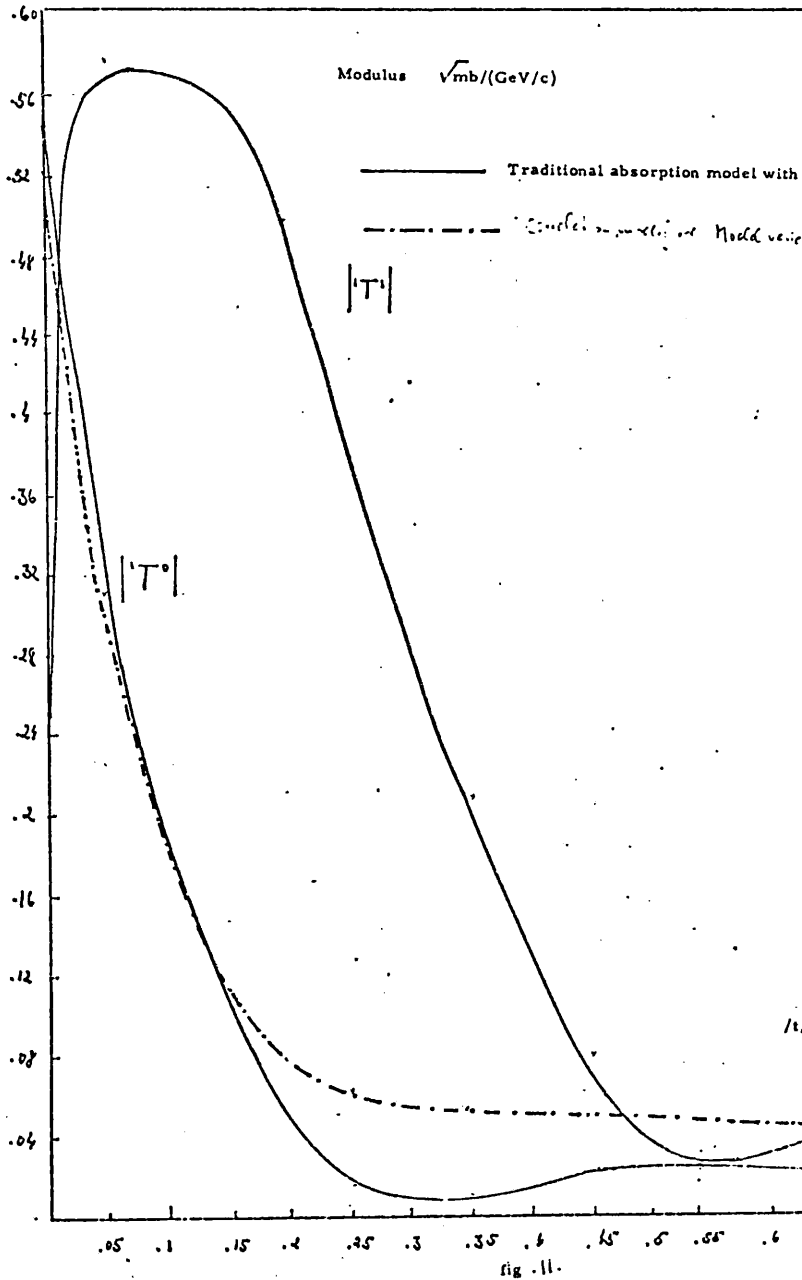
Polarization chart for model variant Ib with complex correlation

t	$\text{Re } T^0 \times \text{Im } T^1 - \text{Im } T^0 \times \text{Re } T^1$		$d\sigma/dt$		Polarization		
			th	exp	th	exp	
.00	.458	$\times .00$	-	.275	.362 \pm .07	.00	.00
.05	.282	$\times .387$	-	.387	.523 \pm .03	.3	.13 \pm .02
.15	.109	$\times .519$	-	.281	.266 \pm .02	.316	.18 \pm .0
.25	.051	$\times .309$	-	.127	-.110 \pm .012	.361	.18 \pm .0
.35	.035	$\times .185$	-	.051	.038 \pm .005	.451	.15 \pm .0
.45	.027	$\times .081$	-	.01	.013 \pm .002	.464	.12 \pm .0
.55	.025	$\times .021$	-	.0029	.0059 \pm .0011	.023	.07 \pm .0
.65	.023	$\times (-.032)$	-	.0031	.0055 \pm .004	-.95	.04 \pm .0
.8	.019	$\times (-.057)$	-	.0042	.0082 \pm .0059	-.626	.00 \pm .0
1.00	.015	$\times (-.05)$	-	.0028		-.465	
1.2	.010	$\times (-.031)$	-	.0012		-.433	
1.4	.0065	$\times (-.015)$	-	.00035		-.515	
1.6	.0056	$\times (-.005)$	-	.0001		-.42	
1.8	.0029	$\times (-.001)$	-	.00001		-.624	
2.00	.0018	$\times (+.001)$	-	.00001		+ .452	

Traditional reggeized absorption model with λ cut = 1.00

Differential cross-section measured in $\text{mb}/(\text{GeV}/c)^2$





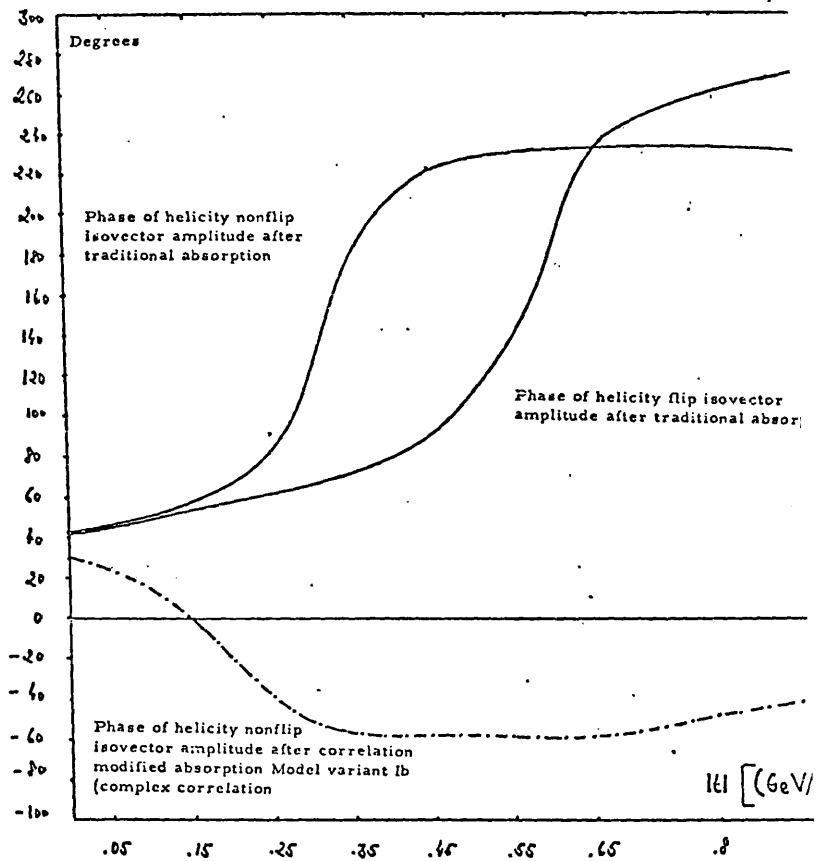


fig. 12

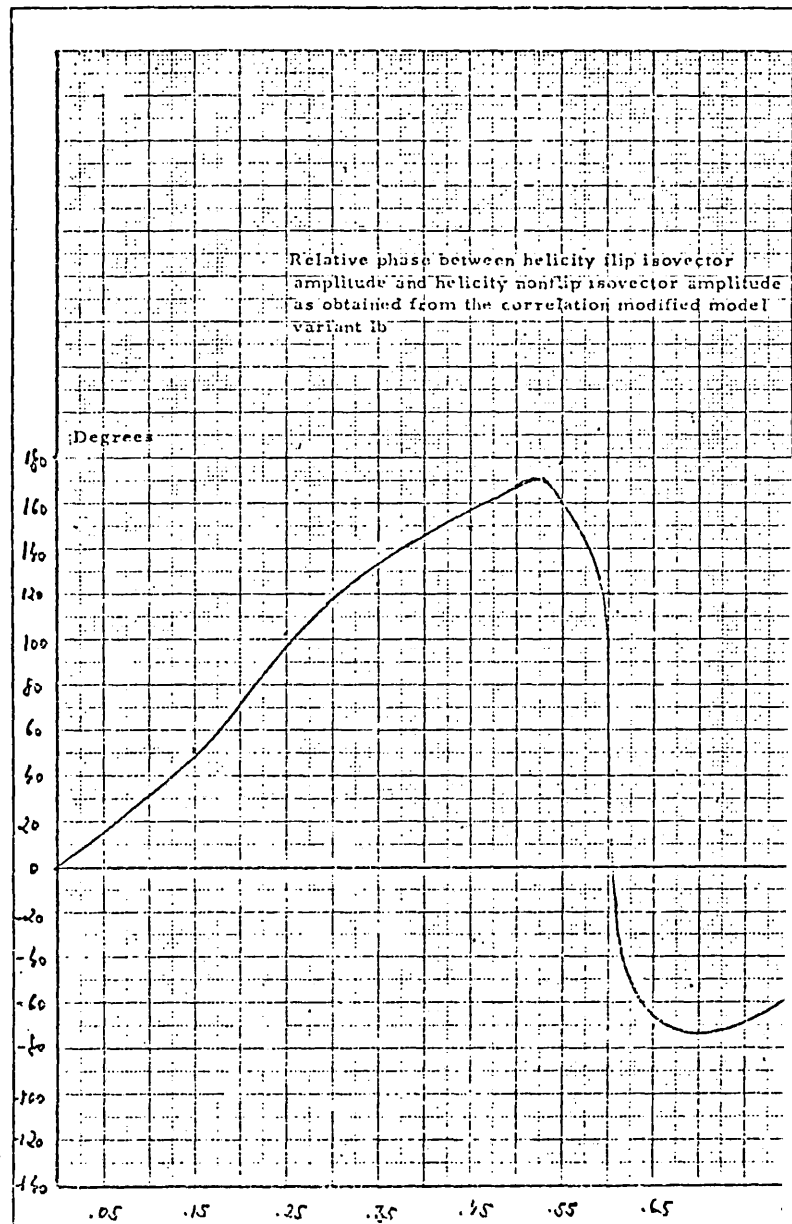


Fig. 13

Traditional absorption model (purely imaginary and stationary Pomeron
and λ cut = 1.00)

See Table IIa for numerical values

—————> Helicity nonflip pole
- - - - -> Absorbed amplitude

Numbers indicate $|t|$ values

Scale =

$$1 \text{ cm} = .019 (\text{mb})^{1/2} / \text{GeV}/c$$

- - - - ->

Correlation modified model variant Ib
See Table III for numerical values

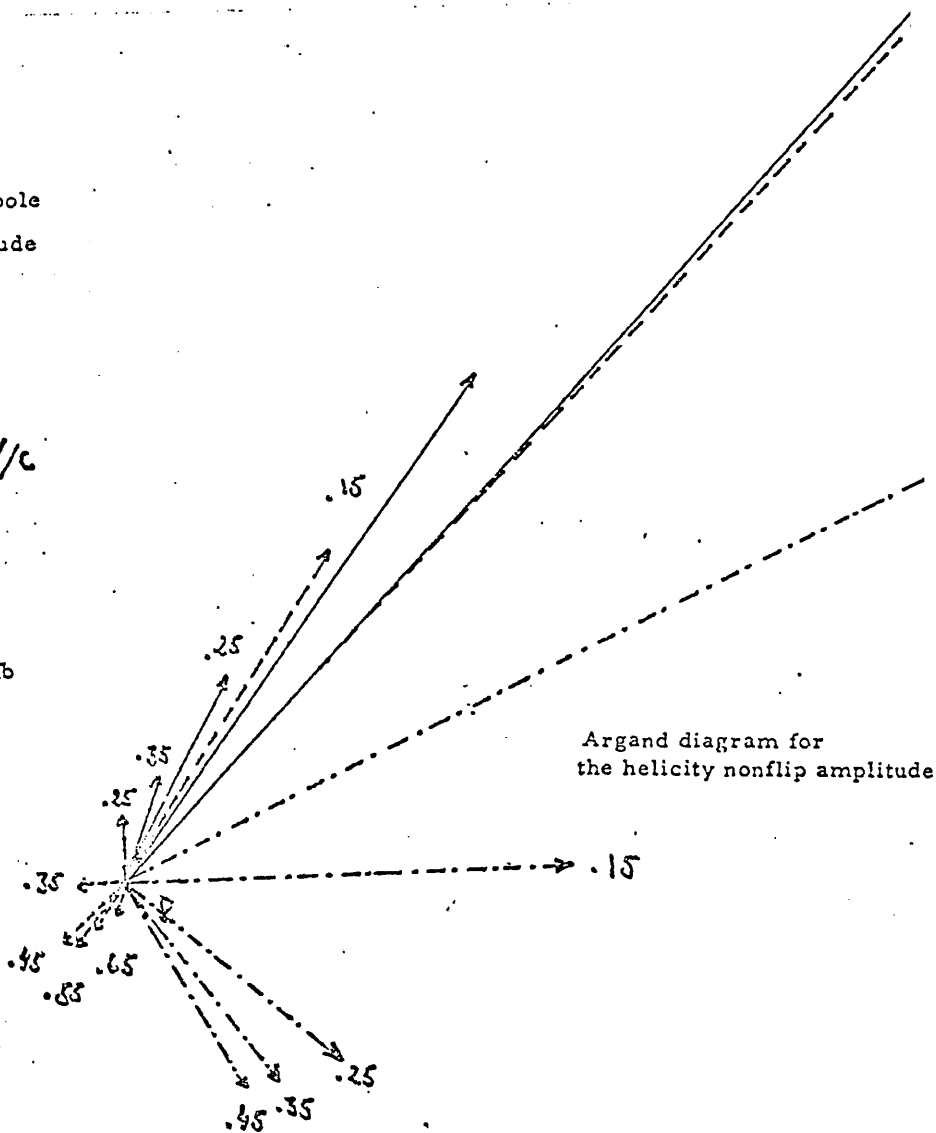


fig. 14

Argand diagram for the helicity nonflip isovector amplitude obtained with the traditional absorption model (purely imaginary and stationary Pomeron and correlation modified model Ib

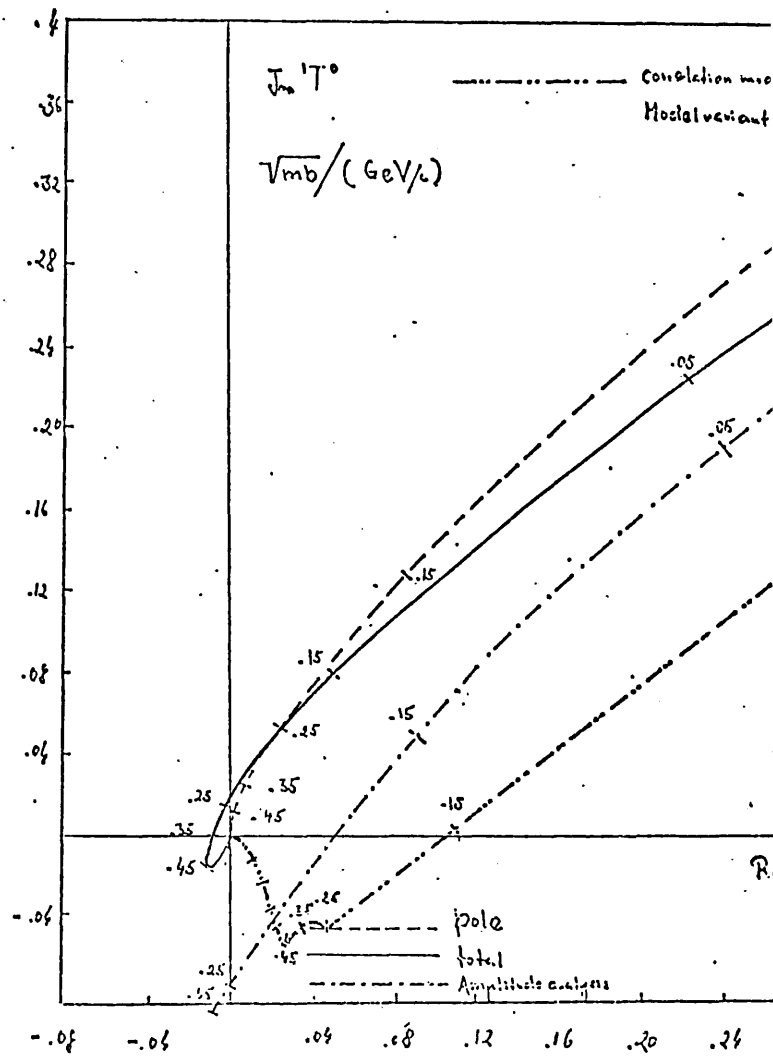


fig. 15

VI. III. 3 - PURELY REAL AND NEGATIVE CORRELATION MODIFIED MODELS AS A CROSSING SYMMETRY PRESERVING SOLUTION TO THE PHASE PROBLEM

A more convenient way to manipulate the terms of the Gribov cut in complex vector representation as written on pages 107 to 119, is to rewrite it as on pages 145 and 146 with the relevant terms explicitly expressed for fixed and variable energies as done on pages 147 to 152. For certain purposes it is specially instructive to write the energy dependence term in powers of $\ln s$ as done for example for the non-rotating part on pages 151 and 152. The vector representations of pole and cut enable us to obtain a great deal of insight into how the phases behave, and we learn that the necessary modifications in order to restore the most profound failures of the absorption cut, as discussed on page 127, can be accomplished for either a purely imaginary and stationary pomeron together with a complex "c" as we have seen, or for a pomeron with a significant real part at all t values, e.g. an initial phase of 101° and a slope of $\alpha'p = .6$, together with a purely real "c". Indeed, as one can see from the explicit formulas of the Gribov cut represented in vector form, the imaginary part of the "c" can, to a certain extent, be exchanged against the slope of the Pomeron.

A concrete model (Model V introduced on page 154) with the parameters as in Table I - and in addition -

$$\begin{array}{ll} \operatorname{Re} c^0 = -1.5 & \operatorname{Im} c^0 = 0 \\ \operatorname{Re} c^1 = -1 & \operatorname{Im} c^1 = -1 \end{array}$$

has been given with numerical details. Rather than describe all the details of the combined effect due to the "interaction" of the "Gribov c" and the real part of the Pomeron, we are going to draw several possible variations II, III, IV, V, VI, on the theme: "Gribov c" and Pomeron real part, while demonstrating how these joint effects as purely real c and real part of the Pomeron accomplish the necessary phase modification. This has been shown in figs. 18 to 23.

* e.g. the stabilisation of the energy dependence (see p. 160)

Helicity nonflip

$$\Psi_i^{\infty} = \frac{(2\sqrt{\pi})^{-1} \lambda_{ca} \beta_p^{(c)} \beta_r^{(c)} (S/s_0)^{\alpha_p^{(c)}-1}}{\left\{ (\text{Re } b_i^{\infty})^2 + (\text{Im } b_i^{\infty})^2 \right\}^{1/2}}$$

$$\Psi_{\perp}^{\infty} = \frac{\text{Re } a_i^{\infty} \text{Re } b_i^{\infty} + \text{Im } a_i^{\infty} \text{Im } b_i^{\infty}}{(\text{Re } b_i^{\infty})^2 + (\text{Im } b_i^{\infty})^2}$$

$$\Phi_{\perp}^{\infty} = \frac{\text{Im } a_i^{\infty} \text{Re } b_i^{\infty} - \text{Re } a_i^{\infty} \text{Im } b_i^{\infty}}{(\text{Re } b_i^{\infty})^2 + (\text{Im } b_i^{\infty})^2}$$

$$\phi_1^{\infty} = \hat{\delta}_p^{\infty} - \text{quartz} \frac{\text{Im } b_1^{\infty}}{\text{Re } b_1^{\infty}}$$

$$\phi_2^{\infty} = -\text{quartz} + \hat{\delta}_p^{\infty} - \text{quartz} \frac{\text{Im } b_2^{\infty}}{\text{Re } b_2^{\infty}}$$

Helicity flip

$$\chi_i^{01} = \frac{(2\sqrt{\pi})^{-1} \lambda_{out}^i \beta_p^0 \beta_p^i \{(\text{Re} d_i^{01})^2 + (\text{Im} d_i^{01})^2\}^{1/2} (s/s_0)^{\alpha_p^{(01)} - 1}}{(\text{Re} b_i^{01})^2 + (\text{Im} b_i^{01})^2}$$

$$\Psi_i^{01} = \frac{\text{Re} a_i^{01} \cdot \text{Re} b_i^{01} + \text{Im} a_i^{01} \cdot \text{Im} b_i^{01}}{(\text{Re} b_i^{01})^2 + (\text{Im} b_i^{01})^2} \quad \Phi_i^{01} = \frac{\text{Im} a_i^{01} \cdot \text{Re} b_i^{01} - \text{Re} a_i^{01} \cdot \text{Im} b_i^{01}}{(\text{Re} b_i^{01})^2 + (\text{Im} b_i^{01})^2}$$

$$\phi_i^{01} = \delta_{iP}^0 - 2g_{iP} \frac{\text{Im} b_i^{01}}{\text{Re} b_i^{01}} + g_{iP} \frac{\text{Im} d_i^{01}}{\text{Re} d_i^{01}}$$

At a fixed energy however the relevant quantities read as follows -

$$\text{Re } a_1^{00} = \text{Re } \hat{\lambda}_P^0 \hat{\lambda}_{P_1}^0 + \text{Re } c (\text{Re } \hat{\lambda}_P^0 + \hat{\lambda}_{P_1}^0) + \bar{\text{Im}} c \frac{\bar{u} \alpha'_P}{2}$$

$$\bar{\text{Im}} a_1^{00} = \bar{\text{Im}} c (\hat{\lambda}_P^0 + \hat{\lambda}_{P_1}^0) - \frac{\bar{u} \alpha'_P}{2} (\hat{\lambda}_{P_1}^0 + \text{Re } c)$$

$$\text{Re } b_1^{00} = \text{Re } \hat{\lambda}_P^0 + \hat{\lambda}_{P_1}^0 + 4 \text{Re } c$$

$$\bar{\text{Im}} b_1^{00} = 4 \bar{\text{Im}} c - \frac{\bar{u} \alpha'_P}{2}$$

$$\delta_{1P}^0 = \delta_P^0 - \bar{u}/2$$

$$\text{Re } a_2^{00} = \text{Re } a_1^{00} + \bar{u} \alpha'_P (\bar{\text{Im}} c - \frac{\bar{u} \alpha'_P}{2})$$

$$\bar{\text{Im}} a_2^{00} = \bar{\text{Im}} a_1^{00} - \bar{u} \alpha'_P (\text{Re } \hat{\lambda}_P^0 + \text{Re } c)$$

$$\text{Re } b_2^{00} = \text{Re } b_1^{00}$$

$$\bar{\text{Im}} b_2^{00} = \bar{\text{Im}} b_1^{00} - \bar{u} \alpha'_P$$

$$\delta_{2P}^0 = \delta_{1P}^0 - \bar{u} \alpha'_P \cos \theta$$

In the case of fixed energy -

Non rotating

$$\text{Re } a_1^{01} = \text{Re } \hat{\lambda}_p^0 \hat{\lambda}_p^1 + \text{Re } c (\text{Re } \hat{\lambda}_p^0 + \hat{\lambda}_p^1) + \bar{J} m c \frac{\bar{u} \alpha_p}{2}$$

$$\bar{J} m a_1^{01} = \bar{J} m c (\text{Re } \hat{\lambda}_p^0 + \hat{\lambda}_p^1) - \frac{\bar{u} \alpha_p}{2} (\hat{\lambda}_p^1 + \text{Re } c)$$

$$\text{Re } b_1^{01} = \hat{\lambda}_p^0 + \hat{\lambda}_p^1 + 4 \text{Re } c$$

$$\bar{J} m b_1^{01} = 4 \bar{J} m c - \frac{\bar{u} \alpha_p}{2}$$

$$\delta_{1p}^0 = \delta_p^0 - \bar{v}/2$$

$$\text{Re } d_1^{01} = \text{Re } \hat{\lambda}_p^0 + 2 \text{Re } c$$

$$\bar{J} m d_1^{01} = 2 \bar{J} m c - \frac{\bar{u} \alpha_p}{2}$$

Rotating

$$\text{Re } a_2^{01} = \text{Re } a_1^{01} + \bar{u} \alpha_p (\bar{J} m$$

$$\bar{J} m a_2^{01} = \bar{J} m a_1^{01} - \bar{u} \alpha_p (\text{Re } \hat{\lambda}_p^0$$

$$\text{Re } b_2^{01} = \text{Re } b_1^{01}$$

$$\bar{J} m b_2^{01} = \bar{J} m b_1^{01} - \bar{u} \alpha_p$$

$$\delta_{2p}^0 = \delta_{1p}^0 - \bar{u} \alpha_p$$

$$\text{Re } d_2^{01} = \text{Re } d_1^{01}$$

$$\bar{J} m d_2^{01} = \bar{J} m d_1^{01}$$

In order to stabilize the energy dependence of the phase we provide the parameter C with a slow energy dependence

$$\operatorname{Re} a_1^{\infty} = (\lambda_p^0 + \alpha_p' \ln(s/s_0))(\lambda_p^0 + \alpha_p' \ln(s/s_0)) + \operatorname{Re}(c_1 + c_2 \ln(s/s_0))(\lambda_p^0 + \alpha_p' \ln(s/s_0) + \lambda_p^0 + \alpha_p' \ln(s/s_0)) + \operatorname{Im}(c_1 +$$

$$\operatorname{Im} a_1^{\infty} = \operatorname{Im}(c_1 + c_2 \ln(s/s_0))(\lambda_p^0 + \alpha_p' \ln(s/s_0) + \lambda_p^0 + \alpha_p' \ln(s/s_0)) - (\lambda_p^0 + \alpha_p' \ln(s/s_0) + \operatorname{Re}(c_1 + c_2 \ln(s/s_0)))$$

$$\operatorname{Re} b_1^{\infty} = \lambda_p^0 + \alpha_p' \ln(s/s_0) + \lambda_p^0 + \alpha_p' \ln(s/s_0) + \frac{1}{2} \operatorname{Re}(c_1 + c_2 \ln(s/s_0))$$

$$\operatorname{Im} b_1^{\infty} = \frac{1}{2} \operatorname{Im}(c_1 + c_2 \ln(s/s_0)) - \pi \alpha_p' / 2$$

$$\operatorname{Re} a_2^{\infty} = \operatorname{Re} a_1^{\infty} + \pi \alpha_p' (\operatorname{Im}(c_1 + c_2 \ln(s/s_0))) - \pi \alpha_p' / 2$$

$$\operatorname{Im} a_2^{\infty} = \operatorname{Im} a_1^{\infty} - \pi \alpha_p' (\lambda_p^0 + \alpha_p' \ln(s/s_0) + \operatorname{Re}(c_1 + c_2 \ln(s/s_0)))$$

$$\operatorname{Re} b_2^{\infty} = \operatorname{Re} b_1^{\infty}$$

$$\operatorname{Im} b_2^{\infty} = \operatorname{Im} b_1^{\infty} - \pi \alpha_p'$$

With explicit energy dependence for the 'non rotating' contribution

$$\text{Re } a_1^{01} = (\lambda_p^0 + \alpha_p' \ln(s/s_0)) (\lambda_p^1 + \alpha_p' \ln(s/s_0)) + \text{Re} (c_1 + c_2 \ln(s/s_0)) \times (\lambda_p^0 + \alpha_p' \ln(s/s_0) + \lambda_p^1 + \alpha_p' \ln(s/s_0)) + \text{Im} (c_1 + c_2 \ln(s/s_0))$$

$$\text{Im } a_1^{01} = \text{Im} (c_1 + c_2 \ln(s/s_0)) (\lambda_p^0 + \alpha_p' \ln(s/s_0) + \lambda_p^1 + \alpha_p' \ln(s/s_0)) - \frac{\pi \alpha_p'}{2} (\lambda_p^1 + \alpha_p' \ln(s/s_0) + \text{Re} (c_1 + c_2 \ln(s/s_0)))$$

$$\text{Re } b_1^{01} = \lambda_p^0 + \alpha_p' \ln(s/s_0) + \lambda_p^1 + \alpha_p' \ln(s/s_0) + \frac{1}{2} \text{Re} (c_1 + c_2 \ln(s/s_0))$$

$$\text{Im } b_1^{01} = \frac{1}{2} \text{Im} (c_1 + c_2 \ln(s/s_0)) - \frac{\pi \alpha_p'}{2}$$

$$\text{Re } d_1^{01} = \lambda_p^0 + \alpha_p' \ln(s/s_0) + 2 \text{Re} (c_1 + c_2 \ln(s/s_0))$$

$$\text{Im } d_1^{01} = 2 \text{Im} (c_1 + c_2 \ln(s/s_0)) - \frac{\pi \alpha_p'}{2}$$

$$\delta_p^0 = \delta_p^1 - \pi/2$$

For the "rotating" contribution

$$\operatorname{Re} a_2^{o1} = \operatorname{Re} a_1^{o1} + \pi \alpha_p' \left(\operatorname{Im} (c_1 + c_2 \ln(s/s_0)) - \frac{\pi \alpha_p'}{2} \right)$$

$$\operatorname{Im} a_2^{o1} = \operatorname{Im} a_1^{o1} - \pi \alpha_p' \left(\chi_p^o + \alpha_p' \ln(s/s_0) + \operatorname{Re} (c_1 + c_2 \ln(s/s_0)) \right)$$

$$\operatorname{Re} b_2^{o1} = \operatorname{Re} b_1^{o1}$$

$$\operatorname{Im} b_2^{o1} = \operatorname{Im} b_1^{o1} - \pi \alpha_p'$$

$$\operatorname{Re} d_2^{o1} = \operatorname{Re} d_1^{o1}$$

$$\operatorname{Im} d_2^{o1} = \operatorname{Im} d_1^{o1}$$

$$\int_{2P}^o = -\pi \alpha_p'(s) + \delta_{IP}^o$$

$$\begin{aligned} \text{Re } a_i^{oo} &= \lambda_p^o \lambda_p^o + \text{Re } c_i^o \{ (\lambda_p^o + \lambda_p^o) \} + \text{Im } c_i^o \left\{ \frac{\bar{\mu} \alpha_p}{2} \right\} \\ &+ \text{Im} \left[(\lambda_p^o \alpha_p^o + \alpha_p^o \lambda_p^o) + \text{Re } c_i^o \{ (\alpha_p^o + \alpha_p^o) \} + \text{Re } c_2^o \{ (\lambda_p^o + \lambda_p^o) \} \right] \\ &+ (\text{Im})^2 \left[\alpha_p^o \alpha_p^o + \text{Re } c_2^o \{ (\alpha_p^o + \alpha_p^o) \} \right] \end{aligned}$$

$$\begin{aligned} \text{Im } a_i^{oo} &= -\lambda_p^o \frac{\bar{\mu} \alpha_p^o}{2} - \text{Re } c_i^o \left\{ \frac{\bar{\mu} \alpha_p^o}{2} \right\} + \text{Im } c_i^o \{ (\lambda_p^o + \lambda_p^o) \} \\ &+ \text{Im} \left[-\alpha_p^o \frac{\bar{\mu} \alpha_p^o}{2} - \text{Re } c_2^o \left\{ \frac{\bar{\mu} \alpha_p^o}{2} \right\} + \text{Im } c_i^o \{ (\alpha_p^o + \alpha_p^o) \} + \text{Im } c_2^o \{ (\lambda_p^o + \lambda_p^o) \} \right] \\ &+ (\text{Im})^2 \left[\text{Im } c_2^o \{ (\alpha_p^o + \alpha_p^o) \} \right] \end{aligned}$$

$$\text{Re } b_i^{oo} = (\lambda_p^o + \lambda_p^o) + 4 \text{Re } c_i^o + \text{Im} \left[(\alpha_p^o + \alpha_p^o) + 4 \text{Re } c_2^o \right]$$

$$\text{Im } b_i^{oo} = -\frac{\bar{\mu} \alpha_p^o}{2} + 4 \text{Im } c_i^o + \text{Im} \left[4 \text{Im } c_2^o \right]$$

$$\begin{aligned} \text{Re } a_i^{oi} &= \lambda_p^o \lambda_p^i + \text{Re } c_1 \{ (\lambda_p^o + \lambda_p^i) \} + \text{Im } c_1 \left\{ \frac{\bar{u} \alpha_p^i}{2} \right\} \\ &+ \text{Im } s \left[(\lambda_p^o \alpha_p^i + \alpha_p^i \lambda_p^o) + \text{Re } c_1 \{ (\alpha_p^i + \alpha_p^o) \} + \text{Re } c_2 \{ (\lambda_p^o + \lambda_p^i) \} \right] \\ &+ (\text{Im } s)^2 \left[\alpha_p^i \alpha_p^o + \text{Re } c_2 \{ (\alpha_p^i + \alpha_p^o) \} \right] \end{aligned}$$

$$\begin{aligned} \text{Im } a_i^{oi} &= -\lambda_p^i \frac{\bar{u} \alpha_p^i}{2} - \text{Re } c_1 \left\{ \frac{\bar{u} \alpha_p^i}{2} \right\} + \text{Im } c_1 \{ (\lambda_p^o + \lambda_p^i) \} \\ &+ \text{Im } s \left[-\alpha_p^i \frac{\bar{u} \alpha_p^i}{2} - \text{Re } c_2 \left\{ \frac{\bar{u} \alpha_p^i}{2} \right\} + \text{Im } c_1 \{ (\alpha_p^i + \alpha_p^o) \} + \text{Im } c_2 \right] \\ &+ (\text{Im } s)^2 \left[\text{Im } c_2 \{ \alpha_p^i + \alpha_p^o \} \right] \end{aligned}$$

$$\text{Re } b_i^{oi} = (\lambda_p^o + \lambda_p^i) + \frac{1}{2} \text{Re } c_1 + \text{Im } s \left[(\alpha_p^i + \alpha_p^o) + \frac{1}{2} \text{Re } c_2 \right]$$

$$\text{Im } b_i^{oi} = -\frac{\bar{u} \alpha_p^i}{2} + \frac{1}{2} \text{Im } c_1 + \text{Im } s \left[\frac{1}{2} \text{Im } c_2 \right]$$

$$\text{Re } d_i^{oi} = \lambda_p^o + 2 \text{Re } c_1 + \left[(\alpha_p^i + 2 \text{Re } c_2) \right] \text{Im } s$$

$$\text{Im } d_i^{oi} = -\frac{\bar{u} \alpha_p^i}{2} + 2 \text{Im } c_1 + \text{Im } s \left[2 \text{Im } c_2 \right]$$

MODEL V

$$\overline{T}_p^0 = 1.042 \sin \frac{\pi}{2} (.52 - .804 |t|) e^{-8.00 |t|} e^{i(43.20 + 72.36^\circ |t|)}$$

$$\overline{T}_c^{00} = -.158 e^{-2.25 |t|} e^{i(20.394 + 40.466^\circ |t|)} + .137 e^{-2.148 |t|} e^{i(-57.32^\circ + 42.}$$

$$e^{-1.74 |t|} e^{i(248.751^\circ + 44.77^\circ |t|)}$$

$$\overline{T}_p^1 = 4.656 (|t|)^{1/2} \sin \frac{\pi}{2} (.52 - .804 |t|) e^{-4.00 |t|} e^{i(43.20^\circ + 72.36^\circ |t|)}$$

$$\overline{T}_c^{01} = -.412 (|t|)^{1/2} e^{-1.98 |t|} e^{i(49.47^\circ + 13^\circ |t|)}$$

$$+ .217 (|t|)^{1/2} e^{-1.94 |t|} e^{i(-17.56^\circ + 38^\circ |t|)}$$

MODEL V Helicity nonflip

<u> t = .00</u>	<u> t = .05</u>	<u> t = .15</u>	<u> t = .25</u>	
$T_p^0 = .76 e^{i 43.20^\circ}$	$= .478 e^{i 46.89^\circ}$	$= .185 e^{i 53.05^\circ}$	$= .06$	
$T_c^0 = .174 e^{i 238.75^\circ}$	$= .156 e^{i 251.00^\circ}$	$= .125 e^{i 255.467^\circ}$	$= .10$	
$T_h^0 = .608 e^{i 36.107^\circ}$	$= .342 e^{i 36.13^\circ}$	$= .082 e^{i 20.502^\circ}$	$= .01$	
<u> t = .35</u>	<u> t = .45</u>	<u> t = .55</u>	<u> t = .65</u>	
$T_p^0 = .032 e^{i 68.526^\circ}$	$= .007 e^{i 75.72^\circ}$	$= .0016 e^{i 83.00^\circ}$	$= .000$	
$T_c^0 = .08 e^{i 264.42^\circ}$	$= .0642 e^{i 268.90^\circ}$	$= .0513 e^{i 273.375^\circ}$	$= .041$	
$T_h^0 = .05 e^{i 83.74^\circ}$	$= .0495 e^{-i 89.305^\circ}$	$= .05 e^{-i 86.322^\circ}$	$= .041 e^{-i 86.322^\circ}$	
<u> t = .8</u>	<u> t = 1.00</u>	<u> t = 1.2</u>	<u> t = 1.5</u>	<u> t = 2.0</u>
$T_p = -.00033 e^{i 101.05^\circ}$	$= .000$	$= .000$	$= .000$	$= .000$
$T_c = .0295 e^{i 283.567^\circ}$	$= .0186 e^{i 66.193^\circ}$	$= .0119 e^{-i 57.381^\circ}$	$= .0062 e^{-i 43.7^\circ}$	$= .0025$
$T_h = .0298 e^{i 75.461^\circ}$	$= "$	$= "$	$= "$	$= "$

MODEL V Helicity flip

<u>1/t/ = .05</u>		<u>1/t/ = .15</u>		<u>1/t/ = .25</u>		<u>1/t/ = .35</u>	
$T_p = .626 e^{i 46.71^\circ}$		$.623 e^{i 54.04^\circ}$		$.441 e^{i 61.29^\circ}$		$.267 e^{i \dots}$	
$T_c = .065 e^{i 261.77^\circ}$		$.106 e^{i 263^\circ}$		$.109 e^{i 264^\circ}$		$.103 e^{i \dots}$	
$T_{th} = .573 e^{i 43.09^\circ}$		$.533 e^{i 48.50^\circ}$		$.343 e^{i 54.23^\circ}$		$.172 e^{i \dots}$	
<u>1/t/ = .45</u>		<u>1/t/ = .55</u>		<u>1/t/ = .65</u>		<u>1/t/ = .8</u>	
$T_p = .136 e^{i 75.76^\circ}$		$.05 e^{i 83.00^\circ}$		$.001 e^{i 90.24^\circ}$		$.055$	
$T_c = .092 e^{i 267^\circ}$		$.082 e^{i 268^\circ}$		$.071 e^{i 269.20^\circ}$		$.055$	
$T_{th} = .049 e^{i 54.37^\circ}$		$.032 e^{i 64.29^\circ}$		$.072 e^{i 90.30^\circ}$		$.09 e^{i \dots}$	
<u>1/t/ = 1.00</u>		<u>1/t/ = 1.2</u>		<u>1/t/ = 1.5</u>		<u>1/t/ = 2.00</u>	
$T_p = .037 e^{i 115.56^\circ}$		$.025 e^{i 130.03^\circ}$		$.012 e^{i 151.74^\circ}$		$.005$	
$T_c = .039 e^{i 271.45^\circ}$		$.027 e^{i 272.65^\circ}$		$.015 e^{i 274^\circ}$		$.005$	
$T_{th} = .071 e^{i 76.78^\circ}$		$.049 e^{i 69.39^\circ}$		$.014 e^{i 60.615^\circ}$		$.005$	

MODEL V Pomeron initial phase 101° slope = .6 $ReC^0 = -1.5$ $ReC' = -1$ $ImC' = -1$ $\lambda_{cut}^{0,1}$

$ t $	$ReT^0 \times ImT'$	$ImT^0 \times ReT'$	k	k	Relativity
			$d\sigma/dt$	$d\sigma/dt$	$d\sigma/dt$
			exp	exp	$exp: Ambrosi P(5) H_{11}$
.00	.491 * .00	- .354 * .00	.369	.362 ± .07	.00
.05	.276 * .392	- .202 * .419	.446	.423 ± .03	.106
.15	.077 * .399	- .029 * .353	.291	.266 ± .02	.141
.25	.015 * .278	- (-.035) * .201	.119	.110 ± .012	.202
.35	.0038 * .146	- (-.05) * .091	.032	.038 ± .004	.317
.45	.0005 * .0399	- (-.057) * .0286	.0057	.013 ± .002	.579
.55	.0032 * (-.032)	- (-.05) * .0032	.0035	.0059 ± .0011	.033
.65	.0056 * (-.072)	- (-.041) * (-.001)	.0069	.0055 ± .0011	.129
.8	.0075 * (-.0853)	- (-.025) * .0076	.0089	.0082 ± .0009	.102
1.00	.0075 * (-.0724)	- (-.017) * .017	.0059		.086
1.2	.0064 * (-.066)	- (-.01) * .0173	.0026		.07
1.5	.0045 * (-.0206)	- (-.0033) * .016	.0006		.143
2.00	.0024 * (-.0053)	- (-.0028) * .0024	.0004		.457

MODEL V - Elastic amplitude differential cross section - Polarization chart

t	$J_m^{\circ} T^{\circ} \cdot Re^{\circ} T^{\circ} - Re^{\circ} T^{\circ} \cdot J_m^{\circ} T^{\circ}$	$\frac{d\sigma_{\text{sym}}^+}{dt} / t $		$\frac{d\sigma_{\text{asym}}^-}{dt} / t $		P^{sym}		P^+	
		th	exp	th	exp	th	exp	th	exp
.20	$6.047 \times .00 - (-1.175) \times .00$	35.14	36.67 ± 1.4	41.49	41.97 ± 1.0		.00		
.005	$4.974 \times .419 - (-1.213) \times .392$	25.32	$26.09 \pm .58$	28.00	$27.61 \pm .29$.191	$.174 \pm .005$.242	
.15	$3.34 \times .353 - (-1.157) \times .399$	12.77	$12.90 \pm .19$	12.8	$12.64 \pm .15$.256	$.171 \pm .006$.297	.20
.25	$2.223 \times .201 - (-1.013) \times .278$	6.29	$6.242 \pm .133$	5.88	$5.72 \pm .10$.239	$.152 \pm .006$.231	.10
.35	$1.462 \times .091 - (-.841) \times .146$	3.03	$3.119 \pm .094$	2.724	$2.789 \pm .072$.18	$.119 \pm .008$.164	.1
.45	$.951 \times .0286 - (-.673) \times .0399$	1.472	$1.615 \pm .044$	1.253	$1.261 \pm .062$.079	$.074 \pm .004$.073	.10
.55	$.610 \times .0032 - (-.525) \times (-.032)$.716	$.834 \pm .048$.587	$.631 \pm .054$	-.046	$.035 \pm .007$	-.042	.0
.65	$.386 \times (-.001) - (-.401) \times (-.072)$.353	$.440 \pm .038$.281	$.376 \pm .027$	-.185	$.009 \pm .004$	-.166	.00
.8	$.187 \times .0076 - (-.259) \times (-.0893)$.126	$.202 \pm .018$.096	$.199 \pm .007$	-.391	$.079 \pm .008$	-.365	.0
1.00	$.064 \times .017 - (-.138) \times (-.0724)$.033		.025		-.614		-.54	
1.2	$.018 \times .0173 - (-.071) \times (-.046)$.0092		.007		-.73		-.642	
1.5	$(-.00084) \times .0116 - (-.024) \times (-.0206)$.0016		.001		-.84		-.720	
2.00	$(-.0018) \times .0024 - (-.0033) \times (-.0053)$.0007		.000041		-.94		-.623	

MODEL V Elastic amplitude differential cross section chart

$ t $	$(J_m^0 T^0 - J_m^1 T^0)^2 + (Re^0 T^0 - Re^1 T^0)^2 + (Re^1 T^1)^2 + (J^- T^1)^2$	$\frac{d\sigma^+}{d\Omega dt}$	$\frac{d\sigma^-}{d\Omega dt}$
.00	$(6.047 - .358)^2 + (-1.175 - .491)^2 + (.00)^2 + (.00)^2$	35.14	36.07 ± 1.4
.05	$(4.974 - .202)^2 + (-1.213 - .276)^2 + (.419)^2 + (.392)^2$	25.32	26.09 ± .74
.15	$(3.34 - .029)^2 + (-1.157 - .077)^2 + (.353)^2 + (.399)^2$	12.769	12.90 ± .19
.25	$(2.223 - (-.039))^2 + (-1.013 - .015)^2 + (.201)^2 + (.278)^2$	6.29	6.22 ± .133
.35	$(1.462 - (-.05))^2 + (-.441 - .0038)^2 + (.091)^2 + (.146)^2$	3.03	3.119 ± .099
.45	$(.951 - (-.057))^2 + (-.673 - .0005)^2 + (.0286)^2 + (.0399)^2$	1.472	1.515 ± .044
.55	$(.610 - (-.05))^2 + (-.525 - .0032)^2 + (.0032)^2 + (-.032)^2$.716	.67 ± .057
.65	$(.386 - (-.041))^2 + (-.401 - .0056)^2 + (-.001)^2 + (-.072)^2$.353	.40 ± .047
.8	$(.187 - (-.029))^2 + (-.255 - .0075)^2 + (.0076)^2 + (-.0483)^2$.126	.202 ± .014
1.00	$(.064 - (-.017))^2 + (-.138 - .0075)^2 + (.017)^2 + (-.072)^2$.033	.025
1.2	$(.018 - (-.01))^2 + (-.071 - .0064)^2 + (.0173)^2 + (-.046)^2$.0052	.007
1.5	$((-.00084) - (-.0043))^2 + (-.024 - .0045)^2 + (.0116)^2 + (-.0206)^2$.0014	.001
2.00	$((-.0018) - (-.0008))^2 + (-.0023 - .0024)^2 + (.0024)^2 + (-.0053)^2$.00007	.000061

VI. III. 4 A PHASE ENERGY DESCRIPTION OF $\pi^- p \rightarrow \pi^0 n$ AT 6 GEV/C AND FNAL ENERGIES WITH A GOOD PREDICTION OF BOTH INELASTIC AND ELASTIC POLARIZATION OF $\pi^- N$ SCATTERING (MODEL V AND MODEL VI)

In Model V we have constructed (see Ardill et al (45)) the isovector helicity amplitude by means of the corrected Gribov absorption model. We absorb with a helicity conserving pomeron pole which possesses a real part $\alpha' p = 1.01^\circ$ and a slope of $\alpha' p = .6$ - see fig. 32 page 179. The same pomeron is used as isoscalar helicity amplitude for the elastic polarization see fig. 33 page 179. By describing the elastic polarization we encounter the same problem in (22,23). We were obliged to give the helicity flip shower factor a strong $|t|$ dependence, such that the double zero turns for $|t| \gg .6$ into a constructive one.

$$\text{Model VI : } \lambda_{cut}^{flip} = (\lambda_1 + \lambda_2 |t|) e^{(\gamma_1 + \gamma_2 |t|) |t|}$$

The imaginary part of the helicity flip amplitude is in that way not only prevented from becoming negative as in "untreated" Model variant V, fig. 27 and 28, but grows and falls rapidly in magnitude - fig. 29 - so as to account for the rise and fall of the elastic polarization beyond the double zero - fig. 33 and 34. The parameters have been given in Table I, but with the addition of -

$$\begin{aligned} \text{Re } c^0 &= -1.5 & \text{Im } c^0 &= 0 & \lambda_1 &= 1 & \alpha' p &= .6 & \gamma_1 &= 2.5 \\ \text{Re } c^1 &= -1 & \text{Im } c^1 &= 1 & \lambda_2 &= -1.8 & \gamma_2 &= -1 \end{aligned}$$

When extrapolating our amplitudes to FNAL energies we stabilize the energy dependence of the helicity nonflip amplitude maximally such that the initial cut phase has minimal energy dependence* and the rotational phase has only a weak energy dependence. We accomplish this by providing the Gribov 'c' with an energy dependence such that

$$c = c_1 + c_2 \ln s$$

which results in a considerably stable polarization over a wide range in energy (fig. 36,37). The smaller s' dependence of the traditional shrinking problem further out in $|t|$ causing a slower fall of $d\sigma/dt$ ($\pi^- p \rightarrow \pi^0 n$) and a spread of trajectories at 6 and 200 GeV/c (fig. 39,40). The parameter values for the energy dependence of c are

$$\begin{aligned} \text{Re } c_1^0 &= -.6225 & \text{Re } c_2^0 &= -.351 \\ \text{Re } c_1^1 &= -.1225 & \text{Re } c_2^1 &= -.351 \\ \text{Im } c_1^1 &= -1 & \text{Im } c_2^1 &= 0 \end{aligned}$$

which coincide with the parameter values found at 6 GeV/c.

* Since our absorptive factor is the full elastic amplitude the initial phase of the Pomeron possesses the experimentally observed energy dependence. This rotates the initial cut phase by a few degrees in clockwise direction and is the only energy dependence of the initial cut phase.

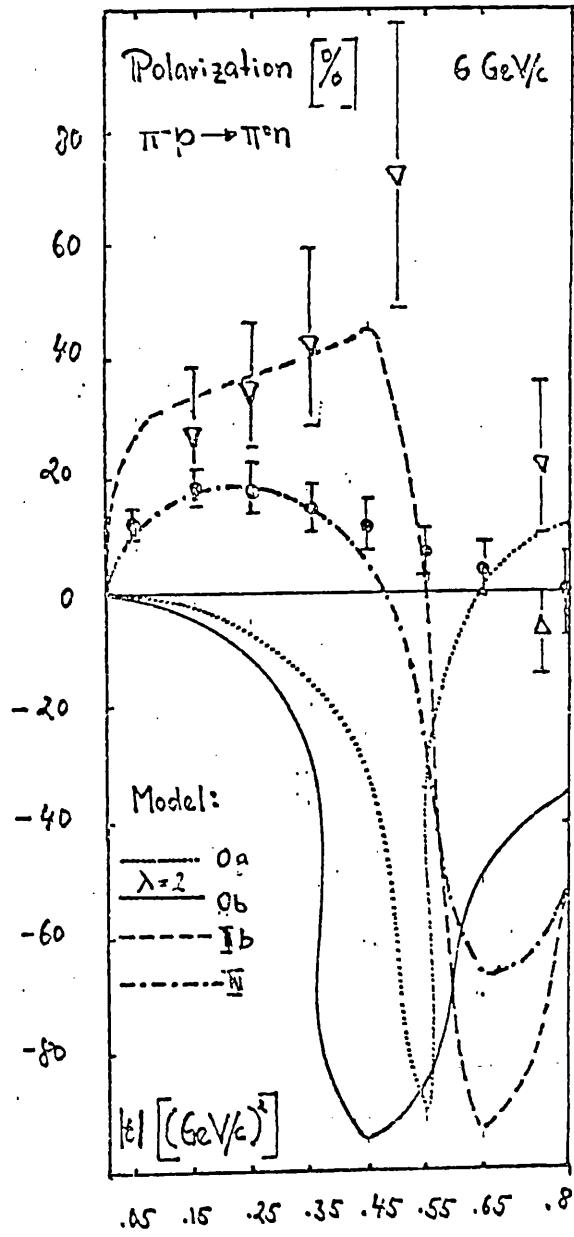


fig 16.

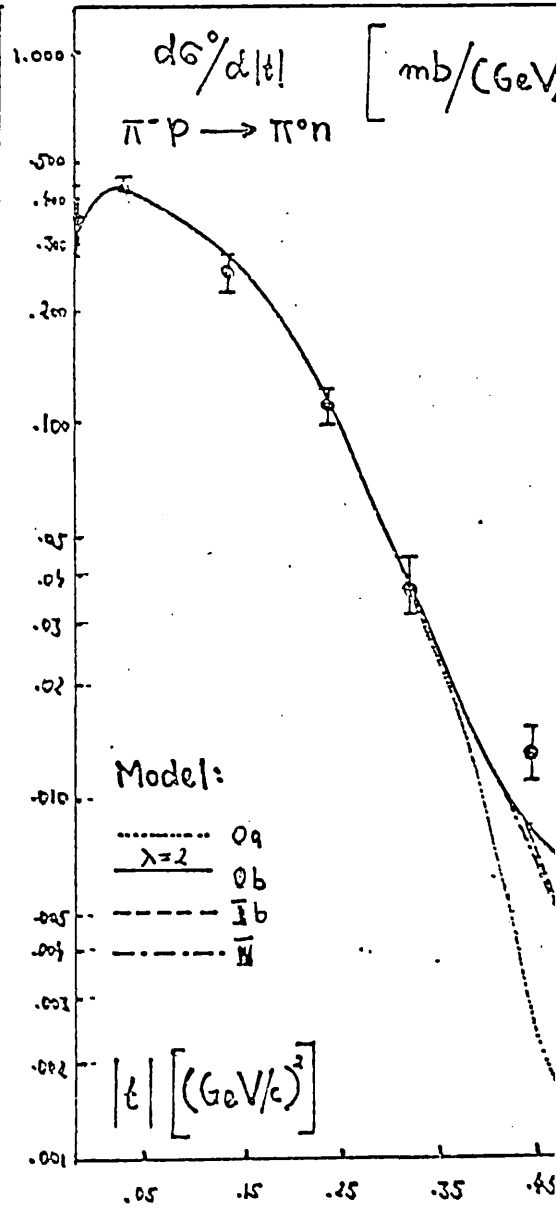







fig. 17.

Im

Re

-  Pole
-  Gribov cut components
-  total Gribov cut
-  total Amplitude (non flip)
-  the critical 180°
-  $1 \text{ cm} = 0.47 \text{ (mb)}^{1/2} / \text{GeV}/c$

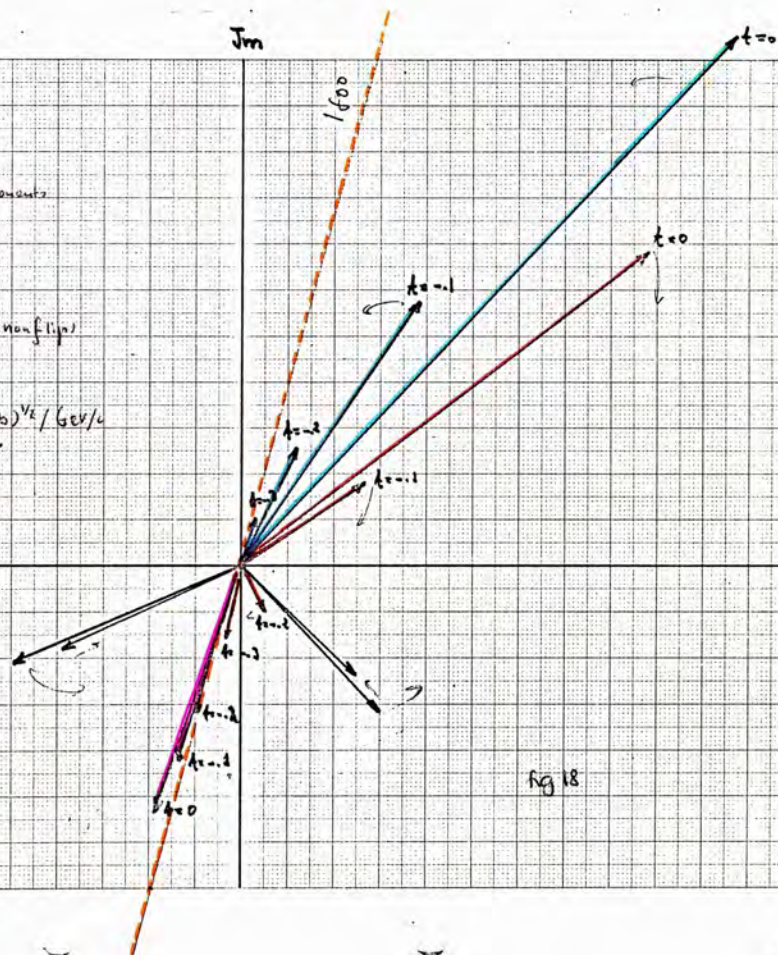


fig 18

Helicity non flip amplitude
scaled by 1

$$|T| = 0.00$$

- 1 Absorption with purely imaginary and stationary Pomero-
- 2 with 10% and stationary Pomero.
- 3 with 10% and moving Pomero - $\rho_0 p = 6$
- 4 hybrid with $c = -1$ and 10% moving Pomero - $\rho_0 p = 6$
- 5 $c = -1.5$
- 6 $c = -2.00$
- 7 $c = -2.1$
- Regge pole
- total Amplitude (theory)
- total " (Experiment - Amplitude)

$1 \text{ cm} = 0.65 (\text{mb})^{1/2} / \text{GeV}^2$

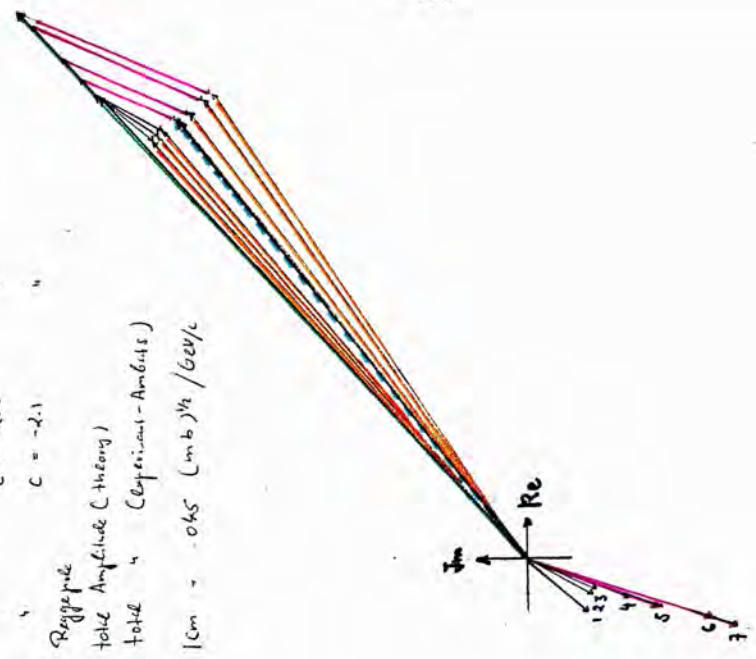


fig 19

$|\zeta| = .05$ scaled by 1.5

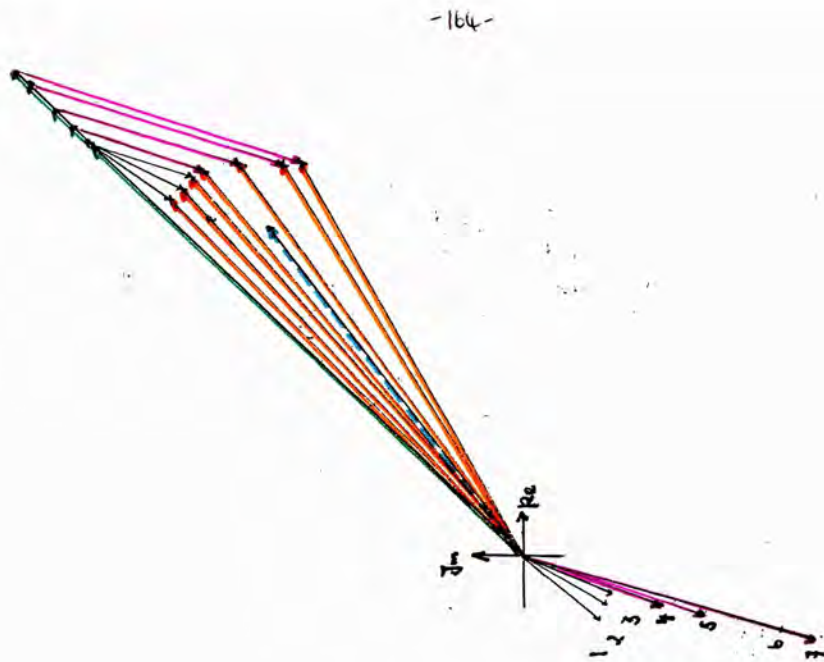
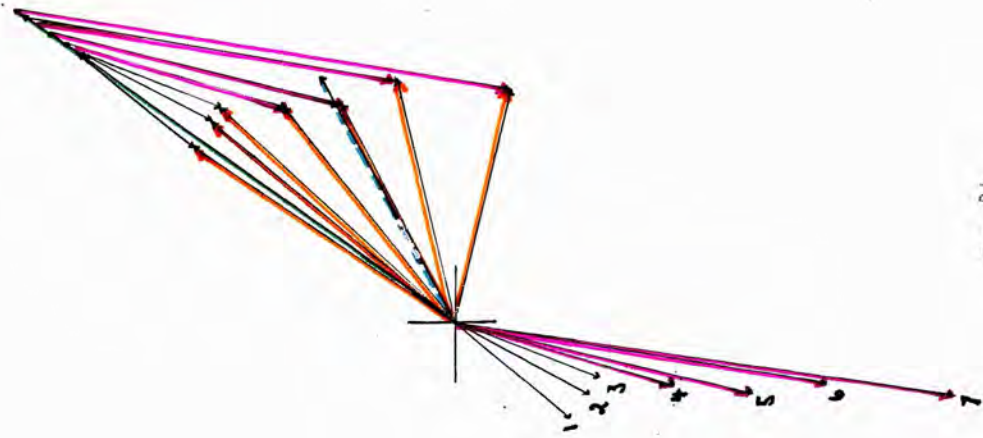


fig. 20

$|t| = .15$ scaled by 3



-165-

fig. 21

$|\zeta| = .25$ scaled by 5

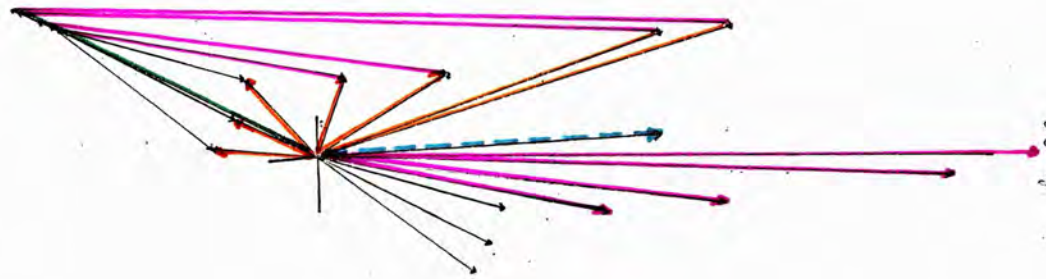


Fig. 22

$|t| = -35$ scaled by 6



fig 23

MODEL VI Helicity flip

<p><u>1/t/ = .05</u></p> <p>$T_p = .626 e^{i 46.71^\circ}$</p> <p>$T_c = .067 e^{i 261.77^\circ}$</p> <p>$T_{th} = .573 e^{i 42.81^\circ}$</p>	<p><u>1/t/ = .15</u></p> <p>$= .623 e^{i 54.05^\circ}$</p> <p>$= .110 e^{i 263^\circ}$</p> <p>$= .529 e^{i 48.29^\circ}$</p>	<p><u>1/t/ = .25</u></p> <p>$= .441 e^{i 61.25^\circ}$</p> <p>$= .1052 e^{i 264^\circ}$</p> <p>$= .346 e^{i 54.51^\circ}$</p>	<p><u>1/t/ = .35</u></p> <p>$=$</p> <p>$=$</p> <p>$=$</p>
<p><u>1/t/ = .45</u></p> <p>$T_p = .136 e^{i 75.76^\circ}$</p> <p>$T_c = .044 e^{i 267^\circ}$</p> <p>$T_{th} = .093 e^{i 70.59^\circ}$</p>	<p><u>1/t/ = .55</u></p> <p>$= .05 e^{i 83.00^\circ}$</p> <p>$= .0024 e^{i 268^\circ}$</p> <p>$= .0472 e^{i 82.78^\circ}$</p>	<p><u>1/t/ = .65</u></p> <p>$= .001 e^{i 90.24^\circ}$</p> <p>$= .04 e^{i 265.20^\circ}$</p> <p>$= .035 e^{i 89.18^\circ}$</p>	<p><u>1/t/ = .8</u></p> <p>$=$</p> <p>$=$</p> <p>$=$</p>
<p><u>1/t/ = 1.00</u></p> <p>$T_p = .037 e^{i 115.56^\circ}$</p> <p>$T_c = .14 e^{i 271.45^\circ}$</p> <p>$T_{th} = .107 e^{i 83.37^\circ}$</p>	<p><u>1/t/ = 1.2</u></p> <p>$= .025 e^{i 130.03^\circ}$</p> <p>$= .149 e^{i 272.65^\circ}$</p> <p>$= .13 e^{i 86.04^\circ}$</p>	<p><u>1/t/ = 1.5</u></p> <p>$= .012 e^{i 151.74^\circ}$</p> <p>$= .114 e^{i 274^\circ}$</p> <p>$= .108 e^{i 88.62^\circ}$</p>	<p><u>1/t/</u></p> <p>$=$</p> <p>$=$</p> <p>$=$</p>

MODEL VI Elastic amplitude differential cross section - Polarization chart

$ k $	$J_m^0 T^0 \times Re^1 T^1 - Re^0 T^0 \times J_m^1 T^1$	$d\sigma/dt$	$d\sigma/dt$	P_{Sym}	P^+			
.00	$6.047 \times .00 - (-1.175) \times .00$	35.14	36.67 ± 1.4	41.432	41.07 ± 1.0	.00	.99	
.05	$4.974 \times .42 - (-1.213) \times .389$	25.32	$26.05 \pm .24$	27.977	$27.44 \pm .25$.192	$.174 \pm .055$.202
.15	$3.34 \times .352 - (-1.157) \times .395$	12.77	$12.90 \pm .19$	12.759	$12.64 \pm .15$.256	$.171 \pm .024$.256
.25	$2.223 \times .201 - (-1.012) \times .242$	6.295	$6.242 \pm .033$	5.85	$5.72 \pm .10$.241	$.152 \pm .026$.233
.35	$1.462 \times .092 - (-.841) \times .168$	3.037	$3.115 \pm .058$	2.73	$2.785 \pm .022$.19	$.119 \pm .023$.182
.45	$-.951 \times .031 - (-.673) \times .088$	1.478	$1.515 \pm .044$	1.262	$1.241 \pm .022$.119	$.074 \pm .014$.120
.55	$-.610 \times .006 - (-.525) \times .0472$.717	.631	.588	$-.631 \pm .02$.087	$.035 \pm .017$.079
.65	$.386 \times .00056 - (-.401) \times .039$.349	$-.480 \pm .014$.278	$-.376 \pm .020$.101	$.005 \pm .02$.091
.8	$.187 \times .0053 - (-.259) \times .06$.121	$-.202 \pm .014$.092	$-.154 \pm .025$.030	$-.079 \pm .014$.273
1.00	$.064 \times .0124 - (-.124) \times .1066$.039		.031		.086		.795
1.2	$-.048 \times .009 - (-.071) \times .13$.024		.021		.034		.782
1.5	$(-.00084) \times .0026 - (-.024) \times .108$.012		.012		.032		.424
2.00	$(-.0018) \times .0009 - (-.0035) \times .04$.00163		.0016		.163		.161

Inelastic amplitude - differential cross section - Polarization chart

MODEL VI : as MODEL V but $\lambda'_{cut} = \lambda' (1/t) = (1-1.8/t) e^{(2.5-1/t)/t}$ λ'_{cut}

$ t $	$Re T^0 \times Im T^1 - Im T^0 \times Re T^1$	t_1	$\frac{d^2\sigma/d\Omega}{d\Omega}$ ρ_p	t_2	ρ_p	$\rho_{p, Ambrose (5)}$	$\rho_{p, Hill}$
.00	.491 x .00 - .358 x .00	.369	.362 ± .07	.00	.00	.00	.00
.05	.274 x .389 - .202 x .42	.445	.423 ± .03	.101	.13 ± .02		
.15	.077 x .395 - .029 x .352	.286	.266 ± .02	.141	.18 ± .03		.13 ±
.25	.015 x .282 - (-.039) x .201	.122	.110 ± .012	.198	.18 ± .03		.20 ±
.35	.0034 x .168 - (-.05) x .092	.039	.038 ± .004	.268	.15 ± .03		.13 ±
.45	.0005 x .088 - (-.037) x .031	.012	.013 ± .002	.302	.12 ± .03		.15 ±
.55	.0032 x .072 - (-.05) x .006	.0048	.0059 ± .001	.188	.07 ± .03		.17 ±
.65	.0056 x .039 - (-.041) x .0056	.0032	.0059 ± .001	.151	.03 ± .05		.02 ±
.8	.0075 x .06 - (-.029) x .0053	.0037	.0082 ± .001	.085	.00 ± .05		$H_1 = .75$ $H_2 = .85$
1.00	.0075 x .1066 - (-.017) x .0124	.0119	.011 ± .002	.170			$H_1 = 1.00$ - .03 ±
1.2	.0064 x .13 - (-.01) x .009	.017	.010 ± .002	.108			$H_1 = 1.15$ $H_2 = 1.25$
1.5	.0045 x .108 - (-.0043) x .0026	.01	.006 ± .001	.099			$H_1 = 1.35$ $H_2 = 1.45$
2.00	.0024 x .04 - (-.0008) x .0004	.0016	.002	.12			$H_1 = 1.65$

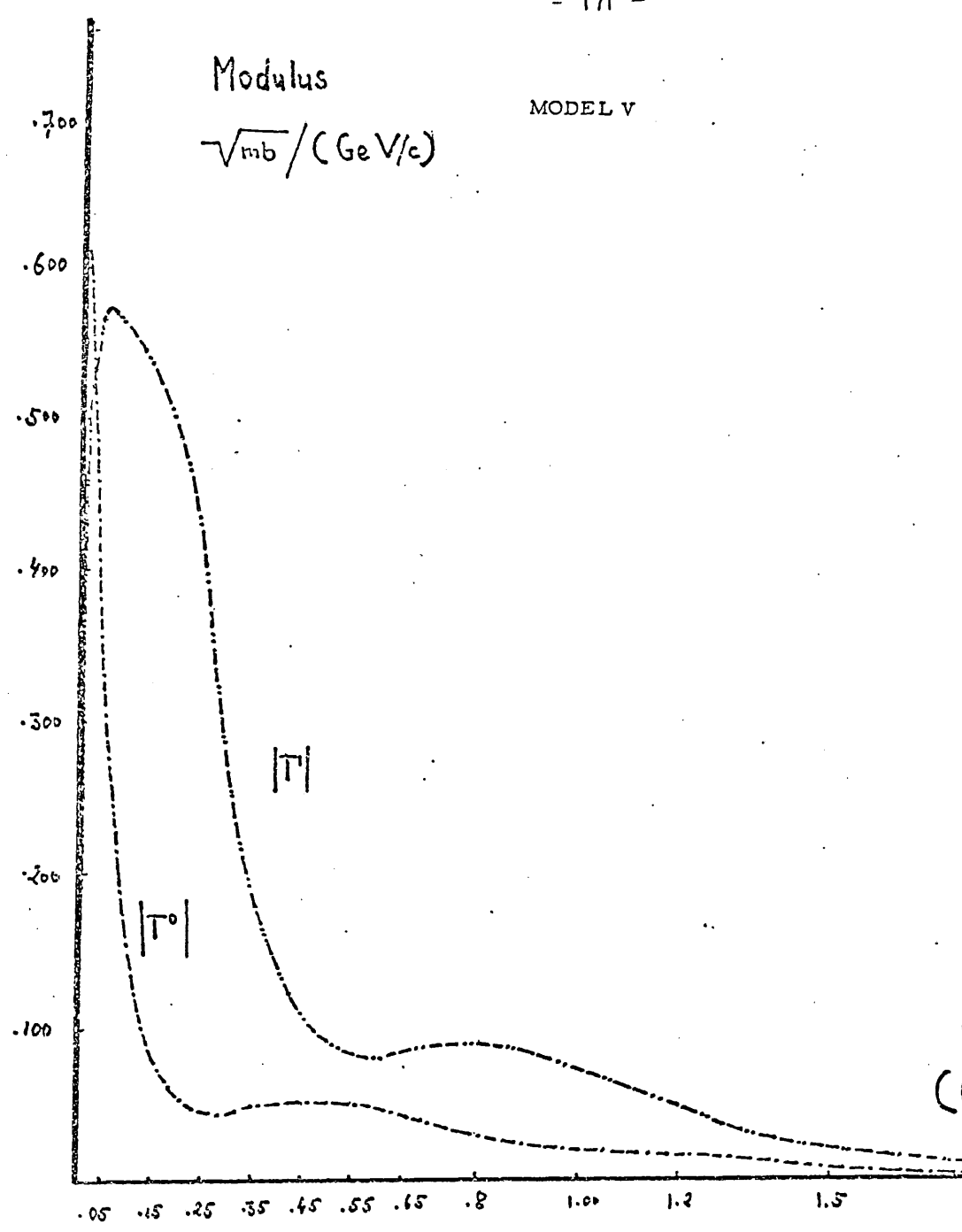
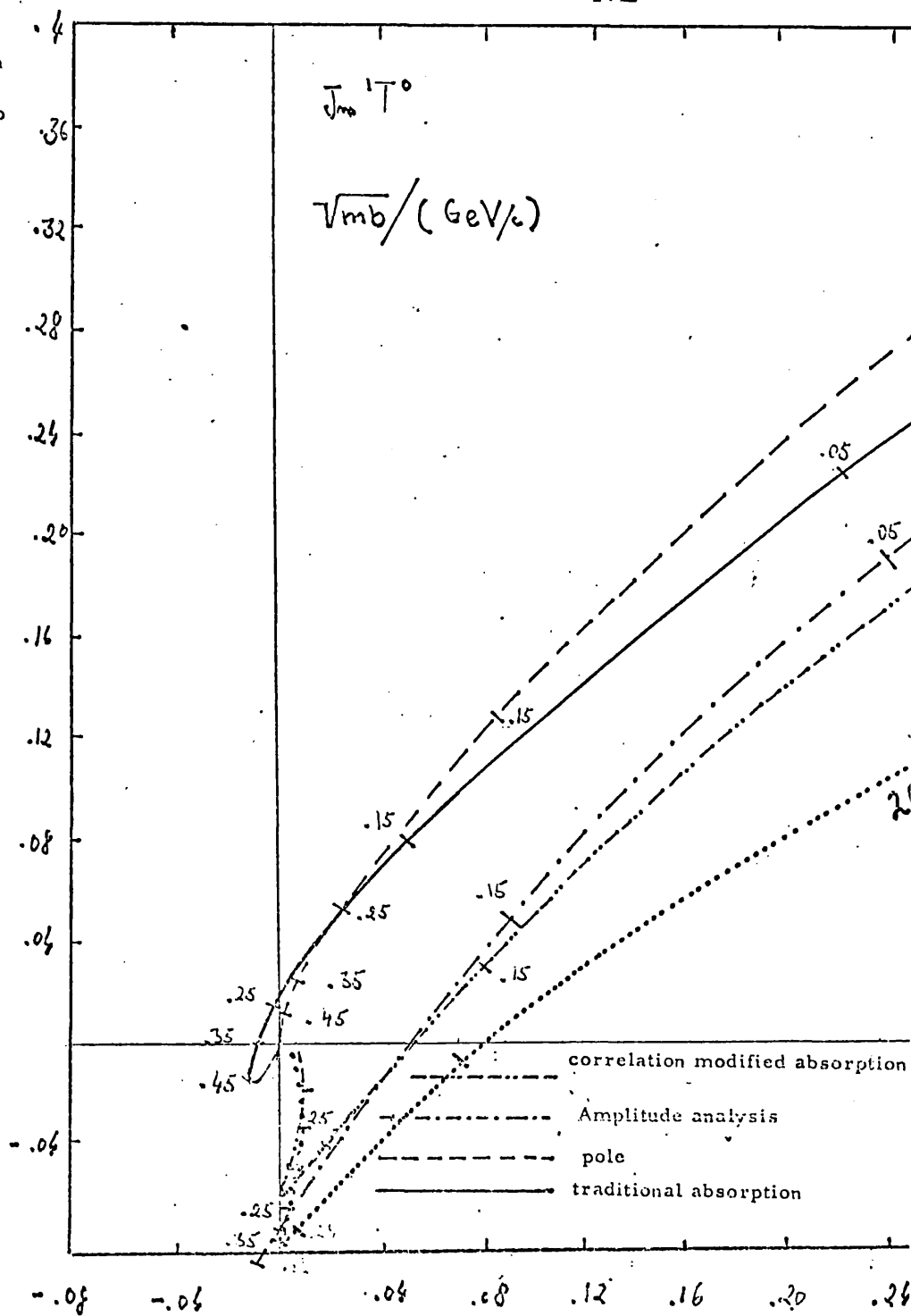
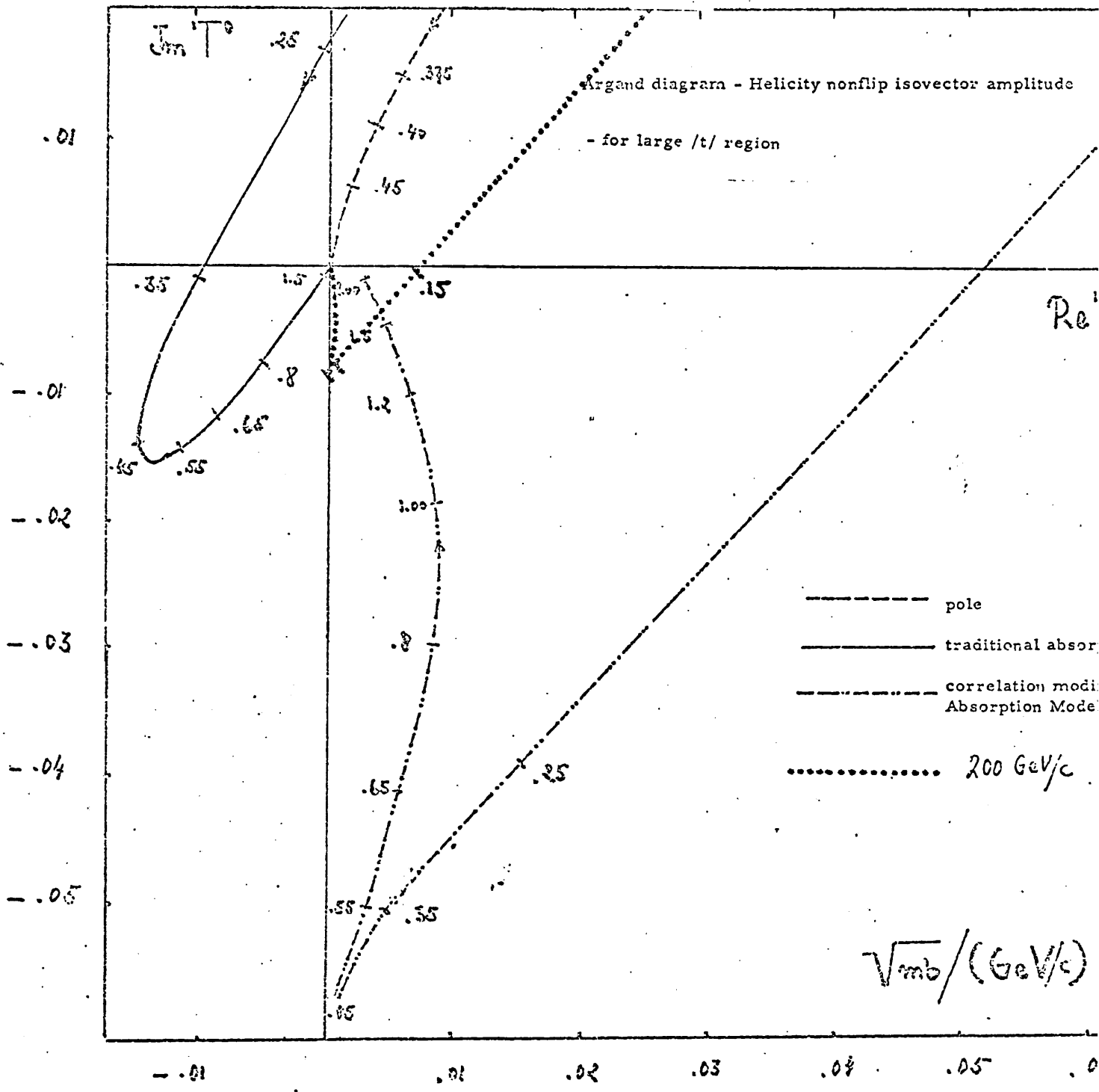


fig. 24

Argand diagram
for the helicity nonflip
isovector amplitude





Argand diagram for the helicity flip isovector amplitude for small $|t|$
The numbers on the curve indicate values in $|t|$.

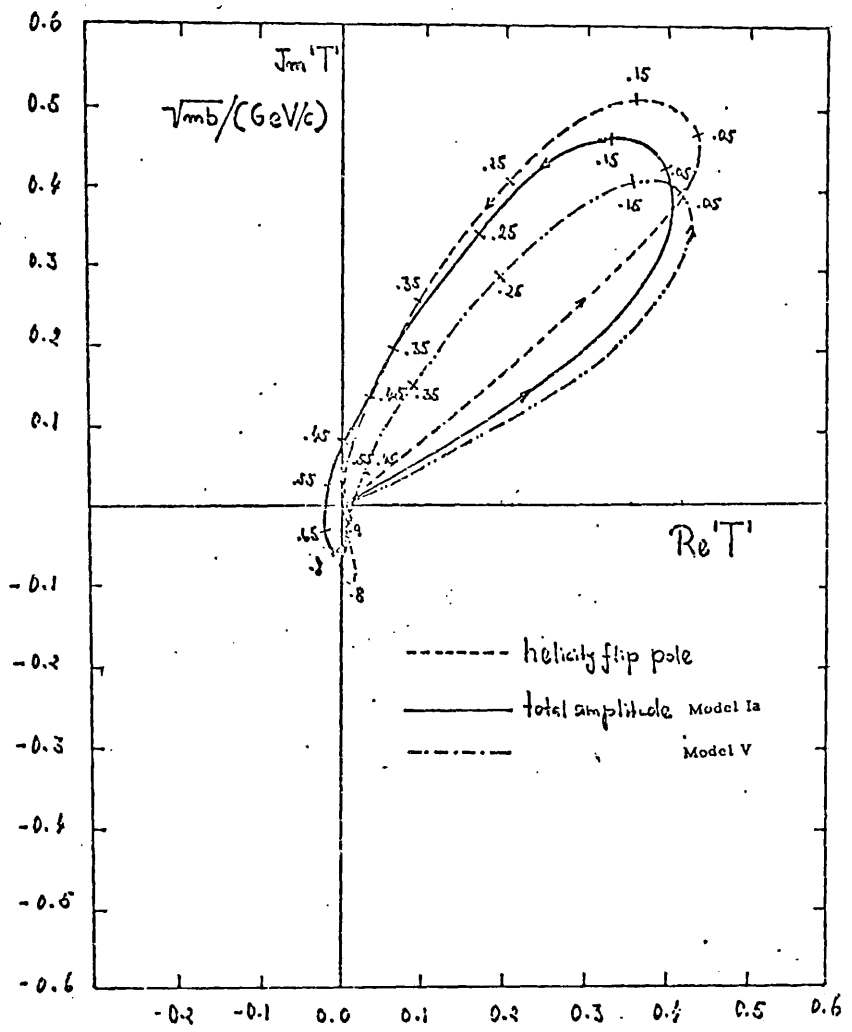
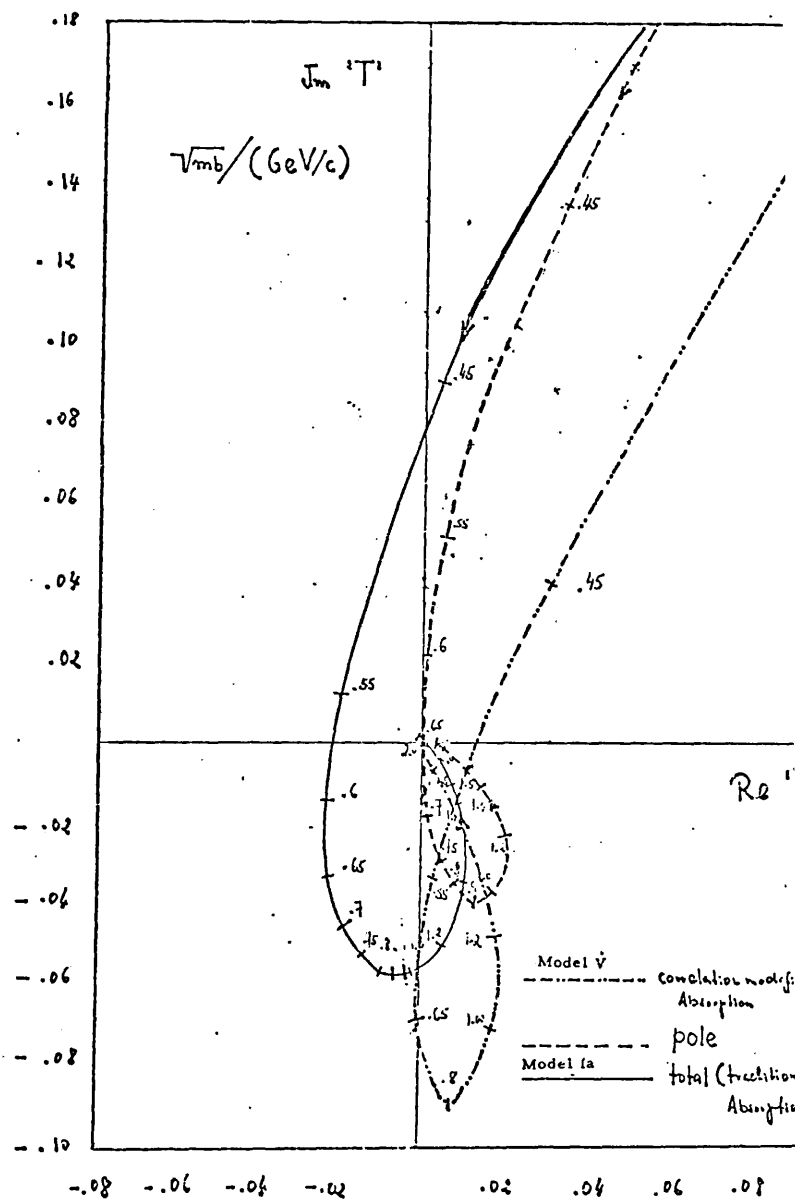


fig. 27

Previous diagram for helicity flip isovector amplitude enlarged for large $|t|$ region



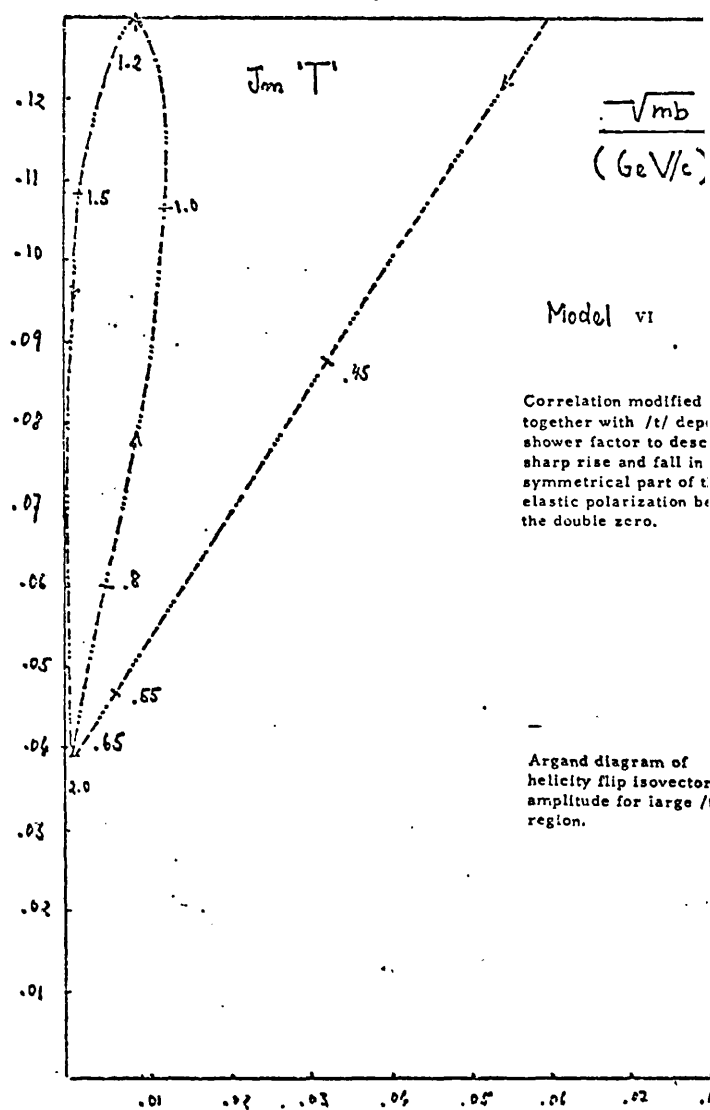
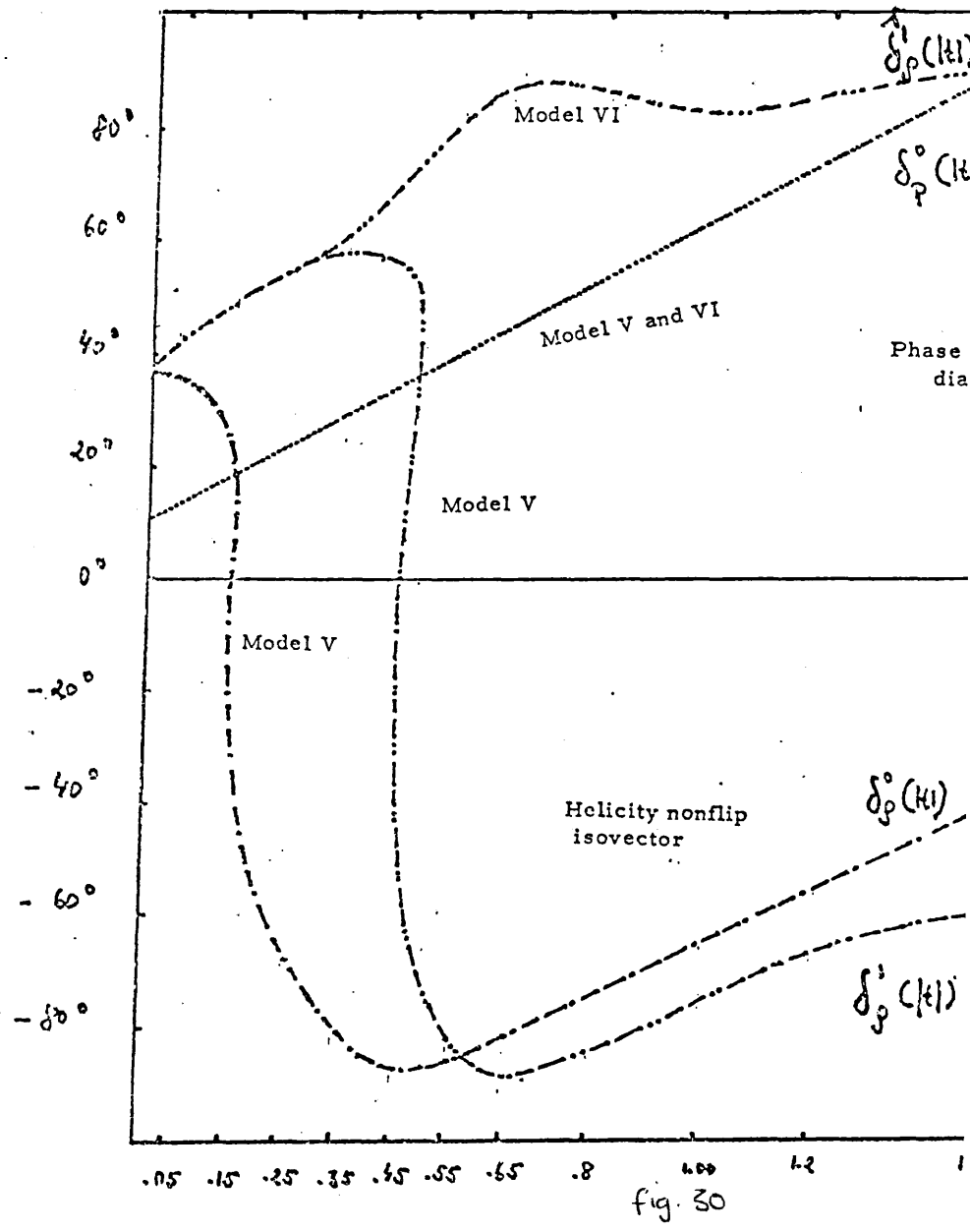


fig. 29



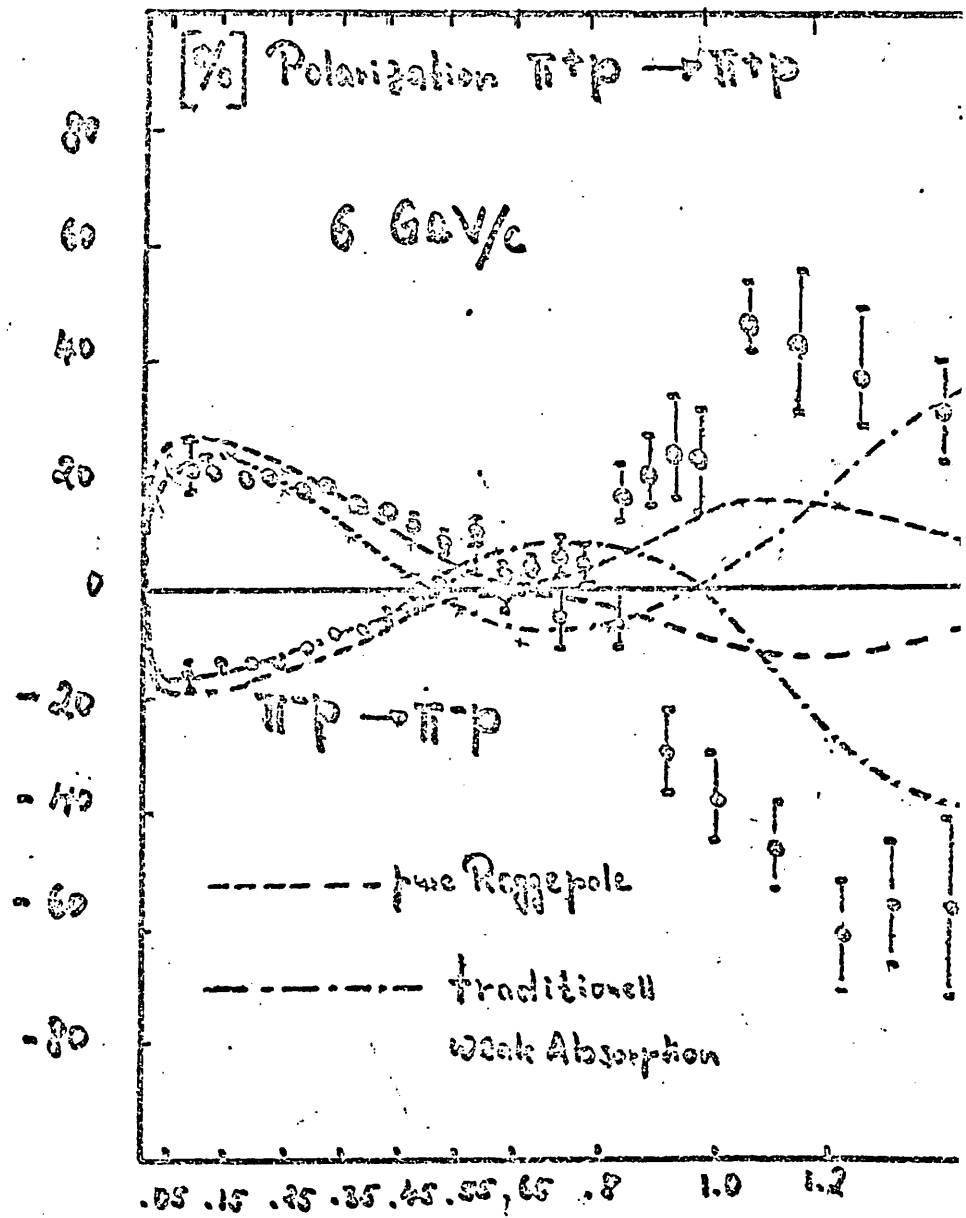


fig. 31.

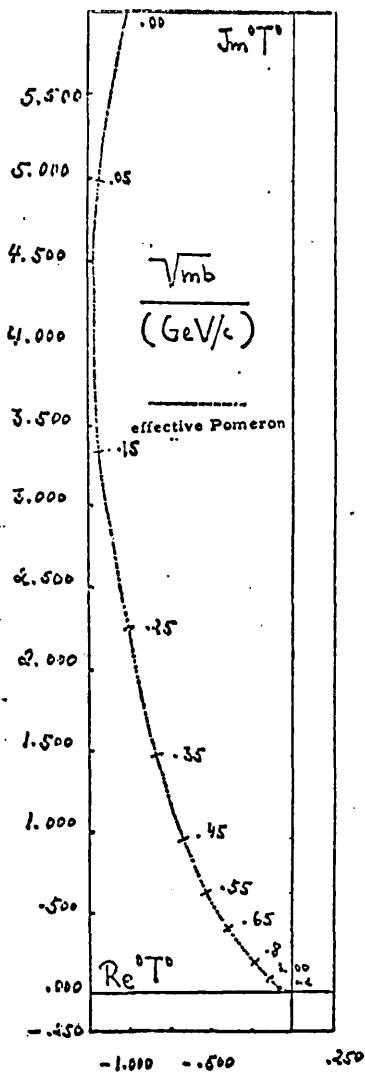


fig. 32

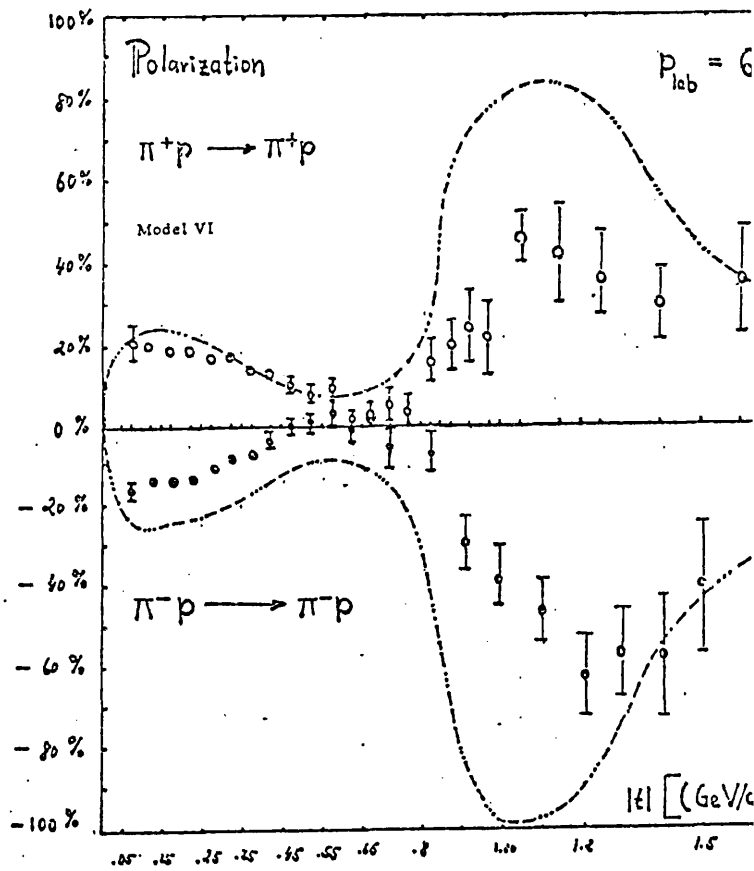


fig. 33.

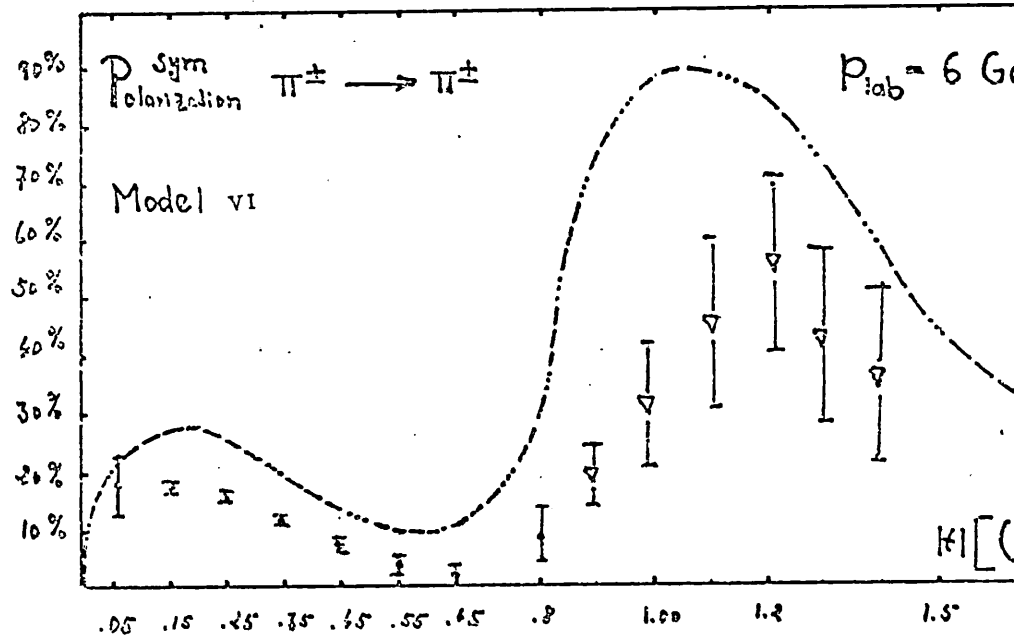


fig. 34

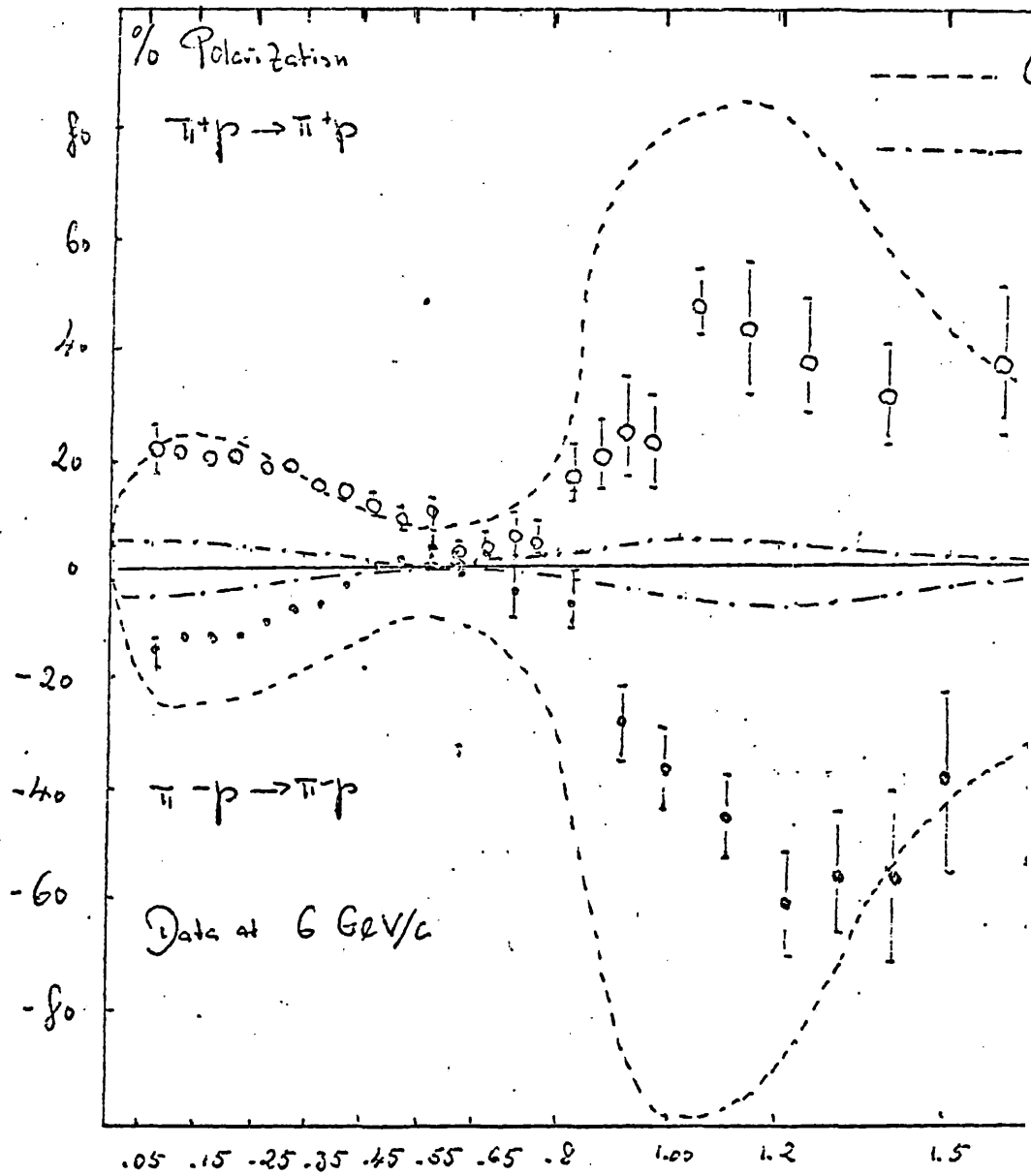


fig. 35

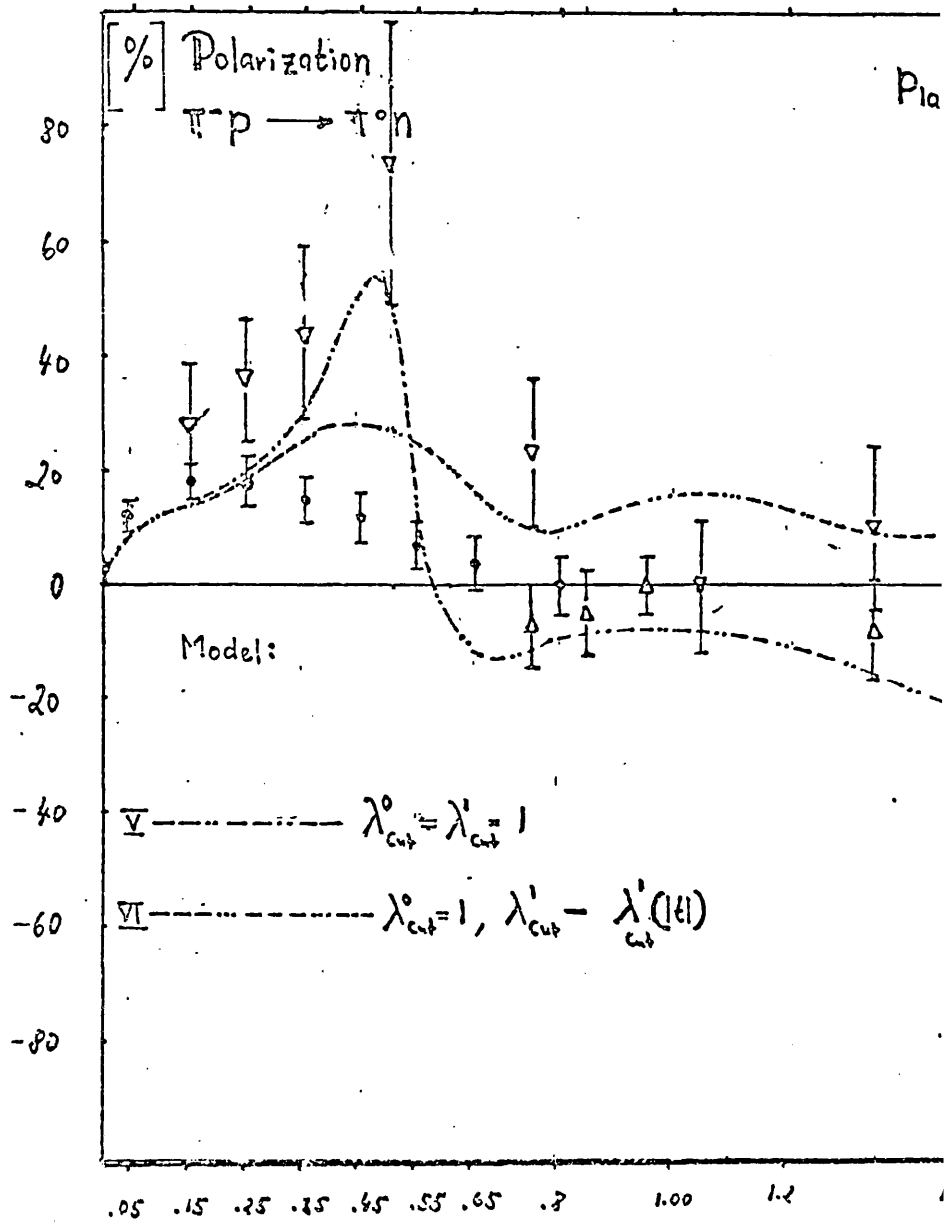


fig. 36

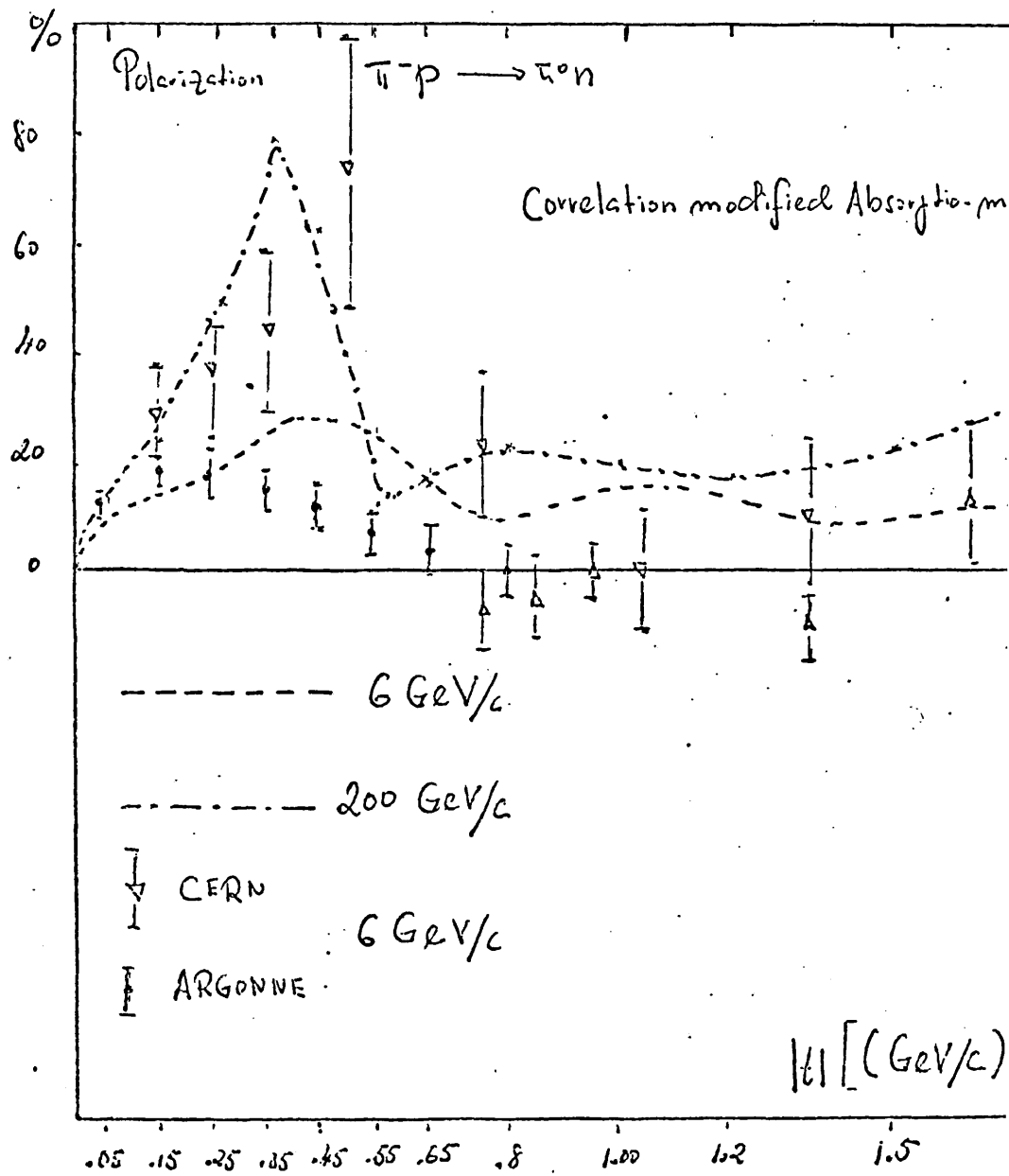


fig-37

$\pi p \rightarrow \pi n$ $d\sigma/d\Omega$ [$\frac{mb}{(GeV/c)^2}$]

Data by Sonderegger
Stirling
Wahlig
Mannelli

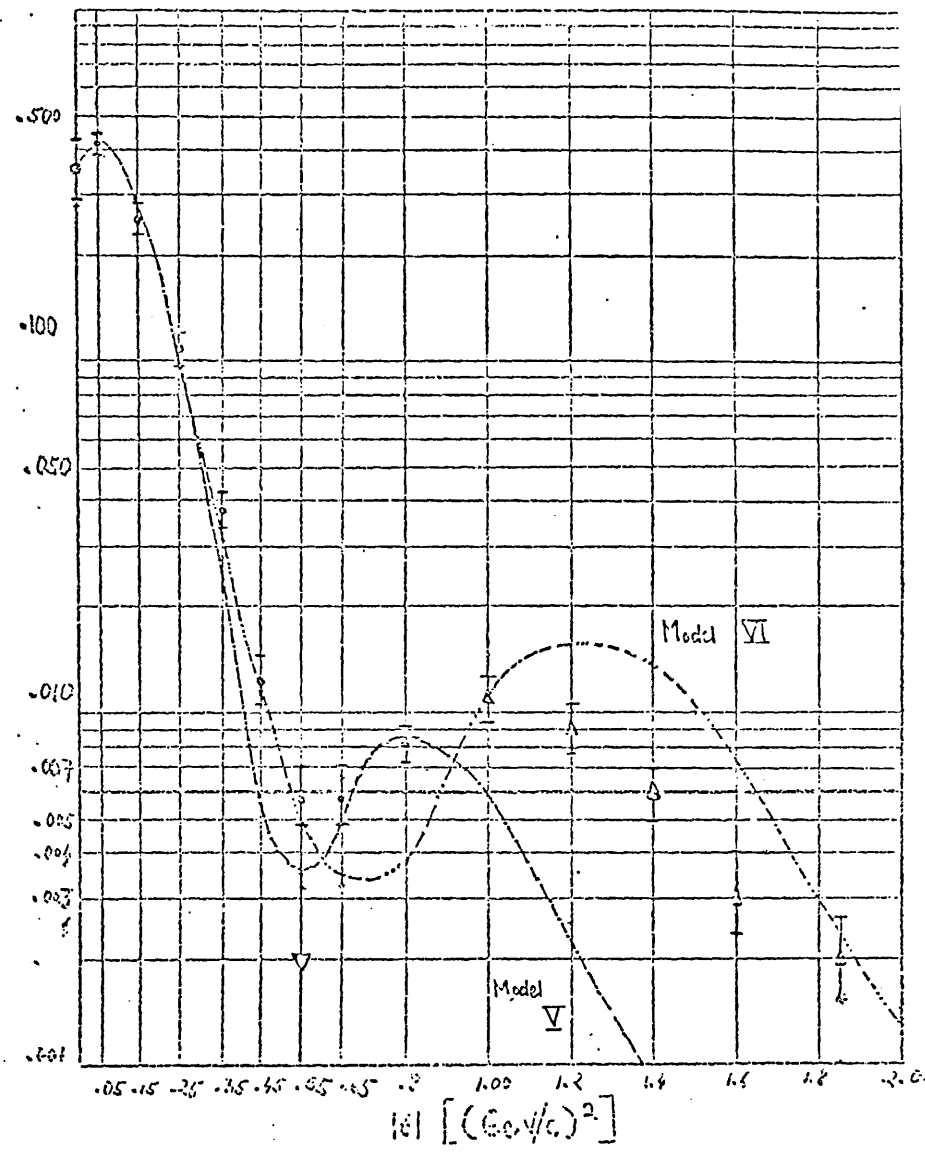


fig. 38

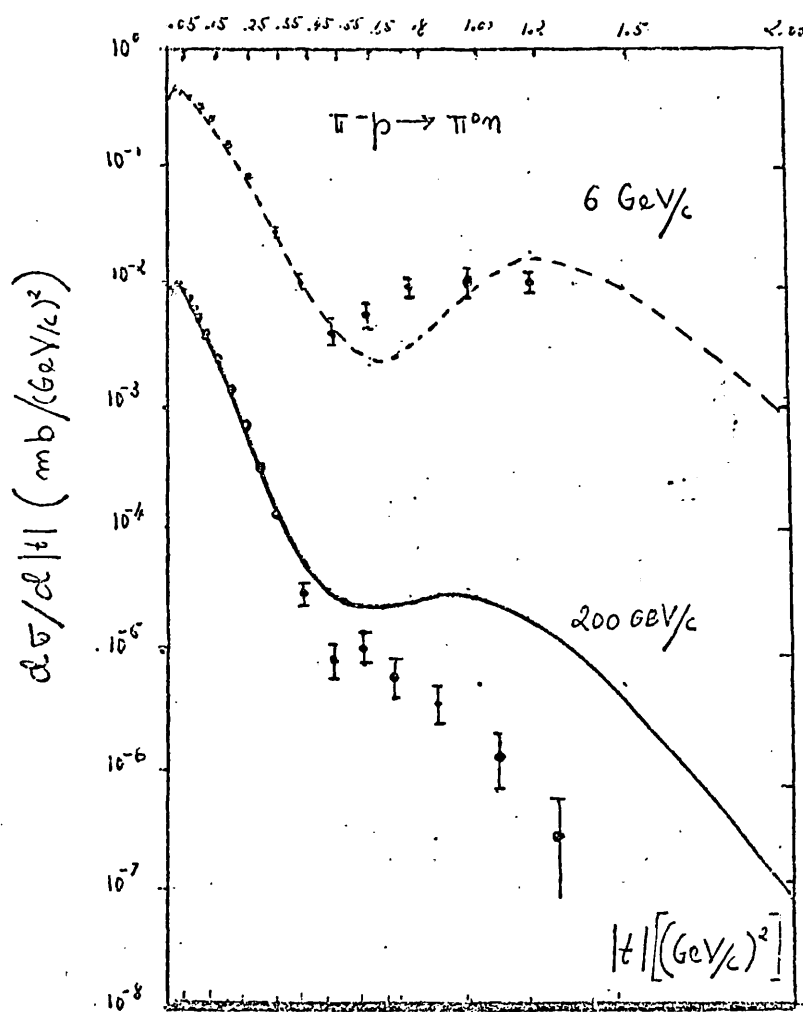


fig. 39

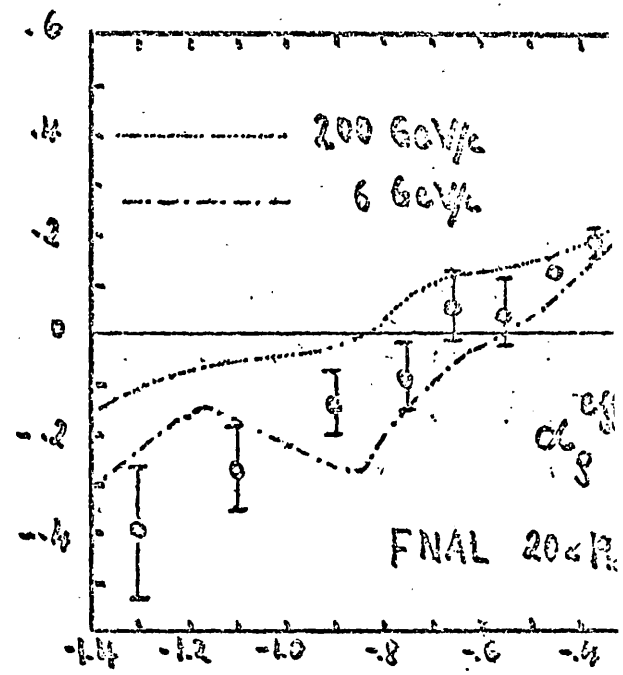


fig. 40

VII - SOME PURELY REAL AND POSITIVE CORRELATION MODIFIED MODELS

VII.1. - THE LARGE POMERON PHASE MODEL

VII.1.1. - The Zero Residue Version (Model VII)

An excellent χ^2 fit can be achieved if we provide the Pomeron with a large real part in forward direction, and also a large Regge pole like slope. If, in addition, we introduce a β -Regge pole-residue parameterized exponentials, the minimisation programme then chooses amplitudes and observables as shown in figs. 41, 42, and happens is that in this case the programme can arrange for an 'ad hoc' zero in the imaginary part of the amplitude to the crossover position without dragging the zero of the real part too closely behind.

We show, in fig. 41, the parallel and perpendicular part (41a and 41b helicity nonflip, and 41c and 41d helicity flip) amplitude and our theoretical curve obtained by means of correlation modified absorption. The transformation complex plane in which we find our theoretical curve and the plane in which amplitude analysis works has been chosen under the circumstances that, first Ambats reference depends on a model assumption for the helicity flip isovector amplitude becomes less valid with increasing $|t|$ from $|t| = .35$ onwards and, second, our theory assumes a different phase for the components near the minimum of the modulus decides unambiguously the sense of rotation of the amplitude origin of the Argand diagram with increasing $|t|$. The failure of the absorption model to obtain the correct sign and hence obtain the correct sense of rotation is displayed in fig. 8 and 6, pages 103 and 101. The incorrect relation between the two helicity amplitudes as seen in fig. 5 and 4, page 100 and 99, causes the polarization to become so disastrous that the proportionality between fig. 2 and fig. 5.

VII.1.2 - The Non-Zero Residue Version (Model VIII)

Case 1
fig. 46
p. 193

Gribov $c = 0$

In this case we do not force a "crossover zero" but still the large phase of the pomeron moves the zero out in $|t|$ with respect to the traditional absorption model.

Case 2
fig. 47
p. 194

Gribov $c = 1.15$

The Gribov c switched on. Had not to arrange the basic modification although it still improves

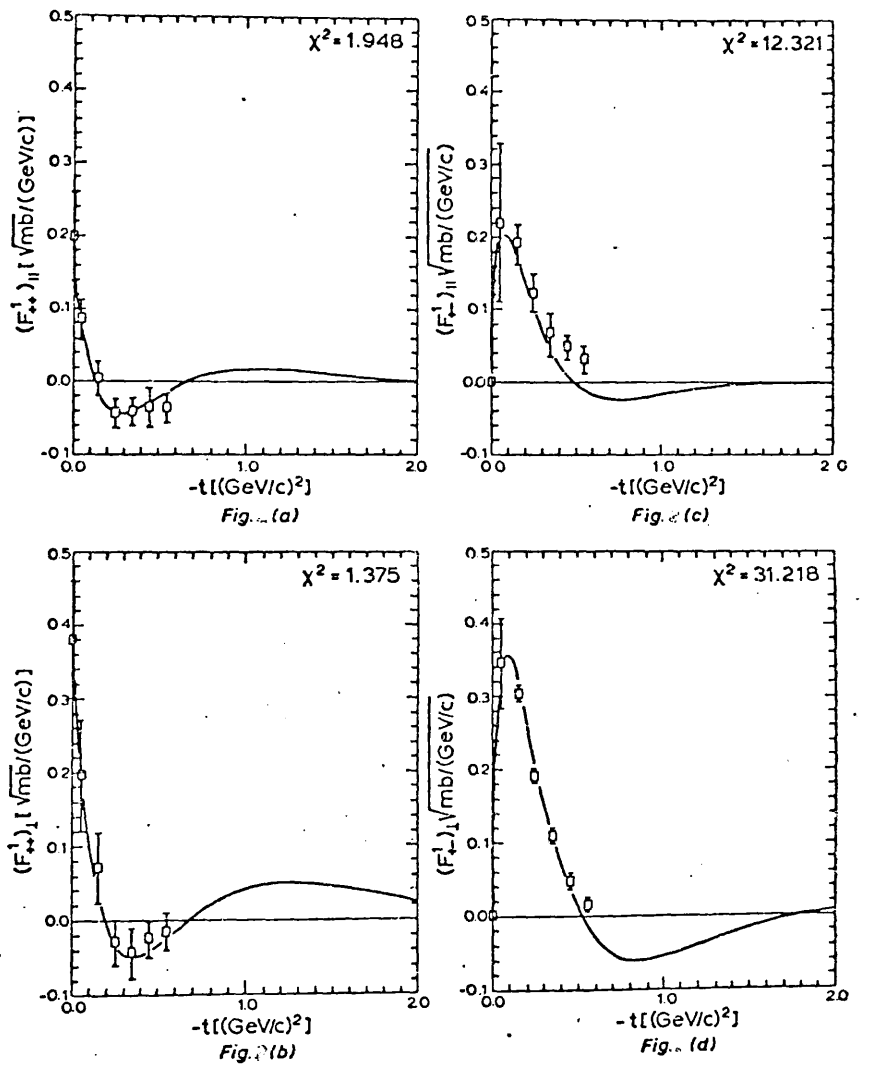


Fig. 41

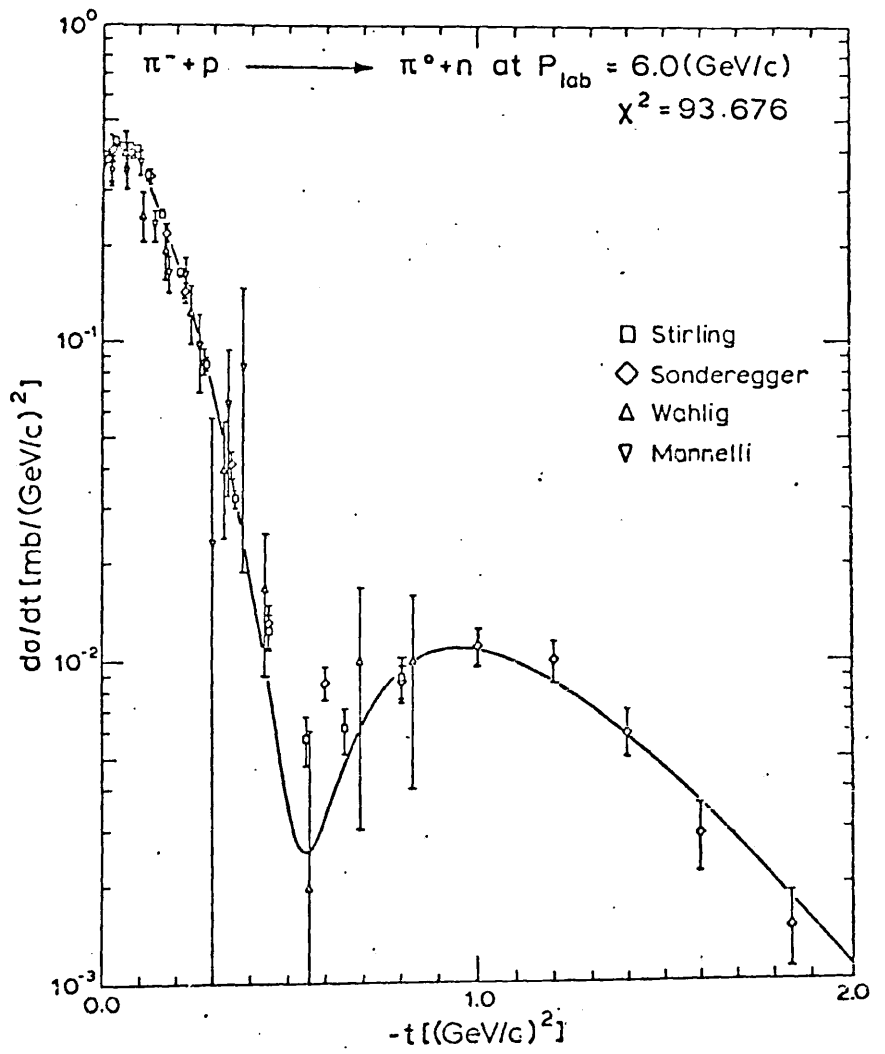


Fig. 42

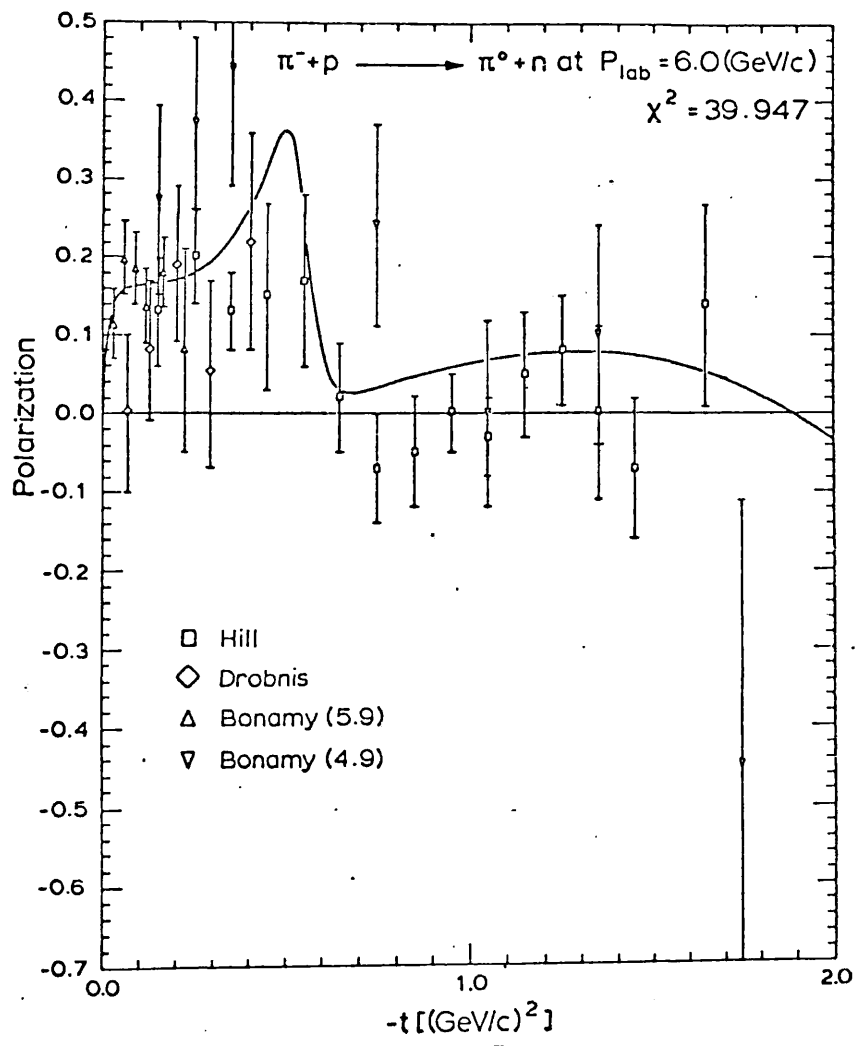


Fig. 43.

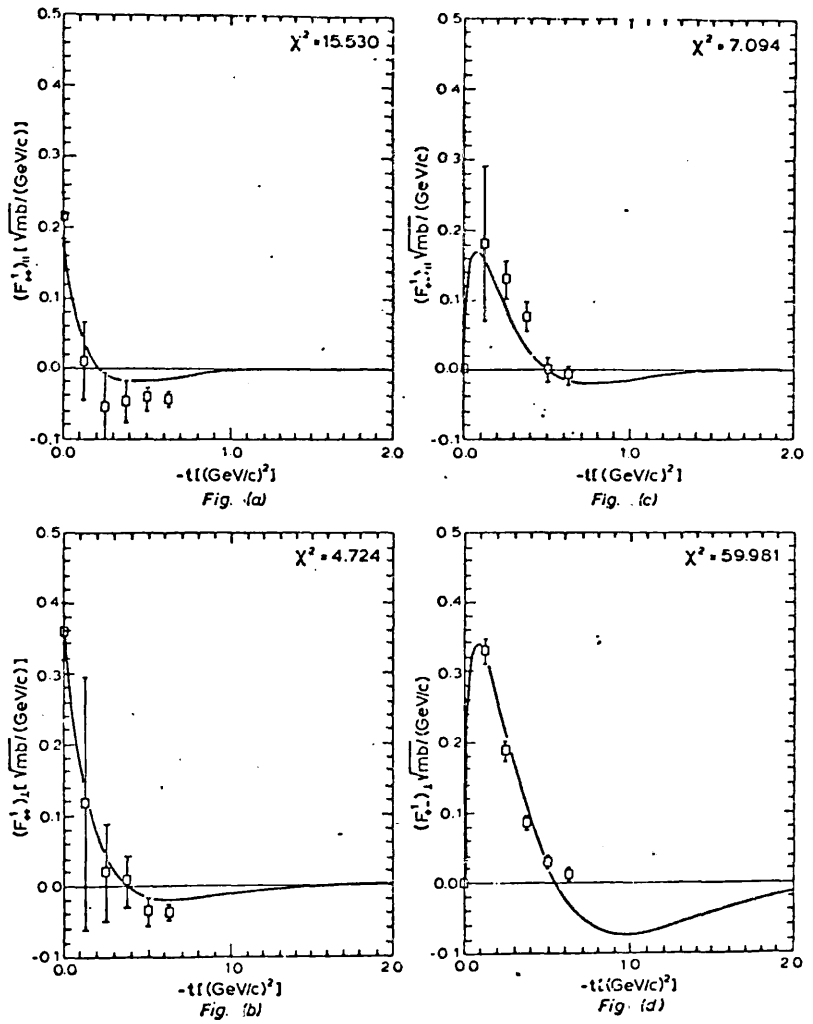


Fig. 44

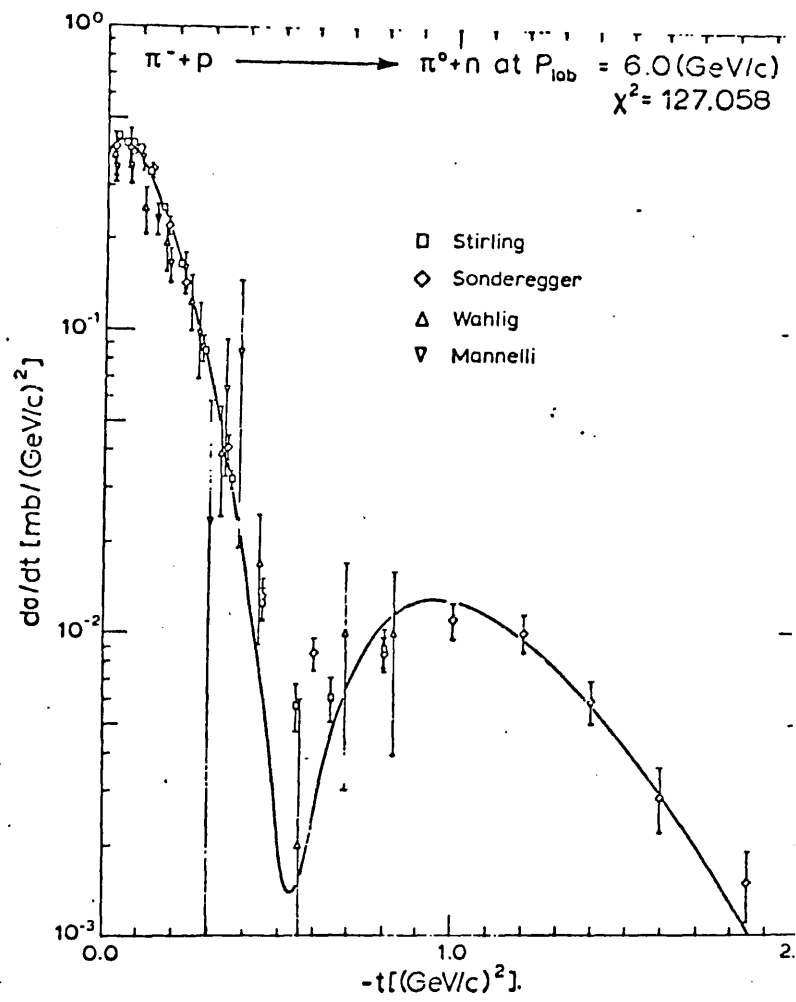


Fig. 45

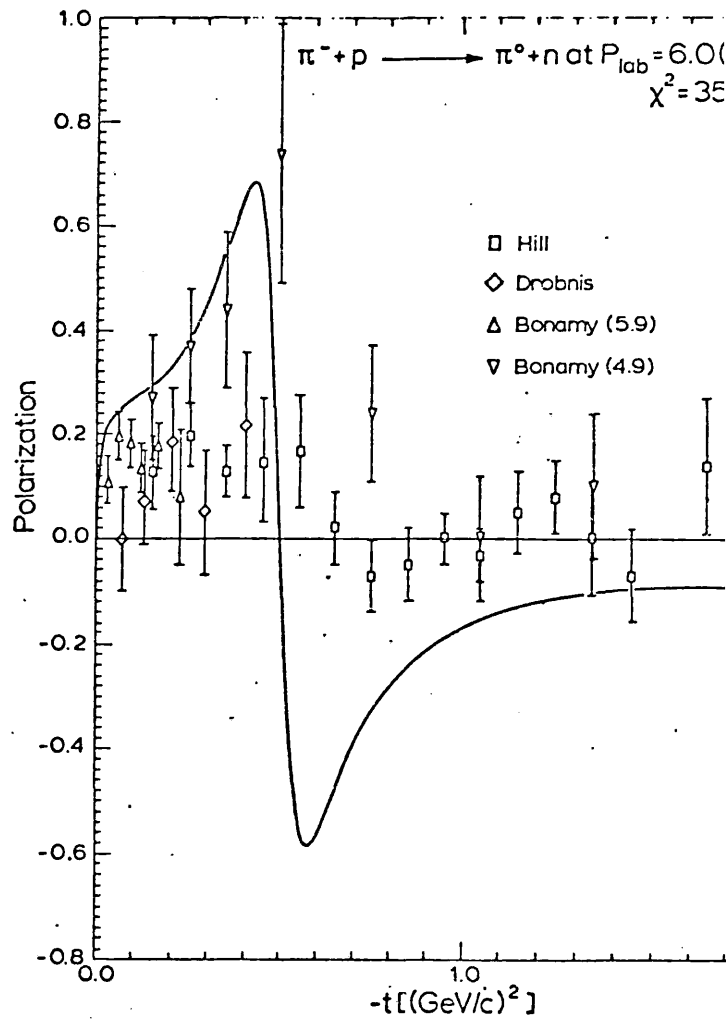


Fig. 4b

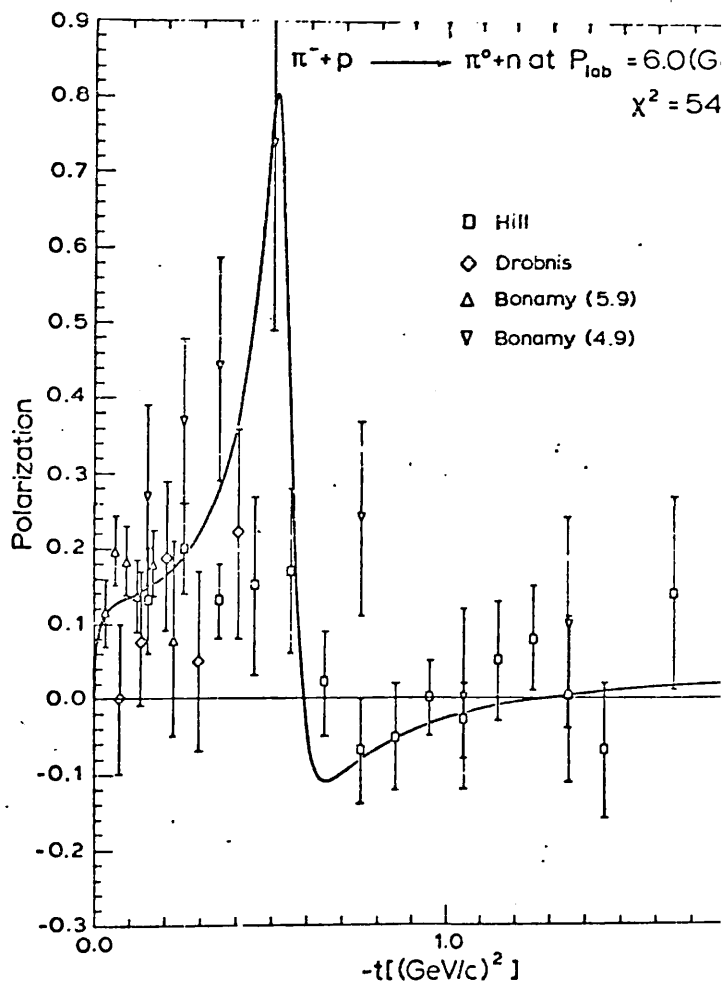


Fig. 14.7

VIII - THE CORRELATION MODIFIED "DERIVATIVE RULE" MODEL (MODEL IX) (46)

We have given, on page 74 the result of the derivative rule as applied to the helicity isovector nonflip amplitude of our correlation modified absorption model.

The parameters, c , A and B as given on page 73 for the helicity nonflip amplitude, are determined by a χ^2 Ambats et al's (5) amplitude analysis data. We find $\text{Re } c = -1.067 (\text{GeV}/c)^{-2}$, $\text{Im } c = -0.629 (\text{GeV}/c)^{-2}$, $A = 0.36467 (\text{mb}/\text{GeV}/c)$ $B = 6.58 (\text{GeV}/c)^{-2}$ with a $\chi^2 = 2.832$ for 14 data points. A comparison of our resonance amplitude analysis data is shown in fig. 48. Our choice of parameters gives a helicity nonflip amplitude which starts at the origin in a clockwise direction as shown in fig. 49. From these figures we note the imaginary zero is at $t = 0$ while the real zero is at $t = -0.228 (\text{GeV}/c)^{-2}$.

Schrempp and Schrempp (47) have shown, in a model-independent way, for the same reaction and energy that one can obtain the s -channel helicity flip amplitude by means of the derivative of the helicity nonflip amplitude as a consequence of the peripheral nature of the process. The proper use of this rule, however, demands an exact fit for the helicity nonflip amplitude to begin with since the derivative rule tends to exaggerate any deviation from the curve which goes through the centre points of the experimental data. How these deviations are amplified can be seen in fig. 50 on page 198 with fig. 48 on page 199. We illustrate in fig. 50 again the parallel and the perpendicular to the helicity flip amplitude which one obtains by rotating the amplitude in the complex plane relative to the isoscalar helicity nonflip amplitude.

As we have already noted, the helicity flip amplitude is extremely sensitive to any deviation in curvature of the curve from the experimental data. Thus, the property of the helicity flip amplitude that it should have a constant phase $-t \approx 0.4 (\text{GeV}/c)^2$ is only maintained out to $-t \approx -0.175 (\text{GeV}/c)^2$ and is rapidly lost beyond this value. This can be seen in fig. 49. This property which is revealed by the amplitude analysis, means that the difference between the phases of the isoscalar helicity nonflip and the isovector helicity flip amplitudes is an approximate constant. This, in turn, seems to indicate that the slope of the Pomeron is similar to the slope of the ρ pole taking the helicity flip amplitude as being approximately Regge behaviour. That we are supposed to see in fig. 51 the behaviour of the isoscalar helicity nonflip amplitude having the same Regge behaviour as the helicity flip amplitude of the isovector exchange as a function of the ρ trajectory. In principle this feature can be seen in fig. 51. However, the larger $|t|$ value loop should never reach into the first quadrant. Of course, fitting data that the Pomeron has a slope as large as the ρ pole could make our effort with a purely imaginary Pomeron only a poor choice. We have already seen that once we have included a nonflat Pomeron the fit will be considerably improved.

The fit to the observables as shown in fig. 32 suffers naturally from the inaccuracy in the nonflip amplitude. In a derivative rule imposes its own nature on to the polarization as can be seen by a comparison between our theoretical polarization curve and the one obtained by Barger and Phillips (48), which are strikingly similar in structure. From this we can see that the zeros in our polarization occur exactly where the phase of the nonflip helicity amplitude has its stationary points, namely between $-t = 0.025 (\text{GeV}/c)^2$ and $-t = 0.05 (\text{GeV}/c)^2$ and shortly after $-t = 0.35 (\text{GeV}/c)^2$. The structure of the polarization results from the effects of competition between a shifted peak and a stationary point of the phase. The apparent peak is caused by the turning point of the phase but is prevented from developing into an actual polarization because of the differential cross section which is, at this point, still large but is falling off very fast such that the minimum is shifted further out in $|t|$. This does not have time to develop a broad shape as we would like to see because the stationary point is forcing the polarization to change sign. Finally, we observe a phenomenon which, although not a consequence of the derivative rule, is also connected with peripherality (49). This is that the rate of change of the differential cross section with respect to scattering angle is equal to the polarization up to a factor which is approximately constant in the range $0 \leq |t| \leq 1.0 (\text{GeV}/c)^2$.

We have seen that by employing a Pomeron which is more rich in structure we could not only improve our fit to the data but also exchange the actual unwanted imaginary part of the parameter in the correlation kernel for a real part of the parameter. Then the correlation kernel could be retained as purely real in character and could, therefore, if it were positive, be a form factor describing the extended structure of the hadrons.

The persistently negative nature of c (apart from the cosmetic c models^{*}) leads us to an interpretation within the parton framework, where care is taken of the particular sub-hadronic nature of the interaction (see. IX).

* Model VII and VIII

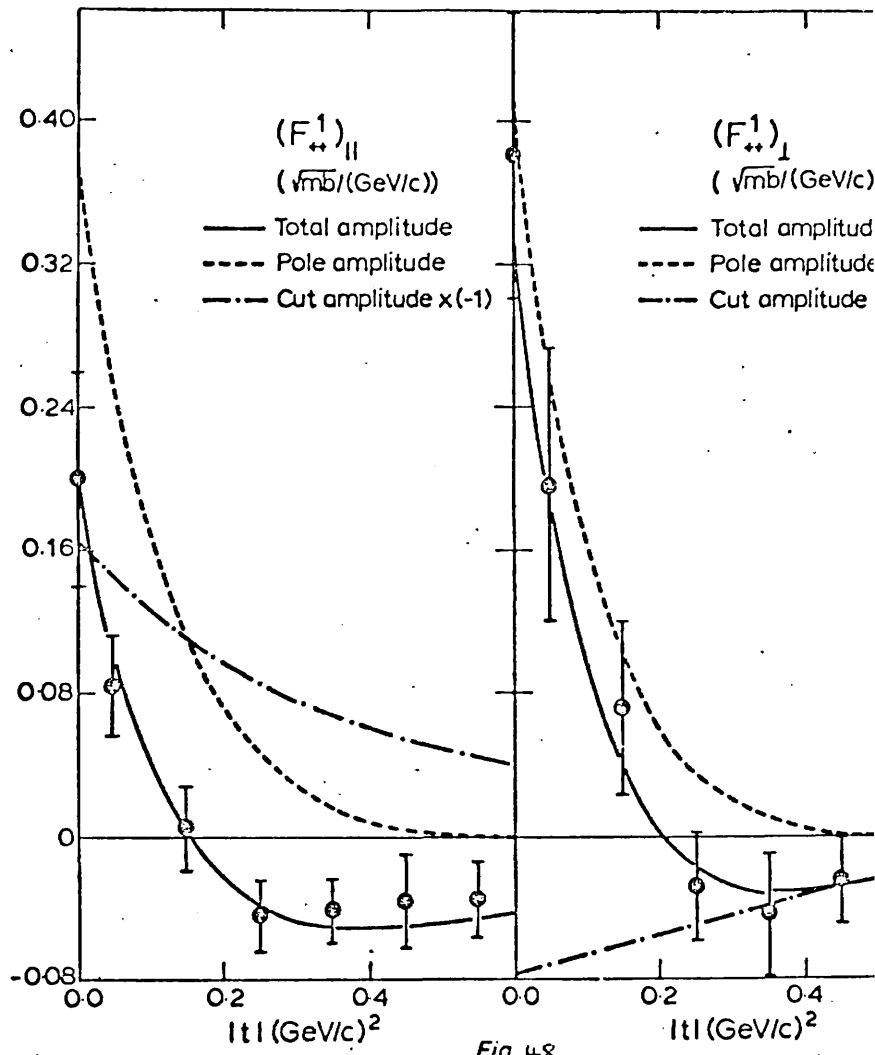
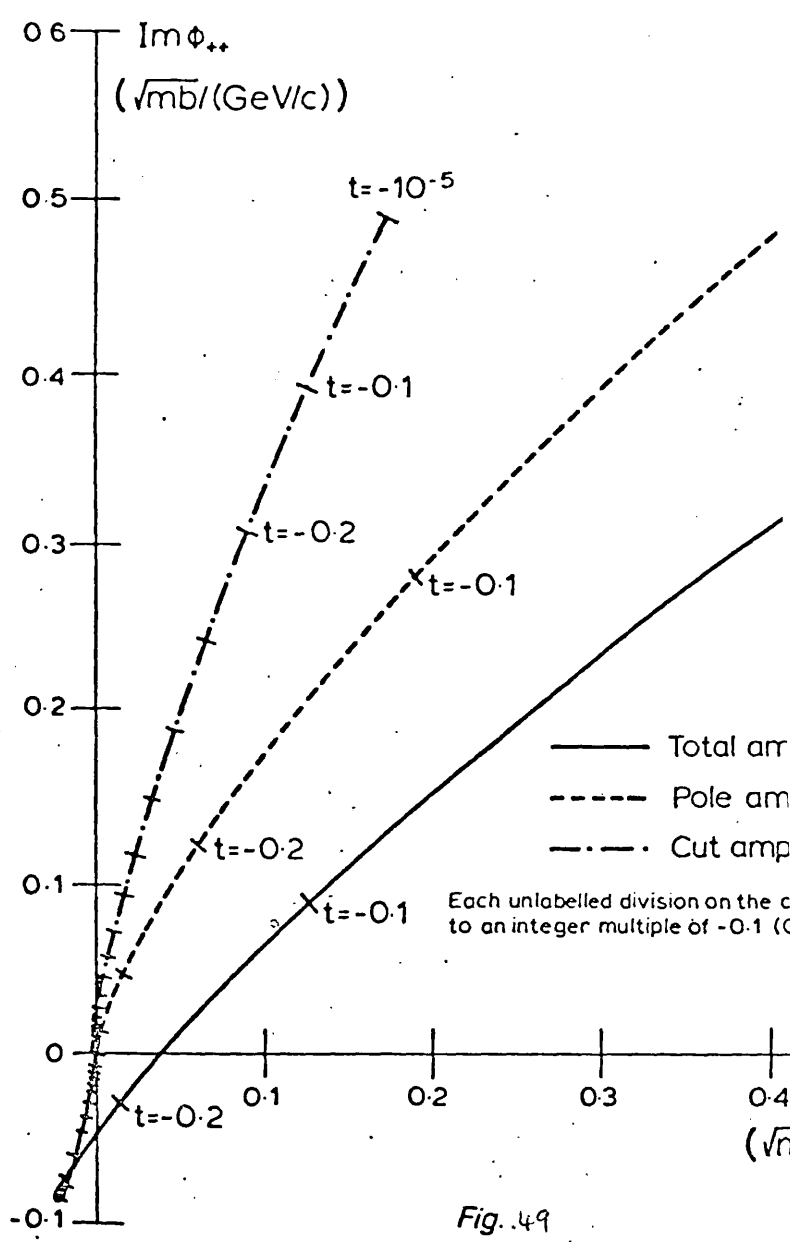


Fig. 48



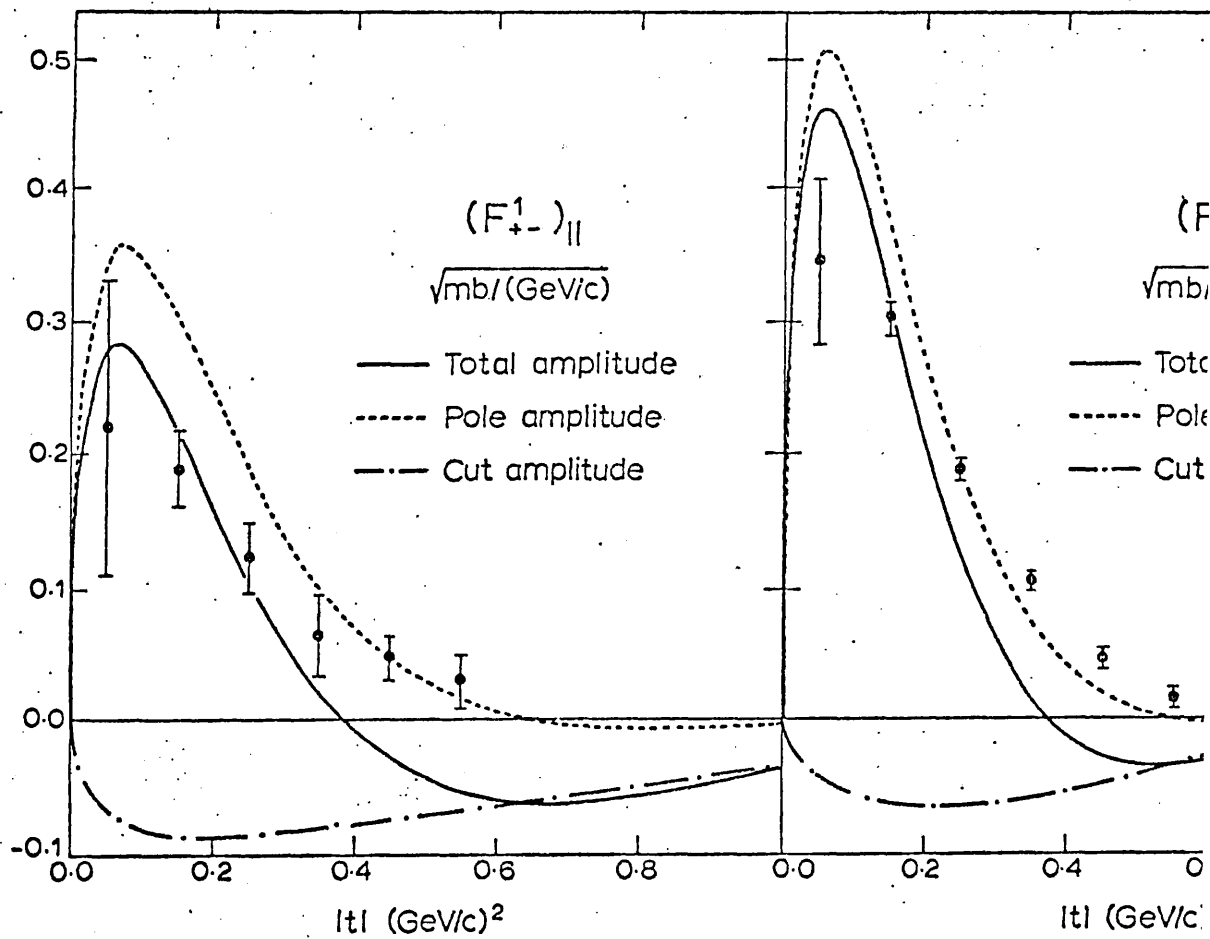


Fig. 150

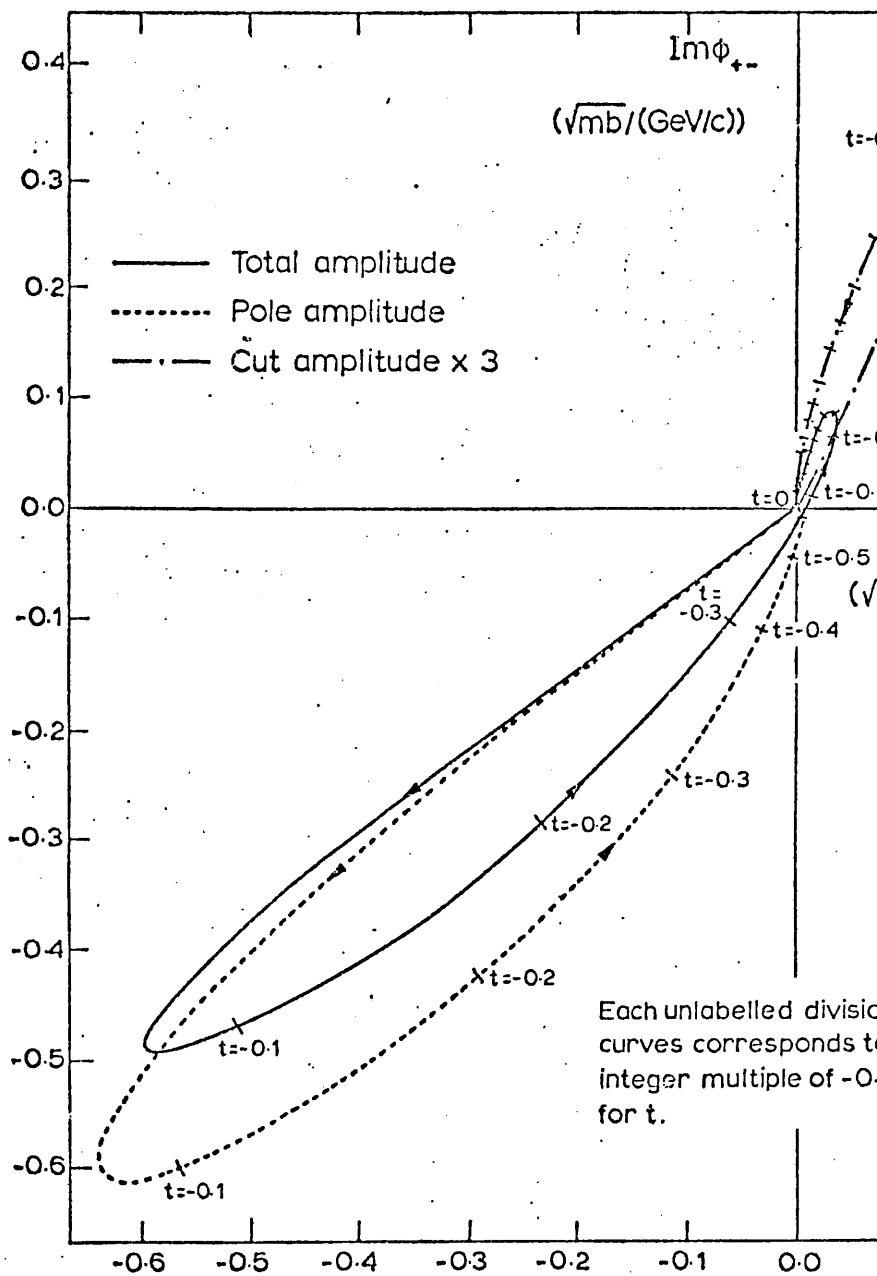


Fig. 51.

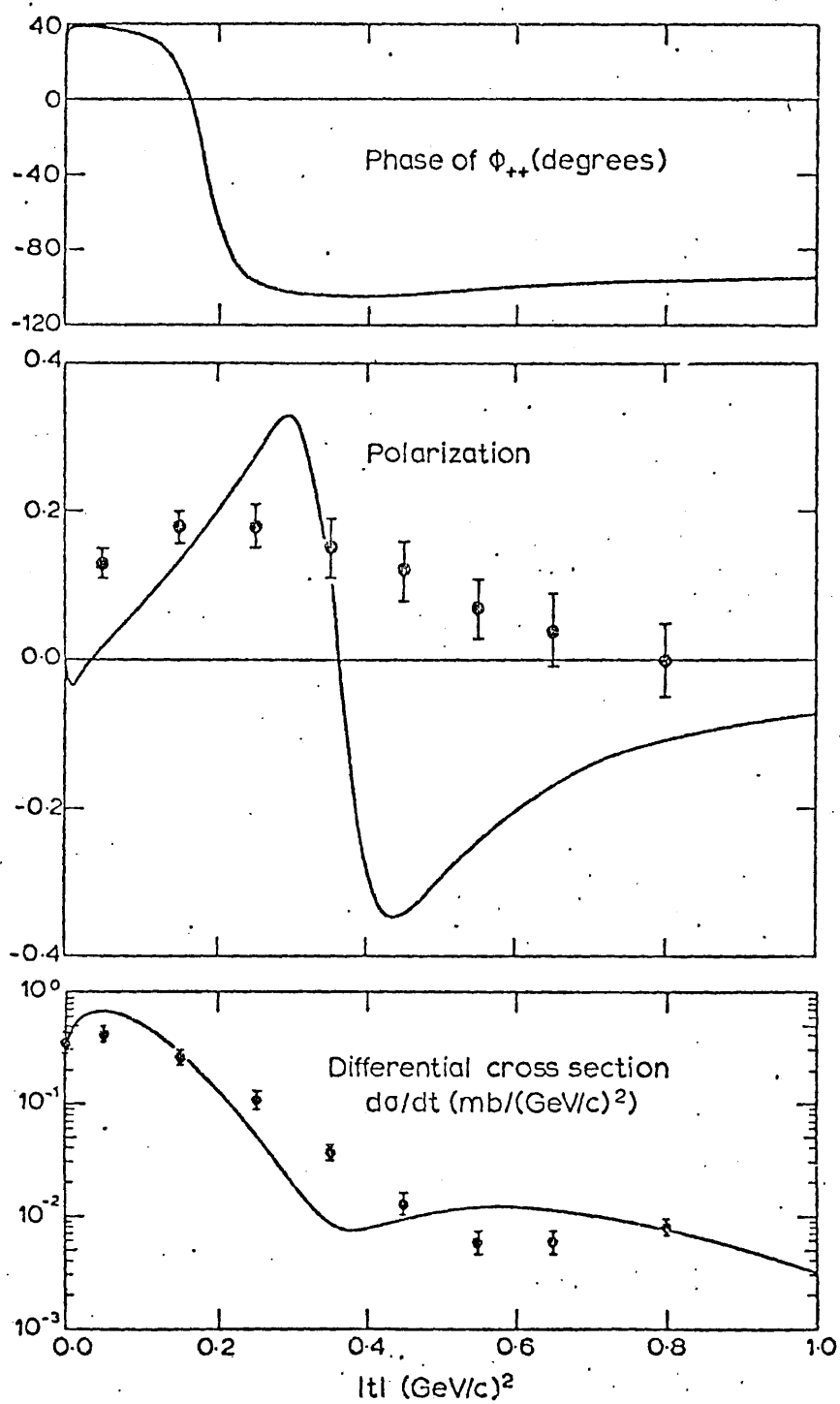


Fig. 52.

IX - AN INTERPRETATION OF THE NEGATIVE SIGN OF THE CORRELATION PARAMETER

We have, in the introduction, remarked upon the need to do the Reggeon-Pomeron convolution with both Reggeon and Pomeron renormalized. The effective interaction range needed to be considerably shorter than is the case for the single exchange. This has been borne out by the necessity to include into the Regge-particle coupling function the mutual orientation of the transverse components of the Reggeons (Pomerons). This in turn provided a way to account for the effective contribution of inelastic intermediate states besides the elastic pole state in the Gribov-Migdal R unitarity condition. Although the formal analogy to nuclear physics suggested parameterization of the modification of the absorption model by including a parameter which seemed to simulate the oscillator length of a quark-antiquark bound state, the actual persistently negative value of this parameter implying the shortening of the interaction range defied such a simple picture.

There has meanwhile emerged an intuitive interpretation (15, 50, 51) of the Gribov graphs based on the simultaneous presence of multiperipheral and diffractive discontinuities in the two body amplitude. Seen in the light of several convergent views such as the multiperipheral model, the parton picture and the diffusion analogy via the Green's function formalism it might be possible to understand the meaning of the negative sign of "c". In the intuitive picture of hadronic interaction it is understood that fast hadrons at distance b in impact parameter and at a certain "time" l_{ns} cannot interact and reduce their energy by emitting a shower of virtual particles, ^{which} populate the Impact parameter plane and are separated by distances of the order of a Compton wave length due to Gribov's finite mass hypothesis.

Every produced particle is a step in the random walk across the impact parameter plane performed by the Reggeon, reducing the energy of the colliding hadrons so as to bring them closer to each other. The higher the initial energy the more steps have to be done, i. e. the more virtual particles are produced in a multiperipheral chain. The initial position of the colliding hadrons is the vector sum of the distances the produced particles are apart from each other. They define an interaction range which has a specific Regge component and boundaries due to the colliding hadrons. Due to the approximate absence of long range correlations it happens that the Regge interaction region is growing linearly with initial energy: the more steps to go, i. e. more particles produced. The average squared value of the vector sum of the impact parameter values of the produced particles is then the defined effective interaction region between

colliding hadrons. The steepness of the exponentially parameterized Regge residues is then the non-shrink of the interaction region. The introduction of the Gribov "c" seems to reduce the size of this region in the It reduces the size by comparison to the single graph and also by comparison to the traditional absorption n is preserved.

Why is this? In general the colliding hadrons produce several showers from which slower partons can e of hadrons then takes place via the simultaneous interaction of the partons. The parton is reduced in ene) Each has $\frac{\sqrt{s}}{4}$ in the c.m. system.

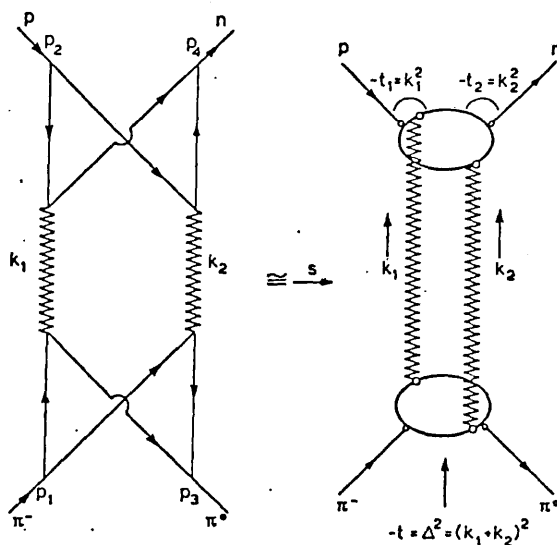


Fig. 53

They are also closer in impact parameter. They enter the diffusion slowing down process from their "s) by contrast to the "space,time" components of the initial single Regge exchange, where the hadron interact It seems to be plausible that the effective interaction range of each individual parton interaction is now bei with the first order interactions. That is to say it is the "size" of the partons which in higher orders is m size of the hadron.

X - AN OUTLOOK TOWARDS A UNITED DESCRIPTION OF HADRONIC TWO BODY INTERACTIONS

We do not wish to end on the speculative note of the last paragraph without emphasizing that the good results on the phase modifying nature of the negative Gribov "c" encouraged us to pursue the subject further, in particular to connect the isoscalar amplitude which could shed new light on the phase of the pomeron as probed by the elastic polarization scattering around and beyond the residue zero. That is to say a correlation modified moving Pomeron might be connected to the elastic polarization beyond the residue zeros and a helicity amplitude which is regge behaved even for $|t| \neq 0.6$ be more satisfying than the adhoc-introduced showerfactor which converts the destructive cut into a constructive one.

Thus, in conclusion we can say we have found a natural solution for the shortcomings of the optical model listed up in the introduction together with a rather adhoc approach to point (2) in order to tide us over until we have constructed an amplitude by means of the Gribov "c". The inelastic differential-cross section is still unsatisfying in the region $0.6 < |t| < 1.0$ and we are still left with the shrinkage problem, see fig. 39 and 40, p.185 and 186, but see the pole dominated model. Work is now in progress to investigate the introduction of Gribov "c"-like couplings into diagrams of the enhanced type, (see fig. 54)

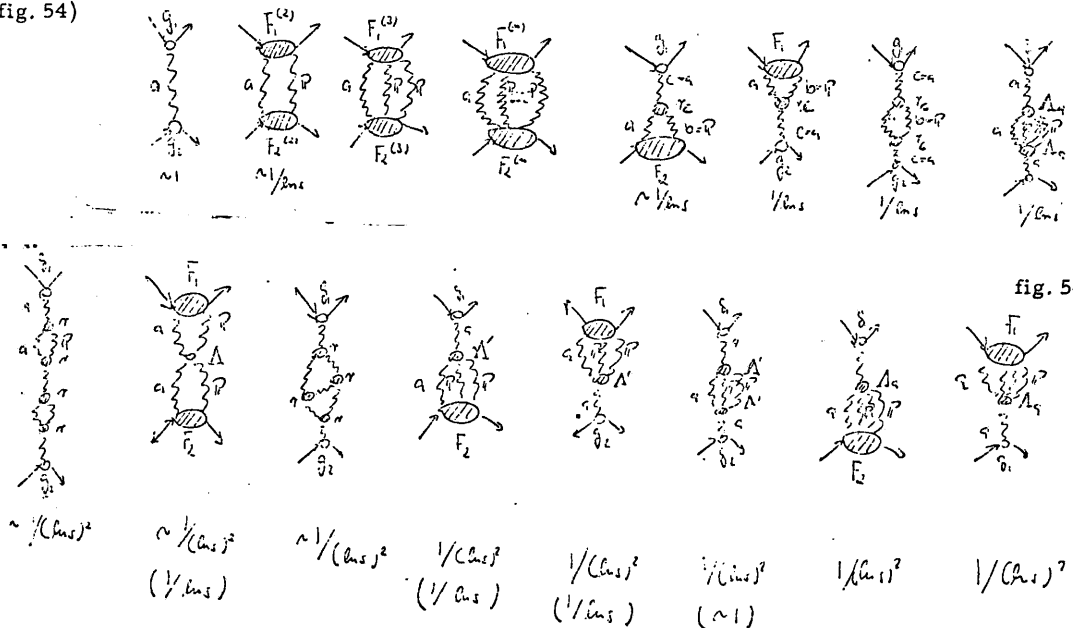


fig. 54

so as to correct the deviations of $\frac{d\sigma}{d|t|} (\pi^- p \rightarrow \pi^0 n)$ and α_p^{eff}

from the FNAL data, while preserving the maximal energy stability of the phase as obtained in our Gribov "c" tree of the unenhanced diagrams.

With the isoscalar amplitude constructed, we could genuinely describe elastic scattering, and, in particular, the cross section and the dip problems in elastic scattering, but see also (37, 53) and for a $\alpha_p' > 0$ model see (54). Another feature of our correlation modified model is that it does not have to treat the real and imaginary part of α differently in order to modify the real and imaginary part of the amplitude differently. Thus the consequences of α modification due to correlation for HCEX will be of interest. See for those reactions in phase modified model as (55) and Egli (5).

The description of the Pion-Nucleon system over a wide range in energy i. e. $6 \lesssim p_{\text{lab}} \lesssim 200 \text{ GeV}/c$ and a relatively large range in momentum transfer i. e. $0.00 \leq |t| \leq 2(\text{GeV}/c)^2$

should provide the basis for a unified description of all two body reactions connected via various symmetry schemes. For example, see (53), once we have obtained the residues for P and P' from $\pi^\pm \rightarrow \pi^\pm p$, the ρ from

the ω from $\pi^- p \rightarrow \eta n$ and the ω from $K_L^0 p \rightarrow K_S^0 p$

one can link, via $\rho(770)$ factorization, quark model and the experimental necessity to account for the fact that Pomeron is not a $\rho(770)$ singlet (use $f-f'$ dominance model), the πN system with the KN system elastic NN scattering i. e. all reactions dominated by the five leading poles.

There lies a vast and fascinating field ahead and models developed within the frame of the Reggeon diagram technique are better suited to explore the systematics of hadronic interactions than traditional absorption.

XI APPENDIX

NORMALIZATION AND UNITS, THE POMERON AND OPACITY

We express, in order to compare with the amplitude analysis by Ambats et al, the relativistic invariant scattering amplitude in the centre of mass-system such that -

$$T(s, t) = \frac{\sqrt{s}}{q^*} T(E^*, \theta^*)$$

With q^*, p^* the three dimensional initial and final momentum, E^* the total energy and θ^* the scattering angle, centre of mass-system. s and t are the invariant total energy and transfer momentum respectively.

The differential cross-section in the centre of mass system reads -

$$\frac{d\sigma}{d\Omega^*} = \frac{1}{(2s_1+1)(2s_2+1)} \frac{p^*}{q^*} |T(E^*, \theta^*)|^2$$

with Ω^* the solid angle in the c. m. system, s_1 and s_2 are the spins of the colliding particles, replacing the invariant amplitude we obtain the invariant differential cross section -

$$\frac{d\sigma}{d\Omega^*} = \frac{\sqrt{s}}{q^* p^*} \frac{d\sigma}{d\Omega^*} = \frac{1}{(2s_1+1)(2s_2+1)} |T(s, t)|^2$$

Our normalization is therefore $N = 1$ and in consequence the optical theorem reads -

$$\sigma_{\text{tot}} = 4\sqrt{s} \operatorname{Im} T^{\circ}_{\text{elastic-P}}(s, t=0)$$

where the upper right hand \circ indicates helicity nonflip. We decompose now the elastic helicity nonflip amplitude in the stars. We denote the elastic amplitude by P (Pomeron). Thus we find -

$$\frac{q}{\sqrt{s}} T^{\circ}_{\text{P}}(s, t) = \frac{i}{2q} \sum_{j=0}^{\infty} (2j+1) T^{\circ j}_{\text{P}}(s) P_j(\cos\theta)$$

projecting out the partial waves and putting $\cos\theta = z$ we write -

$$\int_{-1}^{+1} \frac{q}{\sqrt{s}} T^{\circ}_{\text{P}}(s, t) P_j(z) dz = \frac{i}{2q} \int_{-1}^{+1} \sum_{j=0}^{\infty} (2j+1) T^{\circ j}_{\text{P}}(s) P_j(z) P_j(z) dz$$

and obtain with the help of the orthogonal relation

$$\frac{2 \delta_{jj'}}{2j+1} = \int_{-1}^{+1} P_j(z) P_{j'}(z) dz$$

the partial wave of the elastic amplitude

$$T_{\mathbb{P}}^{oj}(s) = -i q \int_{-1}^1 \frac{z}{\sqrt{z}} T_{\mathbb{P}}^o(s, t) P_j(z) dz$$

We insert the Pomeron as a function of $|t|$

$$T_{\mathbb{P}}^{oj}(s) = -i q \int_{-1}^1 \frac{z}{\sqrt{z}} (i \beta_{\mathbb{P}}^o e^{i \delta_{\mathbb{P}}^o} e^{-\lambda_{\mathbb{P}}^o |t|}) dz$$

$\delta_{\mathbb{P}}^o$ is the Pomeron phase additional to the traditional value of 90° and, $\lambda_{\mathbb{P}}^o = \dots$

we make use of the relation

$$\int_{-1}^1 P_j(z) dz \longrightarrow \frac{1}{q^2} \int_0^{\infty} \gamma_{1k_1} \rho(\gamma_{1k_1}) J_0(c \& \gamma_{1k_1})$$

and transform into impact parameter space b

$$T_P^0(s, b) = \frac{\beta_P^0}{\sqrt{\pi}} e^{i f_P^0} \int_0^b \sqrt{t} e^{-\lambda_P^0 |t|} J_0(\sqrt{t} b) dt$$

and since $\int_0^b x^{\nu+1} e^{-\alpha x^2} J_0(\sqrt{x} b) dx = \frac{\beta^0}{(\alpha)^{\nu+1}} e^{-\beta^2/4\alpha}$ for $\text{Re } \alpha > 0$
 $\text{Re } \nu > -1$

We obtain the Pomeron
in impact parameter space

$$T_P^0(s, b) = \frac{\beta_P^0 e^{i f_P^0}}{2\sqrt{\pi} \lambda_P^0} e^{-\frac{b^2}{4\lambda_P^0}}$$

This gives $\alpha = -0.134$ which compares with Höhler, Strauss value $\alpha = -0.14 \pm 0.04$

With such a small real part its presence is negligible where the differential cross section in forward direction

the optical point, namely $\frac{\sigma^2_{tot}}{16\pi} (\alpha^2 + 1) = 41.37 \frac{\text{mb}}{\text{GeV}^2}$ here we have used the

In order to return the transformation i. e. from b-space into r/t space we write -

$$\frac{q}{\sqrt{\pi}} T_P^0(c, t) = \frac{i}{2q} \sum_{j=0}^{\infty} (2j+1) T_P^{0j}(c, s) P_j(c)$$

and use the small angle impact parameter dictionary (for elastic scattering $q = p$)

$$\begin{aligned} 2j+1 &\longrightarrow 2qb \\ P_j(\cos\theta) &\longrightarrow J_0(k\sqrt{1-\cos\theta}) \\ \sum_{j=0}^{\infty} &\longrightarrow \int_0^{\infty} q db \\ T_P^{0j}(c, s) &\longrightarrow T_P^0(c, b) \end{aligned}$$

thus we convert the partial wave sum into an impact parameter integral -

$$T_P^0(c, t) = i\sqrt{\pi} \int_0^{\infty} db b T_P^0(c, b) J_0(c)$$

We insert the Pomeron dependence on b , which we have found above such that -

$$T_P^0(s,t) = i \sqrt{s} \int_0^1 db b \left(\frac{\beta_P^0 e^{i \int_0^b \lambda_P}}{2 \sqrt{s} \lambda_P} e^{-\frac{b^2}{4 \lambda_P}} \right)$$

making use of the Fourier-Bessel integral as before but now with $\alpha=0, \beta = \sqrt{s}$

$$-T_P^0(s,t) = i \beta_P^0 e^{i \int_0^1 \lambda_P} e^{-\lambda_P |t|}$$

results in the
Pomeron in $|t|$ space

The elastic differential cross section has been fitted by Ambats et al Ref ()

$$\frac{d\sigma(\pi-p)}{d|t|} = A e^{-B|t|} \frac{mb}{\text{GeV}^2}$$

$$A = 40.2 \pm 0.6 \frac{mb}{\text{GeV}^2}$$

$$B = 7.7 \pm 0.07 (\text{GeV})^{-2}$$

The isospin decomposition for $\pi^+ p \rightarrow \pi^+ p$ reads $T^0 = T_{\rho}^0 + T_{\rho}^0$

and the differential cross section at forward direction -

$$\frac{d\sigma}{d\Omega} \Big|_{t=0} = \left| \operatorname{Re} T^0(t=0) + i \operatorname{Im} T^0(t=0) \right|^2 \frac{mb}{G_{ev}^2} =$$

$$= \frac{\sigma_{tot}^2}{16\pi} (\alpha^2 + 1)$$

The last line follows from the optical theorem which gives in our normalization $N = 1$ the imaginary part amplitude in forward direction such that -

$$\operatorname{Im} T^0(s, t=0) = \frac{\sqrt{s}}{4\pi} \sigma_{tot}$$

Furthermore

$$\alpha = \frac{\operatorname{Re} T^0(t=0)}{\operatorname{Im} T^0(t=0)}$$

Ambats et al's value for all amplitudes are represented with respect to T^0 which possesses at $t/ = 0$ a phase the amplitude from Table XX at page 1206 into the complex plane one obtains at $t/ = 0$

$$\operatorname{Re} T^0 = - .855, \quad \operatorname{Im} T^0 = 6.399 \quad \text{measured in}$$

for $\sigma_{tot}(\pi^+p, 6.6 \text{ GeV}) = 28.2 \text{ mb}$ Since, however $d\sigma/dt$ is measured by Ambats in

$$\begin{aligned}
 28.2 \text{ mb} &\longrightarrow ? \text{ mb/GeV} \\
 28.2 \text{ mb} &= 5.31 \text{ mb} \times 5.31 \text{ mb} \\
 1.00 \text{ mb} &\longrightarrow ? \text{ 1/GeV} \\
 1.00 \text{ mb} &= 2.57 \text{ (GeV)}^{-2} \\
 1.00 \text{ mb} &= 1.603 \text{ (GeV)}^{-1} \\
 \Rightarrow 5.31 \text{ mb} &= 8.513 \text{ (GeV)}^{-1}
 \end{aligned}$$

$$\Rightarrow 28.2 \text{ mb} \longrightarrow 45.202 \text{ mb/GeV}$$

$$\Rightarrow \left(\frac{d\sigma}{dt} \right)_{t=0} = 41.373 \text{ mb/GeV}^2$$

Giacomelli 54.1
Hohler α

If we neglect

$\alpha \rightarrow \alpha = 0$ we obtain $\frac{\sigma_{tot}^2}{16\pi} = 40.65 \frac{mb}{GeV^2}$ whereas the actual measurement lies at $\left. \frac{d\sigma}{dt} \right|_{t=0} = 3$

See also Ambats (5) 10 page 1187

$\left(\frac{d\sigma}{dt} \right)_{\text{optical theorem}} = \frac{\sigma_{tot}^2}{15.5\pi}$ with $\sigma_{tot} \approx 40.615 \frac{mb}{GeV^2}$

and finally Ambats amplitude gives

$$\left(\frac{d\sigma}{dt} \right)_{t=0} = (R_2 T^0(t_{00}))^2 + (J - T^0(t_{00}))^2 = 41.68 \frac{mb}{GeV^2}$$

We found the Pomeron (isoscalar amplitude) in b and ln |t| space -

$$T_P^0(s, b) = \frac{\beta_P^0 e^{i\delta_P^0}}{2\sqrt{s} \lambda_P^0} e^{-\frac{b^2}{4\lambda_P^0}} \quad T_P^0(s, |t_1|) = i\beta_P^0 e^{-\lambda_P^0}$$

On the other hand $T_P^0(s, b) = 1 - S(b)$, $S(b) = 1 - C_{op} e^{-\frac{b^2}{R^2}} \Rightarrow T_P^0(s, b) =$ (

With C_{op} the opacity coefficient and R^2 the radius of the absorbing region

Thus $R_{op} = \frac{\beta_P^0}{2\sqrt{s} \lambda_P^0}$ and $R^2 = 4 \lambda_P^0$

from the parameterization of the elastic differential cross section

by a forward diffraction peak which is to a very good approximation exponential over a small range

$$|t| \lesssim 0.5 \text{ (GeV/c)}^2$$

such that

$$\frac{d\sigma}{d\Omega} / |t_1| = A e^{-3|t_1|}$$

which reads as well as

$$4\pi (\lambda_p^0 C_{op})^2 e^{-3|t_1|}$$

because of the optical theorem as

$$\frac{\sigma_{tot}^2}{16\pi} (\alpha^2 + 1) \quad \text{thus}$$

$$C_{op} = \frac{\sigma_{tot}}{8\pi \lambda_p^0}$$

We can determine

$$C_{op}$$

roughly by the exp. parameterization

$$C_{op} \sim 0.79$$

for $\sigma_{tot} \sim 28.2 \text{ mb}$ $\alpha \sim 1.33$ $\lambda_p^0 \sim 3.85$

$$(\text{GeV})^{-2} \rightarrow 0.39 \text{ mb}$$

$$28.2 \text{ mb} \rightarrow 28.2 \cdot 376 (\text{GeV})^{-2}$$

$$A = 4\pi (\lambda_p^0 C_{op})^2 \frac{\text{mb}}{\text{GeV}^2}$$

$$\text{if } C_{op} = 0.79, \lambda_p^0 = 62 \text{ GeV}^{-2} \quad \Rightarrow \quad A = 35.33 \frac{\text{mb}}{\text{GeV}^2}$$

We now consider the range $|t| = 0$ for the differential cross section. Although the isovector amplitude contributes we assume complete isoscalar dominance in this case we write -

$$\frac{d\sigma}{d\Omega |t|} = |T_P^0 C| |t|^{-2} = (\beta_P^0)^2 |t|^{-2} \hat{\lambda}_P^0$$

and it follows $\frac{B}{2} = \hat{\lambda}_P^0$ and $A =$

$$\lambda \text{ (Ambats exp. value)} = 3.85 \text{ (GeV}^{-2}) \quad \beta_P^0 = 6.34 \frac{\text{mb}}{\text{GeV}^2} \text{ (exp)}$$

We have $\hat{\lambda}_P^0 = \lambda_P^0 + \alpha_P' \ln(\frac{1}{|t|}) - i \frac{\pi \alpha_P'}{2}$ our value for $\alpha_P' = .6$

We have fitted Ambats isoscalar amplitude by $6.16 |t|^{-3.7} e^{-3.7|t|}$ at $6 \text{ GeV}/c$

$\hat{\lambda}_P^0$ is the modulus of a complex radius of interaction and implies $\lambda_P^0 = 2.08$ at

$$\text{Re } \hat{\lambda}_P^0 = 3.58 \quad \text{Im } \hat{\lambda}_P^0 = .943$$

The scattering amplitude for the transition $i \longrightarrow f$ for the spinless case in terms of angular momentum is expressed via the "eikonal matrix" χ^{ij} such that it reads in our normalization -

$$\frac{q}{\sqrt{v_i}} T_P^0(s, t)_{if} = \frac{i}{2q} \sum_{j=0}^{\infty} (2j+1) (1 - e^{i\chi^{ij}}) P_j(z)$$

As we did in the case of the elastic amplitude we project out the partial waves and make use of the orthogonality properties of the Legendre polynomials -

$$\int_{-1}^{+1} \frac{q}{\sqrt{v_i}} T_P^0(s, t)_{if} P_j(z) dz = \frac{i}{2q} \int_{-1}^{+1} \sum_{j'=0}^{\infty} (2j'+1) (1 - e^{i\chi^{ij'}}) P_{j'}(z) P_j(z) dz$$

$$(1 - e^{i\chi^{ij}}) = -iq \int_{-1}^{+1} \frac{q}{\sqrt{v_i}} T_P^0(s, t)_{if} P_j(z) dz$$

As our notation already suggests, we identify the Born amplitude $T_P^0(s, t)_{if}$ with an amplitude for the transition parameterized in a simple Regge pole exchange model i. e. in the case of $\pi^+ p \rightarrow \pi^+ n$ a single β -Regge pole

We take $(1 - e^{i\lambda^0}) \approx -i\lambda^0$ and insert the Regge pole in the form

$$T_g^0(s, t) = (s/s_0)^{\alpha_g^{(n)} - 1} \sum_{\lambda=1,2} \beta_{g_i}^0 e^{-\hat{\lambda}_{g_i}^0 |t|}$$

where we have summed over non rotating and rotating part in which the Pole has been split due to its signature such that -

$$\beta_{g_2}^0 = \beta_{g_1}^0 e^{-i\pi \alpha_g^{(n)}} \quad \text{and} \quad \hat{\lambda}_{g_2}^0 = \hat{\lambda}_{g_1}^0 - i\pi \alpha_g^{(n)}$$

and $\hat{\lambda}_{g_1}^0$ contains the energy dependence such that

$$\hat{\lambda}_{g_1}^0 = \lambda_g^0 - \alpha_g^{(n)} \ln(s/s_0) :$$

thus we obtain by employing the relation

$$\int_{-1}^{+1} P_j(x) dx \longrightarrow \frac{1}{q_2} \int_0^b \sqrt{t_1} dt_1 (V_{t_1}) J_0(b \sqrt{t_1})$$

$$-i \chi(s, b) \approx -i T_g^0(s, b) = -\frac{i}{\sqrt{s}} (s/s_0)^{\alpha_g^{(n)} - 1} \sum_{\lambda=1,2} \beta_{g_i}^0 \int_0^b \sqrt{t_1} e^{-\hat{\lambda}_{g_i}^0 |t_1|} J_0(b \sqrt{t_1}) dt_1$$

The Fourier Bessel integral gives then with

$$\int_0^{\infty} x^{2n} e^{-\alpha x^2} J_0(\rho x) dx = \frac{\rho^0}{(2\alpha)^{2n}} e^{-\frac{\rho^2}{4\alpha}} \quad \begin{matrix} \nu=0 \\ \rho=b \\ \alpha=\hat{\lambda}_{\rho i}^0 \end{matrix}$$

$$T_{\rho}^0(s, b) = -i \chi(s, b) = -i \sum_{i=1,2} \frac{(s/s_0)^{\alpha_{\rho}^{(0)}-1} \beta_{\rho i}^0}{2\sqrt{\pi} \hat{\lambda}_{\rho i}^0} e^{-\frac{b^2}{4\hat{\lambda}_{\rho i}^0}}$$

Thus, for the exchange of one Rho-Reggepole and one Pomeron, we obtain -

$$\frac{q}{\sqrt{s}} T_{\rho}^0(s, t) \otimes T_{\rho}^0(s, t) = -\frac{i}{2q} \sum_{j=0}^{\infty} (2j+1) T_{\rho}^{0j}(s) T_{\rho}^{0j}(s) \mathcal{D}_j(z)$$

$$= -i \sqrt{\pi} \int_0^{\infty} db b T_{\rho}^0(s, b) T_{\rho}^0(s, b) J_0(b\sqrt{H_1})$$

$$= -i \sqrt{\pi} \int_0^{\infty} db b \left(-i \sum_{i=1,2} \frac{(s/s_0)^{\alpha_{\rho}^{(0)}-1}}{4\sqrt{\pi} \hat{\lambda}_{\rho i}^0 \hat{\lambda}_{\rho}^0} \beta_{\rho i}^0 \beta_{\rho}^0 e^{i\delta_{\rho}^0} e^{-\frac{b^2(\hat{\lambda}_{\rho i}^0 + \hat{\lambda}_{\rho}^0)}{4\hat{\lambda}_{\rho i}^0 \hat{\lambda}_{\rho}^0}} \right) J_0(b\sqrt{H_1})$$

$$= \sum_{i=1,2} \frac{\beta_{\rho i}^0 \beta_{\rho}^0 e^{i\delta_{\rho}^0}}{2\sqrt{\pi} (\hat{\lambda}_{\rho i}^0 + \hat{\lambda}_{\rho}^0)} (s/s_0)^{\alpha_{\rho}^{(0)}-1} e^{-\frac{\hat{\lambda}_{\rho i}^0 \hat{\lambda}_{\rho}^0}{\hat{\lambda}_{\rho i}^0 + \hat{\lambda}_{\rho}^0} |t|} = T^0(s, t) \quad \text{Absorption cut}$$

Pomeron in momentum transfer space

Pomeron in impact parameter space

$$T_P^0(s, t) = i \beta_P^0(s) e^{i \hat{\delta}_P^0} e^{-\hat{\lambda}_P^0(s) |t|}$$

$$T_P^0(s, b) = \frac{\beta_P^0(s) e^{i \hat{\delta}_P^0}}{2 \sqrt{\pi} \lambda_P^0(s)} e^{-\frac{b^2}{4 \lambda_P^0(s)}}$$

$$= i 2 \sqrt{\pi} \lambda_P^0(s) C_{op}(s) e^{i \hat{\delta}_P^0} e^{-\hat{\lambda}_P^0(s) |t|}$$

$$= C_{op}(s) e^{-\frac{b^2}{4 \lambda_P^0(s)}}$$

$$= i \frac{\sqrt{s}}{4\pi} \sigma_{tot}^{(s)} e^{i \hat{\delta}_P^0} e^{-\hat{\lambda}_P^0(s) |t|}$$

$$= \frac{\sigma_{tot}^{(s)}}{8\pi \lambda_P^0(s)} e^{-\frac{b^2}{4 \lambda_P^0(s)}}$$

with $\hat{\lambda}_P^0(s) = \lambda_P^0 + \alpha_P' \ln(s/s_0) - i \frac{\pi \alpha_P'}{2}$

$\rightarrow T^0(\sigma_{tot}^{(s)}, |t|, s) = - \sum_{\lambda=1,2} \frac{\sigma_{tot}^{(s)} \beta_i^0}{8\pi (\lambda_P^0 + \lambda_{P_i}^0)} e^{i \hat{\delta}_P^0} (s/s_0)^{\alpha_P^0 - 1} e^{-\frac{\lambda_P^0 \lambda_{P_i}^0}{\lambda_P^0 + \lambda_{P_i}^0} |t|}$
 Absorption cut

XI. - REFERENCES

1. A. C. Irving and R. P. Worden, Phys. Rep. 3, 117, (1977)
2. A. Barnes et al. Phys. Rev. Letts., 37, 76, (1976)
O. I. Dahl et al. Phys. Rev. Letts., 37, 80, (1976)
3. S. Mandelstam, Nuovo Cimento, 30, 1127 (1963a)
S. Mandelstam, Nuovo Cimento, 30, 1148 (1963b)
4. Weak
R. C. Arnold and M. L. Blackmon, Phys. Rev. 176, 2082 (1968)
S. A. Adjei, P. A. Collins, B. J. Hartley, K. J. M. Moriarty and R. W. Moore, Annals of Phys. 75, 405, (1973)
G. Cohen-Tannoudji, A. Morel and H. Navalet, Nuovo Cimento, 384, 1075, (1967)
Strong
F. Henyey, G. L. Kane, Jon Pumplin and M. H. Ross, Phys. Rev. 182, 1579, (1968)
5. I. Ambats, D. S. Ayres, R. Diebold, A. F. Greene, S. L. Kramer, A. Lesnik, D. R. Rust, C. E. W. Ward, A. B. Wicklund and D. D. Yovanovitch, Phys. Rev. 9D, 1179 (1974)
F. Halzen and C. Michael, Phys. Lett. 36B, 367, (1971)
E. Pietarinen, Phys. Lett. 61B, 461, (1976)
M. Ross, Phys. Lett. 38B, 321, (1972)
6. M. Borghini et al, Phys. Letts, 31B, 405, (1970)
R. J. Esterlings et al, Phys. Rev. Letts. 21, 1410, (1968)
7. N. J. Sopkovich, Nuovo Cimento, 26, 186 (1962)
8. J. D. Jackson, Rev. Mod. Phys., 37, 484 (1965)
9. P. D. B. Collins and F. D. Gault, Springer Tracts in Modern Phys. 63, 163, (1972)
10. G. A. Ringland, R. G. Roberts, D. P. Roy and J. Thanh Van, Nucl. Phys. 44B, 395, (1972)
J. Anderson, K. J. M. Moriarty and R. L. Thew, Acta Phys. Austr., 45, 261, (1976)
A. Martin and P. R. Stevens, Phys. Rev. 8D, 2
G. L. Kane and A. Seidl, Rev. Mod. Phys., 48,
S. E. Egli, D. W. Duke and N. W. Dean. Phys. Rev. 1365, (1974)
B. Sadoulet, Nucl. Phys. 53B, 135 (1973)
G. Girardi et al. Nucl. Phys., 47B, 445 (1972)
B. J. Hartley, G. L. Kane, Nucl. Phys. 57B, 15
11. (a) R. P. Worden, Nucl. Phys. 58B, 205 (1973)
(b) D. Barkai and K. J. M. Moriarty Act. Phys 43, 143 (1975)
(c) R. P. Worden, Phys. Letts. 40B, 260 (1972)
12. V. Barger and R. J. N. Phillips Phys. Rev., 18
13. V. Barger and R. J. N. Phillips, Phys. Letts. 5
14. V. N. Gribov, Sov. Phys. JETP, 26, 414 (1968)
15. M. Baker and K. A. Ter-Martirosyan, Phys. I
16. K. A. Ter-Martirosyan, Sov. Journ. Nucl. Phy
17. K. A. Ter-Martirosyan, Sov. Journ. Nucl. Phy
18. V. Yu. Glebov, A. B. Kaidalov, S. T. Sukhorukov Sov. Journ. Nucl. Phys. 10, 609 (1970)
19. P. D. B. Collins and R. A. Swetman, Nuovo Ci 793, (1972)
20. K. G. Boreskov, A. M. Lapidus, S. T. Sukhorul Sov. Journ. Nucl. Phys. 14, 457 (1972)
21. K. A. Ter-Martirosyan, Nucl. Phys. 36B, 56

22. Sh. S. Eremyan, Sov. Journ. Nucl. Phys. 20, 554 (1975)
23. Sh. S. Eremyan, Sov. Journ. Nucl. Phys. 21, 195 (1975)
24. V. Franco and R. J. Glauber, Phys. Rev. 142, 1195 (1966)
25. A. Kerman, H. McManus and R. M. Thaler, Ann. Phys. (N. Y.) 8, 551 (1959)
H. Feshbach and J. Hufner, *ibid*, 56, 268 (1970)
26. C. Lovelace, Proceedings of the Amsterdam International Conference on High Energy Physics (Amsterdam 1971)
27. H. Cheng and T. T. Wu, Phys. Rev. 182, 1853 (1969)
28. A. A. Grigoryan and A. B. Kaidalov, Nucl. Phys. 135B, 93, (1978)
29. V. N. Gribov and A. A. Migdal, Sov. Journ. Nucl. Phys., 8, 583 (1969)
30. D. R. Harrington and A. Pagnamenta, Phys. Rev. 173, 1599, (1968). Phys. Rev. 184, 1908 (1969)
D. R. Harrington, Phys. Rev. 1D, 260, (1970)
31. John Kogut and Leonard Susskind, Phys. Rep. 8C, 75, (1973)
32. L. Bertocchi, Proceedings of the International Conference on Elementary Particles, Heidelberg 1967.
33. A. R. White, Phys. Rev. 10D, 1236 (1974)
34. Henry D. I. Abarbanel, Rev. Mod. Phys. 48, 41 (1976)
35. A. B. Kaidalov, Sov. Journ. Nucl. Phys. 13, 226 (1970)
36. A. B. Kaidalov, Sov. Journ. Nucl. Phys. 16, 21 (1973)
37. Sh. S. Eremyan, Sov. Journ. Nucl. Phys. 24, 1 (1977)
38. D. G. Ravenhall and H. W. Wyld Jr. Phys. Rev. 21, 1770 (1968)
39. E. Shrauner, L. Benofy and D. W. Cho, Phys. Rev. 184, 2590 (1969), Phys. Rev. 184, 1908 (1969).
40. H. Høgaasen, Proceedings of the VII Rencontre de Physique, CERN 1972, 1, 233, (1972)
41. C. Quigg, University of California-Berkeley UCRL - 20032, (1970, -Unpublished)
C. Quigg, Nucl. Phys. 29B, 67 (1971)
42. A. V. Stirling et al. Phys. Rev. Letts. 14, 763 (1970)
P. Sonderegger et al. Phys. Letts. 20, 75 (1967)
M. A. Wahlig and I. Mannelli, Phys. Rev. 168, 168 (1968)
I. Mannelli et al. Phys. Rev. Letts. 14, 408 (1970)
43. M. Davier, Proceedings of Summer Institute on Particle Physics, Stanford University SLAC 179, Vol. 1, 179 (1970)
44. D. Hill et al. Phys. Rev. Letts. 30, 239 (1973)
D. D. Drobniš et al. Phys. Rev. Letts. 20, 27 (1967)
P. Bonamy et al. Nucl. Phys. 16B, 335 (1970)
P. Bonamy et al. Nucl. Phys. 52B, 392 (1973)

45. R. W. B. Ardill, P. Koehler and K. J. M. Moriarty submitted to Phys. Rev.
46. R. W. B. Ardill, P. Koehler and K. J. M. Moriarty Lett. Nuovo Cimento, 18, 161 (1977)
R. W. B. Ardill, P. Koehler and K. J. M. Moriarty Lett. Nuovo Cimento, 19, 1, (1977)
47. B. Schrempp and F. Schrempp, Nucl. Phys. 96 B, 307, (1975)
48. V. Barger and R. J. N. Phillips, Nucl. Phys. 87 B, 221 (1975)
49. F. Halzen and M. G. Olsson and A. Yokosawa Nucl. Phys. 113 B, 269 (1976)
50. V. N. Gribov, Sov. Journ. Nucl. Phys. 17, 313 (1973)
51. E. M. Levin and M. G. Ryskin, Sov. Journ. Nucl. Phys. 25, 452 (1977)
52. P. D. B. Collins and A. Fitton, Nucl. Phys. 91 B 332, (1975)
53. Sh. S. Eremyan, Sov. Journ. Nucl. Phys. 23, 690 (1976)
54. P. É. Volkovitskiĭ, A. M. Lapidus, V. I. Lisin, and K. A. Ter-Martirosyan, Sov. Journ. Nucl. Phys. 24, 567, (1976)
55. D. Barkai and K. J. M. Moriarty, Nucl. Phys. 50 B, 354, (1972)
56. P. Choudhury, K. J. M. Moriarty and A. Ungkitchanukit, Acta Phys. Austr. 43, 133 (1975)